

ELECTRON SPIN RESONANCE STUDIES OF SOLVATION USING
NITROXIDE RADICALS AS PROBES

A thesis presented for the Degree
of Doctor of Philosophy

In the
Faculty of Science

by
Edward Andrew Smith

University of Leicester 1979

UMI Number: U440994

All rights reserved

INFORMATION TO ALL USERS

The quality of this reproduction is dependent upon the quality of the copy submitted.

In the unlikely event that the author did not send a complete manuscript and there are missing pages, these will be noted. Also, if material had to be removed, a note will indicate the deletion.



UMI U440994

Published by ProQuest LLC 2015. Copyright in the Dissertation held by the Author.
Microform Edition © ProQuest LLC.

All rights reserved. This work is protected against
unauthorized copying under Title 17, United States Code.



ProQuest LLC
789 East Eisenhower Parkway
P.O. Box 1346
Ann Arbor, MI 48106-1346



THESIS
588548
26 " 79

x752976906

To Ruth

ACKNOWLEDGEMENTS

I would like to extend my thanks to the following:

Professor M. C. R. Symons for his help and guidance throughout the course of this work.

Dr. Y. Y. Lim, with whom much of the work described in Chapter 3 was done.

Drs. M. J. Blandamer, T. A. Claxton, T. Lund, K. W. Morcom, G. W. Neilson and D. Waddington for many fruitful discussions on the principles of physical chemistry.

My colleagues in the Physical Chemistry Department, particularly Sue Jackson, who was responsible for the near infra-red data given in Chapter 4 and Vicky Thompson, who was a regular provider of equipment.

Mr. J. A. Brivati, who took responsibility for me whilst I was a member of the University Technical Staff.

Messrs. P. E. Acton, P. Baxendale, G. C. Clemerson and D. J. Hopkins for technical assistance.

Professor M. J. Perkins and his group at Chelsea College, London, for the gift of materials and several helpful discussions.

Miss Vicky Orson-Wright for typing this thesis and Mrs. Ann Crane for drawing the diagrams.

The experimental work described in this thesis has been carried out by the author, in the Department of Chemistry of the University of Leicester, between September 1973 and September 1977, under the supervision of Professor M. C. R. Symons; it has not, and is not concurrently, being presented for any other degree.

E A Smith

E. A. Smith

June 1979

NOTE

The units used for magnetic field strength and energy in this thesis are those most commonly found in the literature. The S.I equivalents of these units are given below:

$$1 \text{ Calorie} = 4.184 \text{ Joules}$$

$$1 \text{ Gauss} = 10^{-4} \text{ Tesla}$$

SYNOPSIS

Over recent years electron spin resonance has been used to investigate solvation phenomena. This technique is useful for measuring processes occurring on a rapid timescale and is therefore suited for examining solutions. Several paramagnetic probes have been employed in such studies. Increasingly, nitroxide radicals have proved to be useful spin probes. The probe concentrations used in e.s.r. investigations of solvation are usually low and do not therefore appreciably effect the solvent composition.

The initial chapters of this thesis are concerned with contemporary theories of solvation and those principles of e.s.r. which are relevant to solvation studies. A broad description of the structure and properties of water and aqueous solutions is given in chapter one. A review of how spectroscopic techniques have been used, by the Leicester group over recent years, to probe solvation effects is also included in this chapter. Chapter two deals with factors perturbing the g and A tensors of nitroxide radicals and the various mechanisms of line broadening encountered.

The use of ditertiary butyl nitroxide as a spin probe in studying binary aqueous solutions is introduced in chapter three. Both the nitrogen hyperfine coupling constant and linewidths of this radical reveal changes in the solvent medium. In the succeeding chapter this study is extended to examine changes in solvation in electrolyte containing solutions. The e.s.r. results recorded in this study of aqueous and methanolic salt solutions are compared with near infra-red studies of similar systems.

The fifth chapter describes a study of Heisenberg Spin Exchange

for ditertiary butyl nitroxide in several solvents. Water is shown to exert an anomalous effect on the observed exchange rate, this is interpreted in terms of water structure effects.

The sixth chapter examines the information which can be obtained from studies of ditertiary butyl nitroxide in frozen solutions. Solid state spectra in frozen matrices are used to estimate the spin distribution in the radical t-butyl-N-benzoyl nitroxide.

The final chapter deals with the rôle of t-butyl-N-benzoyl nitroxide as a spin probe. The data is interpreted in the same manner as the ditertiary butyl nitroxide results and reveals that t-butyl-N-benzoyl nitroxide is less suitable as a probe of the aqueous environment.

Several useful computer programs, which were used to analyse some of the data collected throughout this study, are documented in the Appendix.

CONTENTS

| | <u>Page No.</u> |
|---|-----------------|
| CHAPTER 1 - The Structure and Properties of Water | |
| 1.1 - Introduction | 1 |
| 1.2 - The Water Monomer | 1 |
| 1.3 - The Structure of Liquid Water | 4 |
| 1.4 - Solutions of Non-electrolytes | 10 |
| 1.5 - Electrolyte Solutions | 12 |
| 1.6 - Recent Work at Leicester | 16 |
| CHAPTER 2 - Review of the Principles of Electron Spin Resonance Spectroscopy | |
| 2.1 - Introduction | 26 |
| 2.2 - The Isotropic E.S.R. Spectrum | 27 |
| 2.3 - The Anisotropic E.S.R. Spectrum | 32 |
| 2.4 - Relaxation Effects | 39 |
| 2.5 - The Effects of Rotational Motion on Linewidths | 40 |
| 2.6 - Spin Rotation | 47 |
| 2.7 - Chemical Exchange | 50 |
| 2.8 - Heisenberg Spin Exchange | 53 |
| 2.9 - Dipolar Broadening | 57 |
| 2.10 - Concluding Remarks | 60 |
| CHAPTER 3 - Ditertiary butyl nitroxide as a Probe for Examining Binary Aqueous Solutions | |
| 3.1 - Introduction | 66 |
| 3.2 - Experimental Details | 67 |
| 3.3 - Trends in Linewidths | 68 |
| 3.4 - Trends in Nitrogen Hyperfine Coupling Constant | 83 |
| 3.5 - DTBN in Aqueous Solutions of Urea and the Acid Amides | 96 |
| 3.6 - Conclusions | 101 |
| CHAPTER 4 - Ditertiary butyl nitroxide as a Probe for Examining Aqueous Electrolyte Solutions | |
| 4.1 - Introduction | 108 |

| | <u>Page No.</u> |
|---|-----------------|
| 4.2 - Experimental Details | 109 |
| 4.3 - Methanolic Salt Solutions | 110 |
| 4.4 - Aqueous Salt Solutions | 115 |
| 4.5 - Conclusions | 137 |
| | |
| CHAPTER 5 - Heisenberg Spin Exchange Studies Using Ditertiary butyl nitroxide | |
| 5.1 - Introduction | 143 |
| 5.2 - Experimental Details | 147 |
| 5.3 - Results and Discussion | 148 |
| 5.4 - Conclusions | 168 |
| | |
| CHAPTER 6 - Frozen Solutions of Nitroxide Radicals | |
| 6.1 - Introduction | 172 |
| 6.2 - Experimental Details | 174 |
| 6.3 - Ditertiary butyl nitroxide - Results and Discussion | 176 |
| 6.4 - t-Butyl-N-benzoyl nitroxide - Results and Discussion | 194 |
| 6.5 - Conclusions | 211 |
| | |
| CHAPTER 7 - Study of t-Butyl-N-benzoyl nitroxide as a Spin Probe | |
| 7.1 - Introduction | 214 |
| 7.2 - Experimental Details | 215 |
| 7.3 - Results and Discussion | 215 |
| 7.4 - Conclusions | 235 |
| | |
| APPENDIX - Computer Programs | |
| A.1 - Introduction | 238 |
| A.2 - The Solid State Simulation Program - PLOWSY | 239 |
| A.3 - The Proton Envelope Simulation Program - SWACK | 243 |
| A.4 - Program to Calculate Rotational Correlation Times - REXTAU | 243 |
| A.5 - Program to Analyse the Concentration Dependence of Linewidths - TUGGER | 245 |
| A.6 - Listings | 246 |

CHAPTER ONE

The Structure and Properties of Water

CHAPTER ONE

1.1 Introduction

The liquid state is the least well understood of the three states of matter. The solid state is seen as a well ordered system and the gaseous state is characterised by its lack of order.¹ The energy of a solid is dominated by its potential energy; the kinetic energy appearing as a small perturbation. Conversely, the kinetic energy dominates in the gaseous state. Liquids are more difficult to treat; since here the potential and kinetic energies are of comparable size. Water is less easily understood than most liquids. However, its use as a solvent and its biological and geological importance,² have aroused much interest in the structure and properties of water. Despite the vast literature on water and aqueous solutions,^{3,4} many aspects of solvation in aqueous systems are not well understood. The rôle of water and aqueous solutions as reaction media, is of great importance. It is hoped to describe the current theories of liquid water and aqueous solutions in the ensuing discussion.

1.2 The water monomer and hydrogen bonding

The properties of the isolated molecule can be obtained from measurements made on water vapour at sufficiently low pressures and temperatures.⁵ The bond length of 0.95718 Å and the bond angle of 104.523°, can be estimated from vibration-rotation spectra. The dipole moment of water is 1.83 D. The fundamental infra-red vibration spectrum shows the three absorptions, the asymmetric OH stretch ν_3 , the symmetric OH stretch ν_1 and the H-O-H band ν_2 (see fig. 1.1).

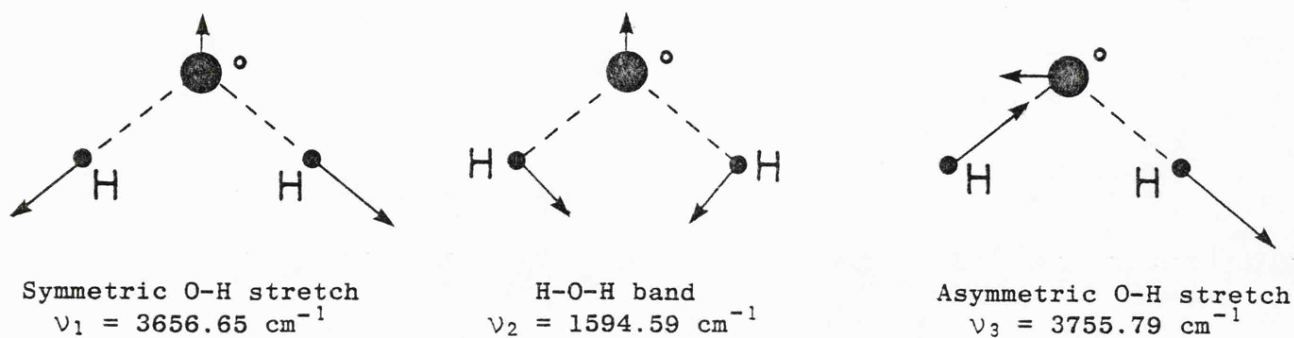


Fig. 1.1 The fundamental vibration modes of the isolated water molecule (taken from ref. 5).

The water molecule can be thought of as a twelve electron molecule, each hydrogen atom contributing its $1s$ electron and the oxygen contributing its $1s^2$, $2s^2$, $2p^4$ electrons to the molecular orbitals. At first sight, one might expect that bonding to oxygen would be in the form of σ bonds between the $2p$ orbitals of oxygen and the $1s$ orbitals of hydrogen. This would lead to a bond angle of 90° , which is inconsistent with experiment. Even the mutual repulsion⁶ of the hydrogen atoms is only sufficient to open up the bond angle to 95° . A better representation is to think of the orbitals on oxygen as being sp^3 hybridised, with the four unbonded electrons in two sp^3 hybrids pointing out into space. This would give a bond angle of $109^\circ 28'$. This picture of the water molecule is still inadequate. Bader⁷ was able to test various wave functions for water by examining the effect of electron density on the nuclear-nuclear repulsions of the hydrogen atoms. Bader found that to balance the nuclear repulsions, he required the bonding hybrids to be of 97% $2p$ character and to be at an angle of 64° to each other. The lone-pairs on this model must be almost pure sp hybrids and should be perpendicular to the plane of the O-H bonds. Recent quantum

mechanical calculations⁸ show that the stable conformation of water should have a bond length of 0.945 Å and a bond angle of 106°. A considerable electron density is to be expected between the nominal bond directions and the lone pairs were found not to have distinctive directionality. Although, this work predicted a dipole moment of 2.19 D, which is higher than found, some of the ideas presented have much in common with Bader's work.⁷ Other calculations⁹ suggest an optimum bond angle of about 109° and a bond length of about 0.974 Å.

It is well known that the hydrides of nitrogen, oxygen and fluorine, have anomalously high melting points and boiling points. This is due to the phenomenon known as hydrogen bonding. In a hydrogen bond; a hydrogen atom is apparently bonded between two electronegative atoms. Hydrogen bonds^{10,11} are normally linear and have a bond strength of the order of 2-10 k cal mol⁻¹. The position of the hydrogen atom varies; in the hydrogen bonded ion HF₂⁻, the hydrogen is equidistant from both fluorines; in ice the hydrogen atom is nearer one oxygen atom (1.0 Å) than the other (1.76 Å). The hydrogen bond^{10,11} is largely electrostatic in nature and can be attributed to a partial positive charge on hydrogen and a partial negative charge on the electronegative atom. The strongest known hydrogen bonds¹¹⁻¹² are of the order 50-60 k cal mol⁻¹.

In the bulk liquid or solid, the lone-pairs on oxygen of the water molecules become much more significant chemically. The lone-pairs are now free to participate in hydrogen bonding and there is a tendency for each molecule to become tetrahedrally hydrogen bonded to four other water molecules. The effect of this four co-ordination is to give water in the solid state a very open structure. Estimates of the strength of the hydrogen bond in ice can be made from the heat of sublimation of

ice; a value of about 5 k cal mol⁻¹ has been suggested by Pauling.¹¹ Eisenberg and Kauzmann⁵ outline the difficulties in obtaining precise values for the bond strength of the hydrogen bond in ice. Hydrogen bonding has a pronounced effect on the infra-red spectrum of water and ice. In the vibrational spectrum of ice, the three sharp bands in the vapour are replaced by a broad coupled stretching band at 3220 cm⁻¹ and a broad coupled bending band at 1650 cm⁻¹. Pauling estimates that on melting only 15% of the hydrogen bonds in ice are broken.

It is both the ability to hydrogen bond through its acidic hydroxyl functions and its basic lone-pair functions; and the tendency for water to be tetrahedrally co-ordinated that influence the solvating power of this liquid.

1.3 The structure of liquid water

Before discussing the structure of liquid water, it is instructive to examine two important solid forms of water. These are the hexagonal (common) form of ice and the clathrate hydrates; as both have proved key features of several models for liquid water.¹³⁻¹⁷

There are several forms of ice;^{5,18,19} Kamb gives the number of ice polymorphs to be 13. Most of the ice polymorphs are metastable and only exist at low temperatures and high pressures. The common form of ice is ice 1h, which has an open tetrahedral structure, consisting of interconnected hexagonal "cyclohexane type" rings in the chair conformation. The structure of ice 1h is shown in figure 1.2. The oxygen-oxygen separation is 2.76 Å, and the O-H bond length is 1.01 Å. The H-O-H bond angle is not significantly different from that in the isolated molecule.⁵ From entropy arguments^{5,16} the distribution of

hydrogen atoms along the O---O axes is random, subject to the condition that distinct H₂O units are conserved.

The rare gas or clathrate hydrates have aroused considerable interest. The structure and properties of this series of compounds has recently been reviewed by Davidson.²⁰ The simpler clathrate hydrates consist of a guest non-polar molecule housed inside an extensively hydrogen bonded water network. The water lattice is made up of interconnected pentagonal dodecahedra.

There are two basic structures:-

Type I, which has a cubic unit cell of 46 water molecules, with a side of length 12 Å. The unit cell is composed of two pentagonal dodecahedra and six tetrakaidecahedra. Guests of diameter smaller than 5.3 Å can be accommodated within the voids at the centre of the polyhedra.

Type II, has a cubic unit cell of 136 water molecules and has a side of length 17 Å. The unit cell is made up of 16 pentagonal dodecahedra and 8 hexakaidecahedra. Guests of diameter between 5.6 Å and 6.6 Å tend to form this structure.

In addition to the two basic clathrate structures a variety of distorted clathrate and semi-clathrate structures exist. An indication of the variety of structures and hosts is given in figure 1.3. Clathrate structures were first observed for simple non-polar guests such as the rare gases, however clathrate type compounds are known for some polar compounds and some bulky ions with alkyl residues. These clathrate compounds are found to be stable at low temperatures, their stability being gained by the formation of an extensive hydrogen bonded network around the guest molecule. The formation of clathrate compounds is accompanied by a considerable loss of entropy.

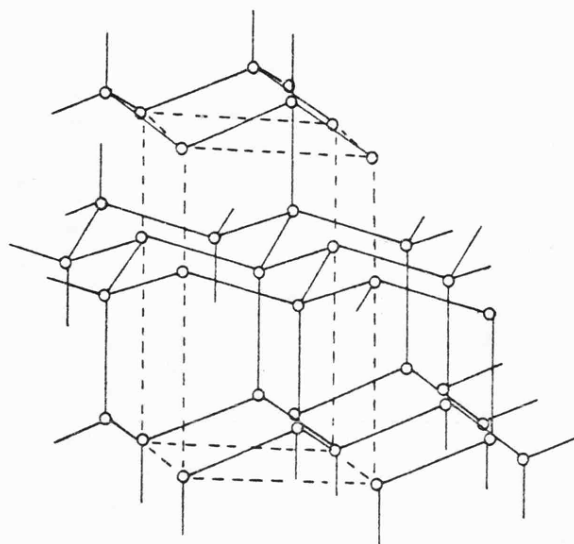


Figure 1.2 The structure of ice Ih, only the oxygen atoms are shown (from ref. 5).

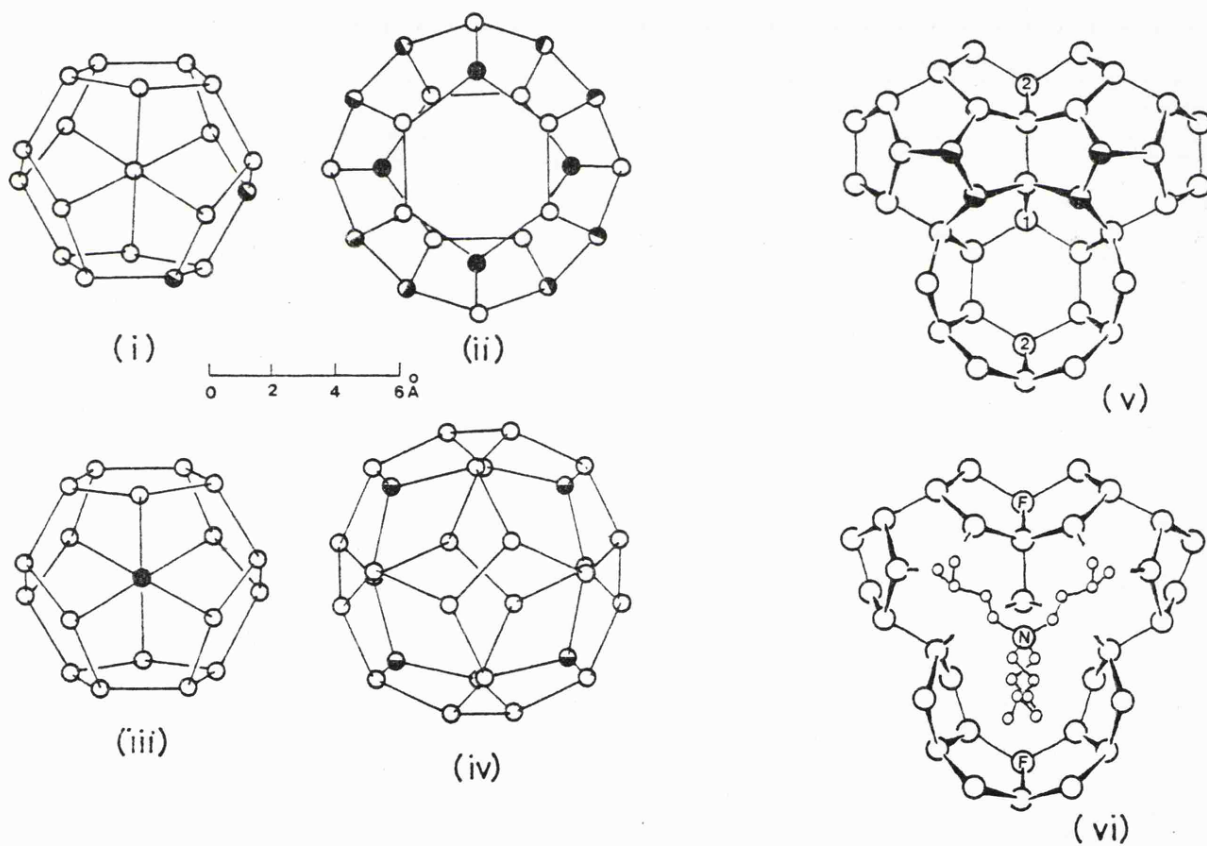
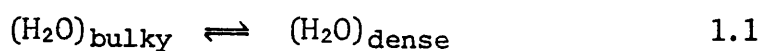


Figure 1.3 Various clathrate structures. (i) and (ii) are the cages of Structure I, (iii) and (iv) are the cages of Structure II. (v) is the ideal hexagonal structure. (vi) is the structure of $(\text{iso-C}_5\text{H}_{11})_4\text{NF}$, which is (v) modified to accommodate the salt. (From ref. 20.)

Water has several physical and chemical properties, which are quite different from those expected for a simple liquid. The high melting point and boiling point have already been mentioned, other properties which are unexpected are the existence of a temperature of maximum density (TMD) at 4°C, the high heat capacity, and the response of water to pressure. Several structural models have been proposed^{13-17,21-22} to account for the above and several other properties of liquid water. Two types of model have been invoked; the continuum models^{13,14,22} and the mixture models.^{15,16,17,21}

Continuum models picture water as being composed as a single structural entity, which may change homogeniously with change in temperature. Bernal and Fowler¹³ described water as being ice 1h-like at temperatures below 4°C, changing gradually to a less open quartz-like structure at normal temperatures. Finally, a dense ammonia type structure is achieved at temperatures above 200°C. Probably, the most popular continuum model is that of Pople.¹⁴ Here water is viewed as a broken down ice-type structure, in which hydrogen bonds are bent as opposed to being broken on melting. Bernal²² has proposed that in liquid water each water molecule forms four hydrogen bonds, although some bonds may be distorted. These linked four co-ordinate water molecules form an irregular lattice of rings. Five membered rings are the most common, although larger and smaller rings may also be found.

Mixture models picture water as existing in several distinct forms in the liquid state. One form is bulky with an open structure, the second is a dense form of water, which may be monomeric. The two forms of water are thought to be in equilibrium with each other as shown below.



The model of Frank and Wen is a very useful one. These workers picture water as being formed of clusters of unspecified open structure, which because of the co-operative nature of hydrogen bonding are able to spontaneously form and collapse on a time scale of 10^{-11} seconds. These "flickering clusters" are in equilibrium with monomeric water and have a meaningful existence of the order of 10^2 to 10^3 molecular vibrations. The short lifetime of these clusters was invoked to explain the dielectric relaxation properties of liquid water, which relaxes with a single relaxation time of about 10^{-11} seconds. Pauling¹⁶ has proposed a clathrate hydrate type model for liquid water, here the bulky form is seen as a clathrate hydrate framework, with some of its voids filled with monomeric water molecules. Samoilov¹⁵ has proposed a similar model, with the bulky form being ice-like in structure, and the monomeric water occupying the voids between the planes of the rings.

The above models have been used to explain certain of the properties of water. For example, the TMD is easily explained in terms of a competition between thermal expansion and the movement towards closer packing (continuum) or the movement of equilibrium 1:1 to the right (mixture). The X-ray diffraction pattern is often taken as a guide to the validity of the model. The models of Pople,¹⁴ Samoilov¹⁵ and Bernal²² have been judged⁵ to give a good fit to the experimental X-ray diffraction pattern. Danford and Levy²³ have shown that the Pauling¹⁶ model gives a poor fit to the X-ray data. The infra-red and Raman spectra of dilute solutions of D_2O in H_2O have yielded much useful information, especially in the OD stretching region. These results have been interpreted in terms of both the continuum and mixture models.^{5, 24-26}

Frank and Quist¹⁷ have examined the Pauling model in more detail,

using the methods of statistical thermodynamics. They were able to fit most of the calculated thermodynamic data to the observed properties of water. Some properties, notably the heat capacity could only be accounted for by considering a third form of water known as "State III". "State III" is described as being made up from molecules, which have just melted from a Pauling cluster and have not yet been incorporated into a new one. Némethy and Scheraga²⁷ have placed the flickering cluster theory on a semi-quantitative basis, assuming a distribution of species forming zero, one, two, three and four hydrogen bonds; those at the edge form less. Using statistical thermodynamics they were able to reproduce the thermodynamic properties of water to a reasonable degree of accuracy. The average cluster size was found to be about 90 molecules at 0°C and about 21 molecules at 100°C. Perram and Levine²⁸ showed that Némethy and Scheraga²⁷ had over-estimated the number of unbonded water molecules, their own calculations based on the lattice theories of simple liquids pointed to a continuum model for water. Refinements^{29,30} of the Némethy and Scheraga work have shown a reduction in cluster size, down to less than 10 water molecules.³⁰ Lentz et alia³⁰ show that liquid water contains a large number of ring pentamers and hexamers.

"Computer models" seem to have a significant rôle in the elucidation of the structure of water. Moore³¹ gives a simple description of the commonly used approaches: the Monte Carlo and molecular dynamics techniques. Both models use the pair potential i.e. the interaction between two water molecules, as the starting point. The water molecule has been represented as a tetrahedral distribution of point charges, for the purpose of both calculations.^{32,33} Barker and Watts³² used a pair potential derived from the properties of ice and steam, in their

Monte Carlo calculations. They were able to obtain a reasonable agreement between their results and the experimentally known thermodynamic energy, heat capacity at constant volume and the X-ray scattering pattern. Rahman and Stillinger³³ in their molecular dynamics calculations were able to show that water in the liquid state bore no resemblance to any of the ice or clathrate structures. They predict a series of ringed polymers, with pentamers and hexamers being quite common.

1.4 Solutions of non-electrolytes

It is thought that the addition of a solute to water can either enhance or diminish water-water interactions. The former case is known as the "structure making" effect, the latter case is known as the "structure breaking" effect. Most of the water-solute mixtures of wide interest can be classified in terms of the relative magnitudes of their thermodynamic excess functions of mixing. Those aqueous mixtures,³⁴ which are characterised by a positive G^E and a dominant excess entropy of mixing i.e. $|TS^E| > |H^E|$ are known as typically aqueous, TA. At low cosolvent molefractions TA mixtures resemble dilute aqueous solutions of the hydrocarbons, showing enhanced water-water interactions. Beyond this initial "structure making" region there is insufficient water to conserve a three dimensional hydrogen bonded network and the structure enhancement is lost. Those aqueous mixtures having a dominant excess enthalpy of mixing are known as typically non-aqueous, TNA. Alcohols, amines, ketones and ethers are typically aqueous solutes; whilst polyhydric alcohols, hydrogen peroxide, methyl cyanide and carbohydrates form typically non-aqueous mixtures with water. Heat capacity changes,

excess volumes of mixing and changes in the TMD are useful guides to the nature of binary aqueous mixtures.

The behaviour of non-electrolytes in aqueous solutions is expected to be dictated by the hydrophilic nature of the polar group favouring mixing, whilst the hydrophobic non-polar residue should oppose mixing. For non-electrolytes³⁵ with a single polar function; the solution behaviour is largely a function of the apolar residue. This often produces typically aqueous behaviour. Once the number of polar groups is increased, the water-solute mixture will tend towards TNA behaviour. For this kind of solute the relative positions of the polar groups, their freedom of rotation, and their conformation are of great importance. Franks³⁵ has illustrated this point by discussing the solution behaviour of water-urea mixtures and water-glucose mixtures in terms of equilibrium 1:1. He proposes that urea, because of its geometry is excluded from interacting with the tetrahedral water in (H₂O) bulky, and thus has to associate with (H₂O) dense. This pushes equilibrium 1:1 to the right exerting a net "structure breaking" effect. He suggested that glucose possess a geometry suitable for association with the "ice-like" (H₂O) bulky, thus producing a net "structure making" effect.

Detailed treatments of the dissolution of apolar solutes in water in terms of equilibrium 1:1 have been attempted.³⁶⁻³⁸ Frank and Franks³⁶ have re-examined the Frank and Quist¹⁷ treatment of water; they suggest that (H₂O) bulky in water is in the form of a clathrate framework and that (H₂O) dense is a quasi lattice. Hydrocarbons are partitioned between the water species, forming interstitial solutions with (H₂O) bulky and regular solutions with (H₂O) dense. This model is of limited value because it applies only in the limit of infinite

dilution. Mikhailov^{37,38} begins from the Samoilov¹⁵ model of water, in expounding his theory. Here (H₂O) bulky is ice-like, (H₂O) dense is structureless and may exist in a third non-interstitial state. Again the solute can be accommodated interstitially or as a regular solution with the non-interstitial (H₂O) dense. Both treatments³⁶⁻³⁸ use statistical thermodynamics to reproduce thermodynamic properties.

Franks and Ives³⁹ have examined the behaviour of water-alcohol mixtures. They show that the simple alcohols form typically aqueous mixtures with the water. The volume behaviour of the mixtures is of interest, they show that at low alcohol concentrations there is an expansion of the water lattice and that the alcohol apparently contracts in volume. This is consistent with the formation of a clathrate type of arrangement with the alcohol molecules occupying the interstices. Franks and Ives³⁹ suggest that methanol dissolves substitutionally in water, whereas t-butanol dissolves interstitially. Glew⁴⁰ has shown that the maxima of several thermodynamic and spectroscopic properties of aqueous solutions of several polar organic solutes, occur at compositions very close to the stoichiometry expected for the solute in the large cage of a Structure II clathrate hydrate.

1.5 Electrolyte solutions

The analysis of solvation effects in aqueous electrolyte solutions is complicated by the presence of ion-ion interactions. Ionic solutions are essentially three component systems; containing anions, cations and solvent. Since, electrical neutrality must be conserved, it is impossible to vary independently the concentrations of the anion and the cation. Thus the effects of a particular ion are difficult to determine.

Early theoretical treatments of ionic solutions were based on the description of the solvent as a structureless continuum. Although, this is clearly not the case such models have found a fairly wide use. The Born equation⁴¹ provides a method of evaluating the ideal Gibbs free energy of a single ion as the difference between the free energy of the ion in a structureless dielectric and the free energy of the ion in vacuo. At low electrolyte concentrations, the Debye-Hückel⁴² treatment is effective in determining the mean activity coefficients for ionic solutes in solution. Despite their fundamental error in treating the solvent too simply; both the Born⁴³ and Debye-Hückel⁴⁴ type treatments can be useful in elucidating solvation problems. More sophisticated treatments have now been developed,⁴⁵ amongst the most successful has been that of Friedman.⁴⁶⁻⁴⁸ Friedman⁴⁶ begins with an expression for the ion-ion pair potential and transforms this via a statistical mechanical treatment known as the hypernetted chain to produce a correlation function. The correlation function, which is related⁴⁷ to the probability that two particles are a distance r apart, is further treated to give thermodynamic functions. The ion-ion pair potential⁴⁸ is made up of several terms which allows for specific solvation effects to be treated. The potential⁴⁸ comprises of a coulombic attraction term, a repulsion term, a term to describe repulsive cavity effects and the Gurney term, which characterises specific solvation effects.

The precise nature of the solvation shells around an ion is the subject of some controversy. Frank^{21,49} has proposed a model, with the ion surrounded by a tightly bound solvent cosphere; an intermediate region of disordered water molecules lies between the strongly coordinated water and the bulk water (see figure 1.4). This model was

invoked to explain a decrease in viscosity when certain electrolytes are added to water; together with a lower entropy of evaporation than expected. Samoilov⁵⁰ was able to account for the viscosity of aqueous electrolyte solutions, by comparing the lifetime τ_1 of association of two water molecules with the time τ_2 a water molecule spends co-ordinated to an ion. For aqueous solutions exhibiting increased viscosity, e.g. LiF, $\tau_2 > \tau_1$ and for those showing a fall in viscosity, e.g. CsI, $\tau_1 > \tau_2$. Eley⁵¹ offers several objections to Frank's model. Friedman⁴⁵ uses a model which invokes a single solvation shell, covering the region of the solvent that is markedly effected by the presence of the ion. The behaviour observed, when two solute particles come close enough together for their solvation cospheres to overlap is shown in fig. 1.5. In such a process, the Helmholtz free energy change associated with the displacement of some cosphere material to the bulk solvent is related to the Gurney term⁴⁸ in the ion-ion potential.

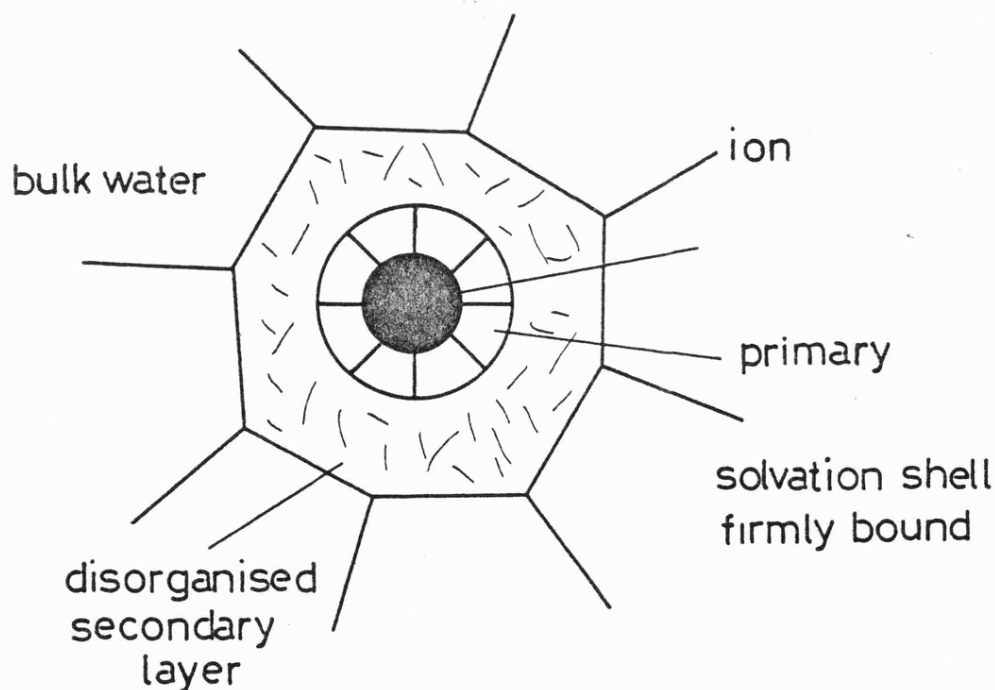


Figure 1.4 Frank's model for a hydrated ion.

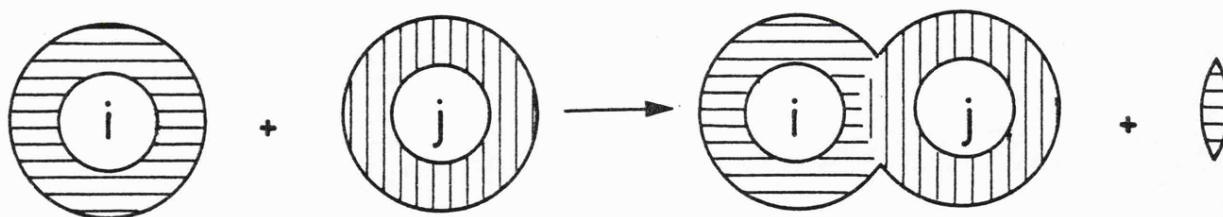


Figure 1.5 Illustration of the effect of cosphere overlap, when the interionic distance gets small. The solvent displaced by overlap relaxes back into the bulk solvent (from ref. 48).

Bulky ions like the tetraalkyl ammonium ions do not exhibit the simple behaviour outlined above. They show³⁵ a large positive partial molar heat capacity and large excess entropy of mixing terms. For the larger ions the entropy changes on mixing with water, shown an increase in solvent ordering. There is a negative concentration dependence of the partial molar volume for the larger tetraalkyl ammonium ions, giving a minimum value at the clathrate composition. Thus bulky ions with alkyl residues in aqueous solution are thought to resemble the other hydrophobic structure formers discussed earlier. If hydroxyl groups are substituted onto the terminal atoms of the alkyl chains of tetraalkyl ammonium ions, a return to normal electrolyte behaviour is observed. Molecules with a polar head group and a single long-chain alkyl residue are of interest. These compounds may be ionic e.g. sodium dodecyl sulphate. In aqueous solutions at low concentrations they tend to be monomeric, but beyond a limiting concentration a clustering process occurs and the solute molecules form aggregates known as micelles. The hydrocarbon chains form the core of the micelle, thus

minimising the unfavourable exposure of hydrocarbon chains to water. The main contribution to the thermodynamics of this aggregation process is the increase in entropy obtained on formation of the miscelle.

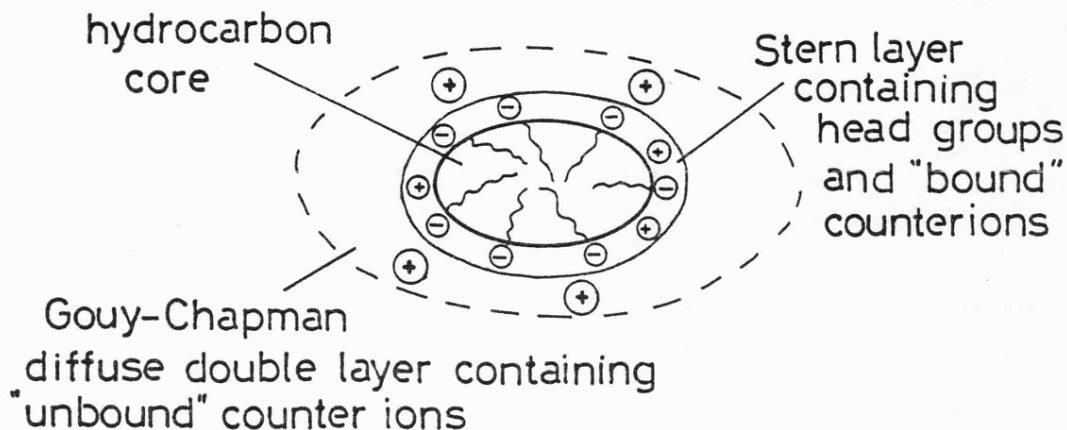


Figure 1.6 Elliptical cross-section of an idealised anionic detergent miscelle (from ref. 52).

1.6 Recent work at Leicester

The discussion here will centre on recent studies of solvation undertaken by Professor Symons' group at Leicester. The emphasis will be placed on spectroscopic studies, which are expected to yield much information on the nature of solvation effects. Symons and Blandamer⁵³ have shown how a wide variety of spectroscopic techniques can be used to investigate the water-tertiary butanol system.

Symons^{54,55} has recently outlined his interpretation of the water structure problem. The structure of liquid water^{54,55} is extrapolated from the known properties of monomeric water and the smaller water polymers. Emphasis is laid on the diacidic and dibasic nature of water; noting that when one of the acidic functions is engaged in hydrogen bonding, the hydrogen bonding capacity of the second acidic function

is reduced, whilst that of the basic functions is increased. Similarly, hydrogen bonding to one of the lone pairs, decreases the basicity of the second lone pair, and enhances the acidity of the protons. Thus the formation of hydrogen bonds is seen as a co-operative process. The formation of cyclic hydrogen bonded structures is looked upon favourably, five and six membered rings being a preferred form. Thus a random three dimensionally hydrogen bonded network is envisaged. The continual making and breaking of hydrogen bonds causes the liquid to be mobile. The random nature of the network, yielding extensive mismatching, will result in there being several lone-pair and hydroxyl groups unable to participate in hydrogen bonding. Between the limits of the free OH groups described above and a completely linear hydrogen bond, lies a continuous distribution of bent or stretched hydrogen bonds. It is suggested,⁵⁵ that clathrate type structures^{20,34,35,40,53} are important in aqueous solutions of non-electrolytes and the Frank^{17,49} model for ionic solvation is rejected.

N.m.r., together with infra-red and Raman data has been used to examine solvation effects in aqueous solutions by direct observation of the water features of the spectrum. Methanolic solutions containing highly charged cations, show a separate hydroxyl resonance due to solvent molecules bound to the cation, in their n.m.r. spectra at low temperatures. This feature has been used by Symons et alia^{56,57} to determine the separate anion and cation contributions to the change in chemical shift of the (OH) resonance on addition of electrolytes to methanol. Secondary solvation⁵⁸ effects have been commented on. Separate cation and anion chemical shifts have also been reported⁵⁹ for aqueous solutions using both this separate solvation shell method and a discontinuity method. Ion-pairing of magnesium salts in methanol at low

temperatures has also been studied,⁶⁰ ion-pairing being manifested by a more rapid movement of the cation solvation shell towards higher field with increasing salt concentration. In pure water the effect of heating is to move the hydroxyl proton resonance to higher field. This is taken as a reduction of hydrogen bonding in the liquid. Davies et alia⁶¹ have measured the hydroxyl chemical shifts of aqueous solutions of tetraalkyl ammonium bromides over a wide temperature range. They were able to show, after subtraction of a positive shift from the bromide ion, that at low temperatures (273 K) water-water interactions are enhanced by the larger tetraalkyl ammonium ions. As the temperature is raised the shifts for the more bulky ions pass through zero and become more positive. This was interpreted in terms of enclathration of the cation at low temperatures. Anderson and Symons⁶² have examined the proton n.m.r. of aqueous t-butanol solutions, the hydroxyl protons move to a lower field, reaching a maximum when the molefraction of t-butanol is about 0.05 mf. These results are explained in terms of enhanced water-water interactions, due to enclathration at lower temperatures. Kingston and Symons have examined the hydroxyl n.m.r. resonances for a wide range of aqueous non-electrolyte solutions.⁶³ They were able to differentiate between the movement to lower field of the hydroxyl protons due to the formation of strong water-base bonds and that due to enhanced water-water interactions; by means of the concentration and temperature dependence of the shifts and the effect of a third component. They conclude that t-butanol strengthens water-water interactions in the low molefraction region and the behaviour of methanol is characterised by strong methanol-water interactions. Harvey et alia⁶⁴ have examined the proton n.m.r. of aqueous glucose solutions and conclude that all the glucose hydroxyl groups are involved in hydrogen bonding.

Infra-red and Raman spectroscopic studies⁶⁵ were carried out on aqueous and methanolic solutions of alkali metal perchlorates; together with infra-red measurements on tetraalkyl ammonium perchlorates in solutions of dichloromethane contaminated with 2% methanol. The peak obtained in the OH stretch region at 3550 cm^{-1} was assigned to a hydroxyl group weakly bound to a perchlorate ion. Symons and Waddington⁶⁶ using this interpretation were able to assign shifts in the residual OH stretching band of the i.r. or Raman spectra to the effect of the cation. The results obtained were similar to the corresponding n.m.r. data.^{56,57,59} The shifts for methanolic solutions were found to be larger than the corresponding water cation shifts. This was attributed to the aqueous solvate having twice as many OH oscillators as the methanolic cation solvate. A solvation number of four for the perchlorate ion was calculated from infra-red and Raman data.⁶⁷ Low temperature⁶⁸ infra-red studies of aqueous and methanolic glasses of salt solutions show narrower bands, the band designated as a hydroxyl group bound to perchlorate moving to lower frequency as the glasses are cooled. The results for aqueous solution demonstrated the presence of unbound OH oscillators as well as OH bound to perchlorate (and of course hydrogen bonded OH). The unbound OH oscillators were thought to be generated by hydration of the cation via the water lone-pairs. Methanol exhibited a pronounced lack of unbound hydroxyl groups. On the basis of their near infra-red results Jackson and Symons⁶⁹ were able to point out the dangers of inferring structure-making and structure-breaking effects from the changes in the spectral feature attributed to un-hydrogen bonded hydroxyl groups. Further low temperature infra-red and room temperature first overtone results⁷⁰ were discussed in terms of secondary solvation to the discredit of the Frank^{21,49} model.

The use of an extra component (with solvent sensitive properties) in small concentrations as a probe for the solvent environment, can be very rewarding. Ultra violet spectroscopic studies using iodide ions or dye molecules as probes have been reviewed.⁵³ Anderson and Symons⁷¹ showed by examination of solvent induced changes in its n.m.r. spectrum, that 1,4-diethyl pyridinium iodide was a useful solution probe. The n.m.r. spectra⁶² of 1,4-diethyl pyridinium iodide in water-t-butanol solutions were insensitive to the presence of added t-butanol up to a molefraction of 0.05, after this initial insensitivity rapid changes occurred, which can be linked with the onset of solvation by t-butanol. Anderson and Symons⁶² also used the ^{19}F resonance of 0.01 molefraction potassium fluoride to probe the solvent environment in t-butanol water mixtures. A rapid change in ^{19}F chemical shift with added t-butanol in the molefraction range 0-0.05 was equivalent to a strong cooling. This rapid change had levelled off by the time the molefraction of t-butanol had reached 0.15 molefraction. The results using both probes were interpreted in terms of a clathrate model for aqueous-t-butanol solutions.

Ultrasonics has proved a useful tool for studying water-alcohol mixtures. Aqueous t-butanol solutions^{53,72} show an initial region of insensitivity to sound, followed by an intense absorption which peaks at 0.1 molefraction of t-butanol. In the insensitive region the t-butanol molecules are thought to be solvated within clathrate type structures. Above 0.04 molefraction, there is insufficient water to maintain each t-butanol molecule in its own clathrate cage and cage sharing is thought to come into effect. Here the two t-butanol molecules sharing a cage are still hydrogen bonded to the cage wall; but interact through their alkyl groups. It is this dimeric unit, which is

said to cause the excess sound absorption. The propyl alcohols⁷³ are found to mimic this behaviour; however dihydric alcohols show a much slower increase in absorption.⁷⁴ The tetraalkyl ammonium ions show a similar behaviour;⁷⁵ but because this behaviour is mimiced in some pure non-aqueous solvents, the rôle of water structure cannot be invoked. This effect is thought⁷⁵ to be due to rotational isomerism of the alkyl groups; this effect having been seen for solutions of tetra ethyl methane in solutions of hydrocarbons.⁷⁶

So far the rôle of electron spin resonance in investigating the nature of solvation has not been mentioned. This will be described in the rest of this thesis.

REFERENCES TO CHAPTER ONE

1. W. J. Moore, "Physical Chemistry", Longmans Green & Co. Ltd., London, 1962, 4th. Edition.
2. F. Franks, Chemistry in Britain, 1976, 12, 278.
3. "Water - A Comprehensive Treatise Vols. 1-4", ed. F. Franks, Plenum Press, New York, 1973.
4. D. T. Hawkins, J. Soln. Chem., 1974, 4, 623.
5. D. Eisenberg and W. Kauzmann, "The Structure and Properties of Water", Oxford University Press, Oxford, 1969.
6. C. A. Coulson, "Valence", Oxford University Press, Oxford, 1961, 2nd. Edition, p.167.
7. R. F. W. Bader, J. Amer. Chem. Soc., 1964, 86, 5070.
8. D. Hankins, J. W. Moskowitz and F. H. Stillinger, J. Chem. Phys., 1970, 53, 4544.
9. M. Dixon, T. A. Claxton and J. A. S. Smith, J.C.S. Faraday II, 1972, 68, 2158.
10. C. A. Coulson, "Valence", Oxford University Press, Oxford, 1961, 2nd. Edition, p.344-356.
11. L. Pauling, "The Nature of the Chemical Bond", Cornell University Press, Ithaca, New York, 1960, 3rd. Edition, p.449-469.
12. J. Emsley, O. P. A. Hoyte and R. E. Overill, J.C.S. Chem. Comm., 1977, 225.
13. J. D. Bernal and R. H. Fowler, J. Chem. Phys., 1933, 1, 515.
14. J. A. Pople, Proc. Roy. Soc., 1951, 205A, 163.
15. O. Ya. Samoilov, "The Structure of Aqueous Electrolyte Solutions and the Hydration of Ions", Trans. by D. J. G. Ives, Consultants Bureau, New York, 1965.
16. L. Pauling, "The Nature of the Chemical Bond", Cornell University Press, Ithaca, New York, 1960, 3rd. Edition, p.472.
17. H. S. Frank and A. S. Quist, J. Chem. Phys., 1961, 34, 604.
18. F. Franks in "Water - A Comprehensive Treatise Vol. 1", ed. F. Franks, Plenum Press, New York, 1973, p.10.
19. B. Kamb in "Water and Aqueous Solutions - Structure, Thermodynamics and Transport Processes", ed. R. A. Horne, Wiley-Interscience, 1972, p.10.

20. D. W. Davidson in "Water - A Comprehensive Treatise Vol. 2", ed. F. Franks, Plenum Press, New York, 1973, p.115-234.
21. H. S. Frank and W. Y. Wen, Disc. Faraday Soc., 1957, 24, 133.
22. J. D. Bernal, Proc. Roy. Soc., 1964, 280A, 299.
23. M. D. Danford and H. A. Levy, J. Amer. Chem. Soc., 1962, 84, 3965.
24. H. S. Frank in "Water - A Comprehensive Treatise Vol. 1", ed. F. Franks, Plenum Press, New York, 1973, p.515-543.
25. G. S. Kell in "Water and Aqueous Solutions - Structure, Thermodynamics and Transport Processes", ed. R. A. Horne, Wiley-Interscience, New York, 1972, p.331-370.
26. C. M. Davis and J. Jarzynski in "Water and Aqueous Solutions - Structure, Thermodynamics and Transport Processes", ed. R. A. Horne, Wiley-Interscience, New York, 1972, p.371.
27. G. Nemethy and H. A. Scheraga, J. Chem. Phys., 1962, 36, 3382.
28. S. Levine and J. W. Perram in "Hydrogen Bonded Solvent Systems", eds. A. K. Covington and P. Jones, Taylor & Francis Ltd., London, 1968, p.115.
29. A. T. Hagler, H. A. Scheraga and G. Némethy, J. Phys. Chem., 1972, 76, 3229.
30. B. R. Lentz, A. T. Hagler and H. A. Scheraga, J. Phys. Chem., 1974, 78, 1531.
31. W. J. Moore "Physical Chemistry", Longmans Green & Co. Ltd., London, 1972, 5th. Edition, p.918.
32. J. A. Barker and R. O. Watts, Chem. Phys. Letters, 1969, 3, 144.
33. A. Rahman and F. H. Stillinger, J. Amer. Chem. Soc., 1973, 95, 7943.
34. F. Franks in "Hydrogen Bonded Solvent Systems", eds. A. K. Covington and P. Jones, Taylor & Francis Ltd., London, 1968, p.31.
35. F. Franks in "Water - A Comprehensive Treatise Vol. 2", ed. F. Franks, Plenum Press, New York, 1973, p.6-19.
36. H. S. Frank and F. Franks, J. Chem. Phys., 1968, 48, 4746.
37. V. A. Mikhailov, J. Struct. Chem., 1968, 9, 332.
38. V. A. Mikhailov and L. I. Ponomarov, J. Struct. Chem., 1968, 9, 8.
39. F. Franks and D. J. G. Ives, Quart. Revs., 1966, 20, 1.
40. D. N. Glew, H. D. Mak and N. S. Rath in "Hydrogen Bonded Solvent Systems", eds. A. K. Covington and P. Jones, Taylor & Francis Ltd., London, 1968, p.195.

41. M. Born, Z. Physik, 1920, 1, 45.
42. P. Debye and E. Hückel, Z. Physik, 1923, 24, 185.
43. See for example, F. M. Van Meter and H. M. Neumann, J. Amer. Chem. Soc., 1976, 98, 1382.
44. See for example, M. J. Blandamer and D. J. Reid, J. Colloid and Interface Science, 1974, 69, 150.
45. H. L. Friedman and C. V. Krishnan in "Water - A Comprehensive Treatise Vol. 3", Ed. F. Franks, Plenum Press, New York, 1973.
46. J. C. Rassiah and H. L. Friedman, J. Chem. Phys., 1968, 48, 2742.
47. J. C. Rassiah, J. Solution Chem., 1973, 2, 301.
48. P. S. Ramanathan and H. L. Friedman, J. Chem. Phys., 1971, 54, 1086.
49. H. S. Frank and M. W. Evans, J. Chem. Phys., 1945, 13, 507.
50. O. Ya Samoilov, Disc. Faraday Soc., 1957, 24, 141.
51. D. D. Eley, Disc. Faraday Soc., 1957, 24, 218.
52. L. R. Fisher and D. G. Oakenfield, Chem. Soc. Revs., 1977, 6, 25.
53. M. J. Blandamer and M. C. R. Symons in "Hydrogen Bonded Solvent Systems", eds. A. K. Covington and P. Jones, Taylor & Francis Ltd., London, 1968, p.211.
54. M. C. R. Symons, Nature, 1972, 239, 257.
55. M. C. R. Symons, Phil. Trans. Roy. Soc., 1975, B272, 13.
56. R. N. Butler and M. C. R. Symons, Trans. Faraday Soc., 1969, 65, 945.
57. R. N. Butler and M. C. R. Symons, Trans. Faraday Soc., 1969, 65, 2559.
58. M. C. R. Symons, Spectrochimica Acta, 1975, 31A, 1105.
59. J. Davies, S. Ormandroyd and M. C. R. Symons, Trans. Faraday Soc., 1971, 67, 3465.
60. R. N. Butler, J. Davies and M. C. R. Symons, Trans. Faraday Soc., 1970, 66, 2426.
61. J. Davies, S. Ormondroyd and M. C. R. Symons, J.C.S. Chem. Comm., 1971, 1204.
62. R. G. Anderson and M. C. R. Symons, Trans. Faraday Soc., 1969, 65, 2550.

63. B. Kingston and M. C. R. Symons, J.C.S. Faraday II, 1973, 69, 978.
64. J. M. Harvey, M. C. R. Symons and R. J. Naftalin, Nature, 1976, 261, 435.
65. D. M. Adams, M. J. Blandamer, M. C. R. Symons and D. Waddington, Trans. Faraday Soc., 1971, 67, 611.
66. M. C. R. Symons and D. Waddington, Chem. Phys. Letters, 1975, 32, 133.
67. M. C. R. Symons and D. Waddington, J.C.S. Faraday II, 1975, 71, 22.
68. I. M. Strauss and M. C. R. Symons, Chem. Phys. Letters, 1976, 39, 471.
69. S. E. Jackson and M. C. R. Symons, Chem. Phys. Letters, 1976, 37, 551.
70. S. E. Jackson, I. M. Strauss and M. C. R. Symons, J.C.S. Chem. Comm., 1977, 174.
71. R. G. Anderson and M. C. R. Symons, Trans. Faraday Soc., 1969, 65, 2537.
72. M. J. Blandamer, D. E. Clarke, N. J. Hidden and M. C. R. Symons, Trans. Faraday Soc., 1968, 64, 2691.
73. M. J. Blandamer, N. J. Hidden, M. C. R. Symons and N. C. Treloar, Trans. Faraday Soc., 1968, 64, 3242.
74. M. J. Blandamer, N. J. Hidden, M. C. R. Symons and N. C. Treloar, Trans. Faraday Soc., 1969, 65, 1805.
75. M. J. Blandamer, M. J. Foster, N. J. Hidden and M. C. R. Symons, Trans. Faraday Soc., 1968, 65, 3247.
76. M. J. Blandamer, M. J. Foster, N. J. Hidden and M. C. R. Symons, J. Phys. Chem., 1968, 72, 2268.

CHAPTER TWO

Review of the Principles of Electron Spin
Resonance Spectroscopy

CHAPTER TWO

2.1 Introduction

Electron spin resonance has proved a powerful technique in the investigation of many physical and chemical problems. Amongst the phenomena studied by e.s.r. are: the structure of organic and inorganic radicals, transition metal complexes, radiation damage and the properties of solvated electrons. The addition of a paramagnetic fragment to a biological molecule and subsequent study by e.s.r. can yield much useful information. This technique is known as spin labelling. Miscelles have been studied using long chain nitroxide radicals, here the nature of the miscelle itself¹⁻³ and the monomer-miscelle exchange rate^{4,5} can be examined. E.s.r. studies of solvation require the use of smaller probes, such as the transition metal ions or small inorganic or organic radicals. The paramagnetic molecule is introduced in small concentrations in order not to appreciably disturb the structure of the solvent system. Chlorine dioxide,⁶ the SO_2^- radical anion,⁶ nitrobenzene derivatives,⁷⁻¹⁰ the semiquinones^{7,11} and the vanadyl¹² ion have proved useful probes in e.s.r. solvation studies. More recently,^{9,13-15} the simple organic nitroxides have proved extremely useful in this type of study. In this thesis, it is hoped to examine solvation effects in aqueous and methanolic solutions by the use of nitroxide spin probes. In this chapter, those aspects of e.s.r. spectroscopy which are useful to the solvation chemist will be described. A comprehensive review of the principles and theory of e.s.r. will not be attempted here. However, it is hoped to usefully describe how the solvation effects predominant in aqueous and non-aqueous solutions of paramagnetic probes, can be determined from e.s.r. measurements.

2.2 The isotropic e.s.r. spectrum

Consider, a paramagnetic molecule with electronic spin S and nuclear spin I , under the influence of a strong magnetic field H . Assuming that the spins only interact with the magnetic field and not with each other, we can write the Hamiltonian of the system as:-

$$\mathcal{H} = \beta H \cdot g \cdot S - \beta_N H \cdot g_N \cdot I \quad (2.1)$$

where g and g_N are the electronic and nuclear g factors respectively, β is the Bohr magneton and β_N is the nuclear magneton. The two terms on the right hand side of equation 2.1 are known as the electronic and nuclear Zeeman interactions respectively. If we now allow the nuclear and electronic spins to interact with each other we can rewrite equation 2.1 in the high field limit as:-

$$\mathcal{H} = \beta H \cdot g \cdot S + I \cdot A \cdot S - \beta_N H \cdot g \cdot I \quad (2.2)$$

where A is the nuclear hyperfine splitting constant, and is the energy of interaction of the nuclear and electronic spins. When the magnetic field is large I and S are good quantum numbers and the hyperfine splitting constant tends to be independent of further increase in field size. For a dialkyl nitroxide at a microwave frequency of 9500 MHz, we can deduce that the nuclear Zeeman term is negligible (1M.Hz), when compared with the magnitudes of the electronic Zeeman (9500 M.Hz) and the nuclear hyperfine interaction (45 M.Hz). Thus, we will omit the nuclear Zeeman term from the rest of our discussion. Figure 2.1 shows the energy levels predicted by equation 2.2 for a single electron coupled to a nitrogen nucleus under the influence of a magnetic field H_0 .

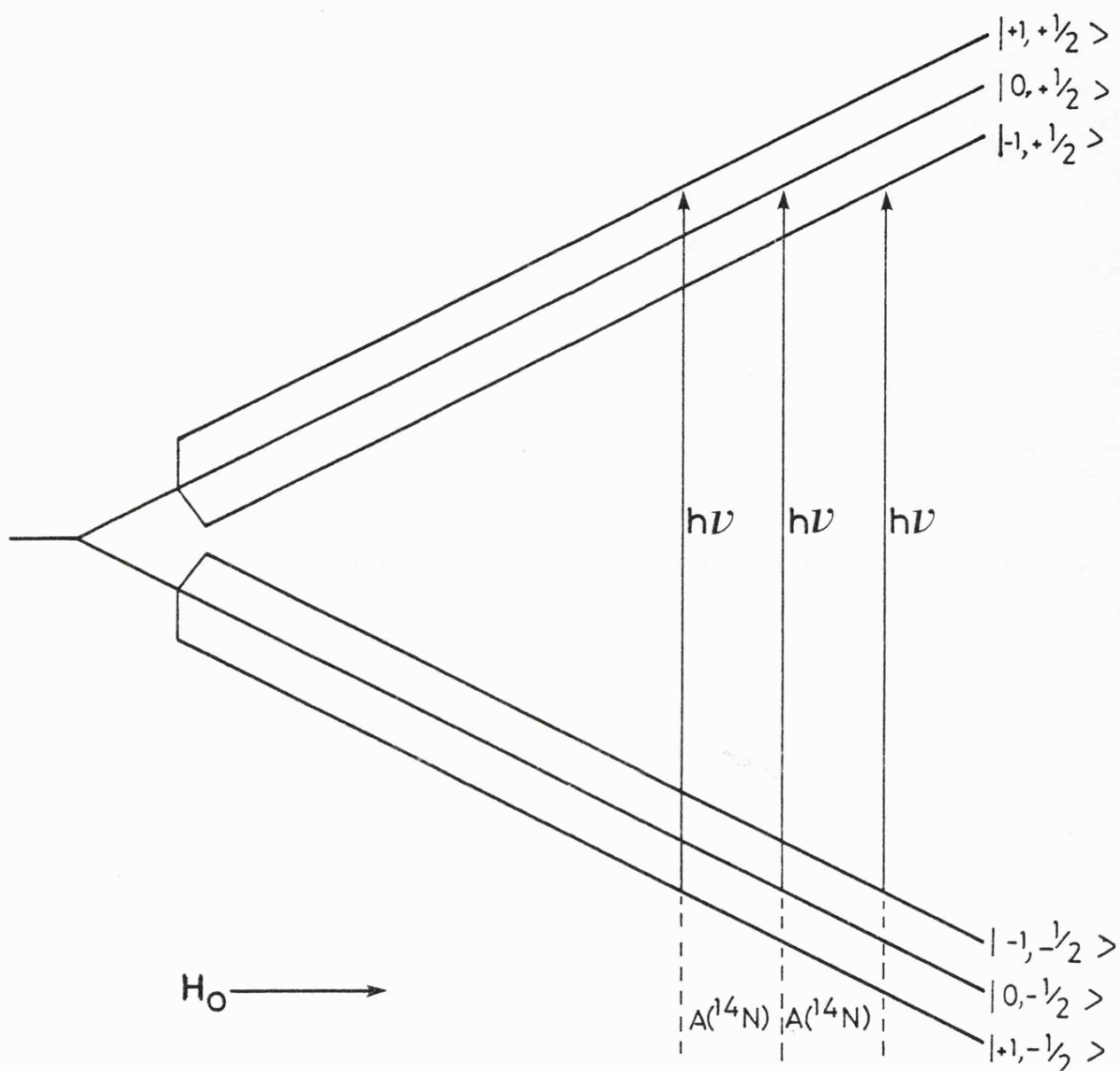


Figure 2.1

The energy levels of the unpaired electron of a dialkyl nitroxide as a function of applied magnetic field H_0 . The functions $|m_S, m_I\rangle$ are the spin wavefunctions of the unpaired electron S and the nucleus I . The energy levels given by equation 2.2 are:

$$E_{+1, +\frac{1}{2}} = \frac{1}{2}g\beta H_0 + a/2; \quad E_{0, +\frac{1}{2}} = \frac{1}{2}g\beta H_0; \quad E_{-1, +\frac{1}{2}} = \frac{1}{2}g\beta H_0 - a/2.$$

$$E_{+1, -\frac{1}{2}} = -\frac{1}{2}g\beta H_0 - a/2; \quad E_{0, -\frac{1}{2}} = -\frac{1}{2}g\beta H_0; \quad E_{-1, -\frac{1}{2}} = -\frac{1}{2}g\beta H_0 + a/2.$$

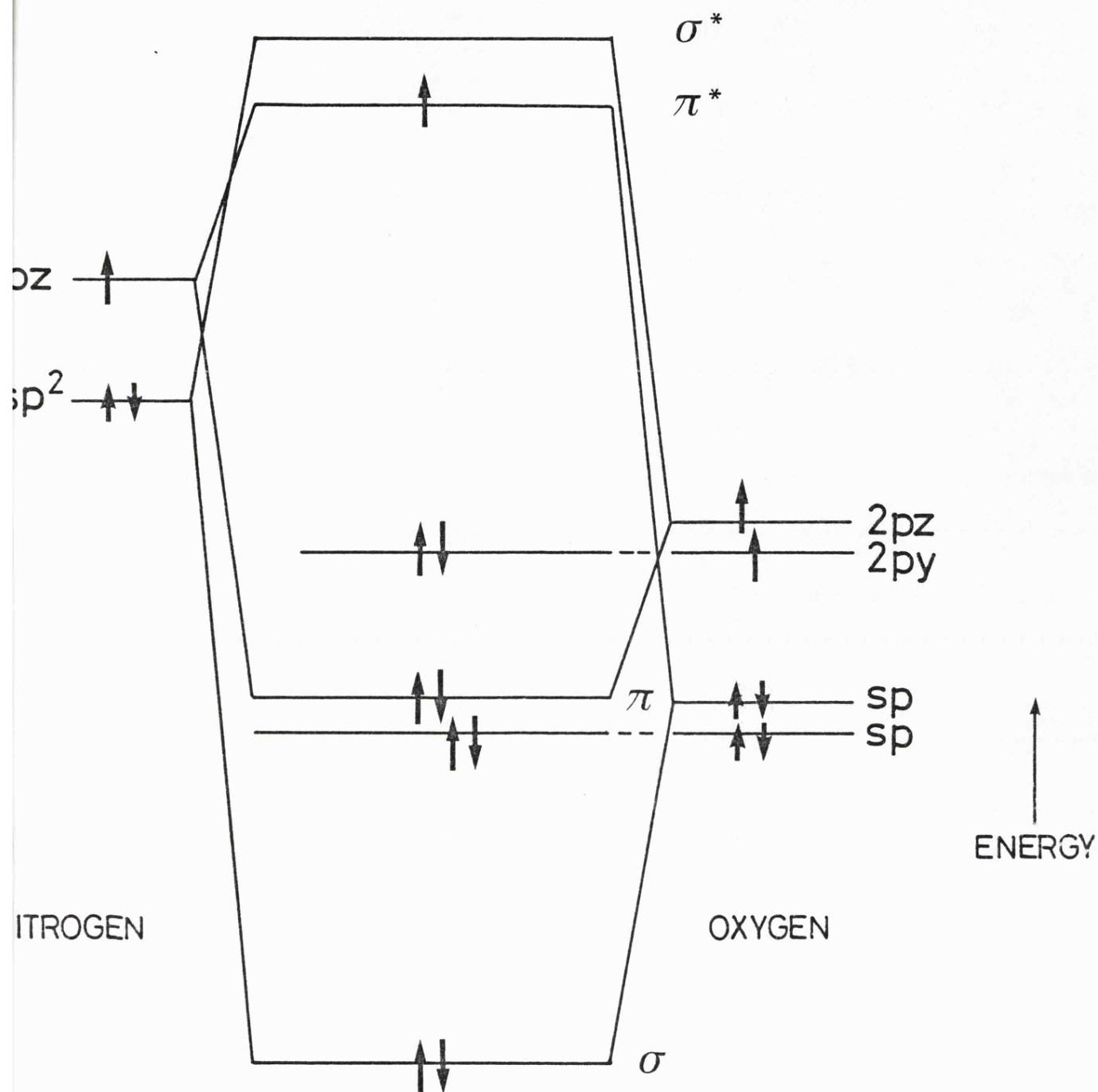


Figure 2.2

Molecular orbital correlation diagram for the N-O fragment of a dialkyl nitroxide. The non-bonding orbitals are essentially a p_y and an sp orbital on oxygen.

If, we examine the molecular orbital diagram in figure 2.2, we can begin to understand the effect of solvation on the Zeeman and hyperfine interaction energies of a dialkyl nitroxide. For a non-hydrogen bonded nitroxide radical, approximately sixty percent of the electron spin is to be found on nitrogen. The unpaired electron is to be found in the lowest energy π^* orbital of the N-O bond. Hydrogen bonding to the non-bonding electrons of oxygen will draw bonding electron density in the N-O group towards the oxygen atom. There will be a compensating drift of antibonding electron density towards nitrogen. This will cause an increase in the nitrogen hyperfine splitting constant $A(^{14}\text{N})$. The deviation from the free spin value of the g factor is determined by the orbital angular momentum of the unpaired electron. Now, electron spin density on oxygen has a greater capacity for orbital motion than that on nitrogen. Consequently, as we hydrogen bond we decrease the spin density on oxygen and hence reduce the deviation of g from free spin. For a dialkyl nitroxide in a non-interacting solvent¹⁶ g is of the order 2.0062 and the value for water is 2.00555.

Rassatt¹⁷ et alia have shown that $A(^{14}\text{N})$ for a dialkyl nitroxide increases linearly with solvent Z value. The Z value being defined by Kosower,¹⁸ as the transition energy (in kcal mol⁻¹) of the longest wavelength charge transfer absorption band of 1-ethyl-4-carbomethoxy-pyridinium iodide in the solvent of interest. Kawamura et alia¹⁶ have shown that for ditertiary butyl nitroxide (DTBN) in a wide variety of solvents, g is directly proportional to $A(^{14}\text{N})$. This investigation also showed that the $n \rightarrow \pi^*$ transition of the N-O chromophore of DTBN experiences a blue shift to higher energies in hydrogen bonded solvents. Knauer & Napier¹⁹ have examined the variation of $A(^{14}\text{N})$ as a function of solvent, using several semi-empirical solvation parameters. The varia-

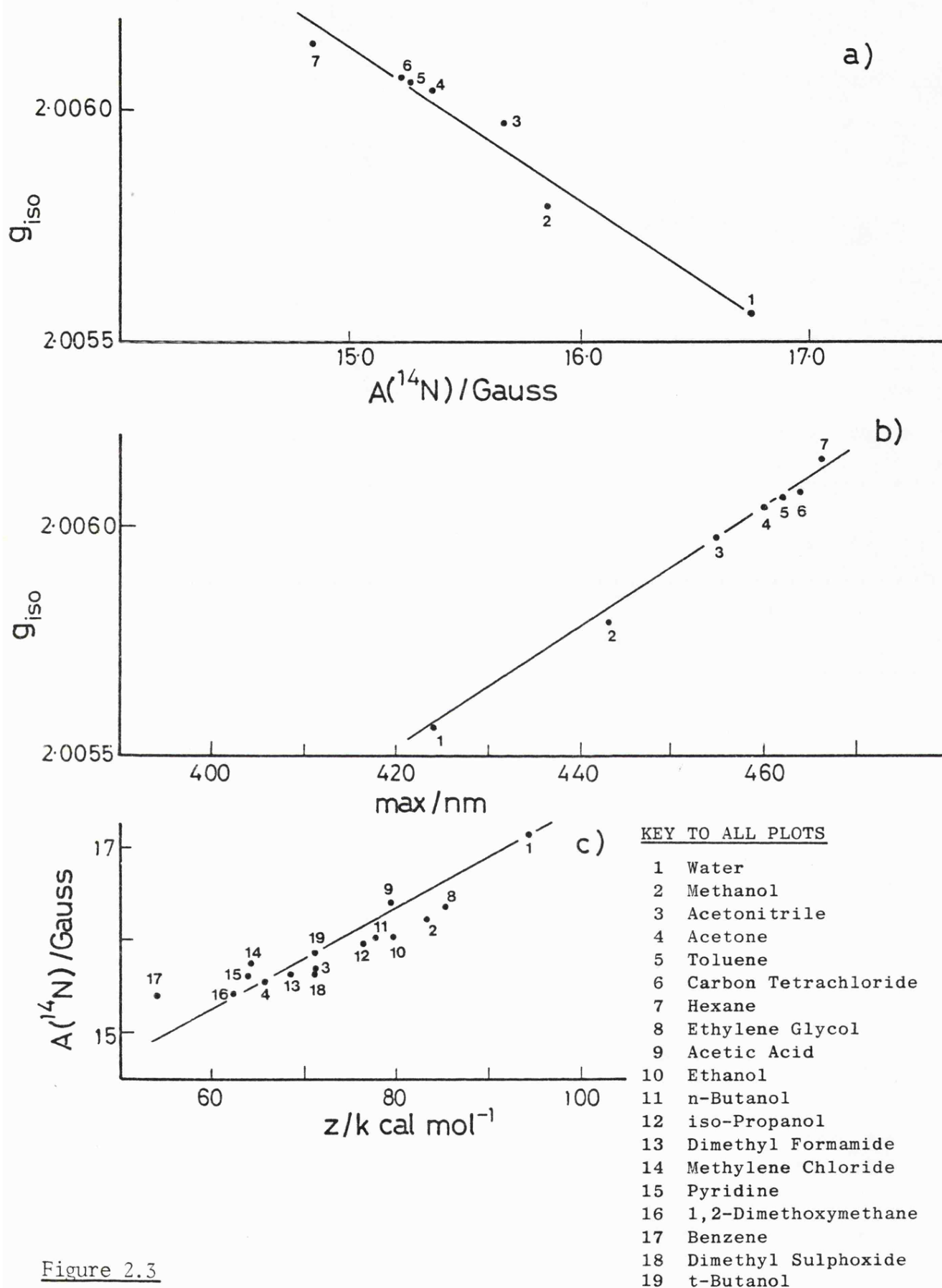


Figure 2.3

- a) Variation of isotropic g-value (g_{iso}) with nitrogen hyperfine splitting constant $A(^{14}N)$ for di-tertiary butyl nitroxide (DTBN) in various solvents. Data from ref. 16.
- b) Variation of g_{iso} with λ_{max} of the $n \rightarrow \pi^*$ transition for DTBN in various solvents. Data from ref. 16.
- c) Variation of $A(^{14}N)$ with Kosower's z-value for DTBN in various solvents. From ref. 19.

tion of g and $A(^{14}\text{N})$ for DTBN in several solvents is summarised in figure 2.3.

2.3 The anisotropic e.s.r. spectrum

The g and A factors are not as simple as the description in the previous section would imply. We need to consider the possibility of a dependence of the g and A factors on orientation to the magnetic field. Let us express the g and A factors as:

$$\begin{aligned} g(\theta) &= g_{\text{iso}} + g' f(\theta) \\ A(\theta) &= A_{\text{iso}} + A' f(\theta) \end{aligned} \quad (2.3)$$

where $g' f(\theta)$ carries the angular dependence of the g factor and $A' f(\theta)$ carries the angular dependence of the hyperfine splitting constant. If the molecule is tumbling rapidly in solution, $g' f(\theta)$ and $A' f(\theta)$ are averaged to zero and the isotropic spectrum characterised by g_{iso} and A_{iso} is seen.

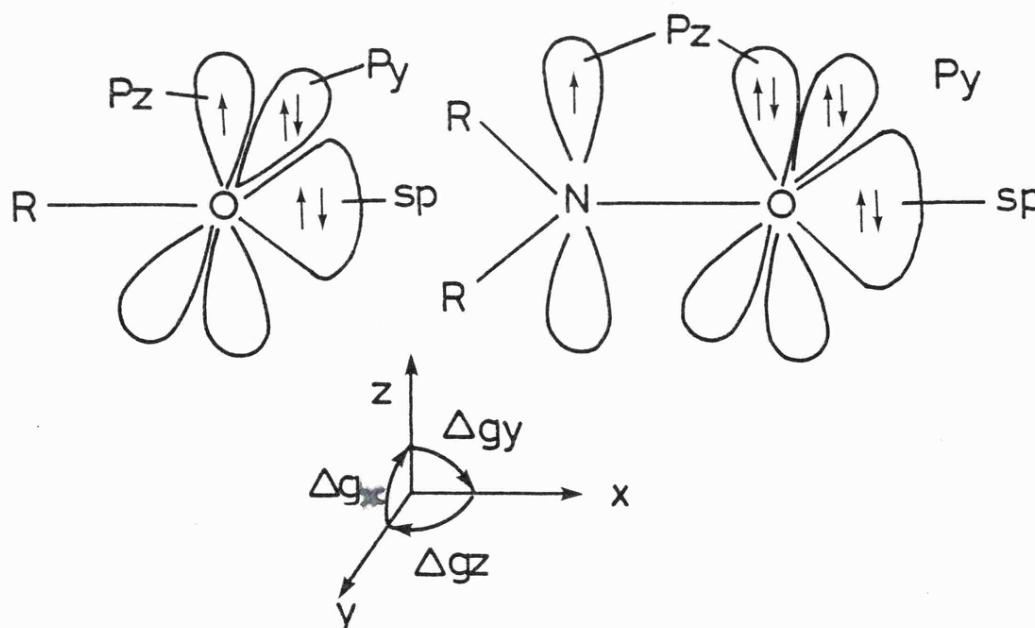


Fig. 2.4 A simplified picture of the p orbital configurations of an alkoxy radical and a nitroxide radical.

With the aid of the descriptions of Ayscough²⁰ and of Atkins and Symons,²¹ let us consider the form of the anisotropic part of g , $g'f(\theta)$. Consider the alkoxy radical shown in figure 2.4 and align the radical so that its R-O bond runs parallel to the applied magnetic field. The unpaired electron feels the sum of the effects of two magnetic fields. The first is due to the applied field, the second is due to the orbital motion of the degenerate p_z and p_y orbitals about the R-O axis. If the p_y orbital were empty and the unpaired electron were in the p_z orbital, then the magnetic field would tend to "drive" the orbital motion in such a way as to oppose the applied field. However, the p_y orbital of the alkoxy radical contains a lone-pair of electrons and so we must think of the applied field as "driving" the orbital motion of a positive hole. This will enhance the applied field, thus causing resonance at a fixed microwave frequency, to occur at lower field and the measured g value to be larger than the free spin value. Let us call $g(\theta)$ measured along the R-O bond g_x . If, we now rotate the molecule through 90° so that the field lies along the Z axis, we can see that the odd electron cannot achieve orbital motion about this axis. Rotating again through 90° so that the field lies along the p_y orbital, we can see that since the p_z and non-bonding sp orbitals are not degenerate orbital motion about the y axis is not easy. We can overcome this barrier to orbital motion through an electronic excitation from the sp bonding orbital to the p_z orbital. We will see a smaller shift in g from the free spin value. This shift is inversely proportional to the energy of the electronic sp (non-bonding) $\rightarrow p_z$ transition. Thus, the g shift is much less than along the y axis and we find that $g_x > g_y > g_z$.

In the case of the dialkyl nitroxide we have reduced the orbital

motion, since approximately 60 per cent of the spin is centred on the nitrogen nucleus, about which there is no orbital motion. A smaller g shift is possible from the 40 per cent of spin on oxygen. Thus, for the dialkyl nitroxide we would expect a smaller spread of g values closer to the free spin value. The p_y and p_z orbitals of the dialkyl nitroxide are no longer degenerate, because the p_z orbital is now involved in the N-O π system, this will reduce angular momentum about the x axis. Hence, g_x will be further reduced from the alkoxy radical case. We can expect some residual orbital angular momentum about the x axis, through the non-bonding $p_y \rightarrow \pi^*$ excitation and about the y axis through the non-bonding $sp \rightarrow \pi^*$ excitation. From figure 2.2 we expect the sp orbital to be lower in energy than the p_y orbital, and hence we may expect $g_x > g_y > g_z$.

Turning our attention to the hyperfine splitting we find that A_{iso} is a direct measure of spin density at the nucleus in question. A_{iso}^{21} can be evaluated from the product of the electron and nuclear magnetic moments and the spin density at the nucleus. Hence we have a direct measure of the s character of the unpaired electron. The anisotropic part of the A value therefore comes from electron density in orbitals having nodes at the nucleus, i.e. p , d and f orbitals. Consider our nitroxide in figure 2.4 with the odd electron nominally in a p_z orbital on nitrogen. If we let the p orbital be inclined at an angle θ to the magnetic field, as in figure 2.5, then the classical dipole-dipole energy of interaction between the electron and nucleus is given by:²¹

$$E \text{ dipole-dipole} = -g \beta g_N \beta_N \left\{ \frac{1 - 3 \cos^2 \theta}{r^3} \right\} \text{ I.S.} \quad (2.4)$$

where r is the distance between the two dipoles. Equation 2.4 will hold

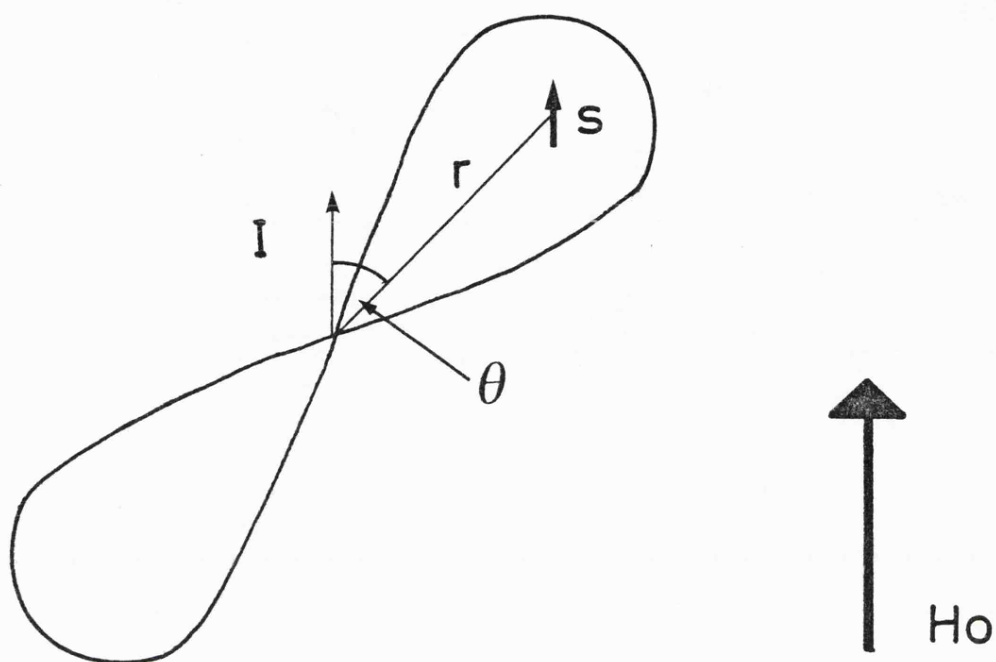


Figure 2.5

Diagram of the interaction of an electronic spin S and a nuclear spin I under the influence of a magnetic field H_0 .

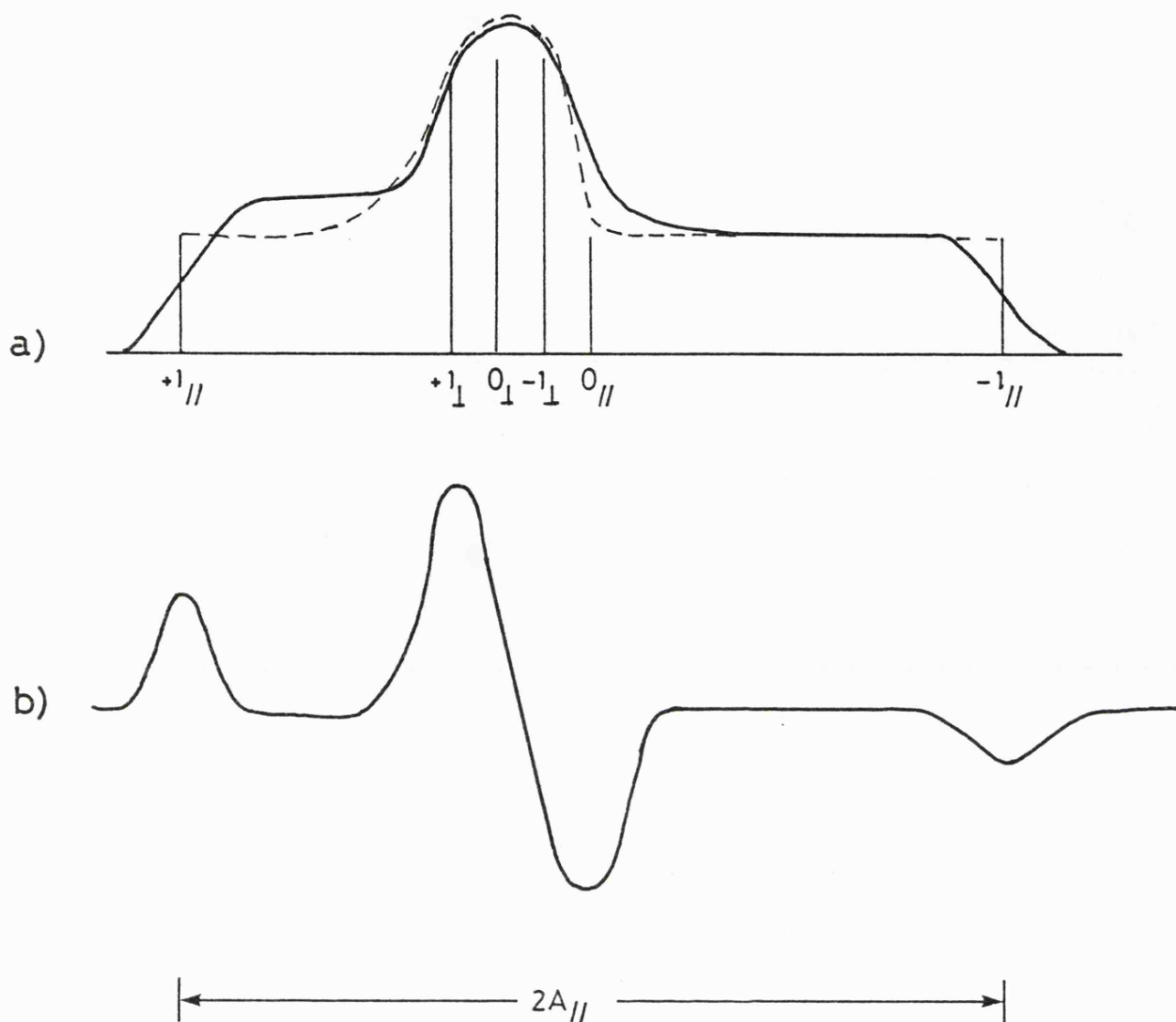


Figure 2.6

The idealised spectrum of dialkyl nitroxide radicals in a rigid matrix at X-band frequencies. Curve a shows the absorption, the dotted curve being due to the ideal absorption; the solid curve is due to each transition being broadened by various relaxation mechanisms thus giving a finite linewidth. Curve b is the first derivative of the solid curve a and is the normally recorded e.s.r. spectrum.

provided that the nuclear and electron spins are aligned with the static magnetic field. If we set $gg_N\beta_N/r^3$ equal to B we can see that:

$$\begin{aligned} A_{\parallel} &= A(0) = A_{\text{iso}} + 2B \\ A_{\perp} &= A(90) = A_{\text{iso}} - B \end{aligned} \quad (2.5)$$

An e.s.r. study of a free radical species diluted in a diamagnetic single crystal, will enable us to examine the effect of orientation on the e.s.r. spectrum. When the crystal is aligned so that the magnetic field is parallel to the orbital containing the unpaired electron, a spectrum centred on g_z with $2I+1$ lines separated by a distance of $A(0)$ gauss is seen. As we rotate the crystal through an orientation of θ to the applied field, we see $2I+1$ lines whose positions are determined by equation 2.3. If we are unable to restrict the orientation of the radical within a single crystal host, then the powder or glass spectrum of figure 2.6 is seen. A broad absorption caused by sampling many spins over all orientations in a randomly orientated glass is seen. The first derivative of this absorption is the e.s.r. powder spectrum normally recorded.

So far we have been restricted to a simple description of the nuclear and electron spins as point dipoles. The spins may be more completely described as vector quantities.

$$\begin{aligned} \mathbf{S} &= S_x + S_y + S_z \\ \mathbf{I} &= I_x + I_y + I_z \end{aligned} \quad (2.6)$$

the Z axis of quantisation being largely determined by the direction of the applied field. I and S are said to be defined by a laboratory frame co-ordinate system. There are nine possible combinations of I and S , hence we need nine measures of the coupling between each component, from

$I_x A_{xx} S_x$ and $I_x A_{xy} S_y$ through to $I_z A_{zz} S_z$. We can represent I and S as a row and column vector respectively, consequently we can represent A as a 3×3 matrix or second rank tensor. The principal axes of the A tensor are defined within the molecular framework and are independent of the laboratory frame. We can characterise the laboratory frame by an orthogonal axis set x, y and z ; and the molecular framework by the orthogonal axis system, α, β, γ . We note that the product $I.A.S.$ is a scalar product and that the scalar product of two vectors is given by

$$X \cdot Y = |X| |Y| \cos \theta \quad (2.7)$$

where θ is the angle between X and Y and $\cos \theta$ is known as the direction cosine. Since, the principal axes of the A tensor and the spins are independent of each other, we now need to introduce two sets of direction cosines of the type $l_{z\alpha}$. The hyperfine Hamiltonian becomes

$$\mathcal{H} = [I_z, I_y, I_x] \left\{ \begin{matrix} l_{z\alpha} & l_{z\beta} & l_{z\gamma} \\ l_{y\alpha} & l_{y\beta} & l_{y\gamma} \\ l_{x\alpha} & l_{x\beta} & l_{x\gamma} \end{matrix} \right\} \left\{ \begin{matrix} A_{\alpha\alpha} & A_{\alpha\beta} & A_{\alpha\gamma} \\ A_{\beta\alpha} & A_{\beta\beta} & A_{\beta\gamma} \\ A_{\gamma\alpha} & A_{\gamma\beta} & A_{\gamma\gamma} \end{matrix} \right\} \left\{ \begin{matrix} l_{\alpha z} & l_{\alpha y} & l_{\alpha x} \\ l_{\beta z} & l_{\beta y} & l_{\beta x} \\ l_{\gamma z} & l_{\gamma y} & l_{\gamma x} \end{matrix} \right\} \left\{ \begin{matrix} S_z \\ S_y \\ S_x \end{matrix} \right\} \quad (2.8)$$

the corresponding Zeeman Hamiltonian becomes

$$\mathcal{H} = \beta [H_z, H_y, H_x] \left\{ \begin{matrix} l_{z\alpha} & l_{z\beta} & l_{z\gamma} \\ l_{y\alpha} & l_{y\beta} & l_{y\gamma} \\ l_{x\alpha} & l_{x\beta} & l_{x\gamma} \end{matrix} \right\} \left\{ \begin{matrix} g_{\alpha\alpha} & g_{\alpha\beta} & g_{\alpha\gamma} \\ g_{\beta\alpha} & g_{\beta\beta} & g_{\beta\gamma} \\ g_{\gamma\alpha} & g_{\gamma\beta} & g_{\gamma\gamma} \end{matrix} \right\} \left\{ \begin{matrix} l_{\alpha z} & l_{\alpha y} & l_{\alpha x} \\ l_{\beta z} & l_{\beta y} & l_{\beta x} \\ l_{\gamma z} & l_{\gamma y} & l_{\gamma x} \end{matrix} \right\} \left\{ \begin{matrix} S_z \\ S_y \\ S_x \end{matrix} \right\} \quad (2.9)$$

For an axial diagonal g and A tensor, with the molecular α axis aligned along the laboratory Z axis; the Hamiltonian expressed by Ayscough²⁰ becomes

$$\mathcal{H} = g_{\parallel} \beta H_z S_z + g_{\perp} \beta (H_x S_x + H_y S_y) + A_{\parallel} I_z S_z + A_{\perp} (I_x S_x + I_y S_y) \quad (2.10)$$

The necessity, for our more rigorous treatment of the spin Hamiltonian can be appreciated from the section on rotational correlation times later in this chapter.

2.4 Relaxation Effects

The solid state spectra described are not composed merely of an envelope of orientation dependent, sharp, infinitely narrow transitions. Each transition will be broadened by relaxation processes. In general, there are two relaxation processes broadening the spectra. The first of these is known as spin-lattice relaxation. Here the population of the higher spin energy levels is reduced by transfer of the excess magnetic energy to the normal vibrational modes of the host lattice. This process is characterised by a single relaxation time T_1 ; the spin-lattice or longitudinal relaxation time. T_1 is defined as the time taken for the spin system to loose $1/e$ th of its excess magnetic energy. If T_1 is long and the microwave power high, saturation may result. A short T_1 will blur the magnetic energy levels by the Heisenberg uncertainty principle and a "life-time" broadening of the lines will occur.

The second relaxation process is the spin-spin or dipolar relaxation. This process occurs, because each unpaired electron experiences a magnetic field comprising of the applied field modified by a small perturbation due to neighbouring magnetic dipoles. Thus, a variety of magnetic environments exist within the lattice and a spread of transition frequencies is seen. The unpaired electron, because of the magnitude of

its magnetic moment, will give the main contribution to spin-spin broadening. Dipolar broadening will fall off as the cube of the separation of the radicals increases. Spin-spin broadening may be reduced by using a diamagnetic medium to dilute the radicals. Spin-spin broadening is characterised by a single relaxation time T_2 , the spin-spin or transverse relaxation time.

We would expect to broaden the features of an e.s.r. spectrum as we increase the radical concentration. This is seen, until the radical concentration is high enough to make orbital overlap between nearest neighbour radicals possible. When overlap between the singly occupied orbitals on neighbouring radicals occurs, then anti-parallel spins on neighbouring radicals tend to be simultaneously reversed. This corresponds to a rapid migration of spins through the system, averaging the dipolar interaction to zero. Thus, the spectral features begin to narrow. This process is known as exchange narrowing.

2.5 The effect of rotational motion on linewidths

Here, only dilute solutions of a radical will be considered, thus reducing the importance of spin-spin broadening. The theory of linewidths of radicals in solution was developed from the n.m.r. theory of Bloembergen et alia.²² Bloembergen showed that the n.m.r. linewidths of a rapidly tumbling species were controlled by the rapid averaging of the dipole-dipole interactions between neighbouring nuclear spins. McConnell²³ adapted these ideas to the investigation of e.s.r. linewidths. A more complete treatment of e.s.r. linewidths in solution was given by Kivelson,²⁴ who used the theory of Kubo and Tommita.²⁵ Carrington and Longuet-Higgins²⁶ have extended these earlier approaches by considering the effects of non-coincidence of the axes of the g and

A tensors. Probably the most elegant treatment is that of Freed and Fraenkel,²⁷ who used the relaxation matrix approach. For the case of a single nucleus and an electron of spin $\frac{1}{2}$, good agreement between the final results of the last three methods is obtained.^{24,26,27}

We begin our treatment of the effect of molecular reorientation from the work of Carrington et alia^{26,28} and of Atherton.²⁹ Carrington and Longuet-Higgins²⁶ begin from the Hamiltonian

$$\mathcal{H} = \beta \sum_{\alpha} H_{\alpha} g_{\alpha\beta} S_{\beta} + \sum_{\alpha} I_{\alpha} A_{\alpha\beta} S_{\beta} \quad (2.11)$$

where the α 's and β 's take the value x through to z. The tensor convention of automatically summing over every Greek subscript which occurs twice in every term or product of terms, is adopted. Equation 2.11 is identical to the expansion of equations 2.8 and 2.9, ignoring the existence of the direction cosine terms. The Hamiltonian can be split into two distinct parts, the isotropic component \mathcal{H}_0 and the anisotropic component $\mathcal{H}(t)$. \mathcal{H}_0 is invariant under conditions of molecular re-orientation and gives rise to the isotropic spectrum. It is the incomplete averaging of $\mathcal{H}(t)$ to zero, which gives rise to the line-widths of each spectral feature. We thus re-arrange equation 2.11 as

$$\mathcal{H} = \mathcal{H}_0 + \mathcal{H}(t) \quad (2.12)$$

where

$$\mathcal{H}_0 = \beta \sum_{\alpha} g_{\alpha} H_{\alpha} S_{\alpha} + \sum_{\alpha} I_{\alpha} A_{\alpha\alpha} S_{\alpha} \quad (2.13)$$

$$\mathcal{H}(t) = \beta \sum_{\alpha} H_{\alpha} g_{\alpha\beta}' S_{\beta} + \sum_{\alpha} I_{\alpha} A_{\alpha\beta}' S_{\beta}$$

and

$$g = \frac{1}{3} \sum_{\alpha} g_{\alpha\alpha} \quad A = \frac{1}{3} \sum_{\alpha} A_{\alpha\alpha} \quad (2.14)$$

$$g_{\alpha\beta}' = g_{\alpha\beta} - g\delta_{\alpha\beta} \quad A_{\alpha\beta}' = A_{\alpha\beta} - A\delta_{\alpha\beta} \quad (2.15)$$

The isotropic g and A tensors are given by equation 2.14 and the anisotropic tensors $g_{\alpha\beta}'$ and $A_{\alpha\beta}'$ are given by equation 2.15. If we consider

the H_{zz}' element of $H(t)$

$$H_{zz}'(t) = (\beta H_z g_{zz}' + I_z A_{zz}) S_z \quad (2.16)$$

It is now necessary to recognise the non-coincidence of the principal axes of the spin vectors and the g and A tensors; and to re-introduce the direction cosines. Thus equation 2.16 becomes

$$H_{zz}'(t) = (\beta H_z l_{z\alpha} g_{\alpha\beta}' + I_z l_{z\alpha} A_{\alpha\beta}) l_{\beta z} S_z \quad (2.17)$$

where the subscripts x , y and z represent the laboratory frame axes and α , β and γ represent the molecular co-ordinates. Using the perturbation treatments of Carrington and Longuet-Higgins the relaxation time T_2 becomes

$$\frac{1}{T_2'} = \frac{1}{2} \left[\overline{ \langle +\frac{1}{2}, m_I | H_{zz}(t) | +\frac{1}{2}, m_I \rangle } - \overline{ \langle -\frac{1}{2}, m_I | H_{zz}(t) | -\frac{1}{2}, m_I \rangle } \right]^2 j(0) \quad (2.18)$$

where $j(0)$ is known as the spectral density and is in general given by the real part of

$$j(\omega) = \int_{-\infty}^{+\infty} e^{i\omega\tau} e^{-|\tau|/\tau_c} d\tau = \frac{2 \tau_c}{1 + \omega_o^2 \tau_c^2} \quad (2.19)$$

where ω_o is the Larmor frequency of any spin transitions associated with the relaxation process. There are no spin transitions associated with equation 2.18 and $j(0)$ becomes $2\tau_c$. The rotational correlation time τ_c is a measure of the tumbling rate of the radical, and is characteristic of the averaging of the anisotropic g and A tensors. We can evaluate the expectation value of $H_{zz}'(t)$ in equation 2.18 by first evaluating the effect of the spin operators on the nuclear and electronic spins, and then averaging the direction cosines over all space. Finally,

evaluating the spectral density term we obtain

$$\frac{1}{T_2'} = \frac{2}{15} \frac{1}{\hbar^2} (\beta H_z g_{\alpha\beta'} + m_I A_{\alpha\beta}) (\beta H_z g_{\alpha\beta'} + m_I A_{\alpha\beta'}) \tau_c \quad (2.20)$$

which becomes

$$\frac{1}{T_2'} = \frac{4}{45} \Delta\gamma^2 H_z^2 + \frac{4}{15} \Delta\gamma b H_z m_I + \frac{1}{5} b^2 m_I^2 \quad (2.21)$$

in the notation of Kivelson.²⁴ Equation 2.21 is said to be the secular contribution to the linewidth. Here $\Delta\gamma$ and b are given by

$$\begin{aligned} \Delta\gamma &= [g_{zz} - \frac{1}{2}(g_{xx} + g_{yy})] \frac{\beta}{\hbar} \\ b &= \frac{2}{3} [A_{zz} - \frac{1}{2}(A_{xx} + A_{yy})] \end{aligned} \quad (2.22)$$

where the A values are measured in units of angular frequency.

Atherton²⁹ obtains the same result using a simplified form of the relaxation matrix treatment of Freed and Fraenkel.²⁷

It is now necessary to treat the elements $\mathcal{H}_{zx'}(t)$ and $\mathcal{H}_{zy'}(t)$ which give rise to electronic spin transitions. The $\mathcal{H}_{xz'}(t)$ and $\mathcal{H}_{yz'}(t)$ elements, which give rise to nuclear spin flips and the $\mathcal{H}_{xy'}(t)$, $\mathcal{H}_{yx'}(t)$, $\mathcal{H}_{xx'}(t)$ and $\mathcal{H}_{yy'}(t)$ elements, which give rise to both nuclear and electronic spin transitions; must all be taken into account. Relaxation process accompanied by electronic transitions are known as non-secular and are characterised by a relaxation time T_1 . This process gives rise to a lifetime broadening. Those terms involving changes in nuclear spin only are known as the pseudosecular terms. The overall relaxation time is given by

$$\frac{1}{T_2} = \frac{1}{T_2'} + \frac{1}{2T_1} \quad (2.23)$$

| | | | |
|---|---------------------------------------|--|-----------------------------|
| Secular terms from $\mathcal{H}_{zz}'(t)$ | $\frac{4}{45} \Delta\gamma^2 H_z^2$ | $\frac{4}{15} \Delta\gamma b H_z m_I$ | $\frac{1}{5} b^2 m_I^2$ |
| Non-secular terms from $\mathcal{H}_{zx}'(t)$ and $\mathcal{H}_{zy}'(t)$ | $\frac{1}{15} \Delta\gamma^2 H_z^2 u$ | $\frac{1}{5} \Delta\gamma b H_z m_I u$ | $\frac{3}{20} b^2 m_I^2 u$ |
| Non-secular terms from $\mathcal{H}_{xy}'(t)$, $\mathcal{H}_{xx}'(t)$, $\mathcal{H}_{yx}'(t)$ and $\mathcal{H}_{yy}'(t)$ | $\frac{7}{40} b^2 I(I+1)u$ | | $-\frac{7}{40} b^2 m_I^2 u$ |
| Pseudosecular terms from $\mathcal{H}_{xz}'(t)$ and $\mathcal{H}_{yz}'(t)$ | $\frac{3}{40} b^2 I(I+1)$ | | $-\frac{3}{40} b^2 m_I^2$ |

TABLE 2.1

Contributions to the linewidth under conditions of rapid re-orientation.

The pseudosecular terms are given by expressions of the type

$$\frac{1}{2T_2'} = \left[\overline{\langle +\frac{1}{2}, m_I | H_{x'z'}(t) | +\frac{1}{2}, m_I \pm 1 \rangle} \right]^2 j(W_n) \quad (2.24)$$

and the non-secular terms by

$$\frac{1}{2T_1} = \left[\langle +\frac{1}{2}, m_I | H_{zx'}(t) | -\frac{1}{2}, m_I \rangle \right]^2 j(W_o) \quad (2.25)$$

where $j(W_n) = 2\tau_c(1 + W_n^2\tau_c^2)^{-1} \approx 2\tau_c$ and $j(W_o) = 2\tau_c(1 + W_o^2\tau_c^2)^{-1}$; W_o and W_n are the nuclear and electronic Larmor frequencies. The complete evaluation of equation 2.23 in terms of secular, nonsecular and pseudosecular terms is given in table 2.1. The relaxation time T_2 is related to the peak to peak linewidth ΔH_{pp} by the expression

$$\frac{1}{T_2} = \sqrt{3} \frac{\pi g \beta}{h} \Delta H_{pp} \quad (2.26)$$

for a Lorentzian line. We can reduce the linewidth expression to the cubic form

$$\frac{1}{T_2} = \alpha + \beta m_I + \gamma m_I^2 \quad (2.27)$$

where α is relaxation due to averaging the anisotropic g tensor, γ is relaxation due to averaging of the anisotropic A tensor and β is the cross term. Where

$$\alpha = \left[\frac{\Delta\gamma^2 H_z^2}{45} (4 + 3u) + \frac{I(I+1) b^2 (3 + 7u)}{40} \right] \tau_c$$

$$\beta = \frac{\Delta\gamma b B_o}{15} (4 + 3u) \tau_c \quad (2.28)$$

$$\gamma = \frac{b^2}{40} (5-u) \tau_c$$

and

$$u = \frac{1}{1 - W_0^2 \tau_c^2} \quad (2.29)$$

The linewidth expressions above have been well tested by both Kivelson³⁰⁻³² and Freed;³³⁻³⁵ producing good agreement between theory and experiment. τ_c can be evaluated independently from the Debye equation

$$\tau_c = \frac{4 \pi r^3 \eta}{3 k T} \quad (2.30)$$

where r is the hydrodynamic radius of the probe, η is the bulk viscosity of the solvent, T is the temperature and k is Boltzmann's constant. This expression fits the data quite well; α , β and γ appear to vary linearly with η/T . It appears that r is solvent dependent and is smaller than the value calculated from molecular models. This "Debye radius" increases with solvent polarity, and is characteristic of specific solvent probe interactions. Freed has shown that small deviations from theoretical non-secular³⁴ and pseudosecular³⁵ spectral densities have a significant effect on the linewidths of nitroxides in solution.

Kivelson³⁰⁻³² has extended his theory to cover probes with large isotropic A values, and has incorporated second order effects. The linewidth expression now becomes a cubic expansion.

$$\frac{1}{T_2} = \alpha + \beta m_I + \gamma m_I^2 + \delta m_I^3 \quad (2.31)$$

where δ is very small. Freed³⁴ has used anisotropic rotation in his

treatment of the linewidths of Fremy's salt in glycerol-water mixtures.

The theory outlined above is only applicable in the limit $\mathcal{H}(t)\tau_c \ll 1$, which corresponds to $\tau_c < 2 \times 10^{-9}$ sec. If the molecule rotates at a rate of between 10^{-6} sec and 10^{-9} sec, we have to use the theory of slow tumbling to evaluate the linewidth. For the purpose of this thesis, linewidths will be measured only in the region of rapid molecular motion with $\tau_c < 10^{-10}$ secs. The theory of slow tumbling will not be dealt with in this thesis.

2.6 Spin Rotation

The m_I independent term in equation 2.27 cannot be fully accounted for by α of equation 2.28. The residual linewidth α'' , left after accounting for all broadening due to the incomplete averaging of the anisotropic g and A tensors, must be evaluated. The theory of spin rotation, developed for the e.s.r. case by Atkins and Kivelson³⁶ and Nyberg,³⁷ can account for α'' . A free radical undergoing rapid reorientation in solution will generate a magnetic moment, because the electrons do not follow precisely the motions of the nuclei and lag fractionally.²⁹ This magnetic moment can then couple to the electron spin, hence causing relaxation. We can represent the spin rotation interaction by the Hamiltonian.

$$\mathcal{H} = \mathbf{S} \cdot \mathbf{C} \cdot \mathbf{J} \quad (2.32)$$

where \mathbf{C} is the spin rotation coupling tensor and \mathbf{J} is the total rotational angular momentum. \mathbf{C} and \mathbf{J} are both time dependent and relaxation occurs as both the spin rotational coupling tensor and \mathbf{J} are averaged by molecular collisions. Fluctuations of \mathbf{C} and \mathbf{J} are characterised by the correlation times τ_c and τ_J respectively. Usually, $\tau_J \ll \tau_c$

and the important spin relaxation comes from the modulation of J.

Thus, we can evaluate the time dependent Hamiltonian as

$$H(t) = C \cdot S \cdot J(t) \quad (2.33)$$

Using the notation of Carrington,^{26,28} we obtain the following perturbation expressions for the relaxation times.

$$\frac{1}{T_2'} = \frac{C^2}{2} \left[\overline{\langle +\frac{1}{2} | S_z | +\frac{1}{2} \rangle} - \overline{\langle -\frac{1}{2} | S_z | -\frac{1}{2} \rangle} \right]^2 j(0) \quad (2.34)$$

$$\frac{1}{2T_1} = C^2 \left[\overline{\langle +\frac{1}{2} | S_x | -\frac{1}{2} \rangle \langle -\frac{1}{2} | S_x | +\frac{1}{2} \rangle} + \overline{\langle +\frac{1}{2} | S_y | -\frac{1}{2} \rangle \langle -\frac{1}{2} | S_y | +\frac{1}{2} \rangle} \right] j(\omega_0) \quad (2.35)$$

Hubbard³⁸ was able to show by comparison with the equation of motion for the linear velocity of a diffusing particle, that an expression for the angular velocity can be found. Atherton²⁹ shows how to evaluate the spectral densities of equations 2.34 and 2.35, using Hubbard's method and obtains the result.

$$j(\omega) = \int_{-\infty}^{+\infty} J_i(t) J_j(t+\tau) e^{i\omega_0 \tau} d\tau = 2\delta_{ij} \frac{kTI}{h^2} \frac{\tau_J}{1 + \omega_0^2 \tau_J^2} \quad (2.36)$$

and we find

$$\frac{1}{T_2} = \frac{kTI}{h^2} C^2 \left[\tau_J + \frac{\tau_J}{1 + \omega_0^2 \tau_J^2} \right] \quad (2.37)$$

Usually, $\omega_0^2 \tau_J^2$ is very small and the function in the brackets can be evaluated as $2\tau_J$. The Debye type expression for τ_J becomes

$$\tau_J = \frac{I}{8 \pi r^3 \eta} \quad (2.38)$$

We are not yet able to evaluate the spin rotational contribution to the linewidth, since we cannot measure C directly. By careful analysis of the total angular momentum of the molecule, it is possible to relate C to Δg , the deviation of the g value from the free spin value. Using this expression for C and equation 2.38 we can see that

$$\frac{1}{T_2} = \frac{kT}{4 \pi r^3} \frac{(\Delta g)^2}{\eta} \quad (2.39)$$

Equation 2.39 shows that, as the temperature of the bulk solvent increases and its viscosity falls, we can expect an increase in the spin rotational contribution to the linewidth. The treatment given above is not completely adequate, since we have assumed isotropic g and C tensors and an isotropic moment of inertia. Correcting for the case of anisotropic g and C tensors equation 2.39 becomes³⁶

$$\frac{1}{T_2} = \frac{1}{12 \pi r^3} [(g_{xx}-2.0023)^2 + (g_{yy}-2.0023)^2 + (g_{zz}-2.0023)^2] \frac{kT}{\eta} \quad (2.40)$$

Spin rotational broadening has been successfully used to account for the residual linewidth of e.s.r. probes in solution in many cases.^{15,16,31,32} However, the theory has proved inadequate³⁹⁻⁴¹ in the analysis of the linewidths of vanadyl β diketonate complexes in solutions at low values of T/η . The radical chlorine dioxide obeys the theory quite well in aqueous glycerol solutions. However, in a non-interacting paraffin solution, chlorine dioxide shows a very weak viscosity dependence. These observations were explained in terms of a break-down of the diffusional model.⁴² Despite the limitations of the theory, no widely accepted alternative has been successfully used to account for α'' . The theory has been well tested for the case of nitroxides in solution^{14,15,33-35} and has been found to be adequate.

Consequently, we will continue to accept spin rotation as the main contribution to α'' , throughout this thesis.

2.7 Chemical Exchange

Chemical exchange is a well known relaxation mechanism in n.m.r. studies. The situation as shown in figure 2.7 is applicable both to n.m.r. and e.s.r. studies. Consider a collection of spins, which can exist in two magnetically inequivalent environments 1 and 2. Each site will be characterised by a different Larmor frequency. If the spins jump from one environment to the other over a period of time, which is long compared to the reciprocal of the difference in their resonance frequencies, then two narrow peaks centred on the undisturbed frequencies w_1 and w_2 are seen. As the exchange rate approaches $1/(w_1 - w_2)$ the two lines broaden and move towards the weighted mean of w_1 and w_2 . Eventually, the peaks coalesce to a single flat-topped broad peak, which sharpens as the exchange rate increases further.

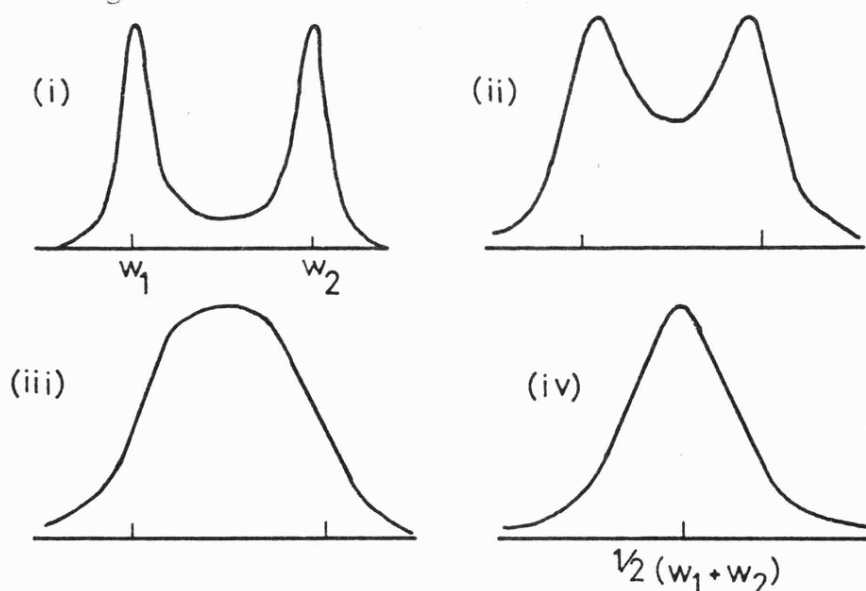


Fig. 2.7 Line shapes for the averaging of two magnetically inequivalent spins. The ratio of the exchange rate to the frequency separation of the peaks, takes the values $1/10$ (i); $1/5$ (ii); $1/\sqrt{8}$ (iii); and $1/2$ (iv). (From ref. 28)

Classically the change in linewidth associated with chemical exchange can be treated by the modified Bloch equations.^{7,28,29} These equations have been applied successfully many times to account for alternating linewidth effects in the dinitrobenzene type radicals⁷⁻⁹ and the semiquinones.⁷ Atherton and Strach¹³ have examined the e.s.r. spectrum of ditertiary butyl nitroxide (DTBN) in aqueous solutions of sodium dodecyl sulphate. They were able to evaluate an exchange frequency of about 4×10^5 radians sec^{-1} at 296 K for DTBN migrating between miscellar and bulk water environments. This corresponds to slow exchange, since the difference in Larmor frequencies of the two states is about 6×10^6 radians sec^{-1} . All the above effects are slower than might be expected for DTBN in water. Freed³⁵ has analysed the behaviour of perdeuterated 2,2,6,6-tetramethyl-4-piperidone-1-oxyl in d^6 ethanol glasses and solutions. He examines the case of rapid exchange between hydrogen bonded and non-hydrogen bonded forms of this radical. Freed concludes that this process is so fast that it does not appreciably contribute to the linewidths. N.m.r. determination of the lifetime of an alcohol-nitroxide hydrogen bonded complex³⁵ is about 4×10^{-12} sec, which is much less than the reciprocal of the microwave frequency. This means that non-secular effects, which characterise the lifetime of a given spin state must be taken into account and this is not possible on the simple Bloch model.

Although some of the solvation effects of interest in aqueous solutions may involve considerably longer lifetimes than Freed³⁵ suggests, we must include non-secular effects in our formulation of chemical exchange. We will use the method of Fraenkel⁴³ to evaluate the line broadening due to chemical exchange. Consider a solution of a nitroxide radical; and let the radical exist in two states A and B

having a lifetime τ_A and τ_B respectively. Let p_A be the probability of finding the nitroxide in state A at a given time and let p_B be the probability of finding it in state B. The mean interval between exchanges τ_{ex} is given by⁴³

$$\tau_{ex} = \frac{\tau_A \tau_B}{\tau_A + \tau_B} \quad (2.41)$$

and the Hamiltonian is given by

$$\mathcal{H} = g \beta H_z S_z + \bar{a} \cdot S \cdot I + [a(t) - \bar{a}] S \cdot I \quad (2.42)$$

where

$$\bar{a} = p_A a_A + p_B a_B \quad (2.43)$$

and, a_A and a_B are the isotropic hyperfine splitting constants associated with states A and B. The third term of 2.42 carries the time dependence, where $a(t)$ is the hyperfine splitting constant at a time t . For simplicity, we assume that $g_A = g_B$. The following expressions for the linewidth are found.

$$\frac{1}{T_2'} = \frac{\gamma e^2}{2} \left[\overline{\langle m_{I, +\frac{1}{2}} | S_z I_z | m_{I, +\frac{1}{2}} \rangle} - \overline{\langle m_{I, -\frac{1}{2}} | S_z I_z | m_{I, -\frac{1}{2}} \rangle} \right]^2 j(0) \quad (2.44)$$

$$\frac{1}{2T_1} = \frac{\gamma e^2}{4} \left[\overline{|\langle m_{I+1, -\frac{1}{2}} | I^+ S^- | m_{I, +\frac{1}{2}} \rangle|^2} + \overline{|\langle m_{I, +\frac{1}{2}} | I^- S^+ | m_{I+1, -\frac{1}{2}} \rangle|^2} \right] j(\omega_0)$$

where $S^\pm = S_x + iS_y$ and $I^\pm = I_x + iI_y$. Following Fraenkel⁴³ we can evaluate the spectral densities as

$$j(\omega) = \int_{-\infty}^{+\infty} [a(t) - \bar{a}] [a(t+\tau) - \bar{a}] e^{i\omega\tau} d\tau = p_A p_B (a_A - a_B)^2 \frac{\tau_{ex}}{1 + \omega^2 \tau_{ex}^2} \quad (2.45)$$

and the linewidths as

$$\frac{1}{T_2} = \gamma e^2 p_A p_B (a_A - a_B)^2 \left[m_I^2 + \left[I(I+1) - m_I^2 \right] \frac{1}{1 + \omega_0^2 \tau_{ex}} \right] \tau_{ex} \quad (2.46)$$

If site A has an associated g value g_A and A value a_A , and site B has different g and A values g_B and a_B , then we have a cross term in the relaxation expression.

$$\frac{1}{T_2} = 2 p_A p_B \frac{\gamma e \beta H_0}{h} (a_A - a_B) (g_A - g_B) m_I \tau_{ex} \quad (2.47)$$

These equations are similar to those of Freed,³⁵ although 2.47 differs by $2H_0$ and 2.46 differs by a factor of $-\frac{1}{2} m_I^2 (1 + \omega_0^2 \tau_{ex}^2)^{-1} \tau_{ex}$ from Freed's equations. Using Freed's values for his nitroxide in d^6 ethanol we find that τ_{ex} must be equal to 1×10^{-9} secs before the m_I dependent terms in equation 2.46 contribute appreciably to the linewidth. In this case the non-secular terms become negligible and the discrepancy between 2.46 and Freed's³⁵ equations becomes unimportant. There is also an m_I independent contribution to the linewidth due to chemical exchange, caused by modulation of the isotropic g tensor. Thus the total chemical exchange broadening may be expressed by an equation similar to equation 2.27. Consequently, it would be very difficult to tell the difference in the contribution from exchange and motional averaging of the anisotropic g and A tensors except when $\tau_{ex} \gg \tau_c$.

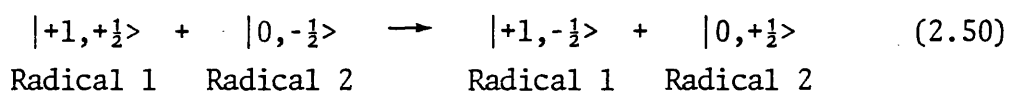
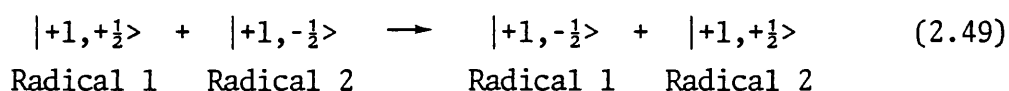
2.8 Heisenberg Spin Exchange

Having examined those relaxation mechanisms, which contribute to the linewidth in very dilute radical solutions, it is now time to examine

more concentrated solutions. As the radical concentration is increased, the lines will broaden monotonically with concentration. We can predict a simple rate law for this process as

$$\frac{1}{T_2} = k_e [X] \quad (2.48)$$

where k_e is the pseudo second order rate constant for Heisenberg spin exchange. Heisenberg spin exchange is a process by which two radicals collide and exchange spins. Only those collisions producing identifiably different spin states will give a line broadening. In the case of a simple nitroxide; of the two collision processes described by equations 2.49 and 2.50, only 2.50 will result in line broadening.



Only those radical-radical encounters, between radicals of different electronic and nuclear spin quantum number will result in line broadening. As in the exchange process described for the solid state in section 2.4, direct orbital overlap is necessary if spin exchange is to occur. In solution intermolecular orbital overlap can only persist for a short time τ_1 ; consequently there is a large uncertainty in the energy of each spin state causing a line broadening essentially by the Heisenberg principle.

The rigorous theory for spin exchange broadening has been developed by Johnson⁴⁴ and Freed.⁴⁵ Both authors use the density matrix method. This involves setting up one density matrix for a given monomeric radical

and a second density matrix for the postulated short-lived dimer. The period between encounters is known as τ_2 : τ_1 is defined above. We also require to introduce J_{ij} ; the exchange integral which is defined as²⁰

$$J_{ij} = \iint \psi_A(r_i)\psi_B(r_j) \frac{e^2}{r_{ij}} \psi_A(r_j)\psi_B(r_i)d\tau_i d\tau_j \quad (2.51)$$

where r_{ij} is the electron-electron separation, e is the electronic charge and the $\psi_A(r_i)$'s indicate the wavefunction of electron A associated with radical i etc. The exchange integral is the probability that, in a collision pair, one electron originally on molecule i will be found on molecule j and vice versa.

The density matrix method is described briefly below. Examine the wavefunction ψ , which is given by

$$\psi = C_a \psi_a + C_b \psi_b \quad (2.52)$$

where the coefficients give the elements of the density matrix as

$$\langle \psi_a | \rho | \psi_b \rangle = \overline{C_a C_b^*} \quad (2.53)$$

The expectation value of an observable represented by an operator O is given by

$$\langle \bar{O} \rangle = \langle \overline{\psi | O | \psi} \rangle = \sum_{a,b} \overline{C_a C_b^*} \langle \psi_b | O | \psi_a \rangle = \sum_{a,b} \overline{\langle \psi_a | \rho | \psi_b \rangle} \langle \psi_b | O | \psi_a \rangle \quad (2.54)$$

Usually, the time dependence of a wavefunction ψ is carried in the coefficients C_a and C_b , and the time dependence of O in equation 2.54 is carried by a time dependent density matrix. Johnson⁴⁴ shows that

the equations for the rate of change of the average density matrix are

$$\frac{d\rho^1}{dt} = \frac{(\text{Tr}_2 \rho^P - \rho^1)}{\tau_2} + i[\rho^1 \mathcal{H}^1 - \mathcal{H}^1 \rho^1] \quad (2.55)$$

$$\frac{d\rho^P}{dt} = \frac{(\rho^1 \times \rho^2 - \rho^P)}{\tau_1} + i[\rho^P \mathcal{H}^P - \mathcal{H}^P \rho^P] \quad (2.56)$$

where the superscripts 1 and 2 refer to monomer radicals 1 and 2 and the superscript p to the collision pair. Tr_2 indicates the trace over the states of the irrelevant nuclei, in order to separate density matrices when the collision pair dissociates. The density matrices of the monomeric forms are ρ^1 and ρ^2 , and the density matrix of the pair is ρ^P . The Hamiltonians of the monomeric radical and collision pair are given by,

$$\mathcal{H}^1 = \beta H_Z \cdot g \cdot S_z^1 + a \cdot I^1 \cdot S^1 \quad (2.57)$$

$$\mathcal{H}^P = \beta H_Z \cdot g \cdot (S_z^1 + S_z^2) + a \cdot (I^1 \cdot S^1 + I^2 \cdot S^2) + J \cdot S^1 \cdot S^2 \quad (2.58)$$

where J is minus twice the exchange integral. After processing the following expression for the linewidth is obtained,

$$\frac{1}{T_2} = f \frac{1}{\tau_2} \frac{J^2 \tau_1^2}{1 + J^2 \tau_1^2} \quad (2.59)$$

where f is the fraction of collisions resulting in exchange. For two nitroxide radicals in collision, each can be in one of six spin states; but for a given spin state of the first radical there will be only two possible spin states of the second which will have different nuclear and electronic spins. Thus, f in equation 2.59 takes the value $1/3$. Freed⁴⁵ uses a τ_2 twice as big as Johnson's,⁴⁴ however both sets of work

give identical results, since Freed's f takes the value of $2/3$.

The Debye type expressions for τ_1 and τ_2 are given by

$$\begin{aligned}\tau_1 &= \frac{\pi r d^2 \eta}{kT} \\ \tau_2 &= \frac{3 r \eta}{4d kT N_A C 10^{-3}}\end{aligned}\tag{2.60}$$

where d is the intermolecular separation at which spin exchange occurs.

In other words $J=0$ if the separation is greater than d . In equation 2.60 k , η , r and T have their usual meanings, N_A is Avogadro's number and C is the molar concentration. In the limit of strong exchange, i.e. $J^2\tau_1^2 \gg 1$, setting $d=2r$ and comparing equations 2.48, 2.59 and 2.60, yields the well-known Smolouchowski rate constant for diffusion. Since spin exchange is a diffusional process the lines should broaden as T increases and η falls.

As in chemical exchange; as we increase the spin exchange rate the lines broaden and the hyperfine splitting decreases. Once the exchange frequency approaches a value comparable to the hyperfine splitting the hyperfine lines overlap a great deal. Once the exchange rate is faster than or equal to the hyperfine splitting, the lines coalesce to a single broad line. Further increase in the exchange frequency causes this feature to narrow, resulting in a single exchange narrowed line. McConnell⁴⁵ has successfully used the modified Bloch equations to examine the problem of Heisenberg spin exchange.

2.9 Dipolar Broadening

In section 2.4 the dipolar spin-spin interaction and its concentration dependence were discussed. The Hamiltonian for the dipolar inter-

action between two spins separated by a distance r is

$$\mathcal{H}_{DD} = g_I \beta_I g_S \beta_S \left[\frac{\mathbf{I} \cdot \mathbf{S}}{r^3} - \frac{3(\mathbf{I} \cdot \hat{\mathbf{r}})(\mathbf{S} \cdot \hat{\mathbf{r}})}{r^5} \right] \quad (2.61)$$

where \mathbf{I} and \mathbf{S} are the electronic spins of species I and S , and r is the distance between them. The subscripts I and S refer to the spins in question and $\hat{\mathbf{r}}$ is the radius vector connecting them. The precise form of this Hamiltonian is shown in Chapter 3 of Carrington and McLachlan's book.²⁸ In a liquid the dipolar interaction is averaged to a low value, by the molecular motions of the spins involved. This leads to a line broadening effect. The slower the molecular motions within the liquid, the greater the line broadening due to the averaging of the dipolar interaction.

In the ensuing discussion, we will quantify the line broadening due to averaging of the dipolar interactions, using the theory of Abragam⁴⁷ as applied by Freed.⁴⁵ When I and S are unlike spins,

$$\begin{aligned} \frac{1}{T_2} = \gamma_I^2 \gamma_S^2 \hbar^2 s(s+1) & \left[\frac{1}{6} J^{(0)}(0) + \frac{1}{24} J^{(0)}(\omega_I - \omega_S) + \frac{3}{4} J^{(1)}(\omega_I) \right. \\ & \left. + \frac{3}{2} J^{(1)}(\omega_S) + \frac{3}{8} J^{(2)}(\omega_I + \omega_S) \right] \end{aligned} \quad (2.62)$$

and when I and S are like spin

$$\frac{1}{T_2} = \gamma^4 \hbar^2 I(I+1) \left[\frac{3}{8} J^{(2)}(2\omega_I) + \frac{15}{4} J^{(1)}(\omega_I) + \frac{3}{8} J^{(0)}(0) \right] \quad (2.63)$$

and the $J^{(l)}(\omega)$'s are the spectral densities. In general the dipolar interaction is averaged by the translational and rotational motion of

the probes. Abragam quotes the translational correlation time of the process as,

$$\tau = \frac{12 \pi r^3 \eta}{k T} \quad (2.64)$$

this is nine times longer than the rotational correlation time. Thus, the discussion will be limited to the translational modulation of the dipolar terms. Freed⁴⁵ shows that, at ambient temperatures where $\tau \geq 10^{-10}$ secs, the spectral densities can be evaluated as

$$J^{(0)}(0) = J^{(0)}(w_I - w_S) = \frac{32 \pi^2 N_A C \times 10^{-3} \eta}{25 k T} \quad (2.65)$$

$$J^{(1)}(w_I), J^{(1)}(w_S), J^{(2)}(2w_I), J^{(2)}(w_I + w_S) \ll J^{(0)}(0)$$

Freed⁴⁵ treats the dipolar interaction between two radicals with differing nuclear spin states as an interaction between two unlike spins. Interactions between radicals with the same nuclear configuration are treated as the like spin case. The linewidth contributions evaluated from equations 2.62 and 2.63 respectively are

$$\frac{1}{T_2} = \frac{8}{45} \hbar^2 \gamma^4 S(S+1) \pi^2 N_A C \times 10^{-3} \frac{\eta}{kT} \quad (2.66)$$

and

$$\frac{1}{T_2} = \frac{4}{25} \hbar^2 \gamma^4 S(S+1) \pi^2 N_A C \times 10^{-3} \frac{\eta}{kT} \quad (2.67)$$

where we are dealing with dipolar broadening in a solution of a radical with nuclear spin I. Combining these equations together, letting $S = \frac{1}{2}$ and making the appropriate transformation to the linewidth, we obtain:

$$\Delta H_{pp} \text{ dipole} = 76456.71672 \frac{\eta}{T} C \quad (2.68)$$

The ratio of the dipolar width to the exchange width is given by:

$$\frac{\Delta H_{pp} \text{ dipole}}{\Delta H_{pp} \text{ exchange}} = 15778072.29 \frac{\eta^2}{T^2} \quad (2.69)$$

From equation 2.69 we can see that dipolar broadening only becomes important for concentrated nitroxide solutions at values of $\eta/T > 6 \times 10^{-3} \text{ cPK}^{-1}$. Our main interest in dipolar broadening is its contribution to the concentration dependent linewidth in Heisenberg spin exchange studies. Nevertheless, n.m.r. studies⁴⁸ of diamagnetic solvent systems contaminated by a paramagnetic solute, can yield much useful chemical information. In this case, the solvent n.m.r. peaks are broadened by the modulated dipolar interaction between the solvent nuclei and the electronic spin.

2.10 Concluding Remarks

In this chapter, we have tried to outline the various pieces of information, which can be obtained from e.s.r. studies of free radicals in solution. The main relaxation mechanisms of interest are summarised in table 2.2.

The discussion of relaxation mechanisms and the g and A tensors is still incomplete. In the case of dialkyl nitroxides, second order corrections to the g and A tensors are small and have been omitted from the discussion. In section 2.5 we neglected to examine line broadening due to the motional modulation of the zero field splitting and the quadrupole interaction. These mechanisms have been covered by Atherton²⁹ and are unimportant in studies of nitroxides, which have an electronic

| <u>MECHANISM</u> | <u>CONTROLLING MOTION</u> | <u>CONCENTRATION DEPENDENCE</u> | <u>COMMENTS</u> |
|---|---|--|--|
| Averaging of the anisotropic g and A tensors | Rotational Diffusion | Independent of concentration | Directly proportional to η/T and molecular radius ³ . |
| Spin Rotation | Rotational Diffusion | Independent of concentration | Directly proportional to T/η and $1/\text{radius}^3$. |
| Chemical Exchange | Rate of interconversion of individual species | Independent of total concentration. Dependent on proportions of individual species | Directly proportional to η/T . Unless, the rate is very slow compared with τ_c , other mechanisms will mask the exchange broadening. |
| Heisenberg Spin Exchange | Translational Diffusion | Directly proportional to radical concentration | Directly proportional to T/η . Depends also on radical size and charge. |
| Averaging of the intermolecular dipolar interaction | Translational Diffusion | Directly proportional to radical concentration | Directly proportional to η/T . Masked by Heisenberg Spin Exchange except at lower temperatures and higher viscosities. |

TABLE 2.2

A Summary of the Main Relaxation Mechanisms occurring at Normal Temperatures and Viscosities

spin $S = \frac{1}{2}$ and a small quadrupole moment.

The relaxation mechanisms outlined are expected to give an adequate representation of the linewidths of radicals in solution. All e.s.r. linewidth studies should be carried out using thoroughly deoxygenated solutions. This is because the oxygen molecule is a triplet state molecule having two unpaired electrons. Thus radical oxygen encounters in solution would broaden the spectral features by a spin exchange mechanism. In the case of the dialkyl nitroxides, the presence of protons in the alkyl groups will further split the nitrogen triplet. This proton super-hyperfine splitting is usually masked by the linewidth. So three lines which are markedly non-Lorentzian in character are now seen. For an adequate description of the linewidth we need to analyse the three nitrogen lines as an envelope of proton lines of width W_H , separated by the hydrogen hyperfine splitting $A(^1H)$. The procedure for this will be described later in this thesis.

In the remainder of this thesis it is hoped to use the described behaviour of free radicals in solution to probe the aqueous environment.

REFERENCES TO CHAPTER 2

1. J. Oakes, J.C.S. Faraday II, 1972, 68, 1464.
2. A. S. Waggoner, O. H. Griffith and C. R. Christensen, Proc. Nat. Acad. Sci., 1967, 57, 1198.
3. A. S. Waggoner, A. D. Keith and O. H. Griffith, J. Phys. Chem., 1968, 72, 4129.
4. K. K. Fox, Ph.D. Thesis, University of Leicester, 1974.
5. K. K. Fox, Trans. Faraday Soc., 1971, 67, 2802.
6. L. C. Dickinson and M. C. R. Symons, Trans. Faraday Soc., 1970, 66, 1334.
7. J. Oakes, Ph.D. Thesis, University of Leicester, 1967.
8. D. Jones and M. C. R. Symons, Trans. Faraday Soc., 1971, 67, 961.
9. D. Jones, Ph.D. Thesis, University of Leicester, 1972.
10. J. Oakes, J. Slater and M. C. R. Symons, Trans. Faraday Soc., 1970, 66, 546.
11. T. A. Claxton, J. Oakes and M. C. R. Symons, Trans. Faraday Soc., 1967, 63, 2125.
12. V. Znamitovschi, O. Cozar and A. Nicula, Mol. Phys., 1974, 27, 273.
13. N. M. Atherton and S. J. Strach, J.C.S. Faraday II, 1972, 68, 374.
14. C. Jolicoeur and H. L. Friedman, Ber. Bunsenges. Physik. Chem., 1971, 75, 248.
15. C. Jolicoeur and H. L. Friedman, J. Solution Chem., 1974, 3, 15.
16. T. Kawamura, S. Matsumani and T. Yonezawa, Bull. Chem. Soc. Japan, 1967, 40, 1116.
17. R. M. Dupreyre, H. Lemaire and A. Rassatt, Tetrahedron Letters, 1964, 27-28, 1775.
18. E. M. Kosower, J. Am. Chem. Soc., 1958, 80, 3253.
19. B. Knauer and J. J. Napier, J. Am. Chem. Soc., 1976, 98, 4395.
20. P. B. Ayscough "Electron Spin Resonance in Chemistry", Methuen & Co. Ltd., London, 1967.
21. P. W. Atkins and M. C. R. Symons, "The Structure of Inorganic Radicals", Elsevier Publishing Company, Amsterdam, 1967.

22. N. Bloembergen, E. M. Purcell and R. V. Pound, Phys. Revs., 1948, 73, 679.
23. H. M. McConnell, J. Chem. Phys., 1956, 25, 709.
24. D. Kivelson, J. Chem. Phys., 1960, 33, 1087.
25. R. Kubo and K. Tomita, J. Phys. Soc. Jap., 1954, 9, 888.
26. A. Carrington and H. C. Longuet-Higgins, Mol. Phys., 1962, 5, 447.
27. J. H. Freed and G. K. Fraenkel, J. Chem. Phys., 1963, 39, 326.
28. A. Carrington and A. D. McLachlan, "Introduction to Magnetic Resonance", Harper & Row, New York, 1967.
29. N. M. Atherton, "Electron Spin Resonance", Ellis Horwood Limited, Chichester, 1973.
30. R. Wilson and D. Kivelson, J. Chem. Phys., 1966, 44, 154.
31. R. Wilson and D. Kivelson, J. Chem. Phys., 1966, 44, 4440.
32. R. Wilson and D. Kivelson, J. Chem. Phys., 1966, 44, 4445.
33. R. G. Kooser, W. V. Volland and J. H. Freed, J. Chem. Phys., 1969, 50, 5243.
34. S. A. Goldman, G. V. Bruno and J. H. Freed, J. Chem. Phys., 1973, 59, 1973.
35. J. S. Hwang, R. Mason, L. P. Hwang and J. H. Freed, J. Phys. Chem., 1975, 79, 489.
36. P. W. Atkins and D. Kivelson, J. Chem. Phys., 1966, 44, 169.
37. G. Nyberg, Mol. Phys., 1967, 12, 69.
38. P. S. Hubbard, Phys. Revs., 1963, 131, 1155.
39. N. S. Angerman and R. B. Jordon, J. Chem. Phys., 1971, 54, 837.
40. J. S. Hwang, D. Kivelson and W. Plachy, J. Chem. Phys., 1973, 58, 1753.
41. T. E. Eagles and R. E. D. McLung, Can. J. Phys., 1975, 53, 1492.
42. J. Q. Adams, J. Chem. Phys., 1966, 45, 4167.
43. G. K. Fraenkel, J. Phys. Chem., 1967, 71, 139.
44. C. S. Johnson, Mol. Phys., 1967, 12, 25.
45. M. P. Eastman, R. G. Kooser, M. R. Das and J. H. Freed, J. Chem. Phys., 1969, 51, 2690.

- 46. P. Devaux and H. M. McConnell, J. Mag. Res., 1973, 9, 474.
- 47. A. Abragam, "The Principles of Nuclear Magnetism", Clarendon Press, Oxford, 1961.
- 48. C. Jolicoeur, P. Bernier, E. Firkins and J. K. Saunders, J. Phys. Chem., 1976, 80, 1908.

CHAPTER THREE

Ditertiary butyl nitroxide as a Probe for Examining
Binary Aqueous Solutions

CHAPTER THREE

3.1 Introduction

A wide variety of organic and inorganic radicals have been used to examine solvation phenomena.¹ Organic nitroxides are particularly suitable for this purpose, because of their chemical stability and the simplicity of their e.s.r. spectra. It has been shown that the nitrogen hyperfine splitting constants, $A(^{14}\text{N})$, of these radicals are sensitive to changes in solvent polarity.^{2,3} Linewidth studies of nitroxides in solution are also expected to produce useful information concerning the solvent environment. Several investigations of the relaxation of these radicals in solution have been reported.⁴⁻⁷

Jones⁸ carried out investigations into the behaviour of several nitroxides; notably ditertiary butyl nitroxide DTBN, in aqueous solution. The main source of solvation information was found to be $A(^{14}\text{N})$ of these radicals, which was found to vary as the probe's environment changes. Relaxation measurements were also made but proved less reliable in reflecting solvation changes.

Jolicoeur and Friedman⁹⁻¹¹ carried out a series of studies on the relaxation of the nitroxides 2,2,6,6-tetramethyl-4-piperidone-1-oxyl, TEMPOO, and 2,2,6,6-tetramethyl-piperidine-1-oxyl, TEMPO, in aqueous solutions. It was expected¹⁰ that the short time scale of measurement of e.s.r. would be capable of providing information concerning rapidly fluctuating hydration structures in aqueous solutions. These authors proposed a two-state model,^{10,11} which depicts a nitroxide molecule as tumbling in different manners in the vicinity of a hydrophobic solute molecule and in bulk water. This conclusion was reached by examining the rotational correlation time τ_c and the spin rotational correlation

time τ_J , of these probes in aqueous solution, measured using e.s.r. spectroscopy.

The purpose of the present study is to extend the work of Jones⁸ and to examine in more detail some of the conclusions of Jolicoeur and Friedman.⁹⁻¹¹ Both linewidth and $A(^{14}\text{N})$ measurements are presented, to obtain the maximum solvation information. The linewidth data should give useful information concerning the rotational freedom of the probe, whilst the nitrogen hyperfine coupling constants should show up any probe-solvent interactions. A wide range of cosolvents has been selected to probe the nature of aqueous solutions more fully. In addition the rôle of urea and several acid amides, which possess both basic and acidic properties, in modifying water structure is examined. Urea was selected for study, because it is well known as the classic "water structure-breaker". Variable temperature studies have also been used as a method of probing the structure of water.

Ditertiary butyl nitroxide was selected as the probe for several reasons. This nitroxide possesses only one polar group, thus any hydrogen-bonding to the probe will occur at one site. The large hydrocarbon residue of this molecule is expected to encourage the formation of a clathrate type solvation structure around itself in aqueous solution. The proton superhyperfine structure of the individual nitrogen envelopes of the e.s.r. spectrum of this radical shows no sign of resolution, except under conditions of low temperature and high solvent viscosity. Finally, $A(^{14}\text{N})$ of DTBN has been shown to be sensitive to changes in solvation.⁸

3.2 Experimental Details

Ditertiary butyl nitroxide was either prepared by the method of

Hoffman¹² or purchased from Eastman. The perdeuterated radical, d^{18} DTBN was prepared by photolysis of d^9 t-nitroso butane in d^4 methanol. The sample was degassed on a vacuum line using the freeze-pump-thaw technique to remove excess oxygen and nitric oxide. Water was twice distilled from alkaline permanganate. Methanol was refluxed over iodine activated magnesium for 30 minutes prior to distillation. Acetone and t-butanol were stored over molecular sieve 4A and fractionated. Methyl cyanide was distilled from phosphorous pentoxide. All other solvents were dried over molecular sieve 4A, with the exception of hexamethyl phosphoramide, which was stored over molecular sieve 13X. Triethylene diamine, TED, was purified by vacuum sublimation.

All solutions were thoroughly degassed, by purging with nitrogen for more than 30 minutes prior to use. Concentrations of DTBN were in the region 5×10^{-5} M in order to prevent broadening by Heisenberg spin exchange. E.s.r. spectra were obtained using a Varian E-3 spectrometer. Sample temperatures were maintained to within $\pm 1^\circ\text{C}$, and were checked using a Comark 1625 electronic thermometer at the beginning and end of each run. N.m.r. spectra were recorded using a JEOL PS100 100MHz spectrometer, using t-butylamine as a shift reference.

3.3 Trends in Linewidths

The basic mechanisms controlling the linewidths of free radicals in solution have been discussed in earlier parts of this thesis. Averaging of the anisotropic g and A tensors and spin rotation are expected to be the main relaxation mechanisms governing the linewidths of DTBN in aqueous solutions. Each of the three nitrogen hyperfine lines of the e.s.r. spectrum of DTBN is comprised of an envelope of 19 proton superhyperfine lines. These superhyperfine features are due to

coupling of the unpaired electron spin with the 18 protons of the two t-butyl groups. To obtain accurate relaxation data, it is necessary to know the widths, W_H , of the individual proton superhyperfine lines.

In order to measure accurately W_H a computer simulation method similar to that of Poggi and Johnson⁴ was used. The computer simulation procedure requires the use of good values of the proton hyperfine coupling constants, $A(^1H)$. Once $A(^1H)$ is known the widths of the proton features can be extracted using a FORTRAN computer program, which calculates an envelope width ΔH_{pp} from a given W_H and $A(^1H)$. The program is documented in the appendix and simulates nineteen lines of binomial distribution separated by a distance $A(^1H)$. Each proton line is assumed to be Lorentzian in shape and to have a width of W_H . The envelope is scanned over 200 points in frequency steps of 5×10^5 rad sec^{-1} from 59.9250×10^9 rad sec^{-1} to 60.0250×10^9 rad sec^{-1} . Figure 3.1 shows a series of plots of computed envelope widths as a function of proton linewidth, for a series of values of $A(^1H)$.

Recently, accurate values of $A(^1H)$ of several nitroxides have been obtained using the n.m.r. technique.¹³⁻¹⁶ This method translates the observed difference in n.m.r. shifts of the protons of the radical and the protons of its nearest diamagnetic analogue, into a value of $A(^1H)$. The free radical must be in a state of rapid relaxation, sufficiently fast to completely average the hyperfine interaction between the nucleus and the unpaired electron. In the case of nitroxides, this condition is obtained, when Heisenberg spin exchange is fast enough to collapse the e.s.r. spectrum into a single exchange narrowed line. The relationship between $A(^1H)$ and the difference in n.m.r. shifts of the probe and its diamagnetic analogue are given by:¹⁷

Figure 3.1

Correlation between the overall linewidths, ΔH_{pp} , and computed individual widths for the separate proton components (W_H) for DTBN for a range of $A(^1H)$ values.

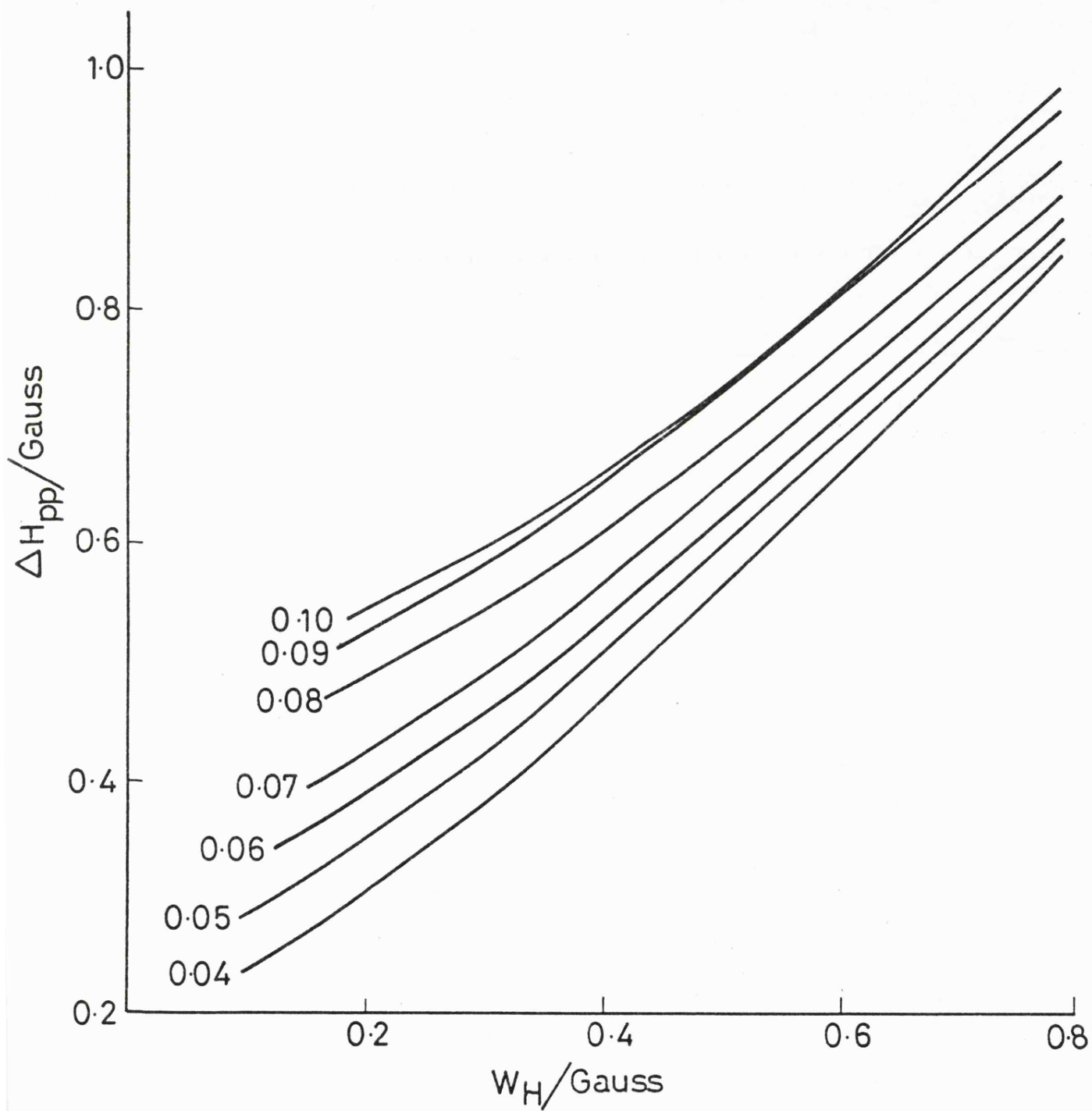


Figure 3.2

100 MHz proton n.m.r. spectrum of DTBN in methanol.

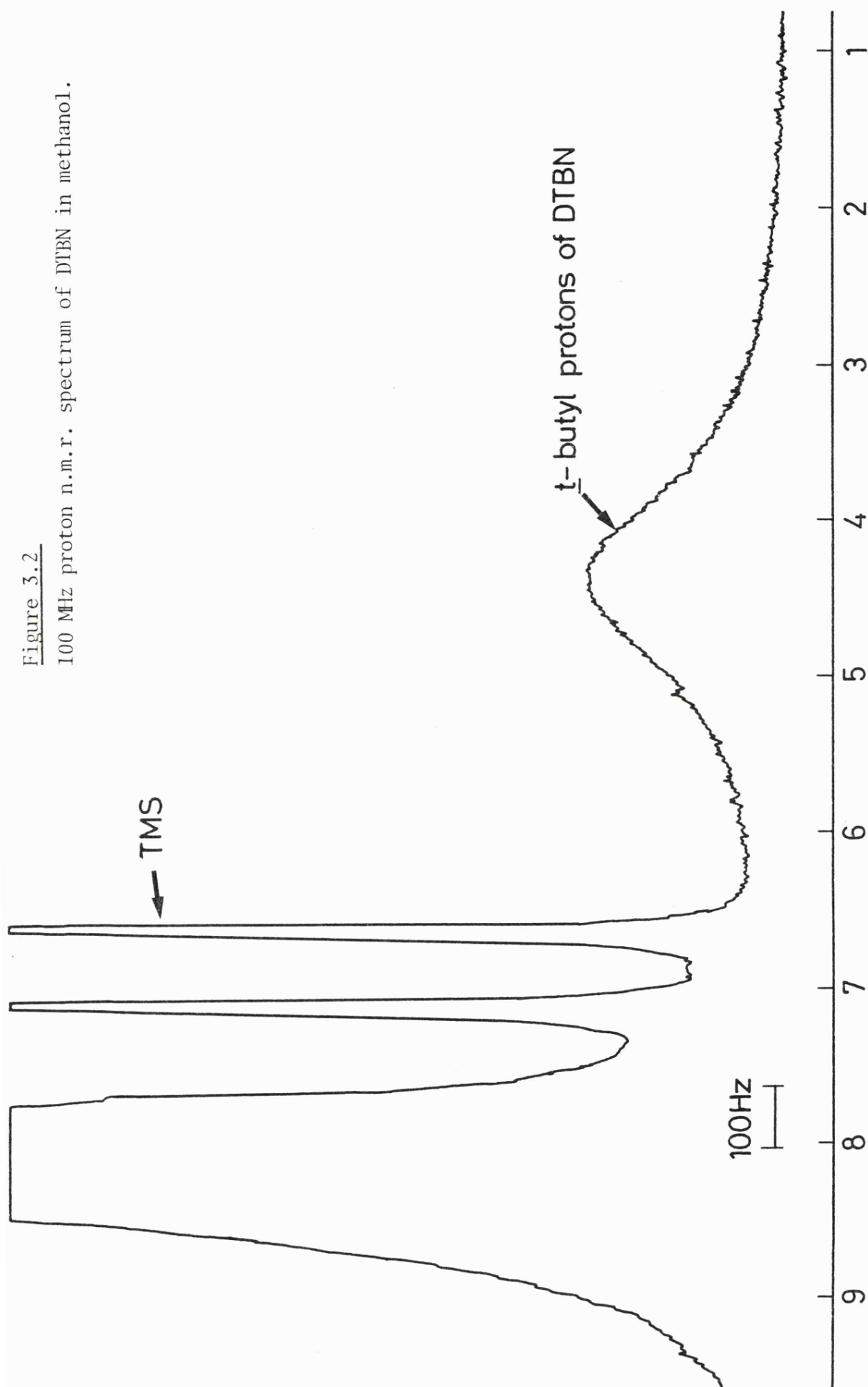
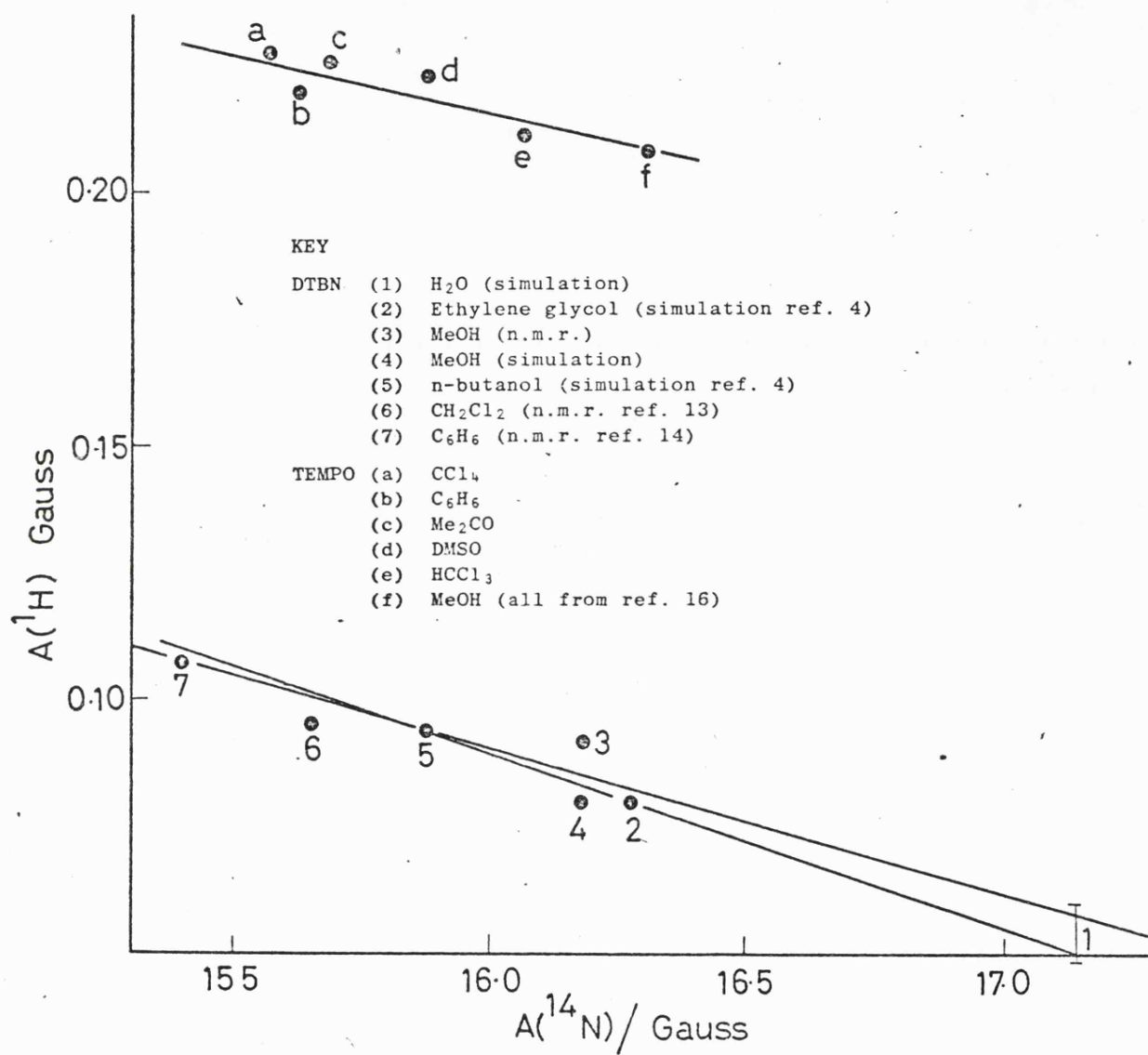


Figure 3.3

Correlation between $A(^{14}\text{N})$ and $A(^1\text{H})$ for DTBN and TEMPO in various solvents.



$$A(^1\text{H}) = - \frac{4 k T}{g_e^2 \beta_e^2} \frac{(\nu_p - \nu_d)}{H_0} \quad (3.1)$$

where ν_p and ν_d are the chemical shifts in Hz of the radical and its diamagnetic analogue respectively.

For the present study values of $A(^1\text{H})$ were obtained either from n.m.r. data appearing in the literature^{13,14} or from the point of resolution given in figure 3.1. In addition to this $A(^1\text{H})$ of DTBN in methanol was obtained using the n.m.r. method described above. Figure 3.2 shows a proton n.m.r. spectrum of DTBN in methanol. Ideally, $A(^1\text{H})$ of DTBN in water should also have been obtained using this method. This was not possible, since DTBN is insufficiently soluble in water to produce the conditions of fast exchange, necessary for accurate n.m.r. measurements. The values of $A(^1\text{H})$ of the t-butyl protons of DTBN obtained from the n.m.r. technique [$A(^1\text{H}) = 0.09$ G] and computer simulation [$A(^1\text{H}) = 0.08$ G] differ significantly. Careful examination of figure 3.1 reveals that this difference, should not significantly effect the linewidth analysis. It has been noted^{11,16} that for the piperidinic nitroxides, $A(^1\text{H})$ is inversely proportional to $A(^{14}\text{N})$. Figure 3.3 confirms that $A(^1\text{H})$ of the t-butyl protons of DTBN also increases as $A(^{14}\text{N})$ decreases.

Throughout this study, the narrowest lines were obtained for solutions of DTBN in water. In aqueous solution resolution of the individual proton lines is never seen, this supports the value of $A(^1\text{H})$ of ca. 0.05-0.06 G indicated by figure 3.3. This is very different from the value of $A(^1\text{H})$ of -0.094 G proposed by Atherton and Strach.¹⁷ Ahn¹⁸ has observed partial resolution of the proton superhyperfine structure of DTBN at -15°C in super-cooled water. A value of $A(^1\text{H})$ of -0.091 G was reported,¹⁸ this agrees well with the value proposed by

Atherton and Strach.¹⁷ The present study includes an examination of the e.s.r. spectrum of DTBN in supercooled water. The linewidths obtained were consistently less than those measured by Ahn,¹⁸ being in the region of 0.36 G as opposed to a minimum width of -0.47 G.¹⁸ In the temperature range 0 to -24°C no resolution of proton superhyperfine coupling was observed. If A(¹H) were as large as suggested by Ahn¹⁸ and Atherton and Strach,¹⁷ then the individual proton components would have been resolved in aqueous solution. It is possible that the larger linewidths observed by Ahn¹⁸ may be due to the presence of dissolved oxygen. However, no explanation of the observed proton features¹⁸ can be offered.

It is usual in relaxation studies to discuss the motional behaviour of the probe in terms of the rotational correlation time τ_c and the spin rotational correlation time τ_J . A selected set of τ_c and τ_J values are presented in tables 3.1 and 3.2. The values of τ_c were calculated from a rearrangement of equation 2.28 proposed by Johnson:⁴

$$\tau_c = \sqrt{3} \frac{\pi g B}{h} \frac{[\Delta H_{pp}^{+1} + \Delta H_{pp}^{-1} - 2\Delta H_{pp}^0]}{b^2 (0.25 - 0.05u)} \quad (3.2)$$

$$\tau_c = \sqrt{3} \frac{\pi g B}{h} \frac{[\Delta H_{pp}^{+1} - \Delta H_{pp}^{-1}]}{b\Delta\gamma B_0 (0.533 + 0.4u)} \quad (3.3)$$

where ΔH_{pp}^{+1} , ΔH_{pp}^0 and ΔH_{pp}^{-1} are respectively the widths of the low, centre and highfield nitrogen hyperfine lines. Because equations 3.2 and 3.3 include non-secular terms a FORTRAN computer program was written to solve these equations using a Newton-Ralphson method. The spin rotational correlation time τ_J was calculated from

$$\tau_J = \frac{\sqrt{3} \pi g B}{h} \frac{\Delta H_{pp}^*}{2kT\{(g - 2.0023)^2 + 2(g - 2.0023)^2\}} \quad (3.4)$$

where ΔH_{pp}^* is the width of the central nitrogen hyperfine line, after broadening caused by averaging of the anisotropic g and A tensors has been subtracted out. At ambient temperatures the errors involved in calculating correlation times are large and the estimated values of τ_c and τ_J are unreliable. It was therefore felt more appropriate to show trends in the experimental linewidths.

In chapter six, the effects of changes in the principal g and A values on the calculation of correlation times is discussed. The g and A values used in calculating the correlation times given in tables 3.1 and 3.2 were calculated using the equations of Cohen and Hoffman^{19,20} and the assumption that $g_{//} = 2.00232$. Using these equations and the measured value of $A(^{14}\text{N})$, band $\Delta\gamma$ can be calculated. This method was used prior to the discovery of the relationships given by equations 6.1 - 6.6 of chapter six. Since calculation of $\Delta\gamma$ and b by both methods are in very good agreement, it was not felt necessary to re-calculate τ_c and τ_J , using b and $\Delta\gamma$ calculated by the second method.

Figure 3.4 shows how the linewidths of the central line of DTBN in aqueous solutions vary with added cosolvent. There is a tendency for ΔH_{pp}^0 to increase as the molefraction of cosolvent increases. There is a similarity between figure 3.4 and the plot of $A(^{14}\text{N})$ of DTBN in aqueous solution as a function of added cosolvent, shown in figure 3.8. The plot of ΔH_{pp}^0 as a function of $A(^{14}\text{N})$ shown in figure 3.5 reflects this similarity. For each solvent ΔH_{pp}^0 shows a linear dependence on $A(^{14}\text{N})$. This type of behaviour would be observed if the envelope width is a function of $A(^1\text{H})$. The figure also includes a plot of $A(^{14}\text{N})$ against W_H , which indicates that changes in $A(^1\text{H})$ are not the sole con-

TABLE 3.1Values of τ_c for DTBN in Water-t-Butanol mixtures at 3.3°C

| Molefraction of t-Butanol | τ_c (s) calculated from Equation 3.2 | τ_c (s) calculated from Equation 3.3 |
|------------------------------|--|--|
| 0.000 | 9.74×10^{-12} | 6.40×10^{-12} |
| 0.011 | 1.27×10^{-11} | 9.69×10^{-12} |
| 0.021 | 2.14×10^{-11} | 8.16×10^{-12} |
| 0.031 | 2.15×10^{-11} | 1.22×10^{-11} |
| 0.043 | 2.43×10^{-11} | 1.95×10^{-11} |
| 0.064 | 3.48×10^{-11} | 2.33×10^{-11} |
| 0.073 | 3.18×10^{-11} | 2.22×10^{-11} |
| 0.087 | 3.40×10^{-11} | 3.05×10^{-11} |
| 0.109 | 3.63×10^{-11} | 2.71×10^{-11} |

TABLE 3.2

 τ_J values for DTBN in DMSO at various temperatures

| T (K) | ΔH_{pp}^0 (G) | W_H (G) | α'' (G) | τ_c (s) | τ_J (s) |
|-------|-----------------------|-----------|----------------|-------------------------|-------------------------|
| 301 | 0.568 | 0.260 | 0.258 | 5.02×10^{-13} | 9.834×10^{-14} |
| 305.2 | 0.588 | 0.295 | 0.284 | 2.715×10^{-12} | 1.068×10^{-13} |
| 310.0 | 0.597 | 0.310 | 0.309 | 3.487×10^{-13} | 1.144×10^{-13} |
| 316.0 | 0.604 | 0.322 | 0.303 | 4.769×10^{-12} | 1.100×10^{-13} |
| 320.0 | 0.597 | 0.310 | 0.300 | 2.267×10^{-12} | 1.076×10^{-13} |
| 325.6 | 0.628 | 0.360 | 0.354 | 1.535×10^{-12} | 1.247×10^{-13} |
| 330.3 | 0.657 | 0.408 | 0.393 | 3.757×10^{-12} | 1.365×10^{-13} |
| 335.5 | 0.649 | 0.395 | 0.389 | 1.338×10^{-12} | 1.330×10^{-13} |
| 341.0 | 0.703 | 0.468 | 0.453 | 3.757×10^{-12} | 1.524×10^{-13} |

Figure 3.4

Linewidths for DTBN in aqueous solutions as a function of the molefraction (m.f.) of added co-solvents. [○ MeOH = methanol, + tBuOH = t-butanol, □ MeCN = methyl cyanide, △ DMSO = dimethyl sulphoxide, ● Me₂CO = acetone, × HMPA = hexamethyl phosphoramidate, ▼ DMF = N,N-dimethyl formamide]

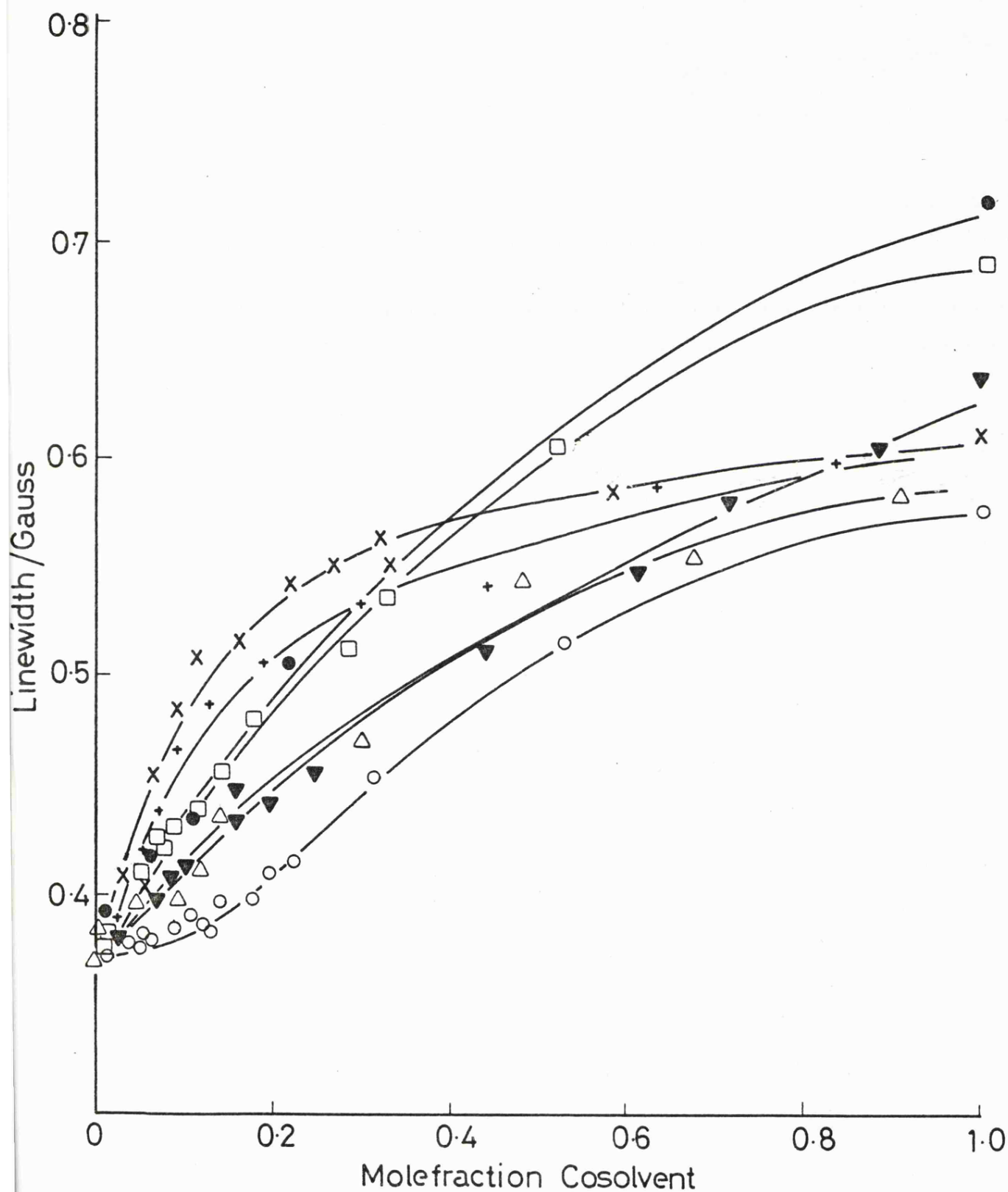
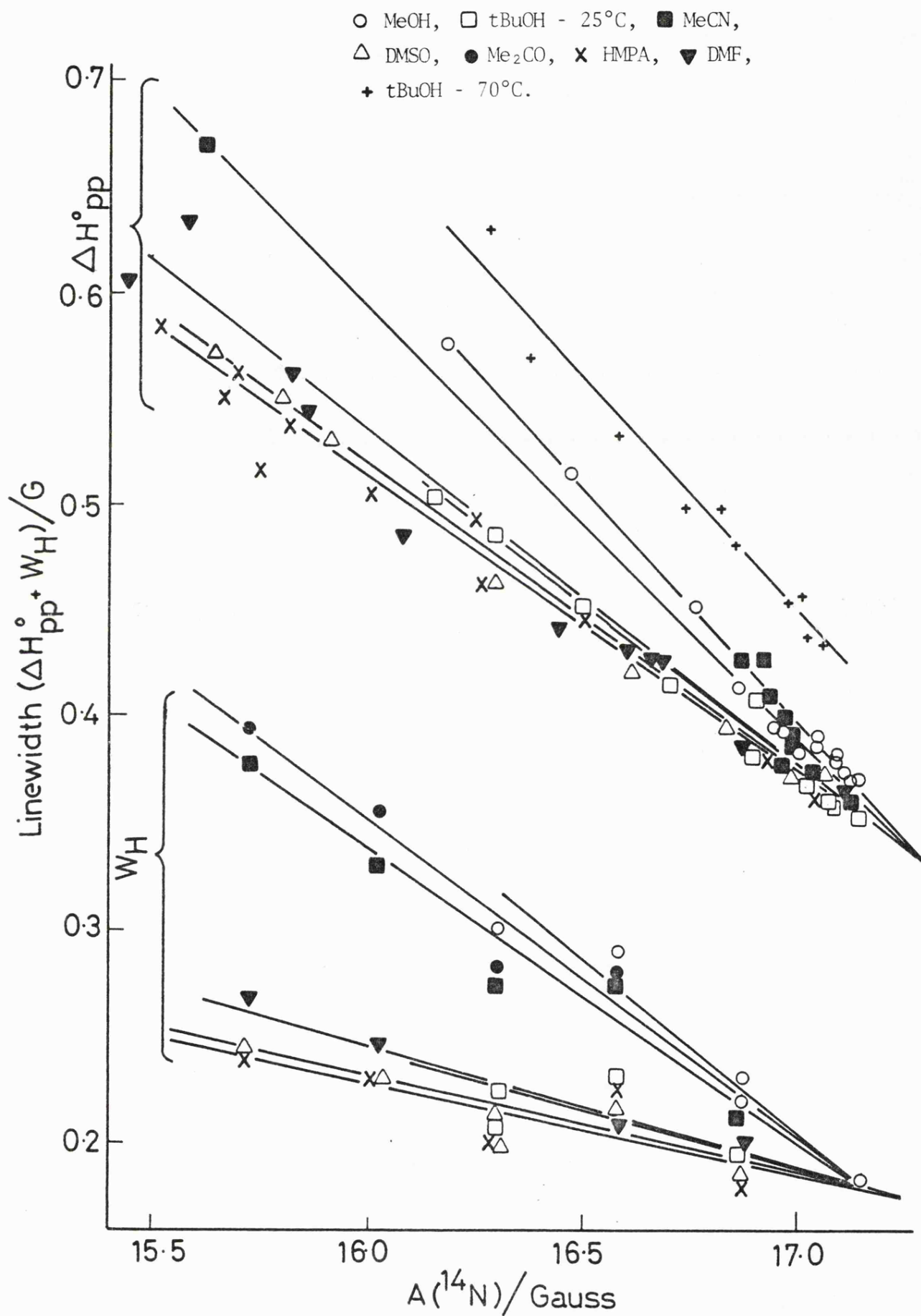


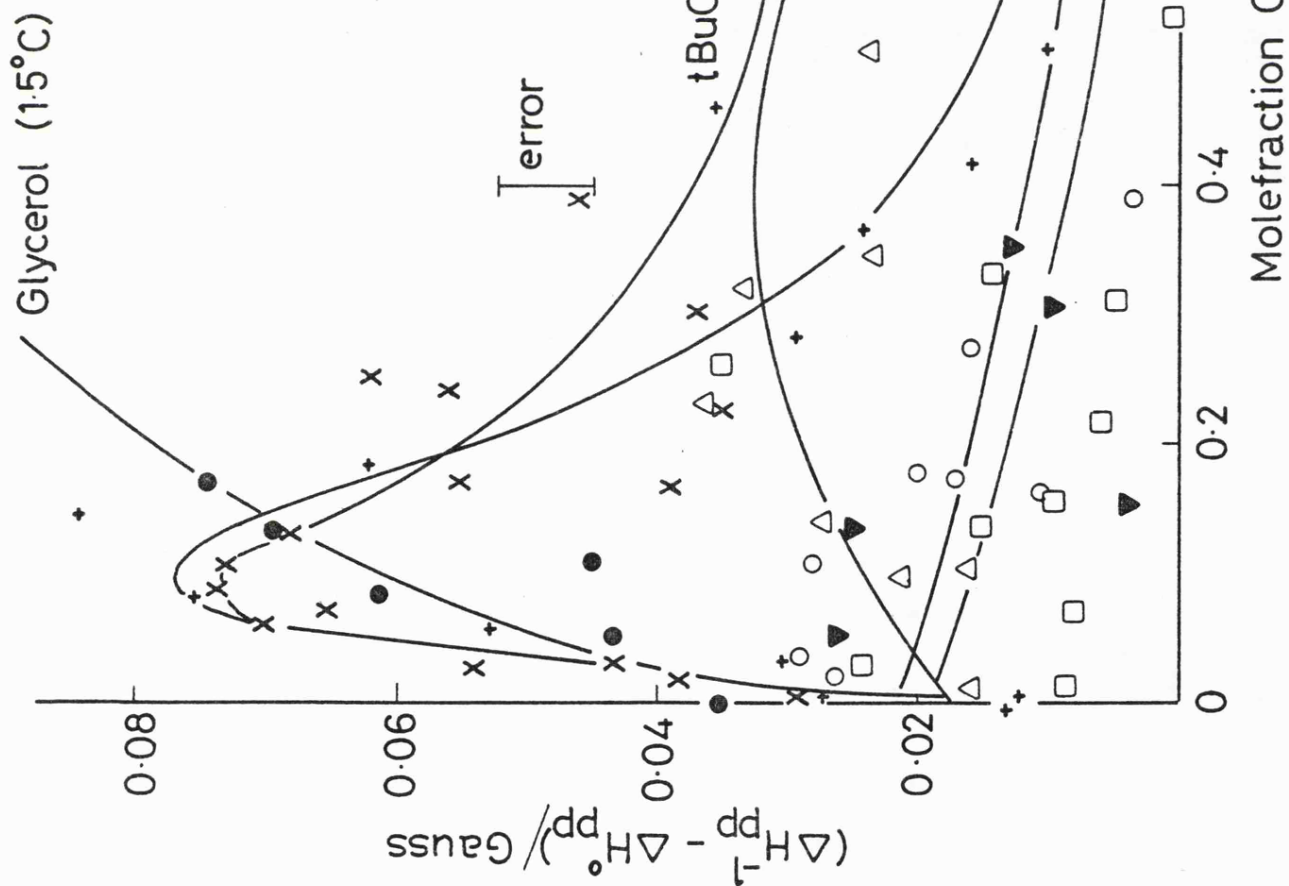
Figure 3.5

Correlation between linewidths (ΔH_{pp}^0 and W_H) and nitrogen hyperfine coupling constants $A(^{14}\text{N})$ for DTBN in various aqueous solutions at 25°C.



Linewidth difference ($\Delta H_{pp}^{-1} - \Delta H_{pp}^0$) for aqueous DTBN as a function of the m.f. of added cosolvents at ca. 0°C.

[● Glycerol, + HMPA, x tBuOH, ▼ Me₂CO, ○ MeCN, △ DMSO, □ HMPA at 25°C.]



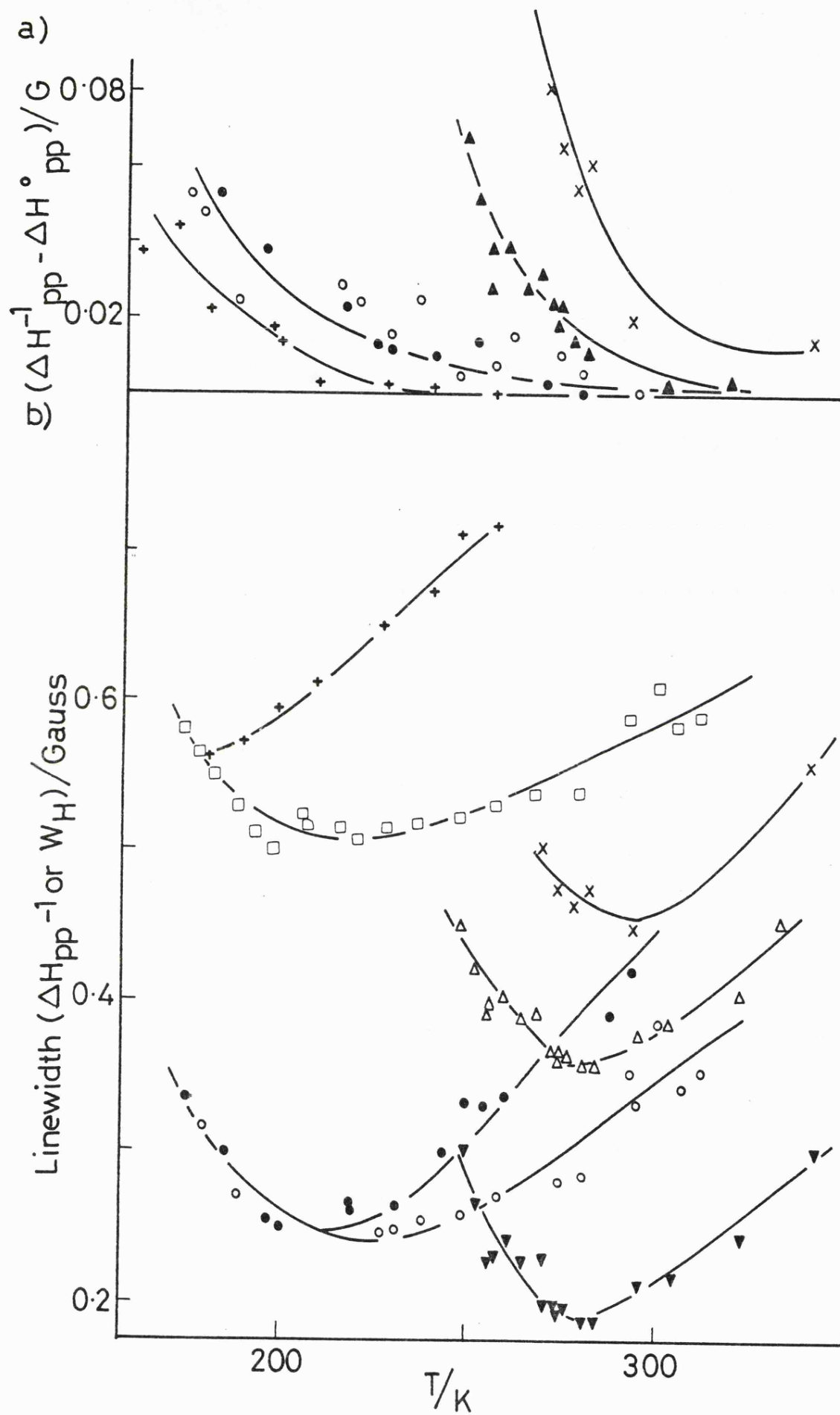


Figure 3.7

Caption to Figure 3.7

(a) ($\Delta H_{pp}^{-1} - \Delta H_{pp}^0$) and (b) linewidth (ΔH_{pp}^{-1} and W_H) as a function of temperature for DTBN and d^{18} DTBN in water, 0.073 m.f. aqueous t-butanol, heptane and MeOH.

(a) \blacktriangle DTBN/ H_2O , \circ DTBN/MeOH, \bullet d^{18} DTBN/ CD_3OD ,
 \times DTBN/ H_2O + tBuOH, $+$ DTBN/heptane.

(b) \triangle DTBN/ H_2O (ΔH_{pp}^{-1}), \blacktriangledown DTBN/ H_2O (W_H), \bullet d^{18} DTBN/ CD_3OD (ΔH_{pp}^{-1}), $+$ DTBN/heptane (ΔH_{pp}^{-1}), \times DTBN/ H_2O + tBuOH (ΔH_{pp}^{-1}), \square DTBN/MeOH (ΔH_{pp}^{-1}), \circ DTBN/MeOH (W_H).

tribution to the linewidth.

At ambient temperatures the effects of asymmetric broadening were small, and all three lines broaden at approximately the same rate. Changes in the asymmetric broadening were measured as $[\Delta H_{pp}^{-1} - \Delta H_{pp}^0]$, the difference in width of the high and centre field nitrogen envelopes of DTBN. Figure 3.6 shows how $[\Delta H_{pp}^{-1} - \Delta H_{pp}^0]$ varies as a function of molefraction of added cosolvent for DTBN in aqueous solutions. Most of the results presented were measured at ca. 0°C, where asymmetric broadening is more pronounced. An indication of the influence of temperature on linewidth is shown in figure 3.7. At high temperatures, the linewidth is controlled mainly by τ_J as shown in figure 3.7b. In the lower temperature region the linewidth control is taken over by τ_c , giving rise to greater asymmetric broadening as shown in figure 3.7a.

In order to demonstrate the importance of the contribution from proton superhyperfine coupling to the linewidths, a series of measurements were made on d^{18} DTBN in d^4 methanol as solvent.²¹ The results are included in figure 3.7. Unfortunately, only a small amount of the perdeuterated material was available and a more comprehensive series of measurements could not be made.

3.4 Trends in Nitrogen Hyperfine Coupling Constant

The rôle of added cosolvent in changing $A(^{14}N)$ for DTBN in aqueous solutions is shown in figure 3.8. As the molefraction of cosolvent increases $A(^{14}N)$ of the probe is reduced. Methyl cyanide and acetone cause a rapid initial fall in $A(^{14}N)$, which becomes more gradual in the base-rich region of the molefraction range. Hexamethyl phosphoramidate, HMPA, produces an even more dramatic initial decrease in $A(^{14}N)$. Methanol and t-butanol have quite different effects as cosolvents.

Figure 3.8

Hyperfine coupling constants $A(^{14}\text{N})$ for DTBN in aqueous solutions as a function of the molefraction (m.f.) of added cosolvents.

[\circ MeOH, $+$ tBuOH, \square MeCN, \triangle DMSO, \bullet Me₂CO, \times HMPA, \blacktriangledown DMF]

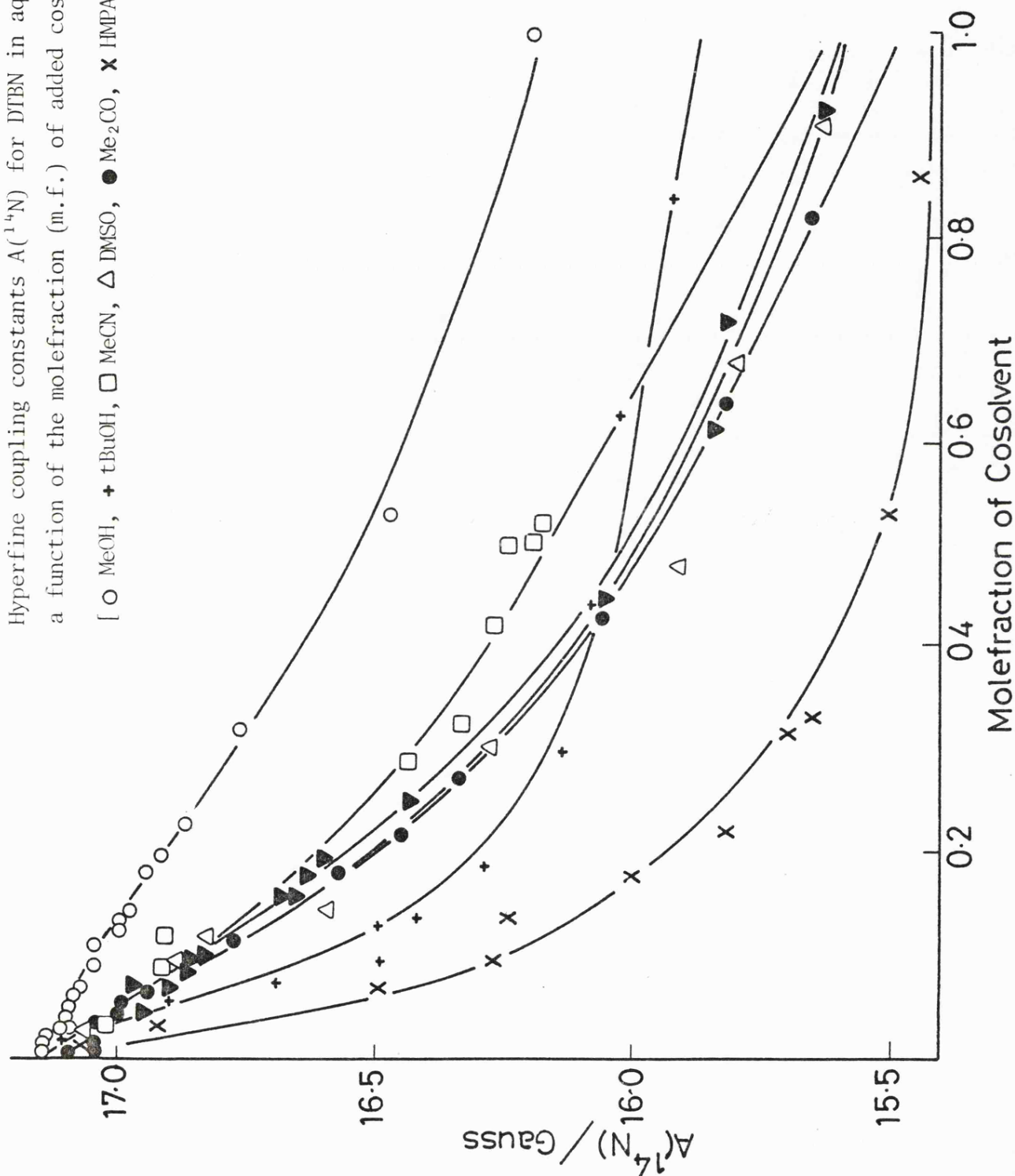
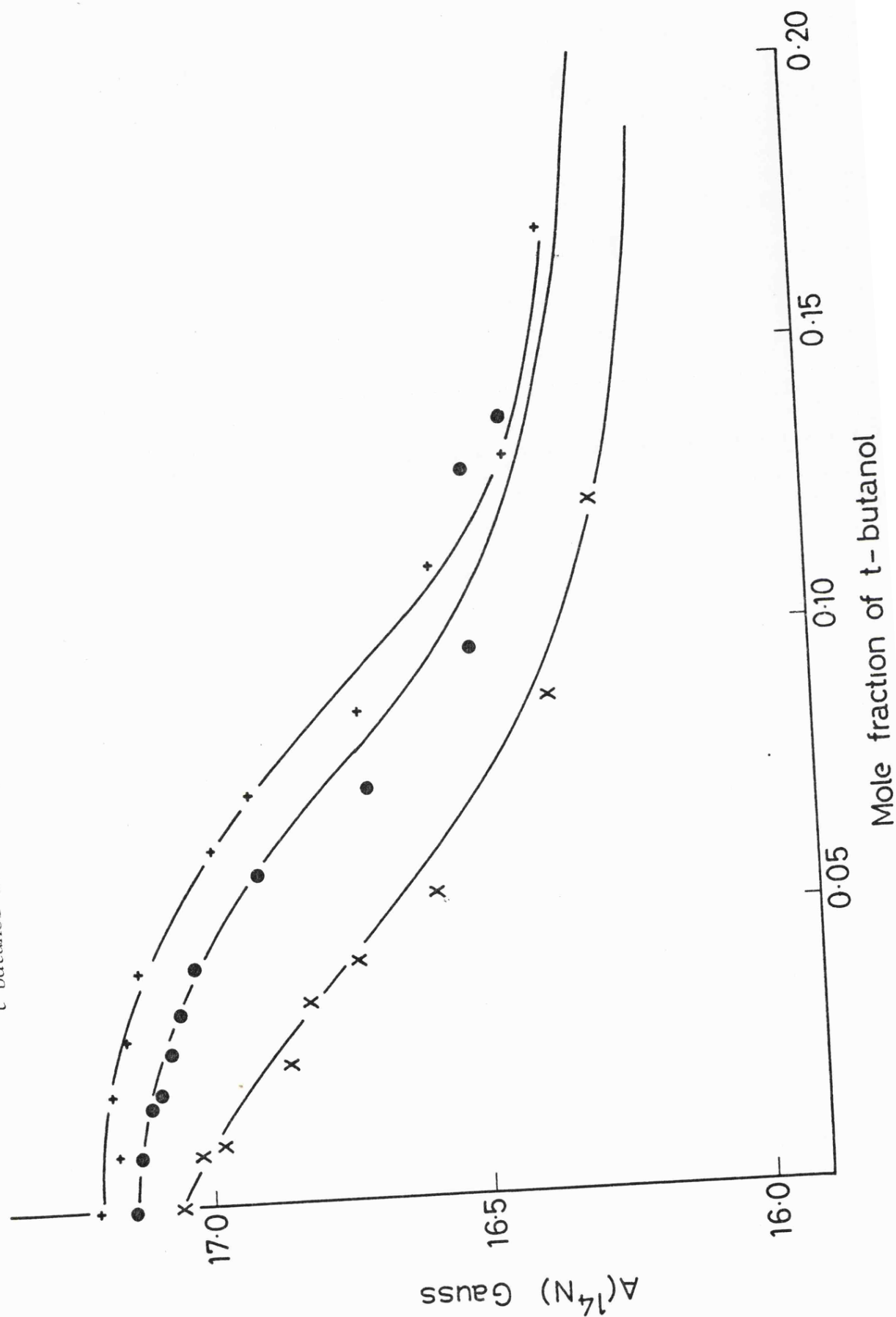


Figure 3.9
 Nitrogen hyperfine coupling constants $A(^{14}\text{N})$ for DTBN in aqueous solutions containing
 t-butanol at: +, 3.3; ●, 25; X, 70°C.



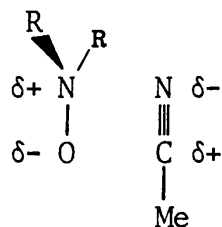
Methanol produces a small steady fall in $A(^{14}\text{N})$. Added t-butanol, on the other hand, initially has little effect on $A(^{14}\text{N})$ of DTBN in water. Once the t-butanol concentration has exceeded ca. 0.04 mf a rapid fall in $A(^{14}\text{N})$ is observed, the final value of $A(^{14}\text{N})$ being almost reached at 0.3 mf t-butanol. This type of behaviour is shown more clearly in figure 3.9, the initial plateau region is most prominent at ca. 0°C and has virtually disappeared once the temperature has reached 70°C.

The fall in $A(^{14}\text{N})$ of DTBN in aqueous solution as the cosolvent concentration increases is probably due to the loss of hydrogen-bonds to the oxygen atom of the nitroxide. The control of $A(^{14}\text{N})$ by hydrogen-bonding or complex formation has been widely discussed.^{2,3,8,19,20} Hydrogen-bonding to the nitroxyl oxygen is thought to attract bonding electron density towards oxygen and to repel anti-bonding (unpaired) electron density towards nitrogen. The overall effect is to increase $A(^{14}\text{N})$, but to reduce the isotropic g-value of the nitroxide.

A variety of studies have probed the nature of hydrogen-bond formation between nitroxides and alcohols. Spectroscopic measurements, made in the visible region, suggest that dialkyl nitroxides form 1:1 complexes with alcohols.^{22,23} Estimates of the strength of nitroxides as bases, can be gained from the compilation of enthalpies of adduct formation for a series of Lewis acid-base pairs, presented by Drago et alia.²⁴ These results suggest that nitroxides and dimethyl sulphoxide show approximately equal strengths as bases in their interactions with a series of alcohols. The strength of a nitroxide-alcohol hydrogen bond has been determined by thermodynamic measurements,²⁵ from n.m.r.²⁶ and e.s.r.²⁷ shifts, and by theoretical means.²⁸ Bond strengths in the range -1.6 to -7.9 k cal mole⁻¹ have been proposed.²⁵⁻²⁸

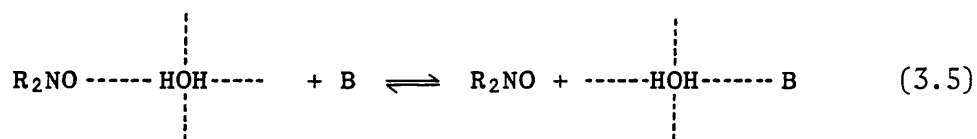
The results presented in figure 3.8 suggest that the extent of

hydrogen bonding is almost complete for water, reduced for methanol and small for t-butanol. The aprotic solvents may also induce small changes in $A(^{14}\text{N})$ due to the formation of dipolar complexes of the form,



the induced dipole producing a small increase in $A(^{14}\text{N})$. This explains why the dipolar aprotics, such as methyl cyanide, produce larger values of $A(^{14}\text{N})$ than completely non-interacting solvents such as the alkanes. Bulky dipolar aprotics, such as HMPA, are expected to be less effective in participating in complex formation than smaller bases such as methyl cyanide.

Basic solvents can be pictured as competing with the nitroxide probe for free hydroxyl groups, $(\text{OH})_{\text{free}}$, present in aqueous solution. An equilibrium of the form



demonstrates this competition for $(\text{OH})_{\text{free}}$. The quantity of added co-solvent will control the relative strengths of the hydrogen-bonds involved in equilibrium 3.5. For instance, a hydrogen bond formed between the base B and a water molecule bound to three other water molecules in a polymeric unit is expected to be stronger than that formed between B and monomeric water.²⁹ The initial slopes shown in figure 3.8 are therefore indicative of the effective base strength of

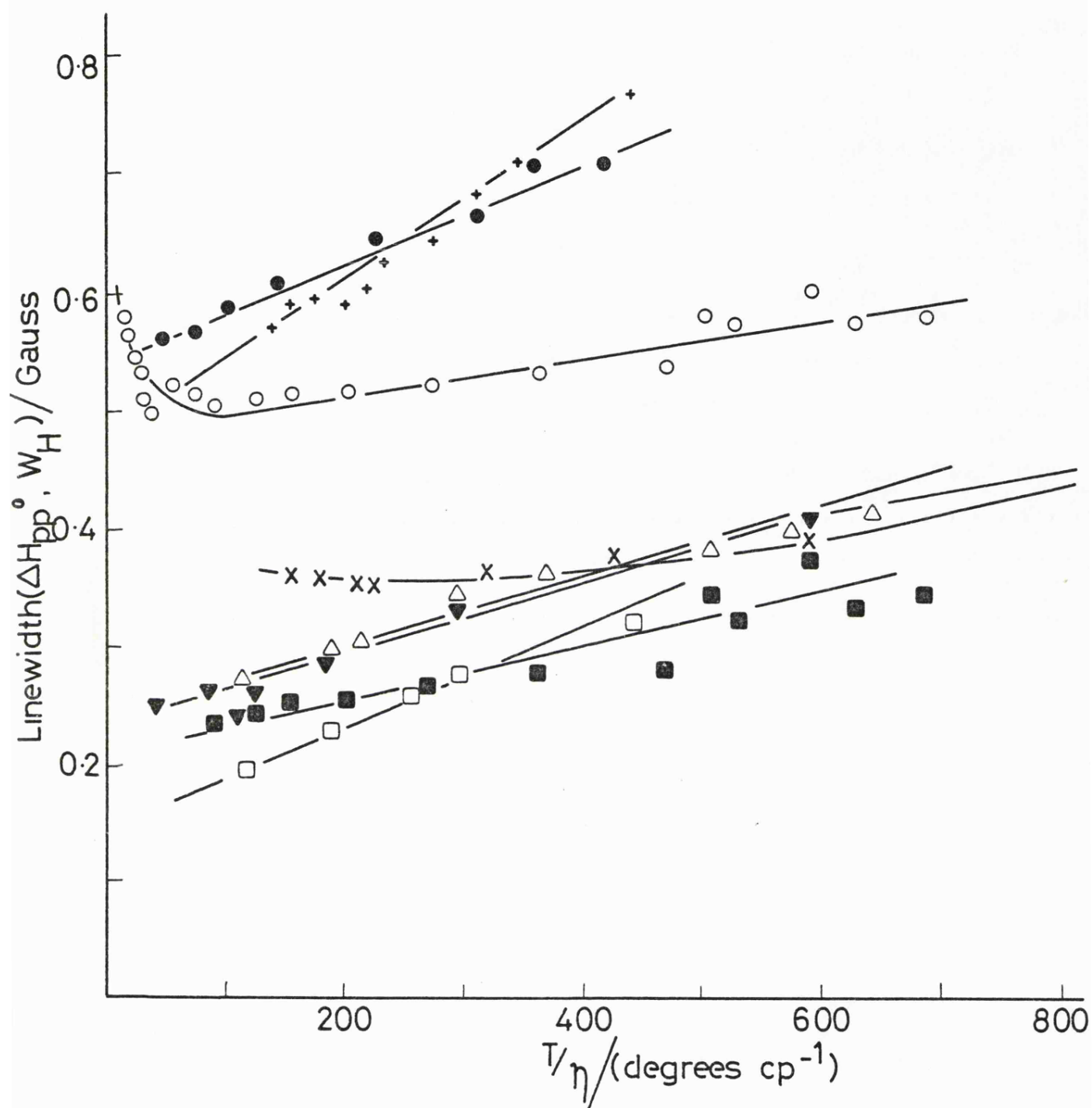


Figure 3.10

Linewidths (ΔH_{pp}^0 and W_H) for DTBN and TEMPO in various solvents as a function of T/η . [Data for TEMPO from ref. 11.]

- + DTBN/DMSO
- DTBN/heptane
- DTBN/MeOH
- W_H for DTBN/MeOH
- x DTBN/water
- ▼ d^{18} DTBN/ CD_3OD
- Δ W_H for TEMPO/EtOH
- W_H for TEMPO/DMSO

the added cosolvents. The order of base strength appears to be



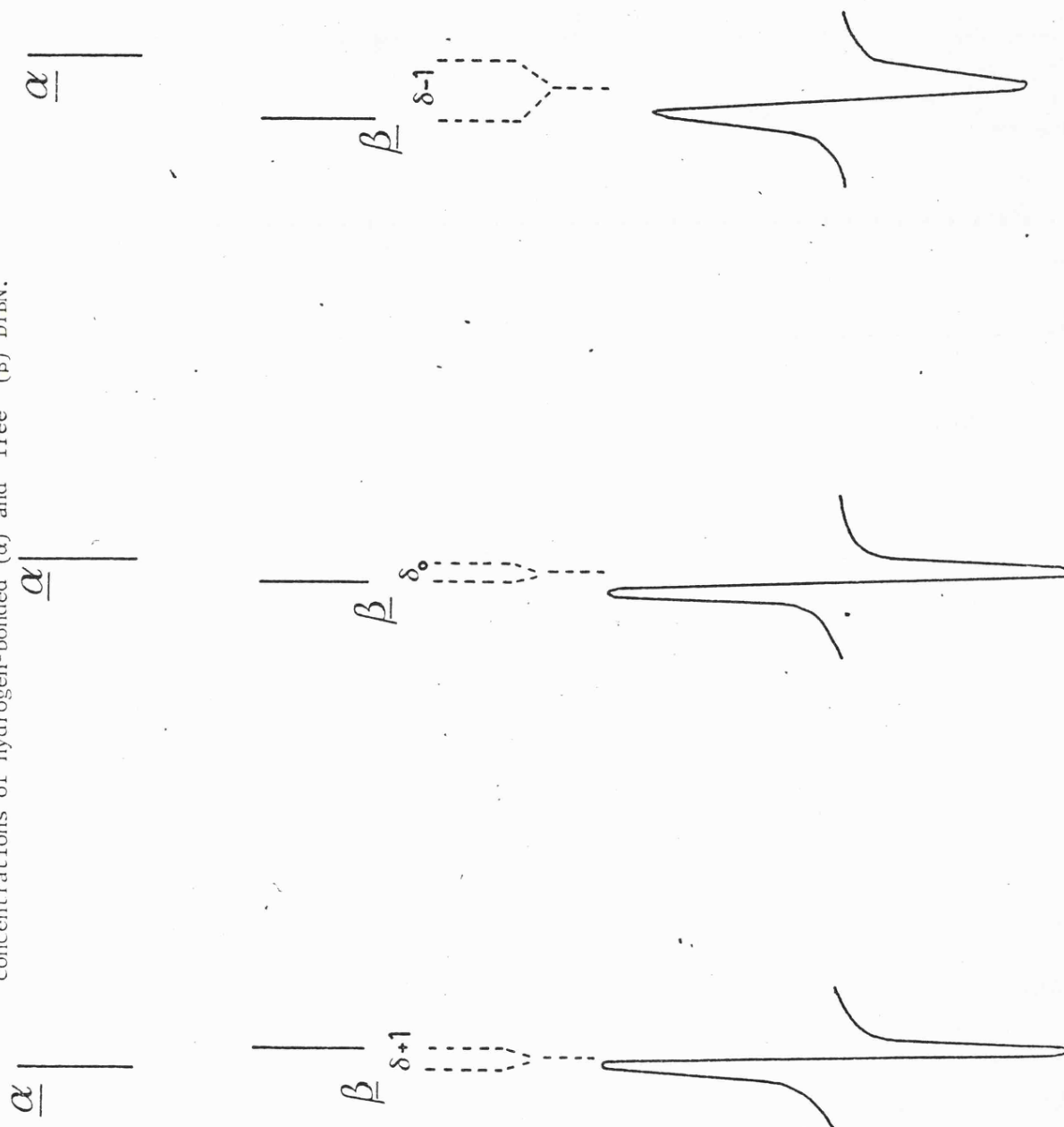
With the exception of HMPA, the above bases are very similar in their power to desolvate the probe in aqueous solutions. This is surprising, but can still be accommodated within the framework of equilibrium 3.5.

Equilibrium 3.5 may exert considerable influence on the variation of linewidths of DTBN in binary aqueous mixtures. It might be expected that a non-hydrogen bonded nitroxide should possess more freedom of rotation than the hydrogen-bonded radical. If spin rotation is the major contribution to the linewidth of DTBN in solution at ambient temperatures, then the degree of hydrogen bonding is expected to exert a large influence on the linewidth. The motional freedom of DTBN in water is viewed as being restricted by hydrogen bonding of the probe to the water "lattice", thus minimising line broadening by spin rotation. As a base is added to an aqueous solution of DTBN, $A(^{14}\text{N})$ falls as the proportion of unbound nitroxide increases and an increase in W_H should be seen, as shown in figure 3.5.

Figure 3.10 illustrates how ΔH_{pp}^0 and W_H of DTBN, in a range of solvents, vary as the solvent temperature: viscosity ratio, T/η , changes. The linewidths of DTBN in aprotic solvents are seen to be sensitive to changes in T/η . This is expected if spin rotation controls the linewidth. In protic solvents, the linewidths are much less sensitive to changes in T/η , as expected if the probe spends much of its time in the hydrogen bonded state. Changes in the anisotropic g and A tensors with changes in solvent, may contribute to the observed differences in linewidth behaviour. The rôle of changes in spectral parameters in determining linewidth behaviour is discussed more fully in chapter six and is shown to be insufficient to account for the

Figure 3.11

Simulation of an exchange broadened spectrum for DTBN in a water + INPA mixture containing equal concentrations of hydrogen-bonded (α) and "free" (β) DTBN.



changes seen in figure 3.10.

Conventionally, the differential linewidths observed for radicals in solution are discussed in terms of averaging of the anisotropic g and A tensors by motional modulation. Equilibrium 3.5 however, suggests that a chemical exchange process may contribute to the differential linewidth. The hydrogen-bonded nitroxide has a high $A(^{14}\text{N})$ and a low g_{iso} , whereas the free nitroxide has a low $A(^{14}\text{N})$ and a high g_{iso} . Figure 3.11 depicts such an exchange process. If the exchange process occurs at a slow enough rate, then a large contribution to the asymmetric line broadening is expected, since in the limit of fast exchange this is proportional to $(\delta_i)^2$. Here δ_i is defined as the frequency separation between the i^{th} line of both the exchanging species.

It is possible to calculate the M_I^2 contribution to the asymmetric broadening from the expression $\frac{1}{2}[\Delta H_{\text{pp}}^{+1} + \Delta H_{\text{pp}}^{-1} - 2\Delta H_{\text{pp}}^0]$. An estimate of the correlation time for chemical exchange, τ_{ex} , can then be obtained from equation 2.46. Estimates made of τ_{ex} for DTBN in *t*-butanol-water and HMPA-water mixtures at ca. 0°C, are in the region 10^{-8} to 10^{-9} sec. These times are probably too long, since no account of line broadening from the normal motion of the radical has been included. These values of τ_{ex} are approximately a 100 times as long as the values of τ_c obtained from equations 3.2 and 3.3, for the same systems. Although τ_{ex} appears to be long, such a process would still be a fast exchange process, since $1/\tau_{\text{ex}}$ is greater than the frequency separations of the two species. For instance, the frequency separation, δ_{-1} between the high field lines of hydrogen and non-hydrogen bonded nitroxide species is estimated to be ca. $5 \times 10^7 \text{ sec}^{-1}$.

It seems reasonable to suppose that in solvent systems, where

$A(^{14}\text{N})$ changes little with solvent composition, the asymmetric line broadening observed for DTBN is due to the averaging of the anisotropic g and A tensors. The results obtained for DTBN in glycerol-water mixtures at ca. 0°C are an example of this type of behaviour. Examination of figures 3.6 and 3.8 indicates that the maximum of $[\Delta H_{\text{pp}}^{-1} - \Delta H_{\text{pp}}^0]$ for DTBN in water-HMPA mixtures occurs when $A(^{14}\text{N})$ is the mean of the pure water and pure HMPA values. This is expected if there is a significant contribution to the asymmetric linewidths from a chemical exchange process. The viscosities of the solutions mentioned in both examples are high. This tends to increase the extent of asymmetric broadening from both chemical exchange and averaging of the anisotropic g and A tensors, in similar ways.

A fundamental difference between the water molecule and the methanol molecule, is that the former possesses equal numbers of lone-pairs and hydroxyl groups, whereas the latter has an excess of lone-pairs. Symons²⁹ has suggested that bulk water forms a hydrogen bonded network of water molecules, with small but equal concentrations of free lone-pairs and $(\text{OH})_{\text{free}}$ groups.²⁹ Bulk methanol, however, shows no detectable free hydroxyl groups, since the excess of lone-pairs is expected to hydrogen bond to any available $(\text{OH})_{\text{free}}$.²⁹ Water is therefore expected to possess enough $(\text{OH})_{\text{free}}$ groups to enable low concentrations of DTBN to be completely hydrogen bonded in this solvent. In methanol, however, the lack of $(\text{OH})_{\text{free}}$ groups is expected to inhibit the formation of hydrogen-bonds to the nitroxide. The value of $A(^{14}\text{N})$ observed for DTBN in methanol is intermediate between the values measured in water and aprotic solvents, suggesting that the radical is ca. 50% hydrogen bonded and 50% non-hydrogen bonded in this solvent. This view is supported by the work of Freed et alia.,⁵ who observed two species

in a solid state spectrum of d^{16} 2,2,6,6-tetramethyl-4-piperidone-1-oxyl in d^6 ethanol solvent. The species having the higher A_z value was attributed to nitroxide hydrogen bonded to the ethanol, the other species being a non-hydrogen bonded nitroxide.⁵ These workers⁵ suggested that ca. 66% of the nitroxide was hydrogen bonded at 77 K. The slow decline in $A(^{14}\text{N})$ of DTBN in aqueous solution, as methanol is added, can be attributed to an increase in competition for $(\text{OH})_{\text{free}}$ from the excess lone-pairs of the alcohol. As more alcohol is added the proportion of hydrogen bonded nitroxide molecules will fall and $A(^{14}\text{N})$ will decrease.

The behaviour of t-butanol, as a cosolvent in aqueous solutions of DTBN, is more complex than that of methanol. The rôle of t-butanol in modifying aqueous solutions has been the subject of a variety of spectroscopic studies.³⁰⁻³² The way in which $A(^{14}\text{N})$ of DTBN in aqueous solution changes with added t-butanol, shown in figure 3.9, parallels the hydroxyl proton shift results obtained from recent n.m.r. studies of t-butanol-water mixtures.^{30,31} The loss of the low temperature plateau effect at high temperature, as shown in figure 3.9, is common to both this and the n.m.r. studies.^{30,31} The n.m.r. results were interpreted as being due to enclathration of the alcohol at low temperatures. As the temperature is raised clathrate structures are thought to break down, since the stability gained from their enthalpy of formation is offset by entropy factors. It seems likely that at low temperatures and low t-butanol concentrations, DTBN and t-butanol are solvated in separate clathrate-type cages. The solute molecules are pictured as being hydrogen bonded to the cage wall; this is borne out by the high value of $A(^{14}\text{N})$ of DTBN in these systems. As the mole-fraction of t-butanol increases, there is insufficient water to maintain

the network of clathrate-type structures and a cage-sharing process is thought to come into play.³² This is expected to aid desolvation of the probe by the alcohol, producing the observed dramatic fall in $A(^{14}\text{N})$. The bulky nature of the t-butyl group makes hydrogen bonding in pure t-butanol an inefficient process, because of steric opposition. Thus, $A(^{14}\text{N})$ of DTBN in pure methanol will be higher than $A(^{14}\text{N})$ of DTBN in pure t-butanol.

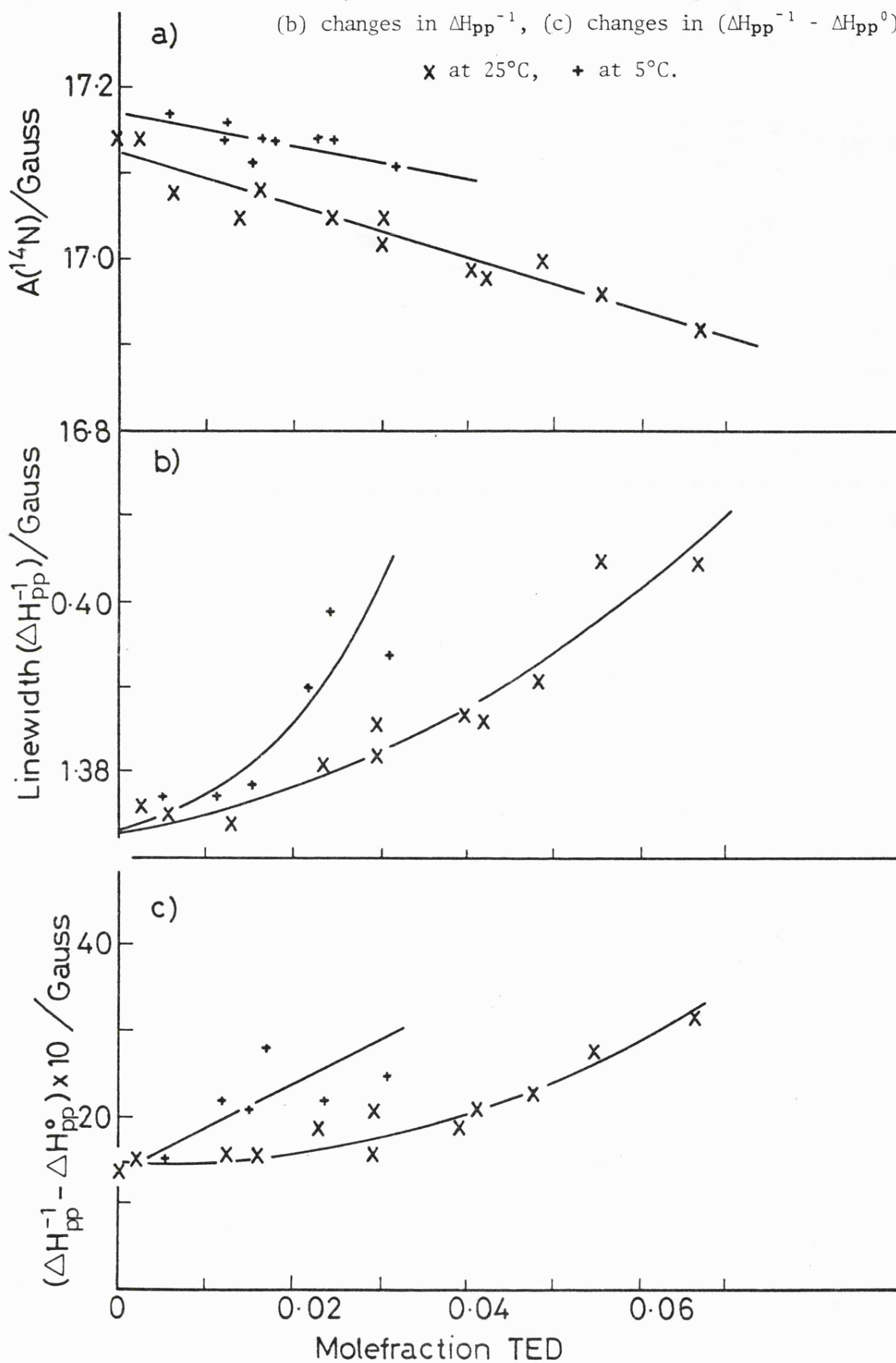
The asymmetric line broadening shown in figure 3.6 for DTBN fits in with the solvation model described above. The viscosity of the t-butanol-water solvent system increases steadily as the concentration of t-butanol approaches 0.05 mf at ca. 0°C.³³ The increase in $[\Delta H_{\text{pp}}^0 - \Delta H_{\text{pp}}^{-1}]$ seen for DTBN in aqueous solutions as t-butanol is added at concentrations below 0.05 mf t-butanol is probably due to a viscosity induced lengthening of τ_c . Once the cage sharing process comes into effect the increase in differential line broadening is probably due to a chemical exchange process. In order to test that water, and not a peculiarity of the t-butanol-DTBN interaction, is responsible for the observed changes in $A(^{14}\text{N})$, the e.s.r. spectrum of DTBN in a series of t-butanol-methanol mixtures was recorded. These results showed a smooth change in $A(^{14}\text{N})$ with solvent composition, confirming the rôle of water in determining the trends of $A(^{14}\text{N})$ of DTBN in t-butanol-water mixtures.

N.m.r. measurements^{30,31} have shown that large, nearly spherical molecules, such as triethylene diamine, TED, are effective in encouraging clathrate formation at ca. 0°C in water. The effect of added TED on the e.s.r. spectrum of DTBN in aqueous solution was examined and the results are presented in figure 3.12. Manifestation of clathrate effects by an initial insensitivity of $A(^{14}\text{N})$ is not as

Figure 3.12

Changes in e.s.r. parameters for DTBN on addition of triethylene diamine (TED); (a) changes in $A(^{14}\text{N})$, (b) changes in $\Delta H_{\text{pp}}^{-1}$, (c) changes in $(\Delta H_{\text{pp}}^{-1} - \Delta H_{\text{pp}}^0)$.

x at 25°C, + at 5°C.



marked as for the t-butanol-water results. This is probably due to the basic nature of the two nitrogen atoms of TED, which will scavenge (OH) free groups and partially desolvate the nitroxide. The increase in differential linewidth seen at 5°C and to a lesser extent at 25°C, may reflect clathrate effects.

3.5 DTBN in Aqueous Solutions of Urea and the Acid Amides

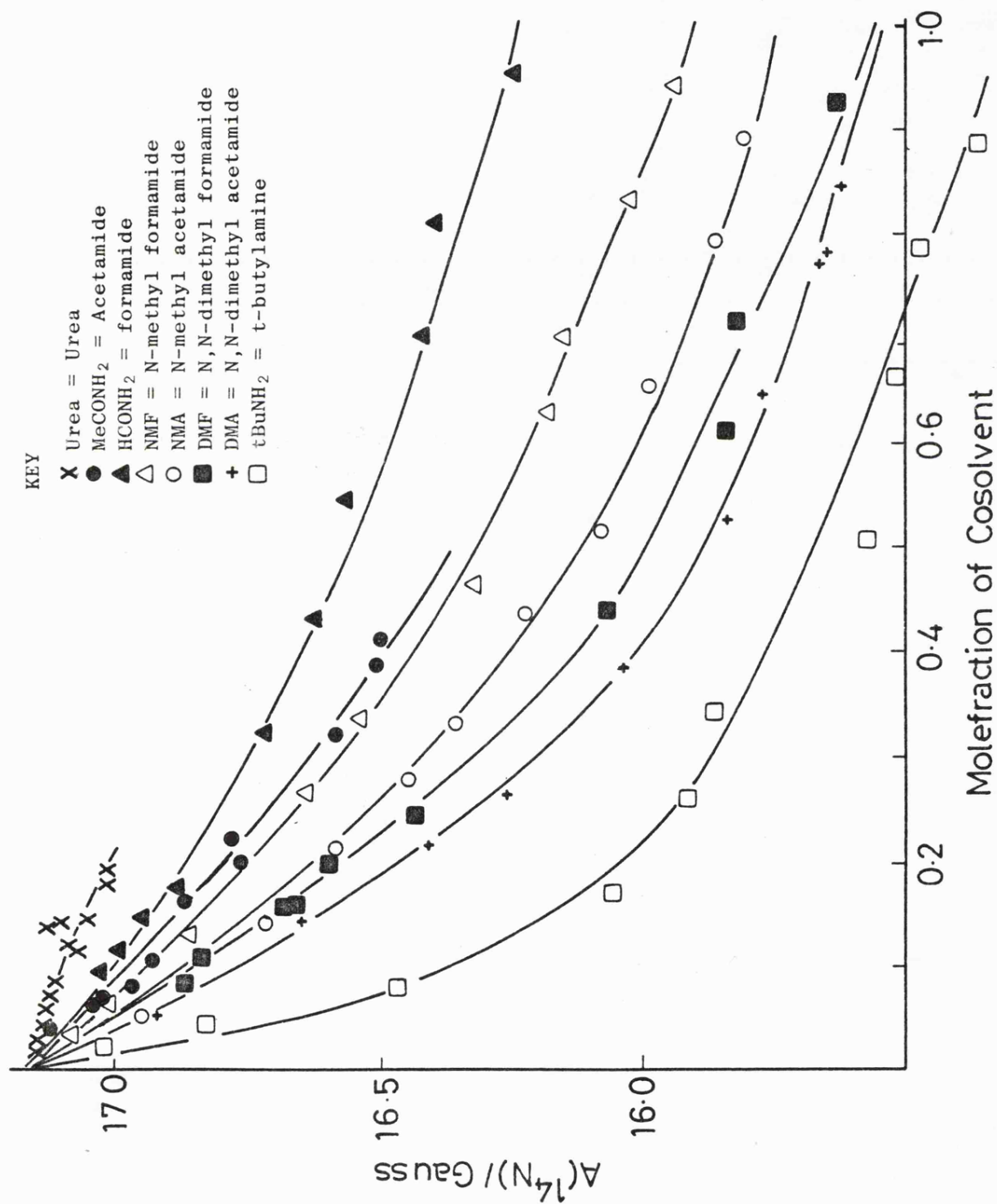
Urea is thought to exert a disruptive influence on the structure of water.³⁴ Recent n.m.r.³⁵ and viscosity measurements³⁶ are consistent with this view and imply that formamide and other acid amides are also structure breakers. Jolicoeur et alia³⁷ have recently made some measurements of the dipolar interaction between the unpaired electron of 2,2,6,6-tetramethyl-piperidine-1-oxyl and the alkyl protons of t-butanol in aqueous solution. The addition of formamide or urea to these solutions resulted in a decrease in the dipolar coupling between the paramagnetic probe and the t-butanol. This Jolicoeur³⁷ took as a demonstration that urea and formamide reduce the "hydrophobic interaction" between the nitroxide and the alcohol.

It was decided to examine the behaviour of DTBN in a range of aqueous solutions of acid amides. The effect of an amine base, t-butylamine, on the e.s.r. spectrum of DTBN in aqueous solution was also investigated. Figure 3.13 shows that $A(^{14}\text{N})$ of DTBN falls as an acid amide is added to an aqueous solution of the radical. The rate of fall of $A(^{14}\text{N})$ is dependent on the nature of the base and follows the order:

tBuNH₂ > N,N-dimethyl acetamide > DMF > N-methyl acetamide >
N-methyl formamide > Acetamide > Formamide > Urea.

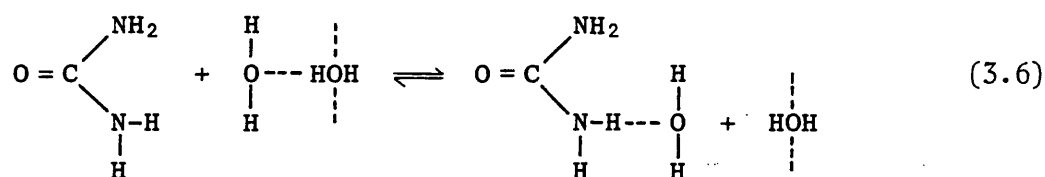
It can be seen that the behaviour of formamide as a base resembles that

Nitrogen hyperfine coupling constants [$A(^{14}\text{N})$] for DTBN in aqueous solutions of amide type bases as a function of the molefraction (m.f.) of added co-solvents.



of methanol, as far as a reduction in $A(^{14}\text{N})$ of DTBN is concerned. On the other hand, t-butylamine seems as powerfully basic as HMPA.

The results can be understood in terms of accepted structures of the acid amides and urea. These compounds are known to act as both weak acids and weak bases, with the N-C bond behaving as a partial double bond.³⁸ Delocalisation of the nitrogen lone-pair onto the carbonyl carbon of urea is expected to make the amide protons acidic in nature. Addition of urea to an aqueous solution is expected to result in the uptake of free lone-pairs by the -NH_2 protons and an uptake of $(\text{OH})_{\text{free}}$ by the basic carbonyl group. The -NH_2 protons can therefore be pictured as generating $(\text{OH})_{\text{free}}$ groups by equilibrium (3.6).

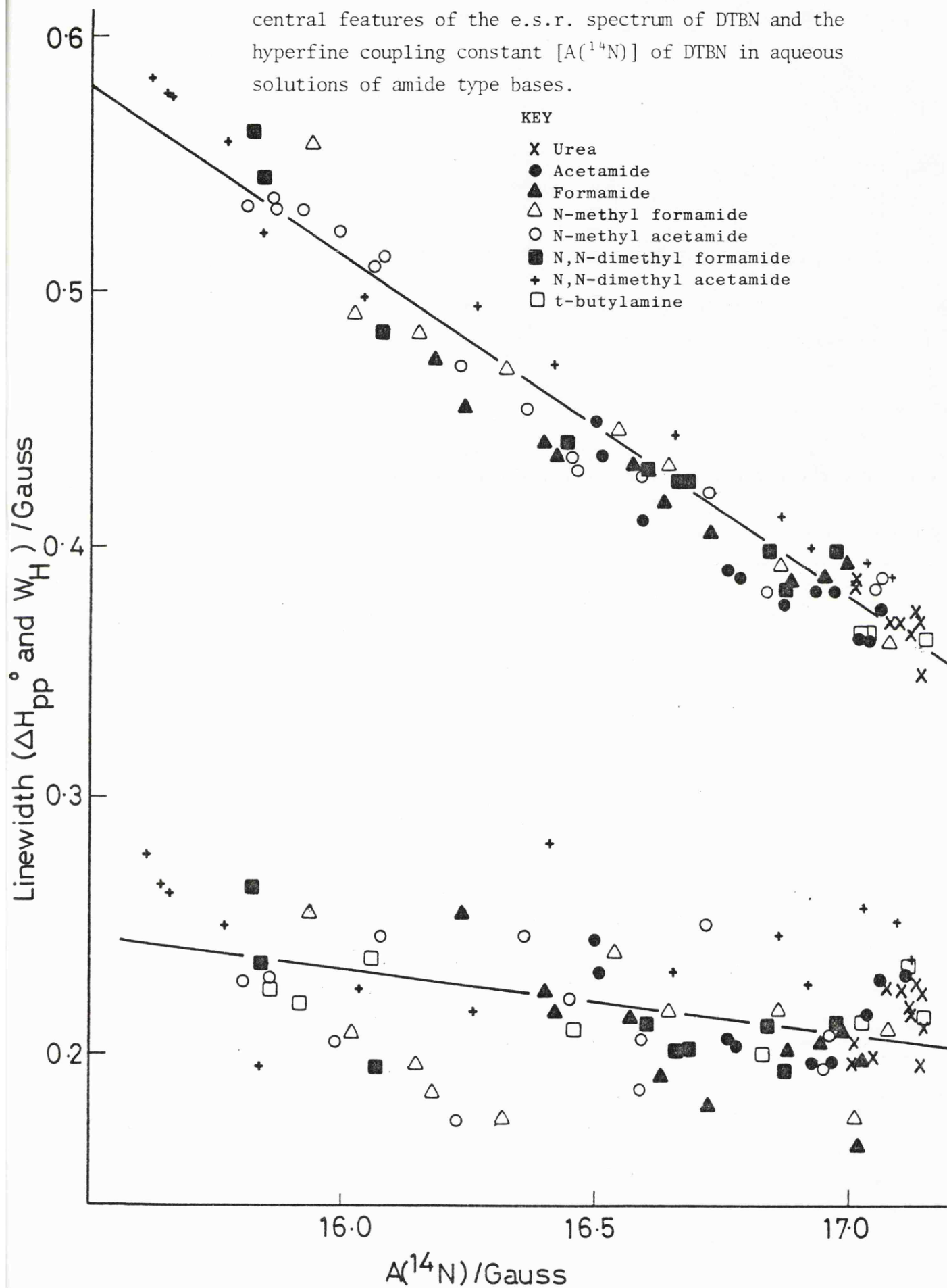


The fall in $A(^{14}\text{N})$ of DTBN in aqueous solution when urea is added can be understood, if the carbonyl group of urea is more successful in scavenging $(\text{OH})_{\text{free}}$ than the amide protons are in generating $(\text{OH})_{\text{free}}$ groups.

The explanation of the acid amide results then follows. Formamide has fewer -NH_2 groups than urea and therefore fewer acidic protons. Hence, it is expected that formamide will be a more powerful base than urea, and will thus produce a greater reduction of $A(^{14}\text{N})$, when added to aqueous solutions of DTBN. Progressive methylation of the amine group further reduces the number of acidic protons and increases the basicity of the acid amide. Thus, the efficiency of dimethyl acetamide and DMF in reducing $A(^{14}\text{N})$ of DTBN in aqueous solution can be understood.

Figure 3.14

Correlation between the linewidths (ΔH_{pp}^0 and W_H) of the central features of the e.s.r. spectrum of DTBN and the hyperfine coupling constant [$A(^{14}\text{N})$] of DTBN in aqueous solutions of amide type bases.



The acetamides are seen to be more effective in reducing $A(^{14}\text{N})$ than the formamides. This is probably due to the positive inductive effect of the methyl group adjacent to $-\text{CO}$, increasing the basicity of the carbonyl of acetamide. The rapid fall in $A(^{14}\text{N})$ seen when *t*-butylamine is added to an aqueous solution of DTBN, is thought to be due to rapid uptake of $(\text{OH})_{\text{free}}$ by the basic lone-pair localised on the *t*-butylamine nitrogen atom.

Figure 3.14 shows ΔH_{pp}^0 and W_{H} of DTBN in aqueous acid amide solutions as a function of $A(^{14}\text{N})$. In common with earlier results ΔH_{pp}^0 appears to be a linear function of $A(^{14}\text{N})$; in this case the data for all solvents appears to lie on a single line. The W_{H} data is somewhat scattered and consequently no clear dependence of W_{H} on $A(^{14}\text{N})$ can be discerned. This may be partially due to the viscous nature of these solutions limiting the rôle of spin rotation in broadening these lines. The above results were recorded at ambient temperatures and no significant trends in differential linewidth were observed.

Recently, Ramachandran and Balasubramanian³⁹ have produced a report describing the behaviour of 2,2,6,6-tetramethyl-4-piperidone-1-oxyl in water-urea mixtures. The results described by these authors differ significantly from those presented above. Linewidth and τ_{c} measurements were used to confirm that urea is a water structure breaker. Initially, a fall in both W_{H} and τ_{c} is seen, indicating increased motional freedom of the probe and a breakdown in water structure.³⁹ At larger urea concentrations, W_{H} and τ_{c} increase; this is said to reflect complex solvent and solute interactions. The complexity of these results are in strong contrast to the DTBN results presented above. The results presented by these workers³⁹ show some discrepancies when compared with the data of Jolicoeur and Friedman¹⁰

for the same radical in aqueous solvent systems. Certainly, W_H and τ_c are not expected to increase together as shown by Ramachandran and Balasubramanian,³⁹ since at the temperatures of measurement spin rotation is expected to contribute significantly to the linewidths.¹⁰ In other words, τ_c would be expected to increase as W_H falls.

3.6 Conclusions

Jolicoeur and Friedman⁹⁻¹¹ concentrated their efforts on examining changes in τ_c of nitroxide probes in aqueous solutions at ca. 25°C. At ambient temperatures, the differences in linewidth of the three nitrogen hyperfine features of the e.s.r. spectra of nitroxide free radicals are small and the experimental errors are large. This and the inaccuracies involved in determining the linewidths of the proton hyperfine components makes the final value of τ_c unsure. The results presented in this thesis confirm that evaluation of τ_c of DTBN in aqueous solutions at ca. 25°C, provides little insight into the nature of the solvent media. If the temperature is reduced to ca. 0°C, then the changes in τ_c as the solvent composition is altered become more obvious. In view of this lack of sensitivity of τ_c to changes in solvent composition at ambient temperatures, the results presented by Ramachandran and Balasubramanian³⁹ are surprising. These authors³⁹ measured τ_c of 2,2,6,6-tetramethyl-4-piperidone-1-oxyl, TEMPOO, in aqueous urea solutions at 27°C, and used the results to propose changes in the structure of water on addition of urea.

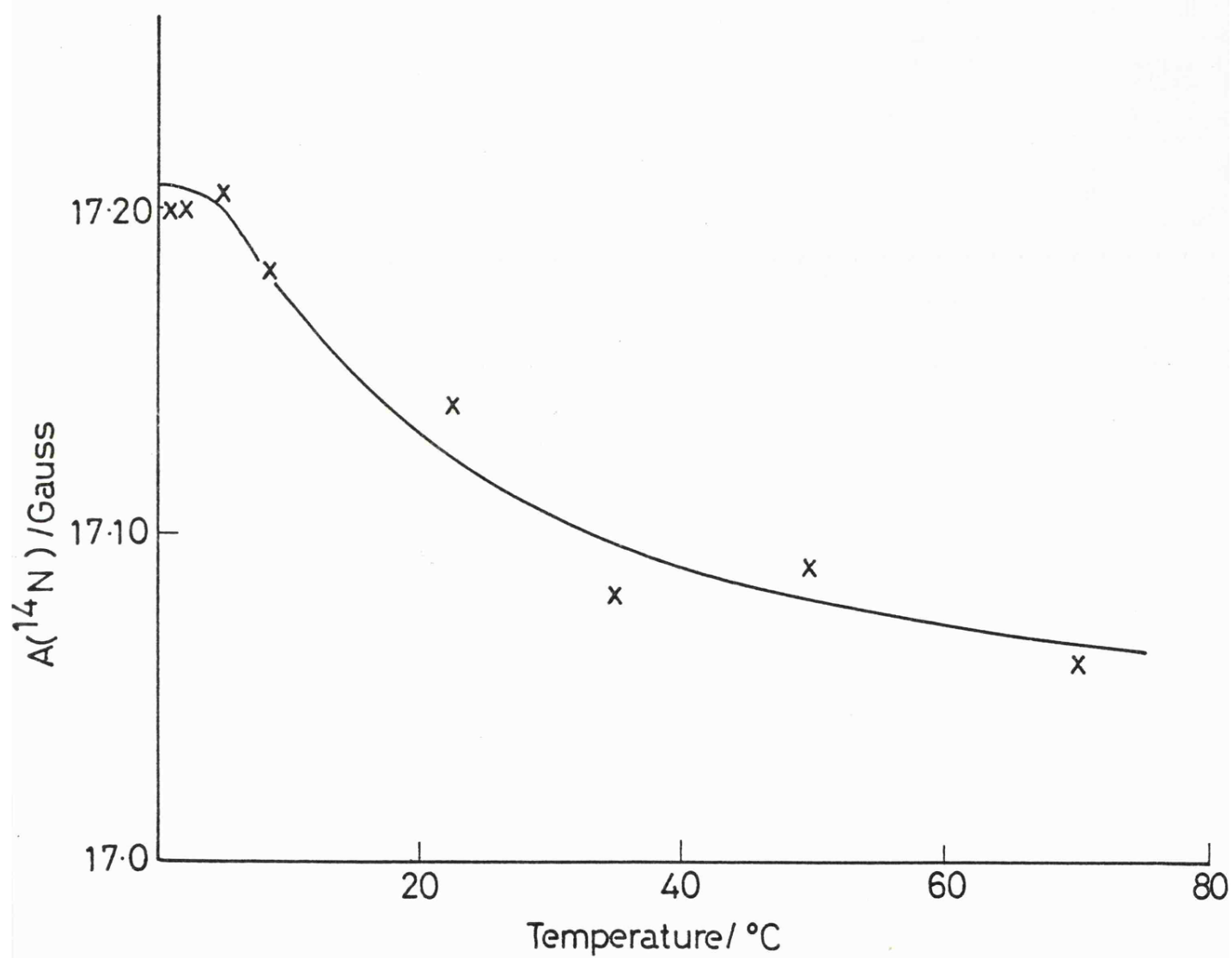
The current work suggests that $A(^{14}\text{N})$ is the most sensitive of the e.s.r. parameters of DTBN, to changes in solvent composition. It is also the largest and most easily measured feature of the e.s.r. spectrum of DTBN. Earlier measurements made by Jones⁸ on DTBN and some of the

piperidinic nitroxides in aqueous solution confirm this point. Jolicoeur and Friedman,⁹⁻¹¹ however, did not find $A(^{14}\text{N})$ a useful parameter to measure; these authors were more interested in relaxation information. The present set of results show that at 0°C asymmetric broadening is often important and is enhanced by certain additives. Under these conditions spin rotational effects are small. The anomalously small increase in linewidth as the temperature is raised, seen for DTBN in aqueous or methanolic solutions has been ascribed to the effects of hydrogen bonding reducing the mobility of the probe.

Jolicoeur and Friedman¹¹ propose that 2,2,6,6-tetramethyl-piperidine-1-oxyl, TEMPO, rotates more freely at ca. 0°C than it does at ca. 25°C. This conclusion was based on an increase in linewidth observed near the freezing point. These authors¹¹ pictured the radical as freely rotating within a clathrate cage, and suggested that this was "the strongest and most direct evidence to date which tends to support the clathrate model of hydration of hydrophobic solutes in liquid water". Such a model requires the probe to be non-hydrogen bonded and hence free to rotate within its host cage. Thus, a fall in $A(^{14}\text{N})$ of the probe in aqueous solution should be seen, as the temperature approaches freezing. A plot of $A(^{14}\text{N})$ of DTBN in water as a function of temperature is shown in figure 3.15; this plot shows no fall in $A(^{14}\text{N})$ as the temperature approaches 0°C. The results presented in figure 3.7 show that the increase in linewidth of DTBN in aqueous solution as the temperature approaches 0°C, is due to an increase in asymmetric broadening. This is consistent with the view that DTBN enjoys less freedom of rotation at ca. 0°C than it does at ca. 25°C, as would be expected if the probe were hydrogen-bonded to the cage wall. The increase in asymmetric broadening observed on addition of t-butanol

Figure 3.15

Changes in $A(^{14}\text{N})$ with temperature for aqueous solutions of DTBN.



is consistent with this view.

Both the current work and the work of Jolicoeur and Friedman^{10,11} employ a model in which the nitroxide probe can exist in two states. The model of Jolicoeur and Friedman,^{10,11} pictures the probe as being in different rotational states in the vicinity of a hydrophobic cosolvent molecule and in bulk water. This model involves no changes in the spectral parameters of the probe. The current work suggests that in a protic solvent medium the probe can exist in hydrogen bonded and non-hydrogen bonded forms as proposed in equilibrium 3.5. Addition of a cosolute to an aqueous solution of DTBN is thought to modify the balance of equilibrium 3.5, by changing the concentration of (OH)_{free} in the solvent. The balance of hydrogen-bonded and "free" nitroxide, should then be reflected in the time-averaged values of $A(^{14}\text{N})$ recorded by e.s.r.

Ramachandran and Balasubramanian³⁹ have used their e.s.r. results to conclude that urea exerts a disruptive influence on the structure of liquid water. The dangers in ascribing water structure making or breaking properties to a given solute have been discussed by Jackson and Symons.⁴⁰ The results presented in this thesis provide no evidence that urea acts as a structure breaker. The data presented in figures 3.13 and 3.14 can be fully explained in terms of the acid-base properties of the cosolvent, and do not require that the cosolvent disrupts water structure. The commonly accepted mixture models of liquid water predict that urea should exhibit structure-breaking properties. Basically, the planar geometry of urea is thought to inhibit interactions with the tetrahedrally co-ordinated "bulky" or structured form of water. Thus, the urea is expected to interact with the "dense" or less structured form of water. This is expected to tilt the equilibrium between the

bulky and dense forms of water, in favour of the dense form producing a structure breaking effect.³⁴ The model of Symons,²⁹ however, does not predict that urea should be a water structure-breaker, since the planar molecule should merely knit into the hydrogen-bonded water "lattice".

REFERENCES TO CHAPTER THREE

1. M. C. R. Symons, Pure and App. Chem., 1977, 49, 13.
2. R. M. Dupeyre, H. Lemaire and A. Rassat, Tetrahedron Letters, 1964, 27-28, 1775.
3. B. Knaeur and J. J. Napier, J. Am. Chem. Soc., 1976, 98, 4395.
4. G. Poggi and C. S. Johnson, J. Mag. Resonance, 1970, 3, 436.
5. J. S. Hwang, R. P. Mason, L. P. Hwang and J. H. Freed, J. Phys. Chem., 1975, 79, 489.
6. M. P. Eastman, R. G. Kooser, M. R. Das and J. H. Freed, J. Chem. Phys., 1969, 51, 2690.
7. M. P. Eastman, G. V. Bruno and J. H. Freed, J. Chem. Phys., 1970, 52, 2511.
8. D. Jones, Ph.D. Thesis, Leicester University, 1972.
9. C. Jolicoeur and H. L. Friedman, J. Phys. Chem., 1971, 75, 165.
10. C. Jolicoeur and H. L. Friedman, Ber. Bunsenges. Physik. Chem., 1971, 75, 248.
11. C. Jolicoeur and H. L. Friedman, J. Solution Chem., 1974, 3, 15.
12. A. K. Hoffmann, A. M. Feldman, E. Gelblum and W. G. Hodgson, J. Am. Chem. Soc., 1964, 86, 639.
13. R. W. Kreilick, J. Chem. Phys., 1966, 45, 1922.
14. K. H. Hausser, H. Brumner and J. C. Jochims, Mol. Phys., 1966, 10, 253.
15. R. W. Kreilick, J. Chem. Phys., 1967, 46, 4260.
16. R. Briere, H. Lemaire, A. Rassat, P. Rey and A. Rousseau, Bull. Soc. Chim. (France), 1967, 34, 4479.
17. N. M. Atherton and S. J. Strach, J.C.S. Faraday II, 1972, 68, 374.
18. M. K. Ahn, J. Chem. Phys., 1976, 64, 134.
19. A. H. Cohen and B. M. Hoffman, J. Am. Chem. Soc., 1973, 95, 2061.
20. A. H. Cohen and B. M. Hoffman, J. Phys. Chem., 1974, 78, 1313.
21. I thank Professor M. J. Perkins for the gift of a small sample of d⁹ t-nitrosobutane.

22. R. E. Cramer, P. L. Dahlstrom and H. Heya, J. Phys. Chem., 1975, 79, 376.
23. Y. Murata and N. Matanga, Bull. Chem. Soc. Japan, 1971, 44, 354.
24. R. S. Drago, G. C. Vogel and T. E. Needham, J. Am. Chem. Soc., 1971, 93, 6014.
25. Y. Y. Lim and R. S. Drago, J. Am. Chem. Soc., 1971, 93, 891.
26. I. Monishma, K. Endo and T. Yonezawa, J. Chem. Phys., 1973, 58, 3146.
27. A. T. Bullock and C. B. Howard, J.C.S. Faraday I, 1977, 73, 465.
28. A. S. Kabankin, G. M. Zhidomirov and A. L. Buchachenko, J. Mag. Res., 1973, 9, 199.
29. M. C. R. Symons, Phil. Trans. Roy. Soc. Lond., 1975, B272, 13.
30. B. Kingston and M. C. R. Symons, J.C.S. Faraday II, 1973, 69, 978.
31. M. Y. Wen and H. G. Hertz, J. Solution Chem., 1972, 1, 17.
32. M. C. R. Symons and M. J. Blandamer, "Hydrogen Bonded Solvent Systems" ed. A. K. Covington and P. Jones, Taylor & Francis, London, 1968.
33. S. Westmeier, Chem. Techn., 1977, 29, 218.
34. F. Franks in "Water - A Comprehensive Treatise, Vol. 2", Ed. F. Franks, Plenum Press, New York, 1973, pp.6-19.
35. E. G. Finar, F. Franks and M. J. Tait, J. Amer. Chem. Soc., 1972, 94, 4424.
36. T. T. Herskovits and T. M. Kelly, J. Phys. Chem., 1973, 77, 381.
37. C. Jolicoeur, P. Bernier, E. Firkins and J. K. Saunders, J. Phys. Chem., 1976, 80, 1908.
38. I. L. Finar "Organic Chemistry Vol. 1 - The Fundamental Principles 5th. Ed.", Longman (London), 1967, p.418.
39. C. Ramachandran and D. Balasubramanian, Chem. Phys. Letters, 1977, 48, 363.
40. S. E. Jackson and M. C. R. Symons, Chem. Phys. Letters, 1976, 37, 551.

CHAPTER FOUR

Ditertiary butyl nitroxide as a Probe for Examining
Aqueous Electrolyte Solutions

CHAPTER FOUR

4.1 Introduction

In the previous chapter the rôle of ditertiary butyl nitroxide, DTBN, in probing solvation effects in aqueous solutions of non-ionic solutes was examined. It is desirable to extend the study of solvation effects using nitroxides as spin-probes, to incorporate studies of solutions containing electrolytes. The usefulness of spectroscopy in probing the nature of ionic solutions has already been discussed. E.s.r. has proved to be useful in examining solvation effects in electrolytic solutions, especially when ion-pairing is of importance.¹⁻² Several ionic-radicals³⁻⁵ have themselves proved to be useful spin-probes in evaluating solvation effects.

Recently, nitroxides have been used to investigate ionic solvation. Several researchers⁶⁻⁹ have used nitroxide probes to examine solutions containing ionic surfactants. Rassat et alia¹⁰ have shown that $A(^{14}\text{N})$ of nitroxides in aqueous solution is sensitive to the addition of an electrolyte. Small cations such as lithium were found to favour the hydrogen-bonded form of the nitroxide in aqueous solution as manifested by an increase¹⁰ in $A(^{14}\text{N})$. Large cations, such as the tetra-ethyl-ammonium ion were found to reduce the amount of hydrogen-bonded nitroxide and therefore reduce $A(^{14}\text{N})$. Anions were found to be less effective in modifying $A(^{14}\text{N})$ of a nitroxide in aqueous solution, than cations.¹⁰ Studies of ion-pairing between cationic and anionic nitroxide radicals have also been made.¹¹ In their studies of hydrophobic effects in aqueous solution, Jolicœur and Friedman^{12,13} have examined the e.s.r. spectra of several nitroxides in aqueous solutions containing certain bulky ions. This work^{12,13} was concerned mainly with relaxation data

and few A(^{14}N) results were reported.

The virtues of DTBN as a spin probe have already been mentioned. It is hoped that the present work will examine solvation effects in solutions containing electrolytes in more detail than earlier investigations.^{10,12,13} Solutions of salts in both methanol and water were examined. Near infrared studies monitoring the first overtone O-H stretching frequency are available for aqueous and methanolic solutions of a similar range of salts.¹⁴ These measurements should reflect the same solvation changes as the e.s.r. results. A comparison of the near infrared and e.s.r. data is included in the current work.

4.2 Experimental Details

Ditertiary butyl nitroxide was purchased from Eastman. Water was doubly distilled from alkaline permanganate under nitrogen. Methanol was refluxed for 30 minutes over magnesium activated with iodine and then fractionated. All salts were dried under vacuum at temperatures between 35°C and 200°C for at least 24 hours, and stored over dry phosphorous pentoxide in a vacuum desiccator.

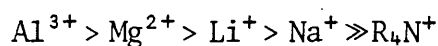
All samples for e.s.r. were deoxygenated prior to measurements being taken. The aqueous samples were degassed by purging with nitrogen for at least half an hour. Methanol was degassed on a vacuum line by the freeze-pump-thaw technique in an apparatus described in chapter 5. The methanolic samples were then made up under an atmosphere of nitrogen and the final samples were placed in capillary tubes. Prior to removal from the nitrogen atmosphere, each capillary was loaded into a 2mm borosilicate tube, which was then sealed using a tight piece of rubber tubing and a 2mm borosilicate stopper. In order to prevent line-broadening due to Heisenberg spin exchange, the concentration of DTBN

in each sample was ca. $5 \times 10^{-5} \text{ mol dm}^{-3}$.

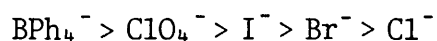
All e.s.r. spectra were measured on Varian E3 or E109 spectrometers. The spectra were calibrated using a $5 \times 10^{-5} \text{ M}$ solution of DTBN in water ($A(^{14}\text{N}) = 17.14 \text{ G}$, $\Delta H_{\text{pp}}^{-1} = 0.370 \text{ G}$). Temperatures were maintained to $\pm 1^\circ$ using a Varian V6040 variable temperature accessory. The sample temperatures were checked at the beginning and end of each run using a Comark 1625 electronic thermometer. N.m.r. spectra were recorded using a Jeol PS100 spectrometer. All UV-visible spectra were recorded using a Pye-Unicam SP700 spectrometer.

4.3 Methanolic Salt Solutions

In protic solvents, $A(^{14}\text{N})$ of DTBN can be used as a guide to the nature of probe-solvent interactions and hence provide information concerning the solvent environment. A high $A(^{14}\text{N})$ corresponds to a high proportion of probe molecules being in the hydrogen-bonded state. In the previous chapter, it was suggested that in methanol ca. 50% of DTBN molecules are in the hydrogen-bonded state and ca. 50% are non-hydrogen bonded. The effect of adding an electrolyte to a methanolic solution of DTBN is shown in figure 4.1. Both the anion and cation can be seen to modify $A(^{14}\text{N})$ of the probe. The magnitude of $A(^{14}\text{N})$ follows the order:



for cations, where R_4N^+ represents the tetraalkylammonium cations. For anions, $A(^{14}\text{N})$ follows the order:



where BPh_4^- represents the tetraphenylboride anion.

Solutions of DTBN in protic solvents are expected to be effected

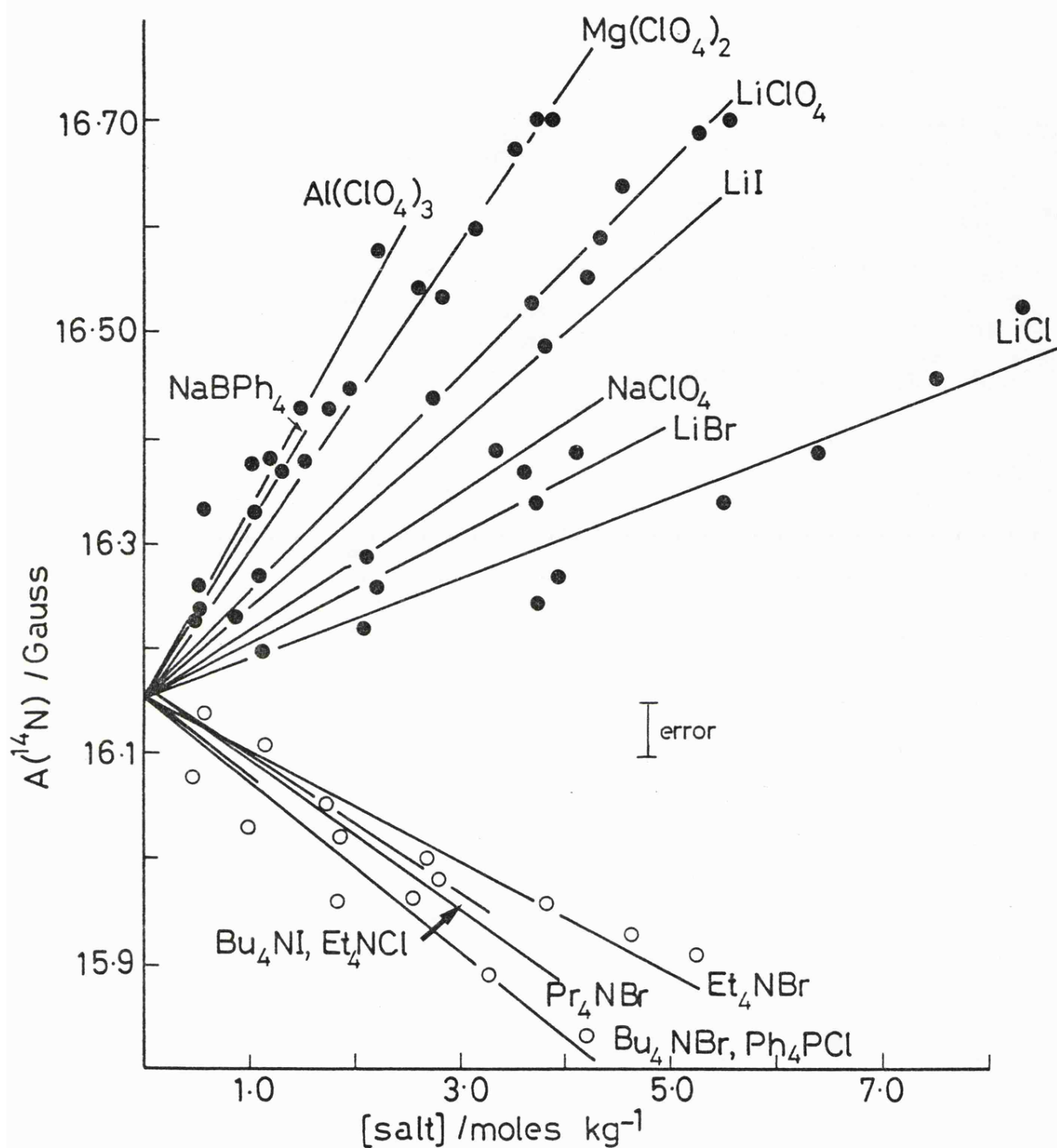
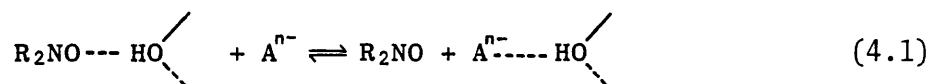


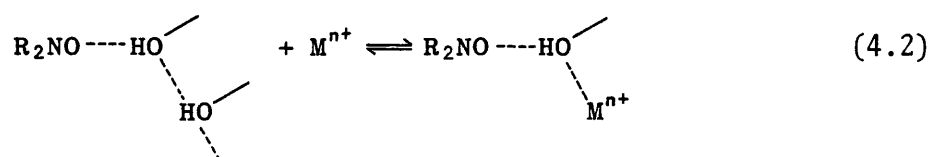
Figure 4.1

Hyperfine coupling constants $A(^{14}\text{N})$ for DTBN in methanolic solutions as a function of the molality of added electrolytes. [Some data points have been omitted for clarity, especially in the low salt concentration region. This applies to all figures.]

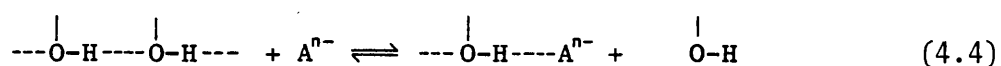
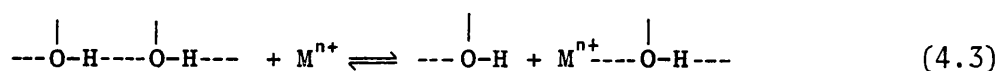
by the addition of salts in several ways. The anion is expected to compete with the nitroxide for free hydroxyl groups, as shown in equilibrium 4.1.



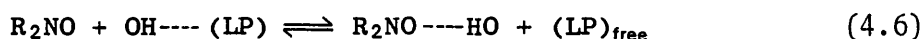
Interaction with cations is quite different, here the probe is thought to interact with the primary solvation shell of the cation.



In addition to these interactions, the salts are expected to adjust the balance of unbound hydroxyl groups, (OH)_{free} in the solvent. The cation is expected to interact with the lone-pairs of the solvent, thereby generating (OH)_{free} groups, whilst the anion is expected to generate free lone-pairs, (LP)_{free}. This situation is depicted in equilibria 4.3 and 4.4:



The (OH)_{free} and (LP)_{free} generated by equilibria 4.3 and 4.4 will recombine to give bulk solvent, if the solvation numbers of the anion and cation are equal. In this case the equilibrium concentrations of (OH)_{free} and (LP)_{free} will not change much. If there is a significant difference in the solvation numbers of the positive and negative ions, then the nitroxide probe should detect a change in the concentration of (OH)_{free}. The nitroxide can then be pictured as interacting with the solvent in the following manner:



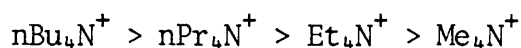
The anion effect is expected to be important even for weakly solvated anions such as the perchlorate or tetrafluoroborate ions,^{15,16} except in concentrated solutions where there is a real shortage of solvent molecules. When either the cation or anion is either weakly solvated or completely non-solvated, equilibria 4.3 to 4.6 are expected to be most important. Small highly charged cations are expected to influence $A(^{14}N)$ of DTBN, through equilibrium 4.2. Since, in methanolic solution the equilibrium between the non-hydrogen bonded and hydrogen-bonded form of the radical, is thought to be delicately balanced, $A(^{14}N)$ of DTBN in this solvent should be sensitive to the above processes. In aqueous solution DTBN is believed to be almost completely hydrogen-bonded, and hence less sensitive to changes in solvation, due to the presence of electrolytes.

The above equilibria can be used to explain the variations in $A(^{14}N)$ observed for DTBN in methanolic solutions of electrolytes. The bulky ions of low charge, such as R_4N^+ and BPh_4^- can be assumed to be unsolvated and therefore should play no part in equilibria 4.3 and 4.4. Thus, the large increase in $A(^{14}N)$ observed for DTBN in methanolic solutions of sodium tetraphenylboride, is probably due to the cation generating $(OH)_{free}$ via equilibrium 4.3, resulting in a larger proportion of hydrogen-bonded probe through equilibrium 4.5. Similarly, the fall in $A(^{14}N)$ of the probe in methanolic tetraalkylammonium salt solutions is thought to be purely an anion effect via equilibria 4.4 and 4.6. The large increases in $A(^{14}N)$ observed on addition of small highly charged cations, such as Li^+ , Mg^{2+} and Al^{3+} are thought to be mainly due to equilibrium 4.2.

These results fit in well with the e.s.r. data reported above. The gain in (OH) weakly bound seen in the near infrared spectrum of sodium tetraphenylboride in methanol, corresponds to the increased proportion of hydrogen-bonded DTBN observed for this system. The smaller increase in $A(^{14}\text{N})$ observed for DTBN in methanolic solutions of perchlorates can be explained in terms of the weakly hydrogen-bonded unit observed by infrared measurements.^{14,20,21}

4.4 Aqueous Salt Solutions

Unlike methanol, water does not possess an excess of free lone-pairs, hence aqueous solutions should be richer in (OH)_{free} groups than their methanolic counterparts.¹⁹ Thus, the addition of an electrolyte to an aqueous solution of DTBN may be expected to produce changes in $A(^{14}\text{N})$, which differ from those described in the previous section. Figure 4.2 shows $A(^{14}\text{N})$ of DTBN in aqueous solution as a function of added electrolyte. The figure shows that $A(^{14}\text{N})$ of the probe in aqueous solution is largely independent of the nature of the anion. This observation is in good agreement with the earlier work of Rassat.¹⁰ The small highly charged cations show a reduction in their power to increase $A(^{14}\text{N})$ when the solvent is changed from methanol to water. The tetraalkylammonium ions now give a clear fall in $A(^{14}\text{N})$, the rate of decline following the order:



in aqueous solution. The behaviour of sodium tetraphenylboride is somewhat anomalous, the increase in $A(^{14}\text{N})$ expected for DTBN in aqueous solutions of this salt is not seen, a reduction in $A(^{14}\text{N})$ being observed instead.

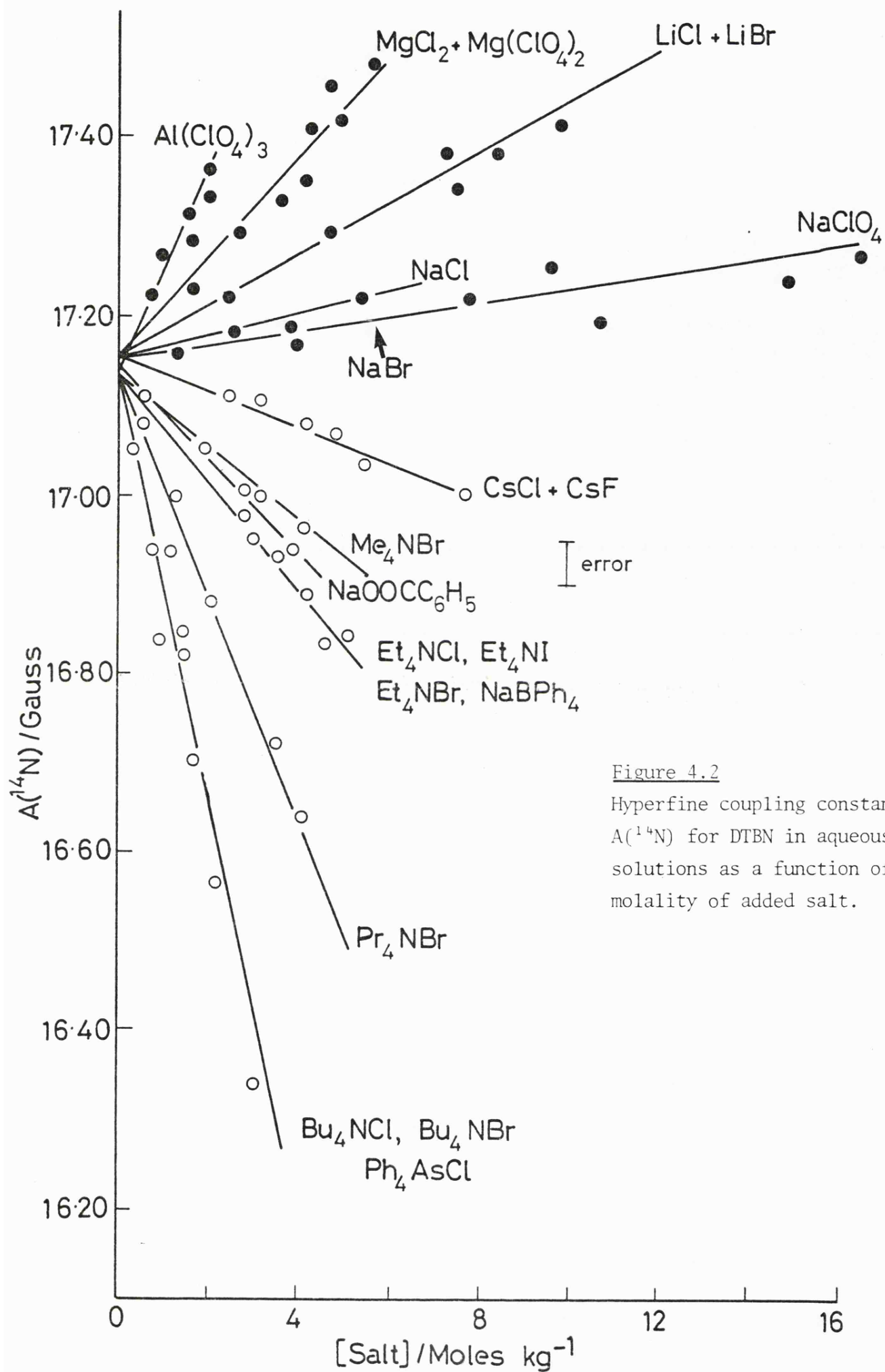


Figure 4.2

Hyperfine coupling constants $A(^{14}\text{N})$ for DTBN in aqueous solutions as a function of the molality of added salt.

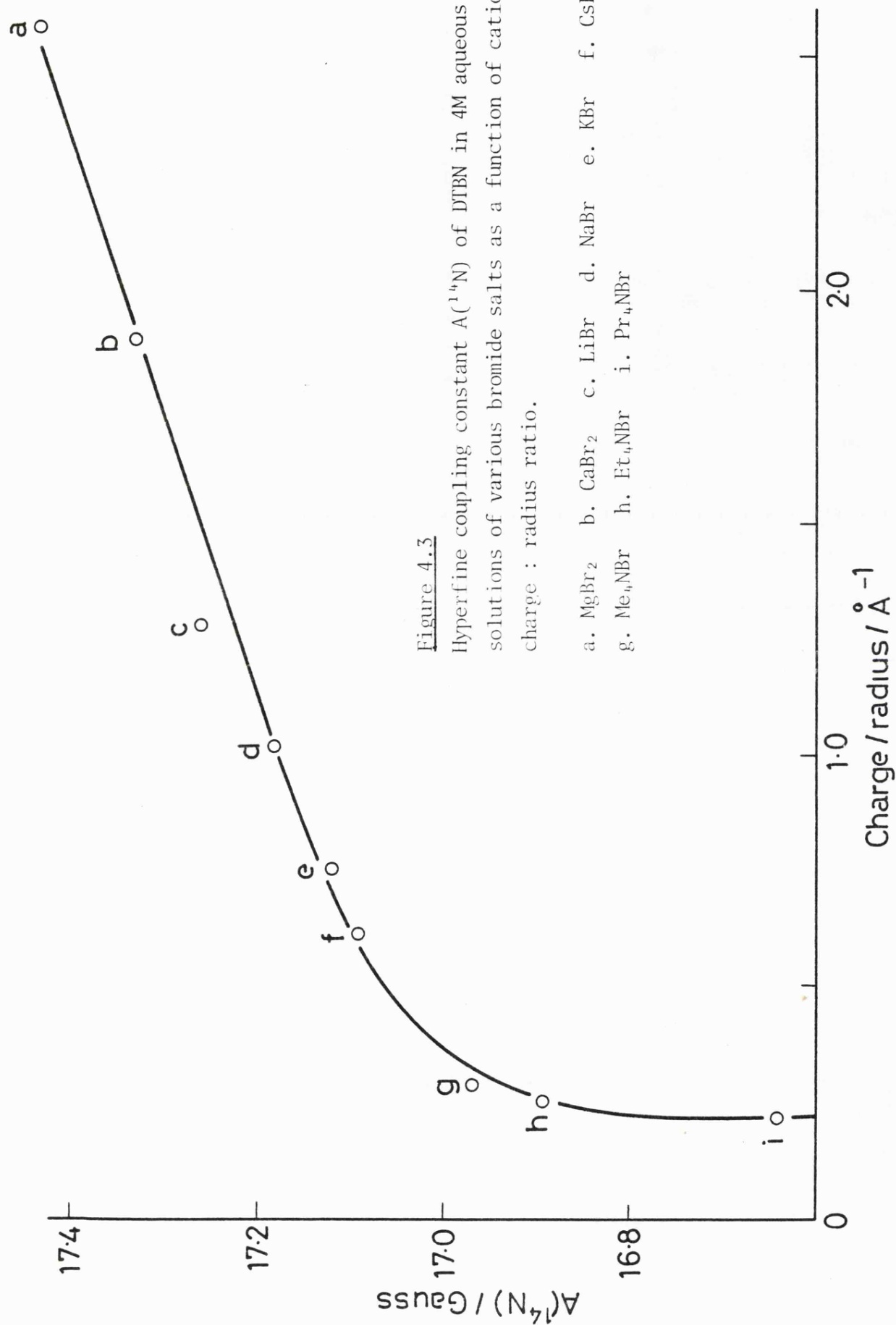


Figure 4.3

Hyperfine coupling constant $A(^{14}\text{N})$ of DTBN in 4M aqueous solutions of various bromide salts as a function of cation charge : radius ratio.

a. MgBr₂ b. CaBr₂ c. LiBr d. NaBr e. KBr f. CsBr
g. Me₄NBr h. Et₄NBr i. Pr₄NBr

In some cases it is possible to analyse spectroscopic data obtained from studies of electrolyte solutions, in terms of separate contributions from the anions and cations. Recent n.m.r.^{22,23} and infrared²⁰ cation shift measurements have shown a correlation with the cation charge : radius ratio. Such a relationship between $A(^{14}\text{N})$ of DTBN in aqueous solutions of various bromide salts and cation charge : radius ratio can be seen in figure 4.3. The cationic radii were obtained from standard sources.^{24,25}

In aqueous solution DTBN is thought to be almost completely in the hydrogen-bonded state, thus the extra $(\text{OH})_{\text{free}}$ groups generated through equilibrium 4.3 on addition of a small highly charged cation are not expected to significantly increase $A(^{14}\text{N})$. This is in marked contrast to the methanol case, when DTBN is thought to be only ca. 50% hydrogen-bonded in the pure alcohol. Thus, any $(\text{OH})_{\text{free}}$ generated by addition of cations should greatly influence $A(^{14}\text{N})$ of DTBN in methanolic solution. In the absence of a worthwhile contribution from $(\text{OH})_{\text{free}}$ generated by equilibrium 4.3, the rise in $A(^{14}\text{N})$ for DTBN in aqueous solutions containing small highly charged cations is expected to be due to equilibrium 4.2. The dramatic fall in $A(^{14}\text{N})$ observed on addition of the tetraalkylammonium cations may be expected to be caused by desolvation of the probe by the anion. This is unlikely, since there is no variation in the rate of fall as the anion is changed. Only the tetraphenylboride or benzoate anions, which are thought to interact with the solvent weakly, if at all, are seen to exhibit a clear anion effect.

There is a clear feature in the near infrared spectrum of aqueous solutions, which can be ascribed to the first overtone O-H stretch of $(\text{OH})_{\text{free}}$ groups. Thus, near infrared measurements on aqueous salt

solutions are expected to give a better guide to the observed variations of $A(^{14}\text{N})$ of DTBN in these solutions, than was the case with the corresponding methanol results. The near infrared data of Jackson¹⁴ is reproduced in figure 4.4. Immediately, it can be seen that sodium tetraphenylboride is efficient in generating $(\text{OH})_{\text{free}}$ in aqueous solution, which conflicts with the drop in $A(^{14}\text{N})$ of DTBN for these solutions seen by e.s.r. A clear dependence of the concentration of $(\text{OH})_{\text{free}}$ on both the cation and anion in aqueous salt solutions can be seen. Indeed, the infrared measurements obtained for aqueous salt solutions bear more resemblance to the $A(^{14}\text{N})$ measurements made in methanolic solution than to those made in aqueous solution. Figure 4.5 emphasises this point. A direct comparison of the measurements of $A(^{14}\text{N})$ of DTBN in aqueous and methanolic salt solutions is given in figure 4.6.

It is still necessary to account for the lack of sensitivity of $A(^{14}\text{N})$ of DTBN in aqueous solution to the nature of the anion. It is possible that the hydrogen-bonding equilibrium for DTBN in water favours the hydrogen-bonded form of the radical so strongly that the concentration of the anions is insufficient to modify this equilibrium significantly. This does not explain the reduction of $A(^{14}\text{N})$ observed for DTBN in aqueous solutions of the tetraalkylammonium salts. The reduction in $(\text{OH})_{\text{free}}$ concentration observed in the near infrared spectra of these solutions is normally explained in terms of the formation of clathrate cages about the cation.^{26,27} In the case of the DTBN results, enclathration of R_4N^+ may be expected to desolvate the nitroxide, and hence reduce $A(^{14}\text{N})$. Equilibrium 4.1 would then be expected to be more effective in reducing $A(^{14}\text{N})$, since the hydrogen-bonding equilibrium for DTBN should be more delicately balanced. If

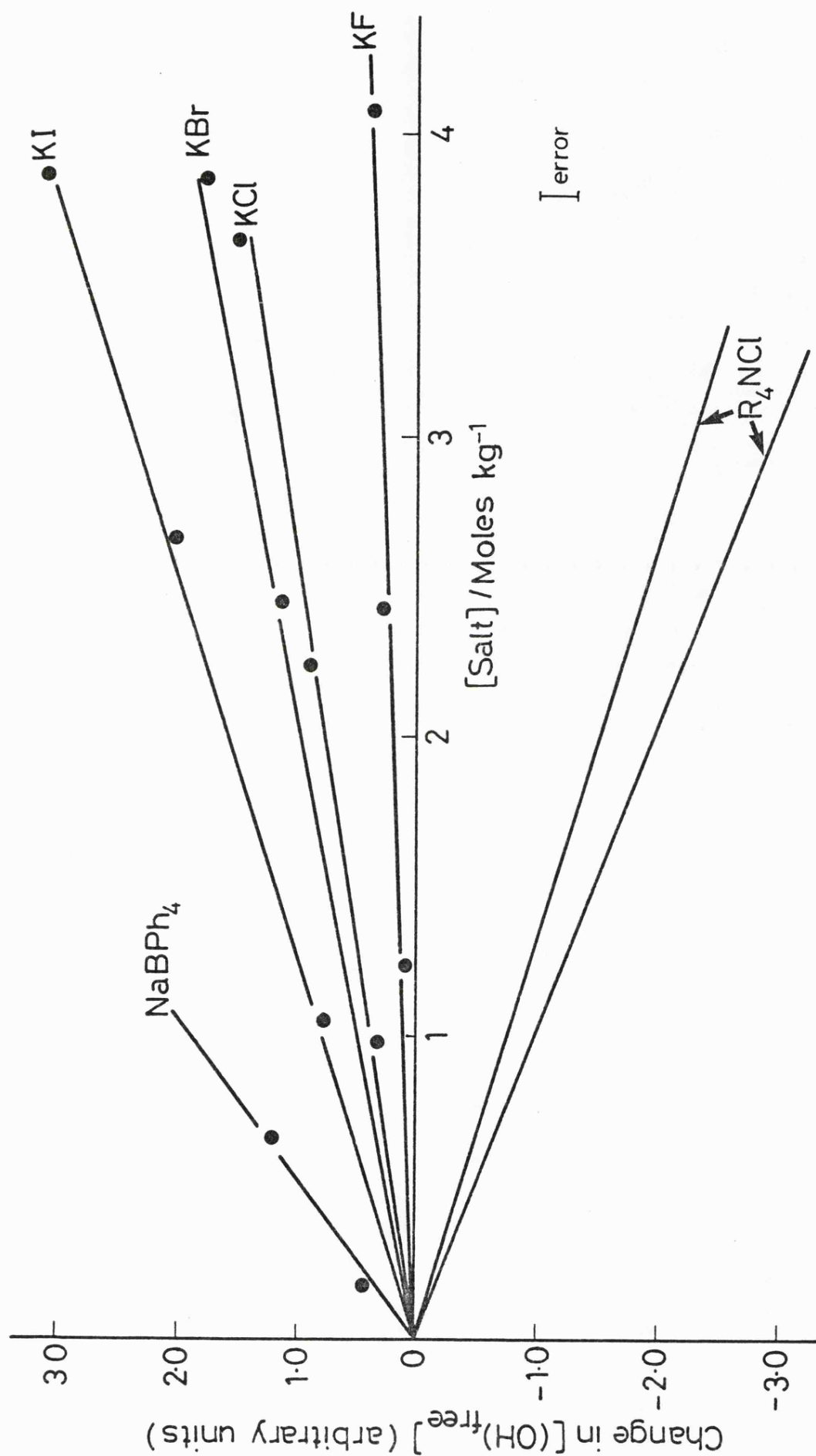


Figure 4.4
Change in $[\text{OH}]_{\text{free}}$ for HOD in D_2O (arbitrary units) as a function of the concentration of added electrolytes. (Taken from ref. 14)

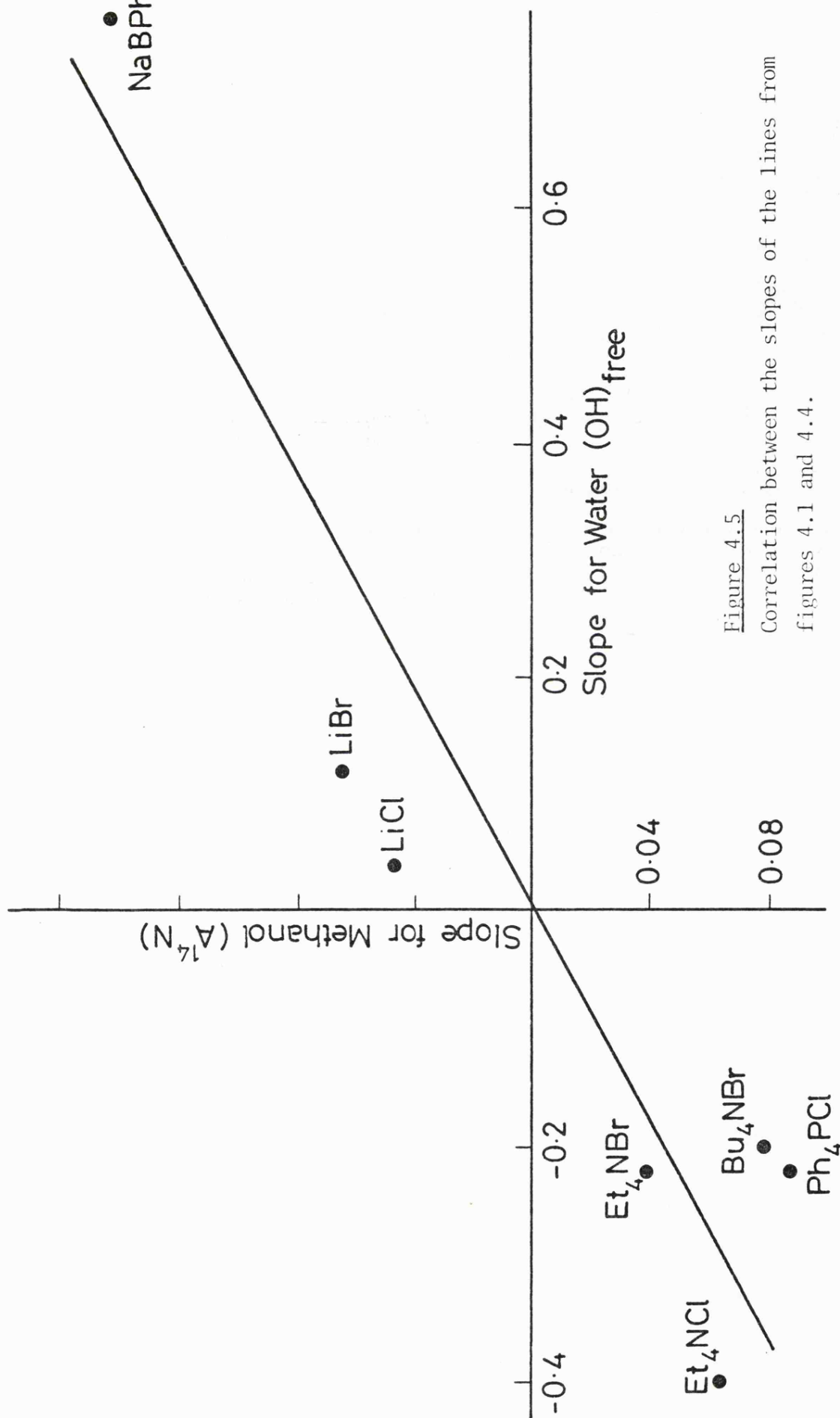
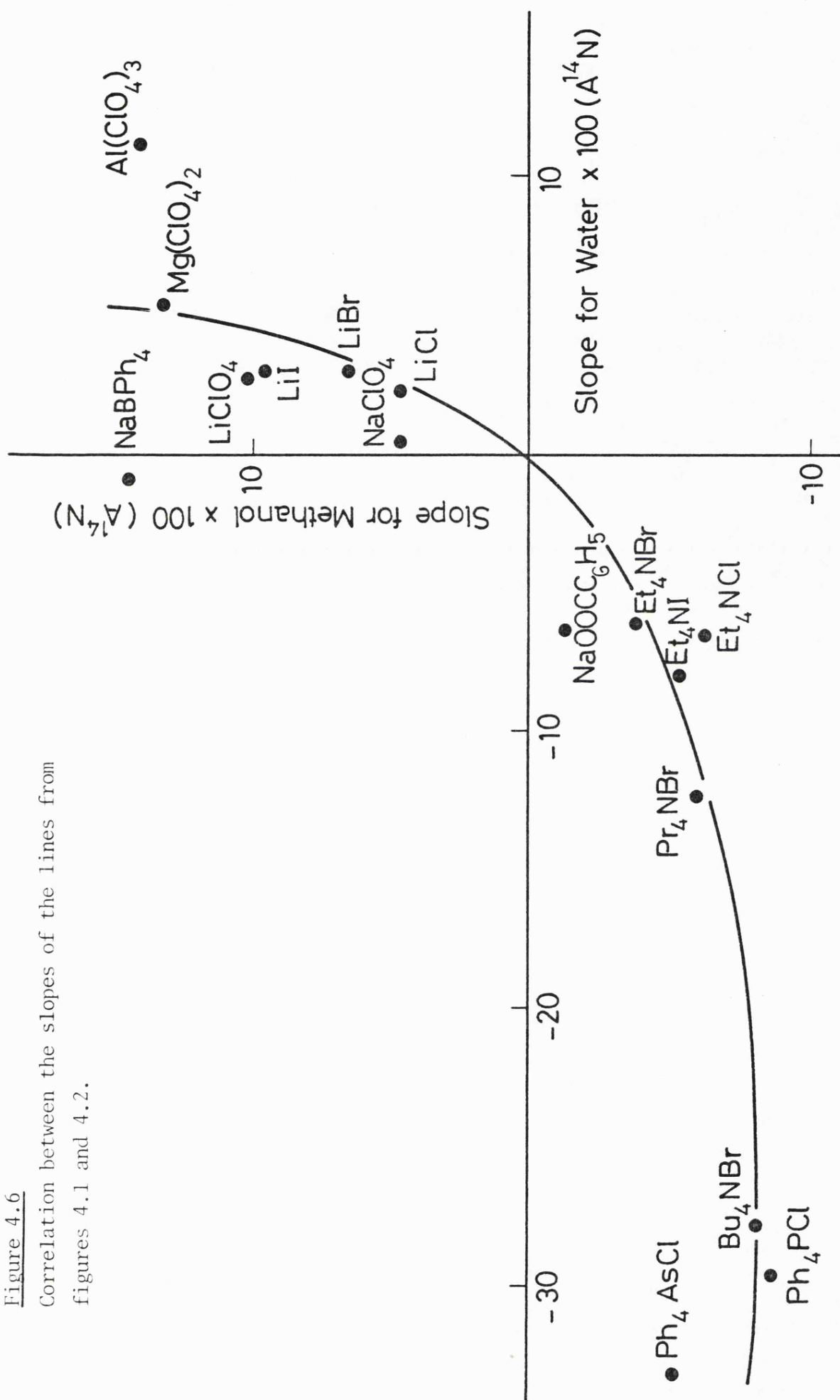


Figure 4.5

Correlation between the slopes of the lines from figures 4.1 and 4.4.

Figure 4.6

Correlation between the slopes of the lines from figures 4.1 and 4.2.



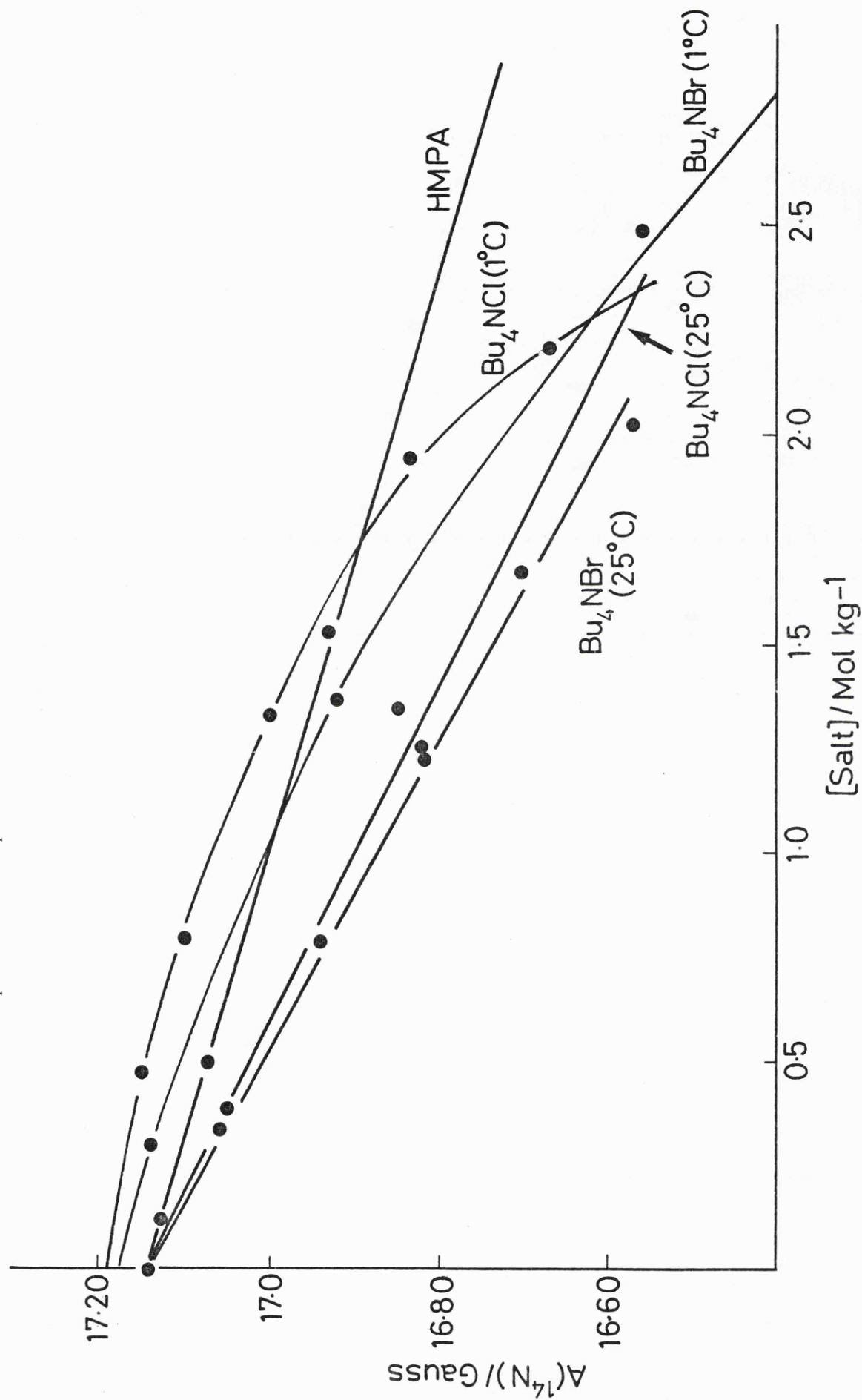
this were the case a clear dependence of $A(^{14}\text{N})$ on the nature of the anion would be seen. A modified form of the cage idea may be used to explain the observed results, if cages are allowed to breed cages. In this argument R_4N^+ ions are thought to induce clathrate-type cages of water molecules around themselves, which in turn form templates on which more cages could be built, with the loss of less entropy than usual. The fall in $A(^{14}\text{N})$ can then be ascribed to DTBN molecules existing as guests within a cage, with no hydrogen bonding between the probe and the cavity walls.

The above hypothesis should be treated with caution, but it is the only explanation that could be found which accounts for the observed results. Figure 4.7 shows a plot of $A(^{14}\text{N})$ for DTBN in aqueous solution as a function of added tetra-n-butyl ammonium salt. A clear temperature effect can be observed, with a weaker dependence of $A(^{14}\text{N})$ on added salt in the low concentration range at low temperature. This is similar to the t-butanol-water results described in the previous chapter. Such a comparison may be meaningful, since t-butanol is also thought to be a cage former in aqueous solution. In the region where $A(^{14}\text{N})$ is less sensitive to added nBu_4N^+ , cage breeding is thought to be inefficient due to the low cation concentration. The effect of the anion in reducing $A(^{14}\text{N})$ is also thought to be small in this region. As a sufficiently high concentration of R_4N^+ ions to promote efficient cage-breeding is reached, the observed fall in $A(^{14}\text{N})$ is expected to occur.

Figure 4.7 also reveals that the fall in $A(^{14}\text{N})$ induced by the tetra-n-butylammonium ion is more rapid than that induced by HMPA, the strongest base examined in the previous chapter. If the cage breeding postulate is correct, then cage effects may play a larger rôle in controlling the initial changes in $A(^{14}\text{N})$ found for aprotic solvents than

Figure 4.7

A comparison of the effects of tetra-alkylammonium salts at (1°C and 25°C) on $A(^{14}\text{N})$ of DTBN in water, with that of HMPA. The HMPA data is obtained from the results reported in chapter 3.



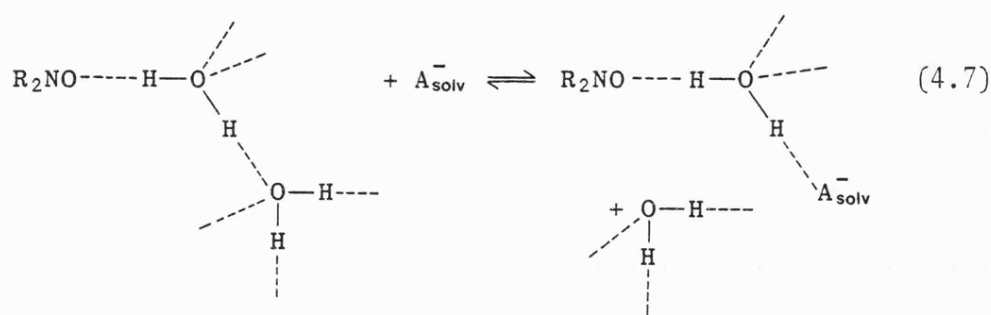
was first thought.

The nature of the interaction between the nitroxide probe and the cation, as depicted by equilibrium 4.2, requires to be examined further. It is necessary to justify the postulate that the probe interacts with the solvation cosphere of the cation, rather than directly with the cation itself. Both methanol and water are expected to exhibit greater power in solvating cations than the nitroxide would; hence a direct interaction between the probe and cation in these solutions seems unlikely. If direct probe-cation interactions did occur, then the e.s.r. spectrum of DTBN in aqueous and methanolic solutions would be expected to exhibit a hyperfine interaction between the unpaired electron and the metallic nucleus. For example, solutions containing ^{27}Al , ($I = \frac{5}{2}$) would be expected to show a spectrum comprising of a sextet of triplets. In the liquid state, this interaction may be averaged to a triplet, but some residual broadening due to the exchange process should then be seen. A clear metal-nitroxide hyperfine interaction has been observed for nitroxides in solutions of the group IIIB metal halides in inert solvents, but this is due to a Lewis acid - Lewis base interaction between the halide and nitroxide.^{28,29} Such solutions are non-ionic in nature.

The e.s.r. spectra of DTBN in aqueous and methanolic salt solutions showed no line-broadening, which could be attributed to averaging of the cation-nitroxide hyperfine interactions, expected if the probe were to be directly bonded to the cation. Several solid state spectra were recorded for DTBN in methanolic glasses containing either aluminium or lithium perchlorates. No evidence of coupling to ^{27}Al or ^7Li could be detected in these glasses, although a rise in A_z is seen as the salt concentration is increased. In the light of these observations the

interaction of DTBN with the solvent cosphere of the cation is favoured as an explanation of the cation effect given in equilibrium 4.2.

It is possible that an anion may also effect $A(^{14}\text{N})$ by a method analogous to that shown in equilibrium 4.2. This is probably only significant in aqueous solutions, but may make a small contribution to the magnitude of $A(^{14}\text{N})$. Such a mechanism is not expected to be large for monovalent anions and is depicted in equilibrium 4.7.



The hydrogen bonds formed between monovalent anions and bulk water are thought to be weaker than those formed between water molecules. This conclusion is reached on the basis of infrared spectroscopic measurements and predicts that the hydrogen-bond formed between the probe and water on the right hand side of equilibrium 4.7 is stronger than that formed on the left hand side. This means that equilibria 4.1 and 4.7 have opposing effects on $A(^{14}\text{N})$. This should produce an increase in $A(^{14}\text{N})$ following the order:



however other effects dominate and no such dependence is seen.

Oakes et alia³⁰ have reported a study of the e.s.r. spectra of nitrobenzene radical anions in alcoholic media. Cations such as lithium or sodium produced a small increase in $A(^{14}\text{N})$, which levels off as the salt concentration approaches 0.005 m.f. The tetraalkylammonium

salts were seen to reduce $A(^{14}\text{N})$ of nitrobenzene anions, this fall in $A(^{14}\text{N})$ extending to higher salt concentrations. This effect was attributed to a displacement of the protic solvent environment of the probe by the aprotic R_4N^+ ions. A fall in $A(^{14}\text{N})$ of the nitrobenzene anion would then be seen.³⁰ In view of the DTBN results, this effect may be explained in terms of the action of the anion operating through equilibria 4.1, 4.4 and 4.6. The cation effect, produced by Na^+ and Li^+ , was attributed to the formation of solvent shared ion-pairs. The rôle of contact ion-pairs was discounted due to the low value of $A(^{14}\text{N})$ of the nitrobenzene radicals measured in etherial solutions of these salts. Comparison of these results with those obtained for DTBN suggests that the formation of solvent shared ion-pairs in alcoholic solutions is important. This ion-pairing process is analogous to equilibrium 4.2. The curvature seen for $A(^{14}\text{N})$ of nitrobenzene radical anions in alcoholic solutions containing sodium salts suggests that this equilibrium is strongly balanced in favour of the solvent shared ion-pair.

Linewidth data from studies of nitroxides in aqueous solutions provide relaxation information and some guide to the nature of the solvent. Two types of linewidth effect are usually encountered. If all three lines of the e.s.r. spectrum of DTBN broaden at equal rates, then the line broadening is normally due to spin rotational effects. Asymmetric linewidth increments are observed for DTBN in aqueous solutions at ca. 0°C . These may be due to either the averaging of the anisotropic g and A tensors by the normal motion of the probe or to a chemical exchange process depicted by equilibrium 3.5 of the previous chapter. The spin rotational process is thought to be important for nitroxide molecules, which are not hydrogen-bonded to the solvent.

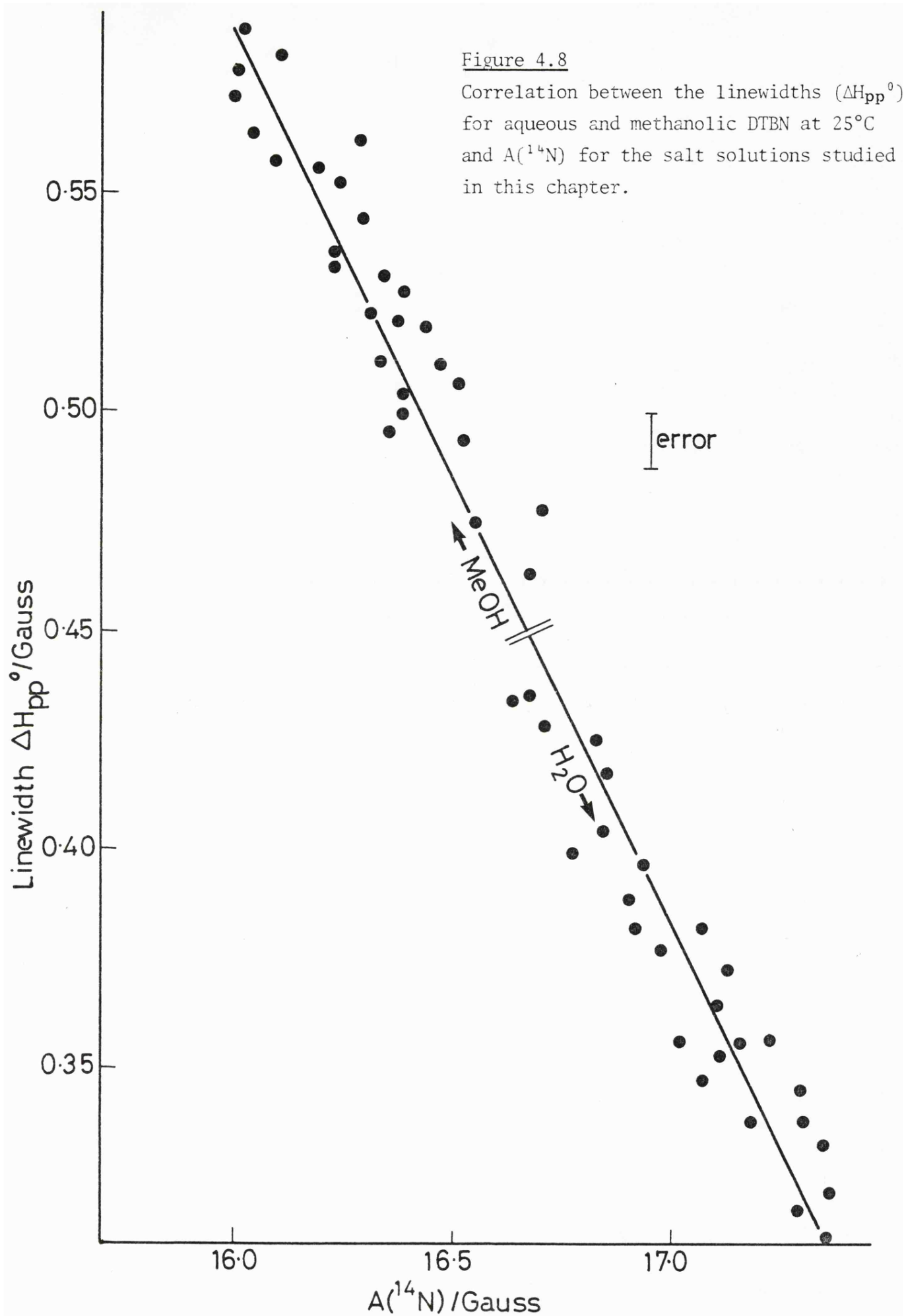
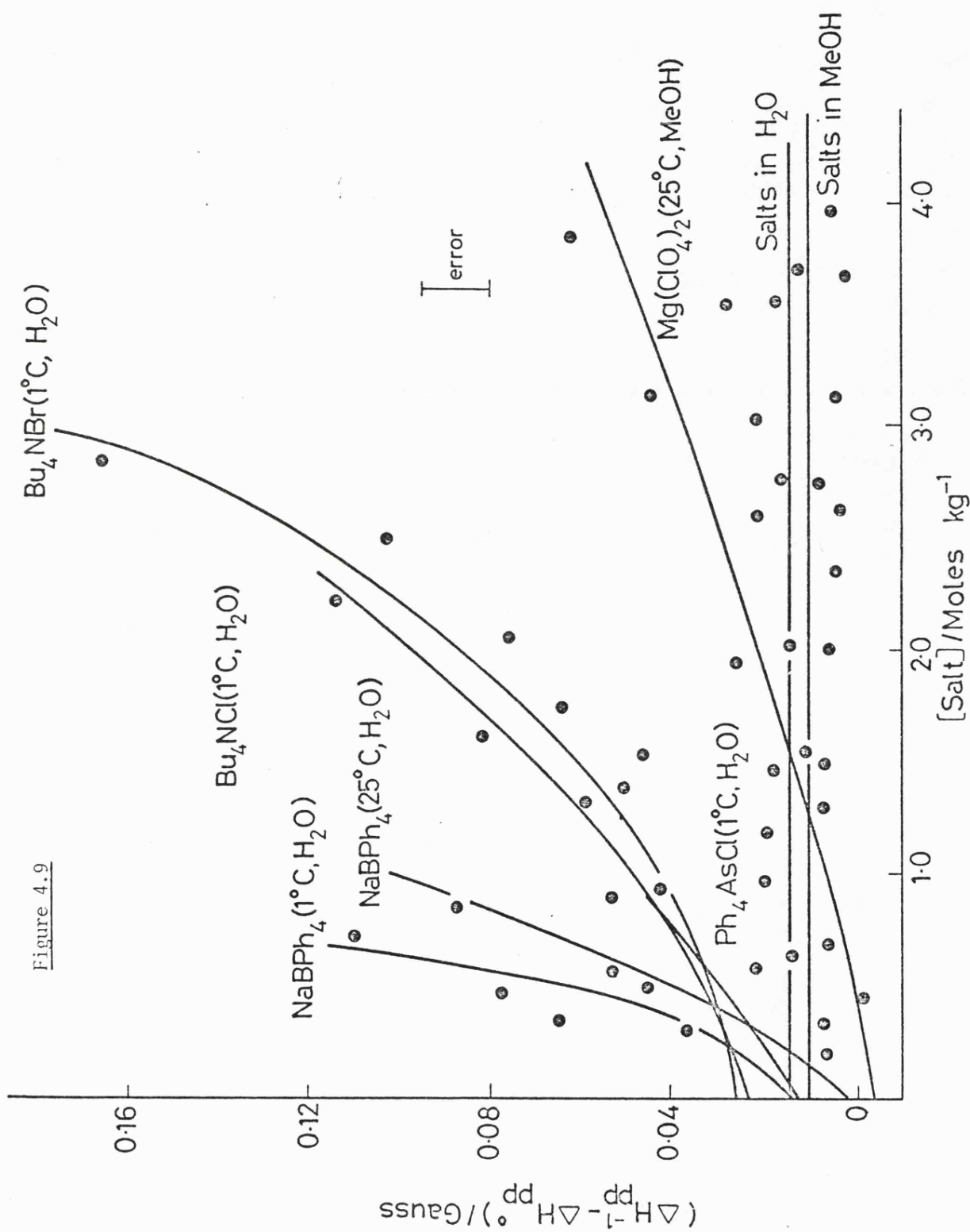


Figure 4.9



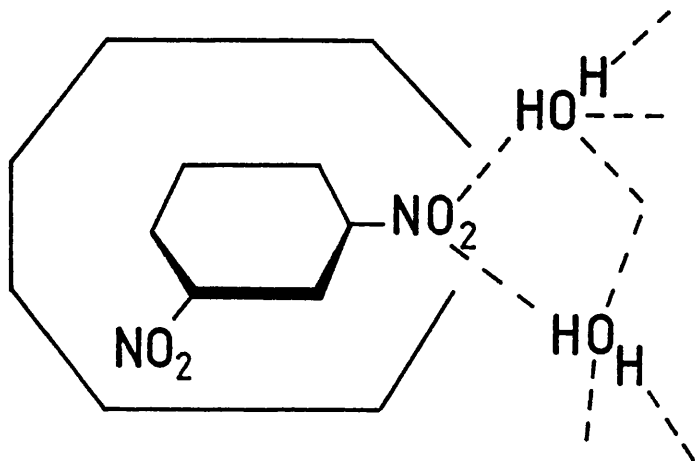
Caption to Figure 4.9

Correlation between linewidth differences ($\Delta H_{\text{pp}}^{-1} - \Delta H_{\text{pp}}^0$) for aqueous and methanolic solutions of DTBN and the concentration of various salts. Salts giving no appreciable change in ($\Delta H_{\text{pp}}^{-1} - \Delta H_{\text{pp}}^0$) include solutions of LiCl, MgCl₂, Mg(ClO₄)₂, LiClO₄, NaClO₄, Ph₄PCl, Ph₄AsCl, nBu₄NBr, nBu₄NCl all in water at 25°C; NaBPh₄ in water at 50°C; and solutions of LiClO₄, NaClO₄, NaBPh₄, Ph₄AsCl, nPr₄NBr, nBu₄NBr, all in methanol at 25°C.

Accurate estimates of τ_J can be obtained only if the effects of super-hyperfine coupling from the alkyl protons of DTBN are accounted for. This is normally done by using computer simulation techniques or perdeuterated radicals. Since the proton hyperfine coupling constant, $A(^1\text{H})$, is inversely proportional to $A(^{14}\text{N})$, the linewidths of the central line (ΔH_{pp}^0) are expected to exhibit an inverse linear dependence on $A(^{14}\text{N})$. The plot of ΔH_{pp}^0 as a function of $A(^{14}\text{N})$, for DTBN in aqueous and methanolic salt solutions, shown in figure 4.8, follows this behaviour. Within the fairly large experimental error, a single straight line is obtained for measurements made in both solvents.

To simplify the analysis, asymmetric line broadening for DTBN in these solutions was recorded as the difference in linewidth, $(\Delta H_{\text{pp}}^{-1} - \Delta H_{\text{pp}}^0)$, between the high and centre field nitrogen envelopes. Figure 4.9 shows a plot of $\Delta H_{\text{pp}}^{-1} - \Delta H_{\text{pp}}^0$ as a function of added salt for DTBN in aqueous and methanolic electrolyte solutions. Normally, the solvent viscosities are expected to control the asymmetric line broadening, but it was not possible to verify that this was the case for DTBN in these solutions. This is because at the low temperatures (ca. 0°C) at which asymmetric line broadening becomes important, it was not possible to obtain the required viscosity data. It seems likely that for all solutions, with the exception of aqueous sodium tetraphenylboride, that viscosity factors control the asymmetric broadening. The excessive asymmetric line broadening observed for nitroxides in aqueous solutions of sodium tetraphenylboride has already been commented on by Jolicoeur and Friedman.^{12,13} These authors^{12,13} suggest that such broadening is caused by the formation of a complex between the probe and anion. This complex was expected to have a long enough lifetime to lengthen the rotational correlation time τ_c .^{12,13}

The nature of any interaction between DTBN and sodium tetraphenylboride should be investigated. The e.s.r. spectrum of DTBN in methanolic solutions of sodium tetraphenylboride shows no excessive asymmetric line broadening and the expected increase in $A(^{14}\text{N})$ is seen. This suggests that the properties of water contribute strongly to the excessive asymmetric line broadening observed for DTBN in aqueous solutions of sodium tetraphenylboride. This effect is most dominant at ca. 0°C , is reduced at ca. 25° and has disappeared at ca. 50°C . Such behaviour would be expected if clathrate effects were involved. Jones and Symons⁵ studied the asymmetric solvation of the m-dinitrobenzene radical anion in various solvents. Only one of the two nitro groups appears to be solvated at any one instant in time, the site of hydrogen-bonding migrating from one site to another rapidly. This process is detected by selective line broadening in the e.s.r. spectrum of m-dinitrobenzene. In methanol the life-time of a hydrogen-bond to any one nitro group is ca. 10^{-9} sec., whereas in water the life-time is ca. 10^{-6} sec. The longer life-time observed in water was attributed⁵ to the formation of clathrate type solvation structure of the form:

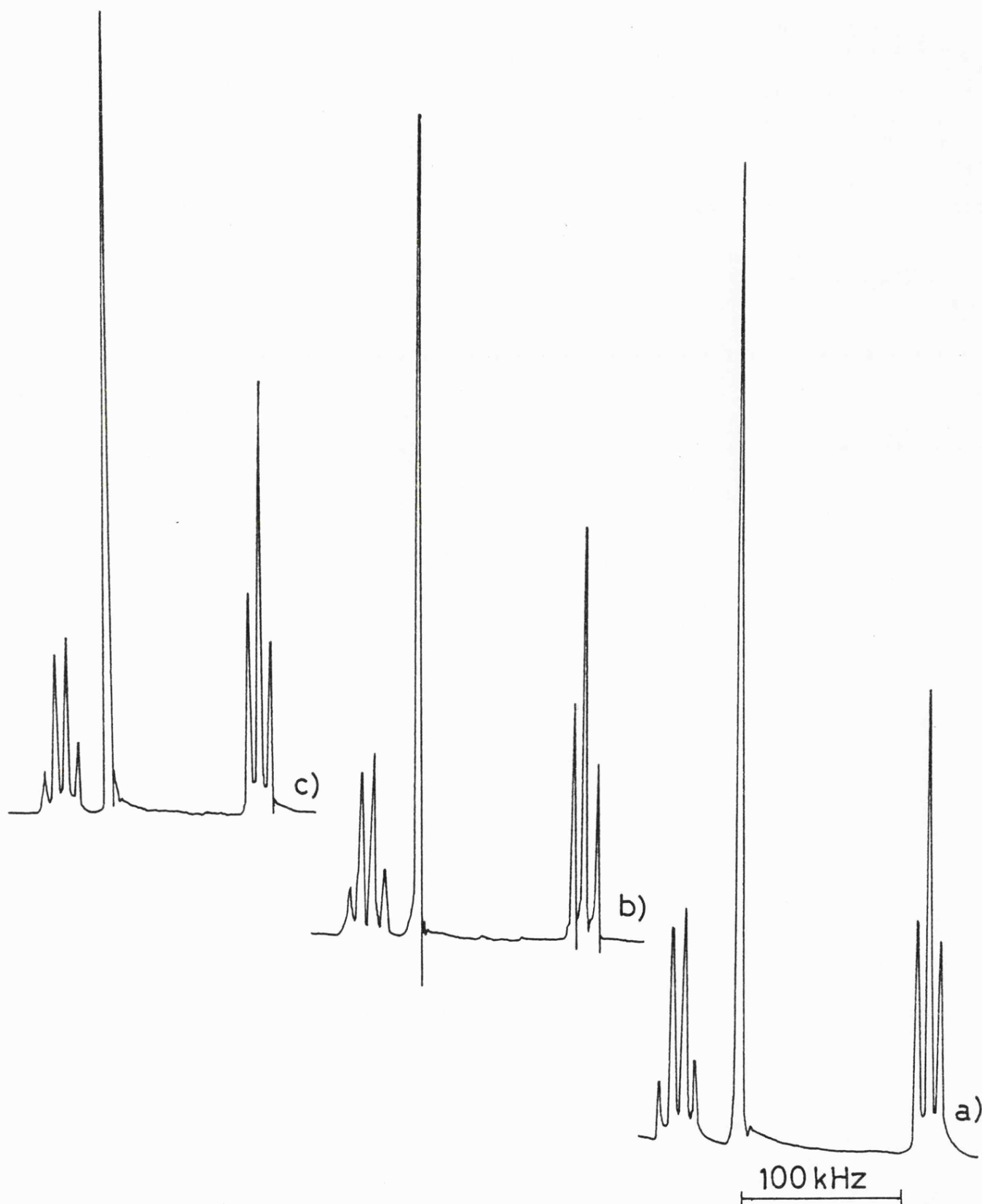


Here one nitro group interacts with bulk water, whilst the rest of the radical anion is enclosed in a clathrate type cage, there being no hydrogen-bonding between the second nitro group and the cage wall. Such a structure would inhibit the switch in solvation from one site to another, thus accounting for the longer life-time of the asymmetric solvate in aqueous solution.

It seems likely that the large asymmetric line-broadening and the associated drop in $A(^{14}\text{N})$, observed for DTBN in aqueous solutions of sodium tetraphenylboride, are due to the formation of a complex between the anion and probe. Such a complex is expected to be a weak charge-transfer type complex, and may have a prolonged life in aqueous solutions due to the formation of clathrate cages. A solvation structure analogous to that proposed for m-dinitrobenzene is envisaged. The small reduction in $A(^{14}\text{N})$ suggests that there is no hydrogen-bonding between the probe and the walls of the complex's host cage. The hypothesis of complex formation was further investigated by studying the proton magnetic resonance spectrum of methylethyl ketone in aqueous and methanolic solutions as a function of concentration of sodium tetraphenylboride. A series of 100 MHz spectra of methylethyl ketone in these solutions is shown in figure 4.10. Methylethyl ketone was chosen as a diamagnetic substitute for DTBN, because of its structural similarity to the nitroxide and its solubility in water. Figure 4.11 displays the results obtained for this study as a plot of $\Delta\delta$, the difference in shift for the methyl and methylene protons of the ethyl group, as a function of concentration of added salt. In all solutions the concentration of methylethyl ketone was kept constant at about 0.65M, this being the minimum concentration which gave a reasonable n.m.r. signal strength. The difference in $\Delta\delta$ measurements for methyl-

Figure 4.10

100 MHz proton n.m.r. spectra of 0.64M methylethyl ketone in aqueous solutions containing a) 0; b) 0.544 and c) 0.901 moles kg^{-1} of sodium tetraphenylboride.



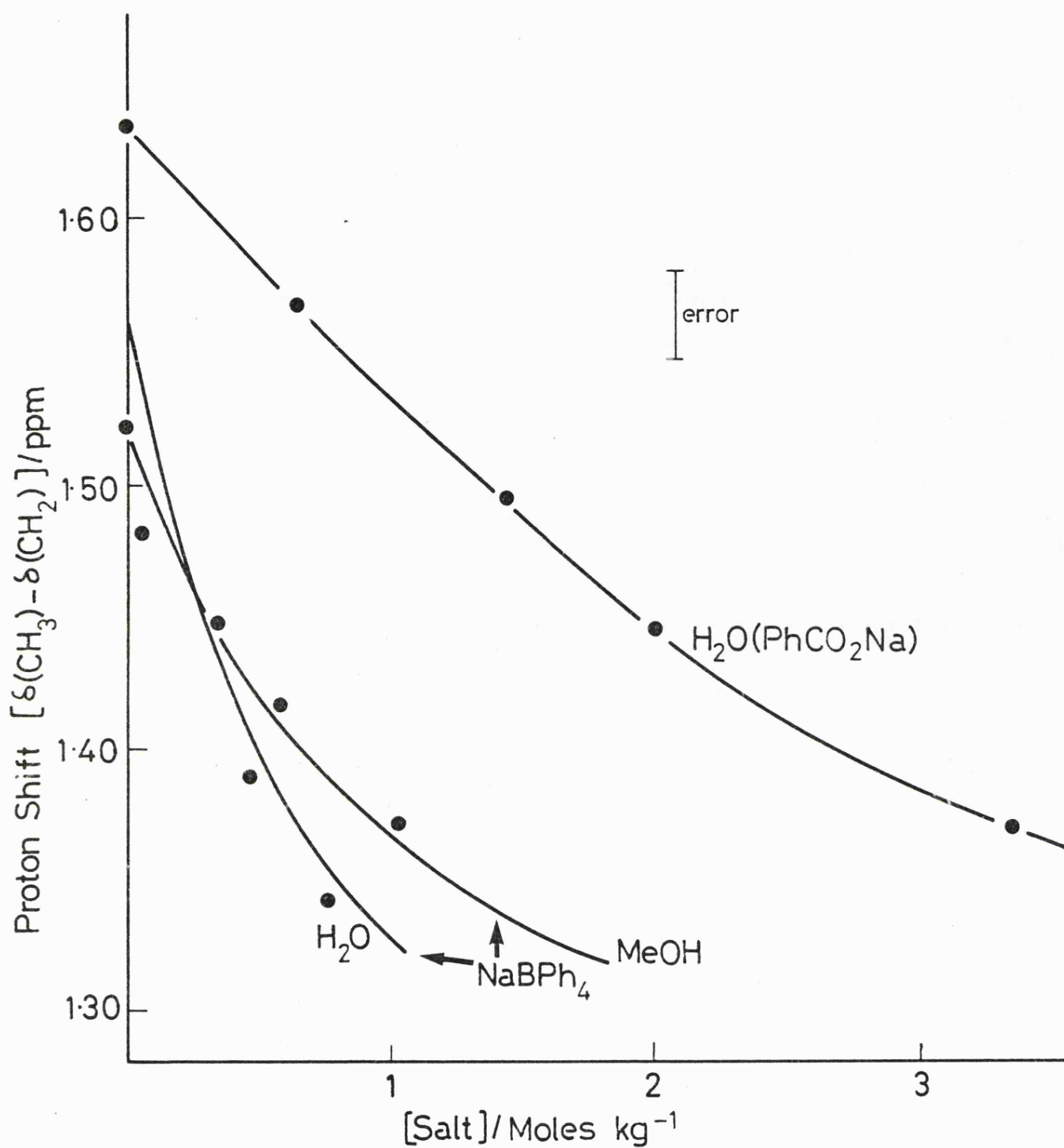


Figure 4.11

Changes in the proton resonance spectrum for dilute aqueous or methanolic methylethyl ketone on adding various electrolytes containing phenyl groups.

ethyl ketone in aqueous and methanolic solutions of sodium tetraphenylboride, shown in figure 4.11, may be due to the slightly higher concentration of ketone used for the methanolic solutions. For most electrolytes, including Ph_4P^+ , $\Delta\delta$ was found to show no dependence on the concentration of added electrolyte. However, sodium tetraphenylboride and to a lesser extent sodium benzoate give a reduction in $\Delta\delta$ as they are added. The e.s.r. spectra of DTBN in aqueous sodium benzoate show a small but significant increase in $\Delta H_{\text{pp}}^{-1} - \Delta H_{\text{pp}}^0$ and a small fall in $A(^{14}\text{N})$. Both the e.s.r. and n.m.r. results suggest that the benzoate and tetraphenylboride anion interact with DTBN in aqueous solution in similar ways.

The changes in $\Delta\delta$ observed in the studies of methylethyl ketone are thought to be due to aromatic ring current effects.³¹⁻³⁵ This would imply that there is some kind of intimate contact between the ketone and anion. It is therefore suggested that there is a weak transfer of electron density from the anion to the ketone. If a charge-transfer interaction is involved there is a possibility that a charge-transfer absorption band may be located in the near ultra-violet. Such a band was searched for in solutions of aqueous sodium tetraphenylboride containing either DTBN or methylethyl ketone. No feature which could be attributed to a charge-transfer interaction could be located at wavelengths above 250 nm, the intense absorption of the cation's phenyl rings making the solution black at wavelengths shorter than this.

Other bulky ions, such as R_4N^+ and Ph_4P^+ which are also thought to promote cage sharing in aqueous solutions, do not increase $(\Delta H_{\text{pp}}^{-1} - \Delta H_{\text{pp}}^0)$ so dramatically when added to aqueous DTBN. This is possibly due to the absence of any complex formation of the type described above. Other factors may contribute. Near infrared studies indicate a loss of

(OH)_{free} groups on addition of R_4N^+ or Ph_4P^+ to water.¹⁴ In addition $A(^{14}N)$ falls when these salts are added to aqueous solutions of DTBN, suggesting that the probe is mainly non-hydrogen bonded in these solutions. Near infrared results¹⁴ suggest that aqueous solutions of sodium tetraphenylboride are rich in (OH)_{free}, implying that the proportion of non-hydrogen bonded nitroxide in these solutions should be low. If as expected the complexed form of the radical tumbles more slowly than the hydrogen-bonded form, which in turn is much less mobile than the non-bonded nitroxide radical, the unique effects of sodium tetraphenylboride can be understood.

4.5 Conclusions

The effects of added electrolyte on the nature of water and methanol as solvents has been probed using the free radical DTBN. The results obtained in aqueous solution show that $A(^{14}N)$ of DTBN depends mainly on the nature of the cation and is almost independent of the nature of the anion. These results are in good agreement with the earlier observations of Rassat et alia.¹⁰ Measurements made on methanolic solutions of DTBN exhibit a clear dependence on both the anion and cation. Bulky weakly solvated ions such as BPh_4^- have little effect on $A(^{14}N)$ of the probe in methanolic solution, whereas small highly charged anions such as Cl^- reduce $A(^{14}N)$. The explanations offered for this behaviour are necessarily more complicated than those offered by Rassat.¹⁰ The anions and cations are thought, from other spectroscopic studies, to modify the number of (OH)_{free} groups in protic solvents. The equilibrium between "free" and hydrogen-bonded nitroxide in methanolic solution is thought to be delicately balanced, hence changes in the concentration of (OH)_{free} on addition of an electrolyte

are expected to have a large effect on $A(^{14}\text{N})$. A contribution to $A(^{14}\text{N})$ from the interaction between the probe and the primary solvation layer of the cation is also expected. This effect is believed to be responsible for the smaller changes in $A(^{14}\text{N})$ observed for nitroxides in aqueous solutions containing small highly charged cations. In water DTBN is expected to be almost completely hydrogen-bonded, hence any increase in available $(\text{OH})_{\text{free}}$ caused by added cations should not effect $A(^{14}\text{N})$. The insensitivity of $A(^{14}\text{N})$ to the nature of the anion in aqueous solutions is attributed to the weak basicity of the anion inhibiting desolvation of the probe. The possibility of a direct interaction between the probe and cation is discounted because of the stronger solvating power of the protic solvents and the failure to find any coupling between the probe and cationic nuclei in the e.s.r. spectra of DTBN in frozen methanolic salt solutions at 77 K.

The e.s.r. results were compared with the near infrared results of Jackson.¹⁴ The presence of (OH) weakly bound units in methanolic solutions of sodium tetraphenylboride was detected by near infrared measurements¹⁴ and this could be correlated with the large increase in $A(^{14}\text{N})$ of DTBN in these solutions. Near infrared results on methanolic perchlorate solutions show the presence of weak hydrogen-bonding between the solvent and anion.¹⁴ This is compatible with the observed e.s.r. results, which show a smaller increase in $A(^{14}\text{N})$ for DTBN in methanolic perchlorate solutions. In aqueous solutions the near infrared results are clearer, due to the presence of a feature ascribed to $(\text{OH})_{\text{free}}$ groups. Jackson¹⁴ was able to demonstrate a dependence of the amount of $(\text{OH})_{\text{free}}$ on the nature of both the anion and cation in aqueous salt solutions. This contrasts with the observed e.s.r. results, especially in the case of sodium tetraphenylboride where the near infrared results

show a large increase in $(\text{OH})_{\text{free}}$ and the e.s.r. results exhibit a fall in $A(^{14}\text{N})$. A good correlation is found between the aqueous near infrared results¹⁴ and the $A(^{14}\text{N})$ values measured in methanol.

Bulky ions like the tetraalkylammonium ions produce anomalous effects on $A(^{14}\text{N})$ of DTBN in aqueous solution. In the absence of a clear anion effect, the rapid fall in $A(^{14}\text{N})$ observed in these solutions was attributed to a cage-breeding process. It is postulated that the bulky tetraalkylammonium ions are guests within clathrate cages in aqueous solution and that these cages form templates on which other cages may grow. If the concentration of R_4N^+ is sufficiently high then DTBN is expected to become a guest in a previously empty cage, but to be unable to hydrogen-bond to its host's cage walls. Support for this hypothesis is given by the similarity between the effects of R_4N^+ and known cage formers, such as t-butanol, on $A(^{14}\text{N})$ of DTBN in aqueous solution.

In addition to changes in $A(^{14}\text{N})$ for DTBN in these solutions, linewidth measurements were also made. There is a single linear dependence of the linewidth of the central line on $A(^{14}\text{N})$ for DTBN in both aqueous and methanolic electrolyte solutions. These linewidth changes are attributed to variations in $A(^1\text{H})$, the proton superhyperfine coupling constant. Very few salts produce any changes in asymmetric line broadening when added to aqueous or methanolic solutions of DTBN. Any observed changes in asymmetric line broadening are attributed to viscosity effects, with the exception of the very large changes in differential linewidths observed for DTBN in aqueous solutions of sodium tetraphenylboride. Similar increases in linewidth were reported for these solutions by Jolicoeur and Friedman,^{12,13} who proposed that the increased asymmetric broadening was due to complex formation between the

probe and tetraphenylboride anion. The current set of results suggest that a weak charge-transfer complex is formed between the nitroxide and tetraphenylboride anion, although no confirmation of a charge-transfer interaction could be obtained using U.V. spectroscopy. Aromatic ring current shifts observed in the proton n.m.r. spectrum of methylethyl ketone, which is structurally similar to DTBN, in aqueous and methanolic solutions of sodium tetraphenylboride suggest that complex formation is likely. It is suggested that the large asymmetric line broadening observed for DTBN in aqueous solutions of sodium tetraphenylboride and the concomitant fall in $A(^{14}\text{N})$ are caused by stabilisation of the probe-anion complex by clathrate effects. In methanolic solutions where cage formation is not possible the linewidth effect disappears and an increase in $A(^{14}\text{N})$ is observed.

Commonly, changes in solvation in aqueous electrolyte solutions are explained in terms of Frank and Wen's model³⁶ of ionic solvation. This model envisages a layer of disordered water molecules interposed between the ion's primary solvation layer and the bulk solvent. The size of this layer of disordered water is thought to dictate whether the ion reinforces or disrupts water structure. Symons et alia^{19,37,38} have often argued that this view of ionic solvation is incorrect and the commonly used criteria for structure making and breaking are unsound. It is unnecessary to invoke either the Frank and Wen theory³⁶ or the concepts of structure making and breaking to explain the DTBN results given above. The current work is fully consistent with Symons' view¹⁹ of ionic solvation, in which the primary solvation layer of the ion is hydrogen-bonded to bulk water.

REFERENCES FOR CHAPTER FOUR

1. H. Sharp and M. C. R. Symons, "Ions and Ion-pairs in Organic Reactions" ed. M. Szwarc, Wiley, New York, 1972.
2. M. C. R. Symons, Pure and Appl. Chem., 1977, 49, 13.
3. T. E. Gough and M. C. R. Symons, Trans. Faraday Soc., 1966, 62, 269.
4. T. A. Claxton, J. Oakes and M. C. R. Symons, Trans. Faraday Soc., 1967, 63, 2125.
5. D. Jones and M. C. R. Symons, Trans. Faraday Soc., 1971, 67, 961.
6. A. S. Waggoner, A. D. Keith and O. H. Griffith, J. Phys. Chem., 1968, 72, 4129.
7. N. M. Atherton and S. J. Strach, J.C.S. Faraday II, 1972, 68, 374.
8. K. Fox, Trans. Faraday Soc., 1971, 67, 2805.
9. J. Oakes, J.C.S. Faraday II, 1972, 68, 1464.
10. R. Briere, A. Rassat, P. Rey and B. Tchouber, J. Chim. Phys. (Fr)., 1966, 63, 1575.
11. D. Pilo-Veloso, R. Ramasseul, A. Rassat and P. Rey, Tetrahedron Letters, 1976, 40, 3599.
12. C. Jolicoeur and H. L. Friedman, Ber. Bunsenges. Phys. Chem., 1971, 76, 248.
13. C. Jolicoeur and H. L. Friedman, J. Solution Chem., 1974, 3, 15.
14. Both the e.s.r. and near infrared data presented here have already been published as:
S. E. Jackson, E. A. Smith and M. C. R. Symons, Disc. Faraday Soc., 1977, 64, 173.
15. G. Brink and M. Falk, Canad. J. Chem., 1970, 48, 2096.
16. D. M. Adams, M. J. Blandamer, M. C. R. Symons and D. Waddington, Trans. Faraday Soc., 1971, 67, 611.
17. W. A. P. Luck, Disc. Faraday Soc., 1967, 43, 115.
18. W. A. P. Luck, Ber. Bunsenges. Phys. Chem., 1965, 69, 69.
19. M. C. R. Symons, Phil. Trans. Roy. Soc. Lond., 1975, B272, 13.
20. M. C. R. Symons and D. Waddington, Chem. Phys. Letters, 1975, 32, 133.

21. I. M. Strauss and M. C. R. Symons, Chem. Phys. Letters, 1976, 39, 471.
22. R. N. Butler and M. C. R. Symons, Trans. Faraday Soc., 1969, 65, 2559.
23. J. Davies, S. Ormondroyd and M. C. R. Symons, Trans. Faraday Soc., 1971, 67, 3465.
24. W. E. Addison, "Structural Principles in Inorganic Compounds", Longmans, Green & Co. Ltd., London 1967, p.172.
25. R. A. Robinson and R. H. Stokes, "Electrolyte Solutions", Butterworths Scientific Publications Ltd., London, 1959, p.125.
26. O. D. Bonner and C. F. Jumper, Infrared Phys., 1973, 13, 233.
27. P. R. Philip and C. Jolicoeur, J. Phys. Chem., 1973, 77, 3071.
28. B. M. Hoffman and T. B. Eames, J. Amer. Chem. Soc., 1969, 91, 2169.
29. C. Hambly and J. B. Raynor, J.C.S. Dalton, 1974, 604.
30. J. Oakes, J. Slater and M. C. R. Symons, Trans. Faraday Soc., 1970, 66, 546.
31. J. P. Coetzee and W. R. Sharpe, J. Phys. Chem., 1971, 75, 3141.
32. G. P. Schiemenz, J. Mol. Struct., 1973, 16, 99.
33. G. P. Schiemenz, Angew. Chem., 1971, 10, 855.
34. G. P. Schiemenz, Tetrahedron, 1973, 29, 741.
35. G. P. Schiemenz, J. Organometallic Chem., 1973, 52, 349.
36. H. S. Frank and W. Y. Wen, Disc. Faraday Soc., 1957, 24, 133.
37. S. E. Jackson and M. C. R. Symons, Chem. Phys. Letters, 1976, 37, 551.
38. S. E. Jackson, I. M. Strauss and M. C. R. Symons, J.C.S. Chem. Comm., 1977, 174.

CHAPTER FIVE

Heisenberg Spin Exchange Studies using Ditertiary
butyl nitroxide

CHAPTER FIVE

5.1 Introduction

The line broadening processes of Heisenberg spin exchange and dipolar broadening have been discussed in chapter two of this thesis. The basic principles of Heisenberg spin exchange were investigated in the late fifties and early sixties;¹⁻⁴ the formal theory was put forward by Johnson⁵ and Freed.⁶ Nitroxides⁶⁻¹⁰ have often been the subject of spin exchange studies. In general good agreement between experiment and theory has been observed in the range of solvents examined. The effects of dipolar broadening have not been examined as carefully as the effects of spin exchange. Freed⁶ has produced a quantitative estimate of the effects of dipolar broadening by extending the work of Abragam.¹¹ In the range of solvent viscosities probed by earlier studies,⁶⁻¹⁰ the effects of dipolar broadening are thought to be negligible. However, as solvent viscosity increases and temperature falls, theory⁶ predicts that the effects of spin exchange diminish, whilst those of dipolar broadening increase. Equation 2.69 of chapter two of this thesis predicts that when the ratio of temperature over solvent viscosity T/η approaches 40 K cP^{-1} , both phenomena contribute equally to the linewidth.

The effects of radical concentration on linewidth are shown in figure 5.1. Figure 5.1(i) shows the three narrow lines associated with a dilute solution of DTBN in a given solvent. As the radical concentration is increased the three lines broaden and begin to converge. The lines further broaden until the limit of fast exchange is reached; here the rate of exchange is greater than the nitrogen hyperfine splitting and the lines coalesce to form a single broad line. This line begins

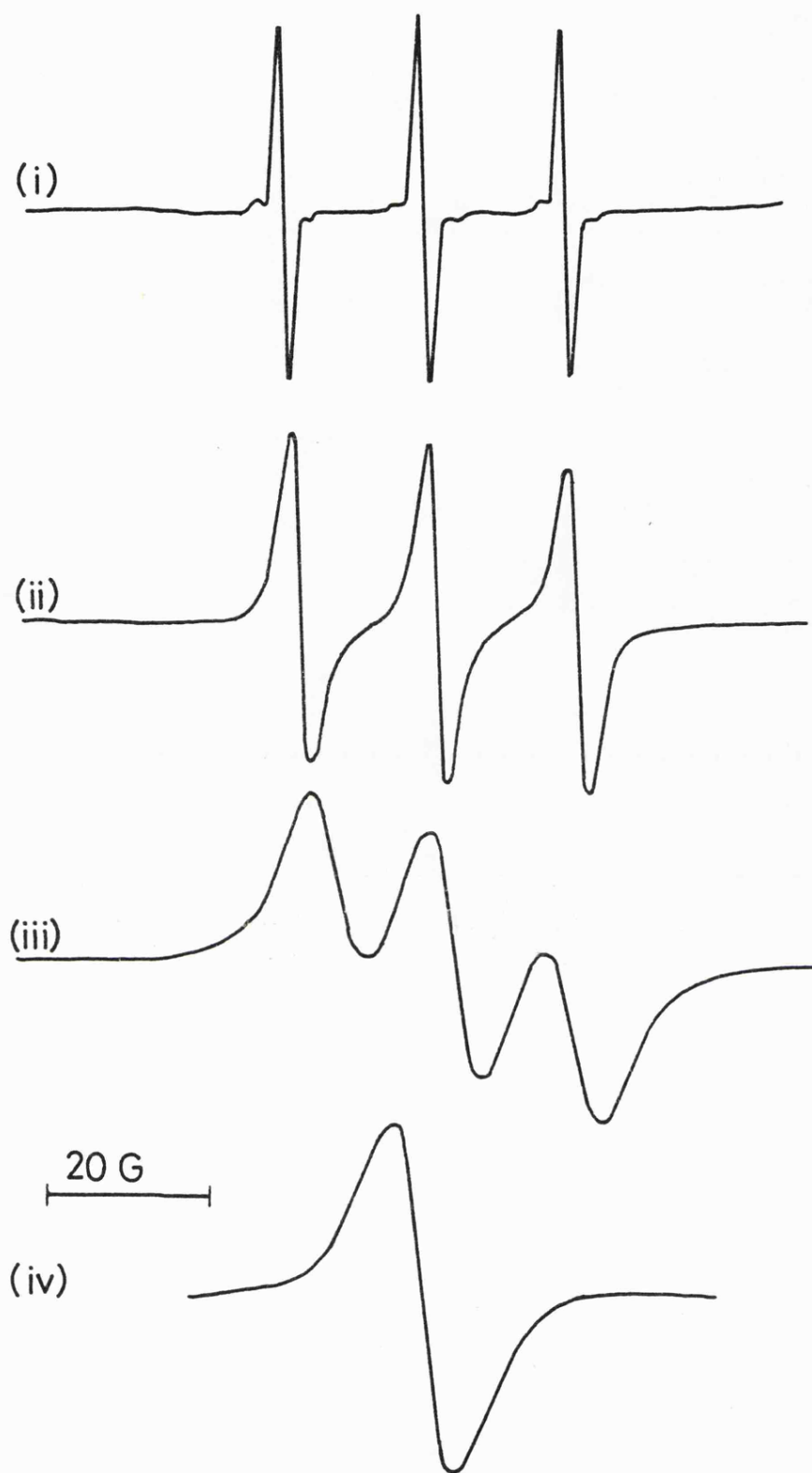


Figure 5.1

Simulated spectra of DTBN undergoing Heisenberg spin exchange in solution, showing:

- | | | |
|--------|-----------------------|---|
| (i) | Negligible exchange | $\omega_{\text{HE}} \ll A(^{14}\text{N})$ |
| (ii) | Slow exchange | |
| (iii) | Intermediate exchange | $\omega_{\text{HE}} < A(^{14}\text{N})$ |
| (iv) | Fast exchange | $\omega_{\text{HE}} \gtrsim A(^{14}\text{N})$ |

to narrow with further increase in DTBN concentration producing a single exchange narrowed line.

The theory of Heisenberg spin exchange implies the formation of a "collision complex", formed by overlap of the singly occupied p orbitals of the colliding nitroxide radicals. This dimeric species is expected to be short-lived. The Stokes-Einstein equation 2.60 predicts a radical-radical encounter time τ_1 of about 10^{-10} secs for a nitroxide in a solvent of viscosity 1 cP at 298 K. Spin exchange⁶⁻⁷ and specific heat studies¹² predict that the exchange interaction between two nitroxides is of the order 8-9 cal mol⁻¹. This is much weaker than the strength of a typical chemical bond. The possibility of the formation of a long-lived dimeric species should be examined, since the existence of such a species would clearly complicate the analysis. Ingold¹³ has discussed the possibility of dimerisation in certain solvents and has shown that diethyl nitroxide in non-interacting solvents at low temperatures is capable of some dimerisation, the dimer forming a transition state in the radical decomposition process. Bis-(trifluoro methyl) nitroxide¹³ also dimerises at low temperatures. However, Rassatt^{12,14,14} has demonstrated that the radical 2,2,6,6 tetramethyl 4 piperidinol-1-oxyl (TEMPO^{OH}), in the pure state and concentrated solutions, prefers to facilitate radical-radical interactions through hydrogen bonding, via the hydroxyl and nitroxide groups, rather than by interactions between nitroxide groups only. Certainly DTBN would not be expected to form long-lived dimers to any great extent, both for steric reasons and because of stability of the 3 electron N-O π bond.¹⁶

Our interest in spin exchange was aroused by the preliminary studies of Jones,¹⁷ which showed that spin exchange studies of DTBN in

water showed some anomalous behaviour. This situation was further probed in these laboratories,¹⁸ and we were able to show that the exchange rate measured for DTBN in water was slower than the rate measured in an isoviscous solvent. However, before this study could be completed Franks et alia¹⁹ published their paper on the effect of solvent on rate of spin exchange.

Franks et alia¹⁹ examined the spin-exchange behaviour of 2,2,6,6-tetramethyl piperidine-1-oxyl (TEMPO) in seven different solvents. They also noticed that the Heisenberg spin exchange rate for the nitroxide in water was slow compared to the rate in isoviscous solvents at the same temperature. This was attributed to the effect of hydrophobic bonding, preventing overlap of the unpaired electrons of colliding radicals. Franks based much of his discussion on a Stokes-Einstein type diffusional analysis, ignoring any possible effects due to dipolar broadening, even when solvent viscosities were high. It has been proposed that hydrogen bonding²⁰ has a significant effect on the e.s.r. spectra of dilute solutions of nitroxides. Franks et alia did not explore any possible effects hydrogen bonding may have on the exchange rate.

In the present study it is hoped to explore more fully the behaviour of nitroxides undergoing spin exchange in solution. By examining spin exchange at temperatures ~273 K it is hoped to exaggerate any anomalies due to hydrophobic effects in aqueous solution. It is appreciated that dipolar effects may become more important at this lower temperature. A wider range of protic and aprotic solvents was studied in order to probe the rôle of hydrogen bonding. The rôle of water structure in determining the exchange rates was further examined by investigating the effect of temperature on the exchange behaviour of

ditertiary butyl nitroxide in water.

5.2 Experimental Details

Ditertiary butyl nitroxide was purchased from Eastman and was used without further purification. All solvents used were of the best available grades. Decane was purified by passage through a column of basic aluminium oxide and silica gel. Heptane was stored over 4B molecular sieves for five days prior to use. Dodecane was used as supplied. Toluene was distilled twice prior to use. Methyl cyanide was dried over and distilled from fresh P_2O_5 . Methanol, ethanol and n-propanol were purified by distillation from magnesium activated with iodine, after being refluxed over this mixture for 30 minutes. n-Butanol was purified by shaking with anhydrous sodium carbonate. The alcohol was then fractionated, the water azeotrope coming over at 92°C and the pure alcohol at 117°C. t-Butanol was purified by fractionation. Water was either doubly distilled from alkaline permanganate or purified using a Millipore water purifier.

All solvents were carefully degassed prior to use. Water was degassed by purging with nitrogen for an hour, and all organic solvents were degassed using the freeze-pump-thaw technique. The degassing cell shown in figure 5.2 was used for freeze-pump-thaw degassing. All solutions were made up volumetrically under a nitrogen atmosphere in a dry box. Each sample was held in a 1 mm capillary tube held within a 2 mm borosilicate tube. The outer tube was sealed using tight fitting rubber tubing and a 2 mm diameter borosilicate stopper. Aqueous solutions were housed in a standard variable temperature aqueous cell, sealed using a rubber bung and parafilm.

All nitroxide concentrations were measured in units of moles dm^{-3} .

In order to correct for solvent contraction at the lower temperatures, at which the e.s.r. spectra were recorded; whenever possible the correction used by Freed was applied.⁶ The solvent density data required to make this correction was obtained from standard sources.²¹ Viscosity data for the alkanes²² and other solvents,²¹ was obtained from standard sources. The work of Westmeier²³ was used to find the viscosities of t-butanol-water mixtures at 274 K. It is well known that at the onset of Heisenberg spin exchange, the effect of exchange on the proton hyperfine^{6,24} components is important. Exchange narrowing of the proton structure can cause the nitrogen manifold to narrow as the nitroxide concentration is increased. This effect is not significant once the proton lines have been completely exchange narrowed, i.e. when the envelope width is very much greater than the proton hyperfine splitting constant. Care has been taken in this study to eliminate the effects of proton hyperfine coupling, by only considering samples giving lines very much broader than the proton hyperfine splitting $A(^1\text{H})$. In aqueous solutions $[A(^1\text{H}) \sim 0.05 \text{ G}]$ only lines broader than 0.5 G were used and for completely non-interacting solvents $[A(^1\text{H}) \sim 0.1 \text{ G}]$ only lines broader than 1 G were considered.

E.s.r. spectra were recorded on Varian E-3 and Varian E109 spectrometers, using a V-6040 variable temperature accessory to maintain the temperature to within $\pm 1^\circ$. The spectrometers were calibrated using a standard $1 \times 10^{-4} \text{ M}$ solution of DTBN in water. Optical density measurements were made using Pye Unicam SP700 and SP1800 spectrophotometers.

5.3 Results and Discussion

The ultra violet absorption of the $\pi \rightarrow \pi^*$ electronic transition of

Vacuum line at a pressure of 10^{-2} mm Hg or less

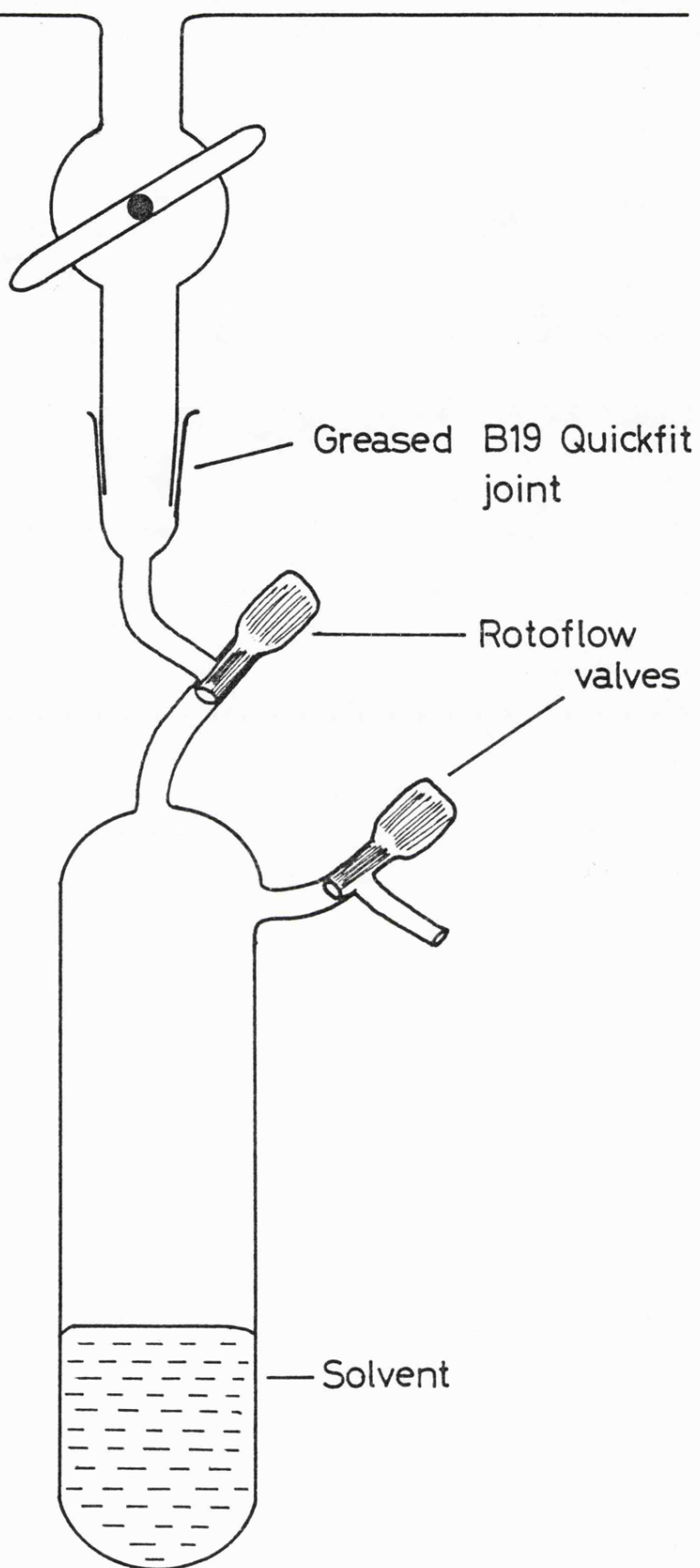
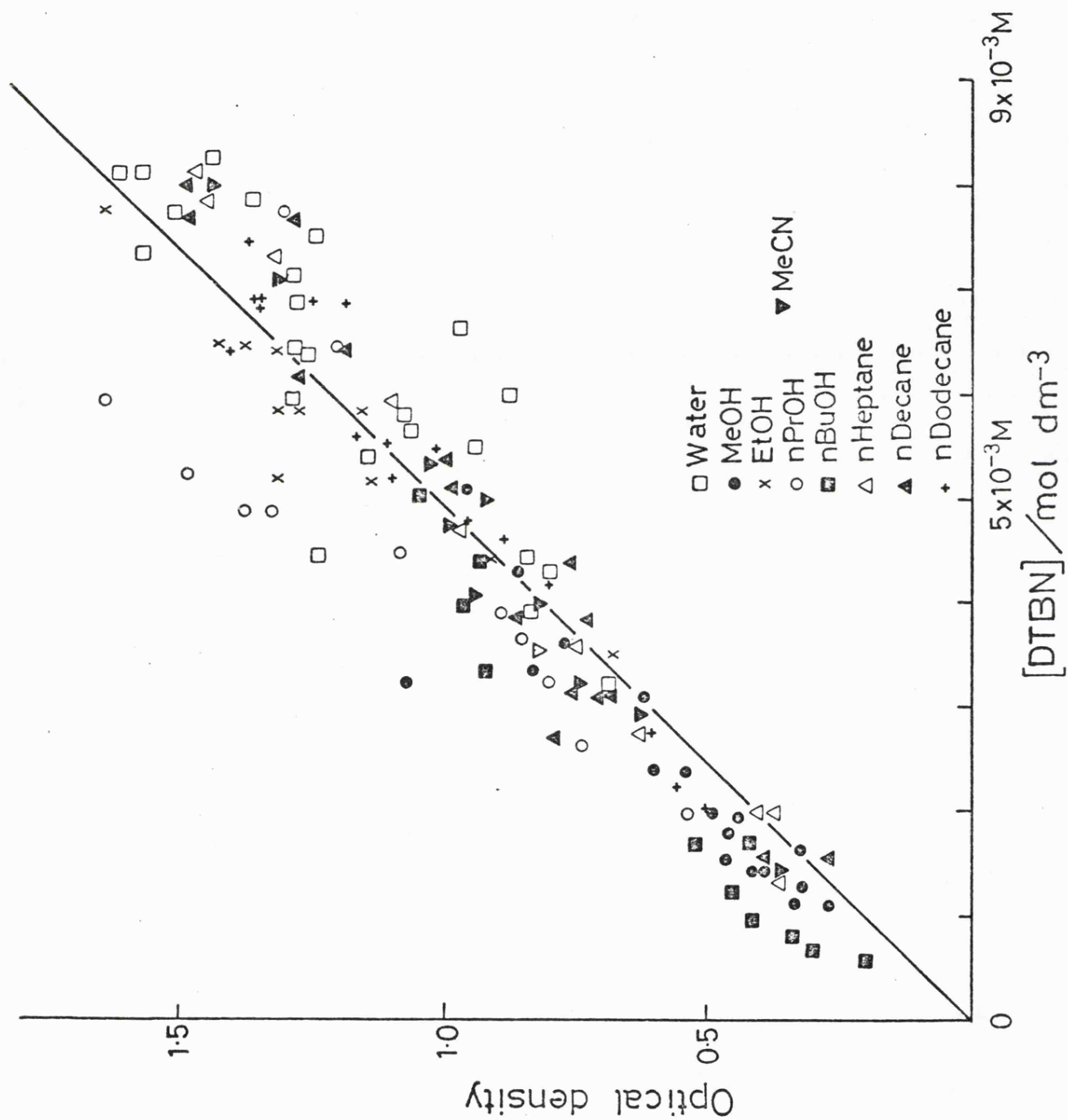


Figure 5.2

The degassing cell used for the degassing of organic solvents.

Figure 5.3

The optical density measured at 238 nm for DTBN in various solvents as a function of DTBN concentration.



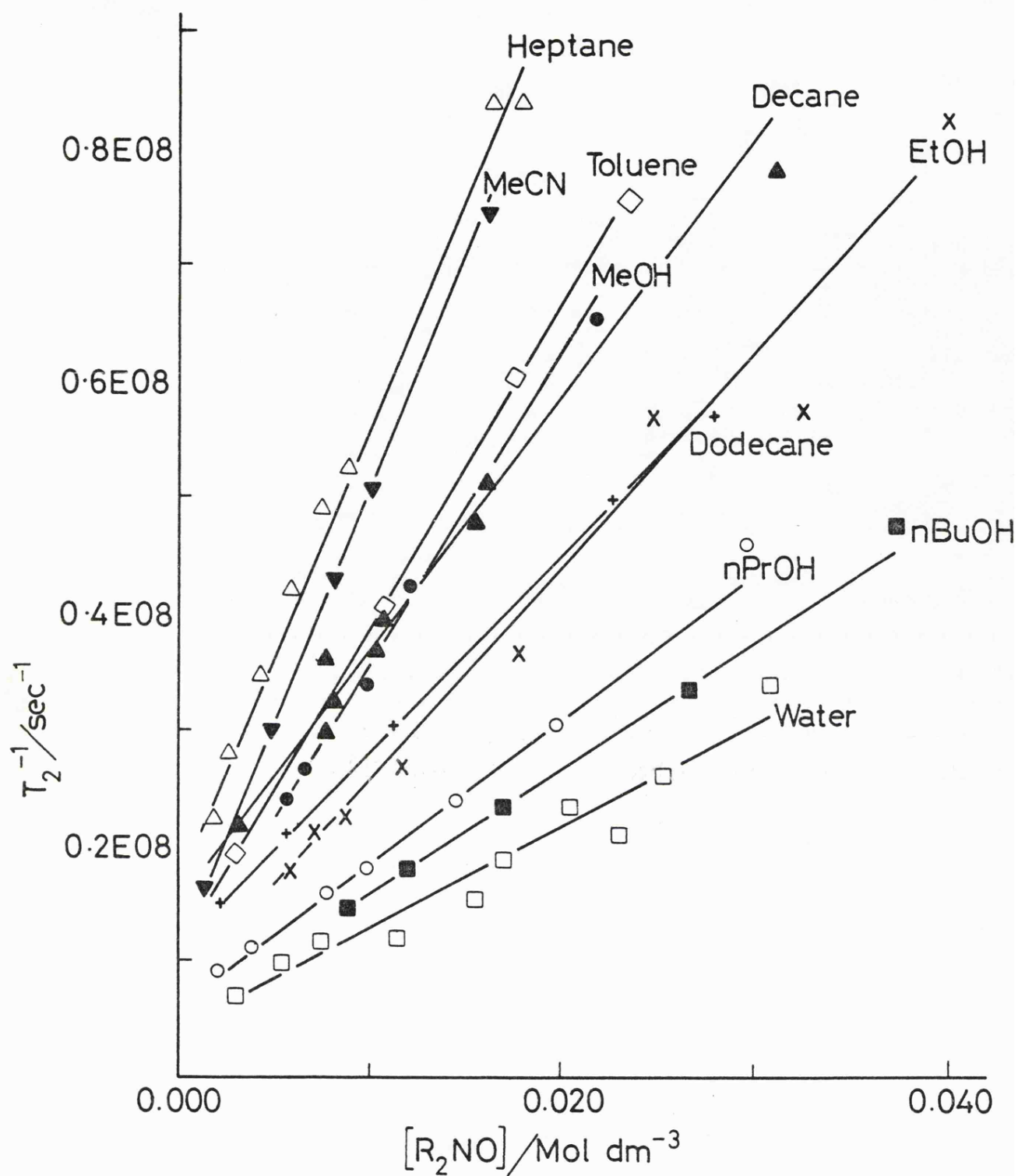


Figure 5.4

Correlation between $1/T_2$ and concentration of DTBN for solutions of DTBN in various solvents.

DTBN at 238 nm has often been used as a concentration check. The extinction coefficient of this transition is $\epsilon = 2140$ at 238 nm.²⁵ In order to check the concentration of our nitroxide solutions, several optical density measurements were made on samples used for e.s.r. measurements. The results of the optical density determinations are shown in figure 5.3. The data shown in figure 5.3 falls on a single straight line, yielding an extinction coefficient of 2033 at 238 nm. This is within five per cent of the literature value. Thus the volumetrically determined nitroxide concentrations are satisfactory, at least to within the limits of the scatter of figure 5.3.

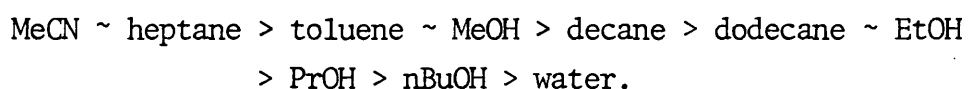
Figure 5.4 shows the variation of e.s.r. linewidths of the nitroxide in each solvent, as a function of nitroxide concentration. It can be seen that the rate of line broadening is fastest for non-viscous solvents such as heptane and acetonitrile, and slowest for the more viscous solvents like n dodecane and the higher alcohols. Water apparently slows down the rate of line broadening to a lower level than even the most viscous solvent, n butanol. All measurements were made at 274 K. Clearly, the results of figure 5.4 can be analysed in terms of equation 2.48, the slope of this plot giving the pseudosecond-order rate constant for Heisenberg spin exchange. The intercepts of the plots in figure 5.4 should give the linewidth of DTBN at infinite dilution in the given solvent. A FORTRAN computer program²⁶ was written to perform a least squares analysis on the results shown in figure 5.4, the results of this analysis are shown in table 5.1. The experimentally determined linewidths of a 5×10^{-5} M solution of DTBN in each of the ten solvents is included in table 5.1 for comparison.

It is well known that as the exchange rate increases the spectrum as a whole begins to contract in overall width. This effect is

| Solvent | k_e calculated ($\text{dm}^3 \text{M}^{-1} \text{sec}^{-1}$) | k_e from graph ($\text{dm}^3 \text{M}^{-1} \text{sec}^{-1}$) | Residual width from graph (Gauss) | Experimental limiting width (Gauss) |
|----------------|---|---|--------------------------------------|--|
| Methyl Cyanide | 4.582×10^9 | $3.969 \pm 0.098 \times 10^9$ | 0.676 ± 0.053 | 0.610 |
| n Heptane | 3.849×10^9 | $3.889 \pm 0.116 \times 10^9$ | 1.051 ± 0.065 | 0.822 |
| Toluene | 2.624×10^9 | $2.747 \pm 0.040 \times 10^9$ | 0.699 ± 0.028 | 0.641 |
| Methanol | 2.470×10^9 | $2.681 \pm 0.170 \times 10^9$ | 0.567 ± 0.129 | 0.520 |
| n Decane | 1.553×10^9 | $2.159 \pm 0.117 \times 10^9$ | 0.980 ± 0.092 | 0.742 |
| Ethanol | 1.142×10^9 | $1.815 \pm 0.113 \times 10^9$ | 0.481 ± 0.143 | 0.580 |
| n Dodecane | 0.889×10^9 | $1.683 \pm 0.043 \times 10^9$ | 0.711 ± 0.034 | 0.722 |
| n Propanol | 0.552×10^9 | $1.240 \pm 0.055 \times 10^9$ | 0.367 ± 0.060 | 0.537 |
| n Butanol | 0.391×10^9 | $1.074 \pm 0.044 \times 10^9$ | 0.316 ± 0.058 | 0.533 |
| Water | 1.172×10^9 | $0.881 \pm 0.051 \times 10^9$ | 0.250 ± 0.054 | 0.336 |

Table 5.1 Summary of the least squares analysis of
the results present in figure 5.4.

initially negligible, but as the nitroxide concentration increases, the outer two lines move closer together. This can be measured as a decrease in $A(^{14}\text{N})$. Figure 5.5, shows $A(^{14}\text{N})$ as a function of nitroxide concentration. We can see that the greater k_e for a nitroxide, the greater the rate of fall of $A(^{14}\text{N})$ with increasing nitroxide concentration in that solvent. The order of rate of fall of $A(^{14}\text{N})$ with radical concentration seems to show the following solvent dependence:-



Unfortunately, it is not easy to present these results in a clear way, since $A(^{14}\text{N})$ is solvent dependent for DTBN at low concentrations. The picture is further complicated, since the slope of the graph in the limit of fast exchange, will be governed by the point at which the spectrum completely coalesces to a single peak, which in turn depends on the value of $A(^{14}\text{N})$ at infinite dilution. The data presented seems to indicate that the rate of fall of $A(^{14}\text{N})$ presents a useful guide to the exchange rate, but not as accurate a guide as linewidth measurements.

Equations 2.59 and 2.60 predict that in the limit of strong exchange, the rate of exchange should be a linear function of the ratio of solvent temperature and viscosity. Figure 5.6 shows the temperature/viscosity dependence of k_e ; it can be seen that there is a single linear dependence for all non-aqueous solvents. This would imply that hydrogen bonding is not a significant factor in determining the rate of spin exchange, since protic and aprotic solvents fall on the same line. A comparison of experimentally determined exchange rate and a theoretically derived value, would be interesting. It is possible to obtain an estimate of the collision rate of two radicals in solution by using the Smoluchowsky equation, which is

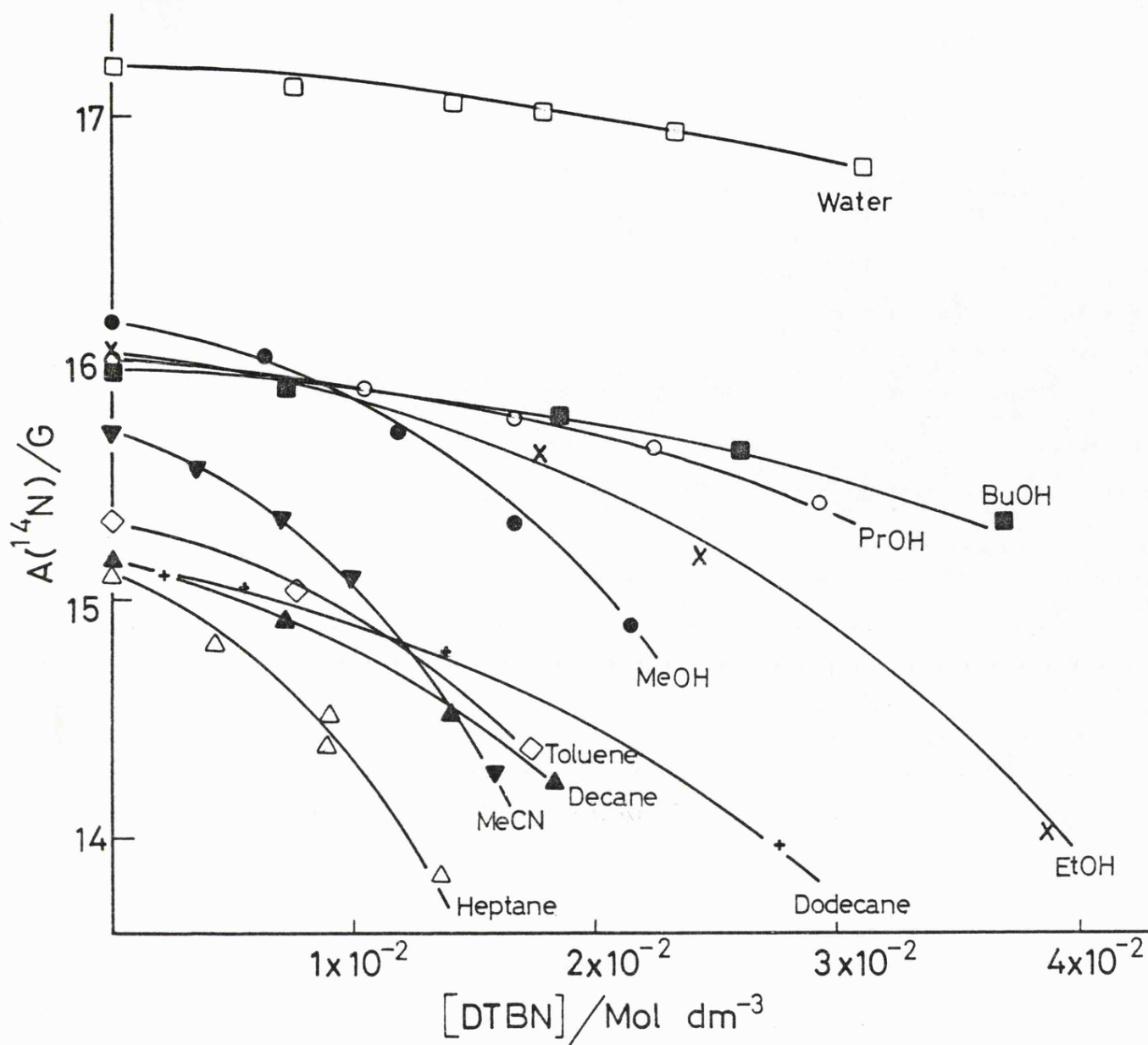


Figure 5.5

The correlation between $A(^{14}\text{N})$ and radical concentration for solutions of DTBN in various solvents at 274 K.

- | | |
|---------|------------|
| □ Water | △ Heptane |
| ● MeOH | ▲ Decane |
| X EtOH | + Dodecane |
| ○ PrOH | ▼ MeCN |
| ■ BuOH | ◇ Toluene |

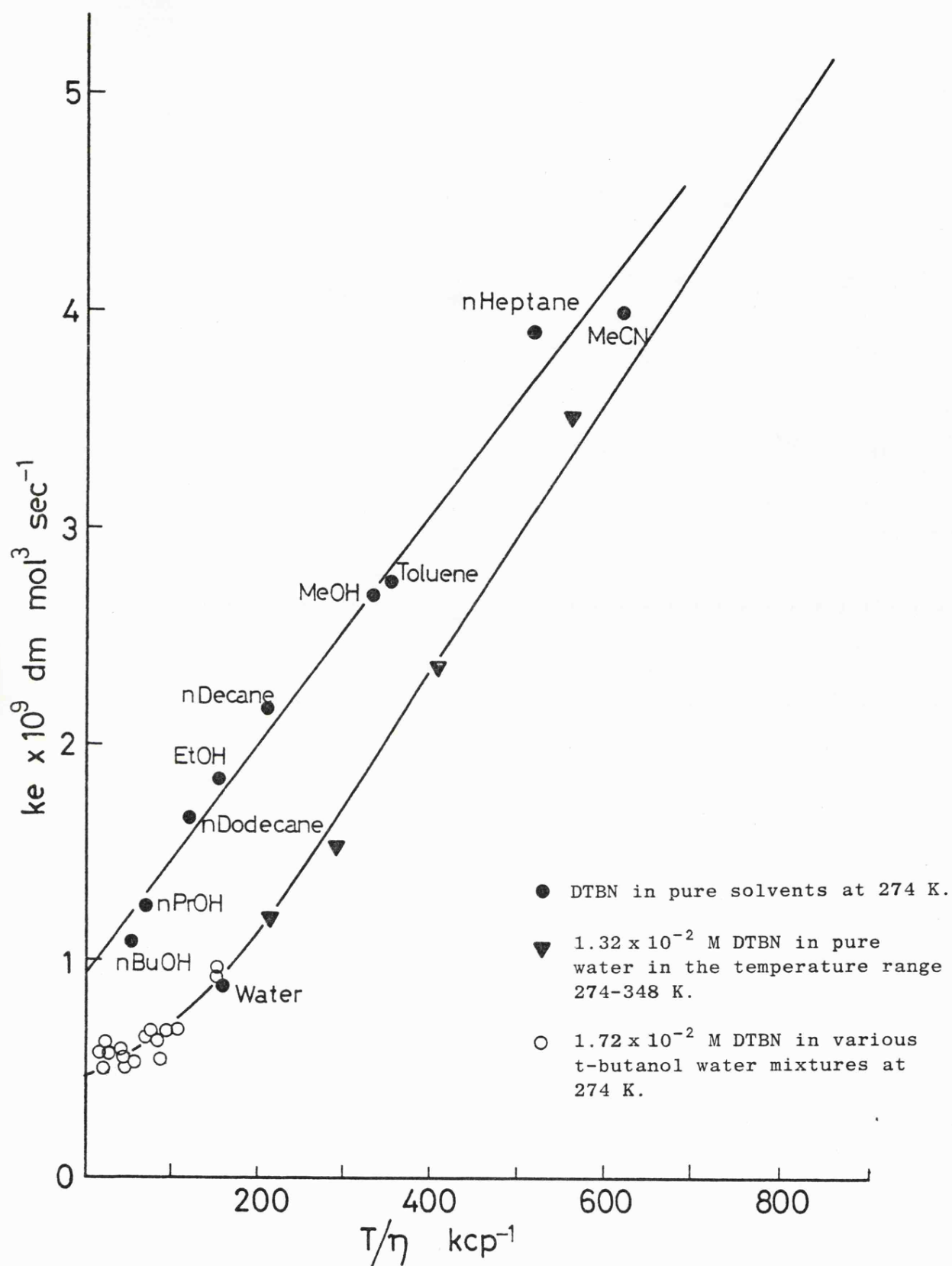


Figure 5.6

The rate constant for Heisenberg Spin Exchange as a function of T/η .

$$k_c = \frac{8 RT}{3000 \eta} \quad (5.1)$$

where k_c is the radical-radical collision rate and R is the gas constant. It can be appreciated that this is three times the pseudo-second order rate constant for spin exchange, since only one third of all collisions will result in exchange. Equation 5.1 can be produced by simple manipulation of equations 2.59 and 2.60 to give a collision rate for the strong exchange limit. Table 5.1 shows a comparison between the experimentally determined exchange rate and the rate calculated as $\frac{1}{3}$ of the result of equation 5.1. For low viscosity solvents agreement between the two is good, however as the viscosity increases the calculated exchange rate becomes increasingly smaller than the observed rate.

Franks et alia¹⁹ have commented on the failure of the Smoluchowsky equation to account for the variation of exchange rate with viscosity. They have shown that the product $k_c\eta$ was not a constant as suggested by equation 5.1. They drew a graph of the product $k_c\eta$ against η ; and hence argued that the product $k_c\eta$ tended towards a limiting value of $14 \times 10^9 \text{ cP dm}^3 \text{ mol}^{-1} \text{ sec}^{-1}$. This conclusion was further supported by obtaining a value of the product $k_c\eta$ of $13.8 \times 10^9 \text{ cP dm}^3 \text{ mol}^{-1} \text{ sec}^{-1}$, calculating k_c from equation 5.2 and obtaining the value of the diffusion coefficient D from pulsed n.m.r. measurements.

$$k_c = 16 \pi r N D \quad (5.2)$$

Equation 5.2 can be derived from the Stokes-Einstein equations of Freed,⁶ by simple algebraic manipulation. The values of $k_c\eta$ thus obtained are about twice the value predicted from the Smoluchowsky rate. Franks et alia¹⁹ proposed that this result provided an accurate measure

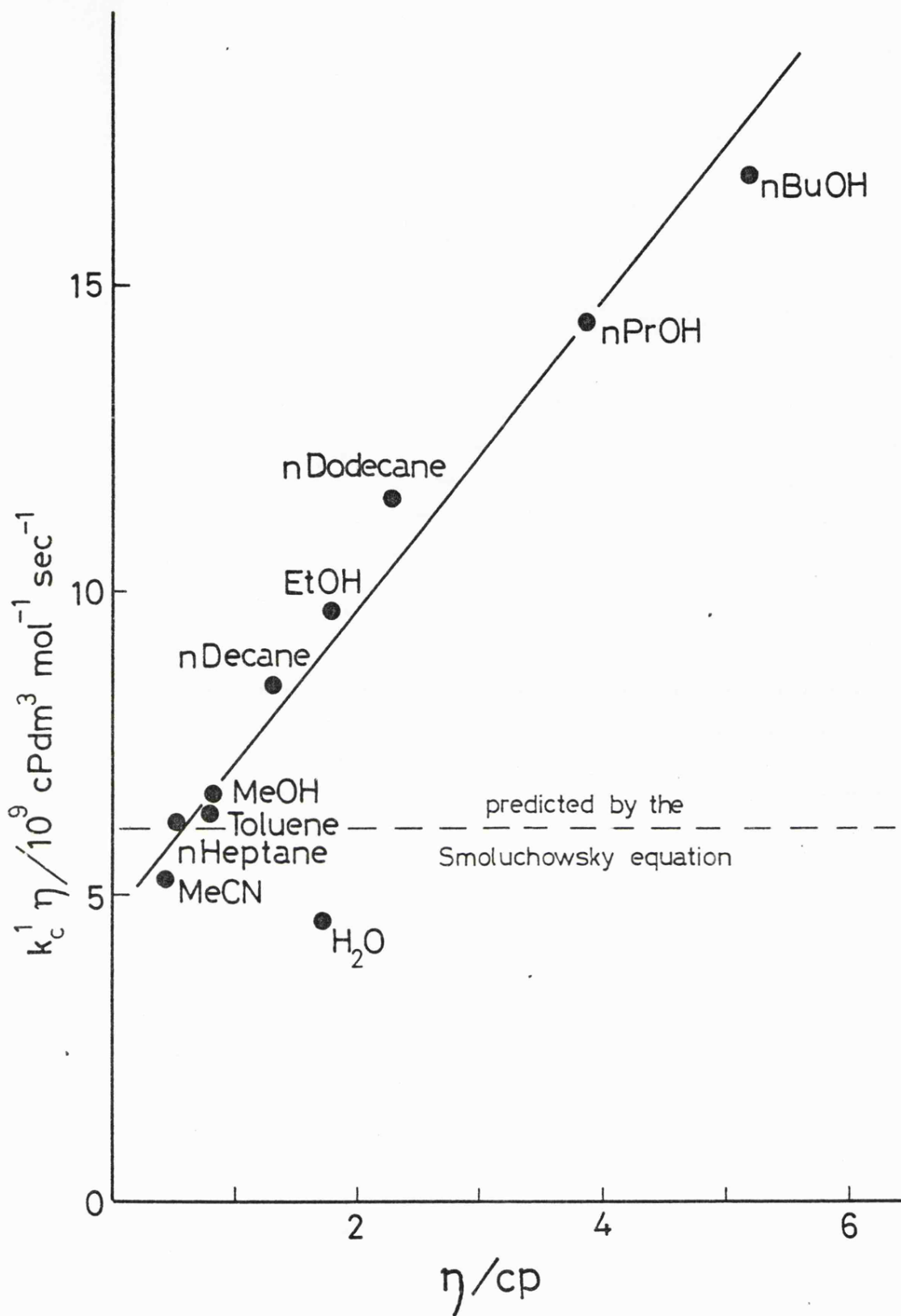


Figure 5.7

The product of radical collision rate constant k_c' and viscosity η as a function of viscosity.

of the diffusion rate of a nitroxide radical in solution. They suggested that at solvent viscosities less than 4cP at 293 K spin exchange is an inefficient process. Using a sticking time of about 10^{-11} sec, for nitroxide-nitroxide collision in a solution of $\eta = 1\text{cP}$ at 293 K; they predicted that the function $J^2\tau_1^2/(1+J_1^2\tau_1^2)$ in equation 2.60 was less than one. Thus, they were able to account for the results at least qualitatively, by postulating spin exchange as an inefficient process becoming more efficient with increasing medium viscosity, until the free diffusion behaviour is reached at $\eta \sim 4\text{cP}$.

In order to compare the results of the present work with those of Franks et alia, a graph of three times the exchange rate multiplied by the solvent viscosity against solvent viscosity was drawn. Unlike the graph of Franks et alia these results, presented in figure 5.7, show no clear tendency to curve off towards an asymptote at $13.8 \times 10^9 \text{ cP dm}^3 \text{ mol}^{-1} \text{ sec}^{-1}$ (this would be $12.9 \times 10^9 \text{ cP dm}^3 \text{ mol}^{-1} \text{ sec}^{-1}$ when corrected for temperature). This suggests that their conclusions are not satisfactory. Since our work was carried out at a lower temperature than that of Franks et alia, we would expect τ_1 to be longer and hence exchange to reach the strong exchange limit a little more quickly. The proposal of a value of 10^{-11} sec for τ_1 ($\eta = 1\text{cP}, T = 293 \text{ K}$) is a factor of ten smaller than the value predicted using equation 2.60. Clearly, the rôle of diffusion processes in determining the exchange rate must be re-examined.

The rôle of dipolar broadening must also be considered. The effect of competing dipolar and contact interactions in the broadening of the n.m.r. spectra of various solvents containing nitroxide radicals, has been examined in some detail.^{27,28} It is not inconceivable that both mechanisms should contribute to the concentration dependent line

broadening of nitroxides in solution. Figure 5.7 shows that on a pure diffusional basis, an efficient spin exchange process can fully account for the observed rate of line broadening at viscosities less than 1cP. The deviation from this "Smoluchowsky type behaviour" increases with solvent viscosity, as would be expected if dipolar broadening was of importance. The theory of Freed⁶ as given by equation 2.69 predicts that at 274 K approximately 36% of the concentration dependent broadening for DTBN in n butanol is due to the dipolar mechanism. This figure reduces to about 6% for ethanol and is further reduced for less viscous solvents. Even at 293 K, we would expect dipolar broadening to contribute ~10% and 20% respectively to the concentration dependent linewidths of TEMPO in DMSO and in sec butanol, as examined in ref. 9. Although this argument seems qualitatively sound, it is not so good quantitatively. It is only possible to account for about sixty per cent of the concentration dependent linewidth of DTBN in n butanol by computing the exchange contribution from equations 2.59 and 2.60, and the dipolar contribution from equation 2.68.

In the absence of any other known contribution to concentration dependent linewidths, we assume that Heisenberg spin exchange and dipolar broadening alone determine the concentration dependent linewidth. There are two probable explanations for the quantitative failure of these mechanisms in accounting fully for the concentration dependent linewidth of DTBN in solution. Firstly, the equations for the dipolar linewidth are approximate⁶ and only allow for relaxation via translational motion^{6,11} modulating the radical-radical dipolar interactions. It is possible that the equations given underestimate the dipolar contribution. The second and probably more likely explanation is the inadequacy of the Stokes-Einstein model of diffusion upon which equations

2.60 and 2.64 are based. It is well known that the Stokes-Einstein type equations cannot predict accurately, the contributions of spin rotation and motional averaging of anisotropic g and A tensors, to the linewidth of a radical in dilute solution. However, both mechanisms follow the predicted dependence on temperature and viscosity.

Buchachenko et alia²⁹ have commented that "experimental results have shown that this (the Stokes-Einstein) model describes the diffusion of large molecules more satisfactorily than it does small ones". However, these authors were able to show that the effects of radical size, solvent viscosity and temperature followed qualitatively the predicted effect on the exchange rate. It seems likely, on the basis of the discussion so far, that the nitroxides have a greater freedom of movement in solution than the solvent's bulk viscosity would predict. This would have the following effects:

- 1) τ_1 would be reduced and the exchange process would be less efficient causing a fall in concentration dependent linewidth.
- 2) τ_2 would be reduced, increasing the exchange rate and hence increasing the linewidth.
- 3) The correlation time for dipolar broadening would be reduced, decreasing the size of the dipolar broadening.

Of the two explanations, the second is favoured, largely because of the known failures of the Stokes-Einstein model. Clearly it would be very fortuitous if this "microviscosity" effect were to produce the linear dependence of the concentration dependent width on T/η .

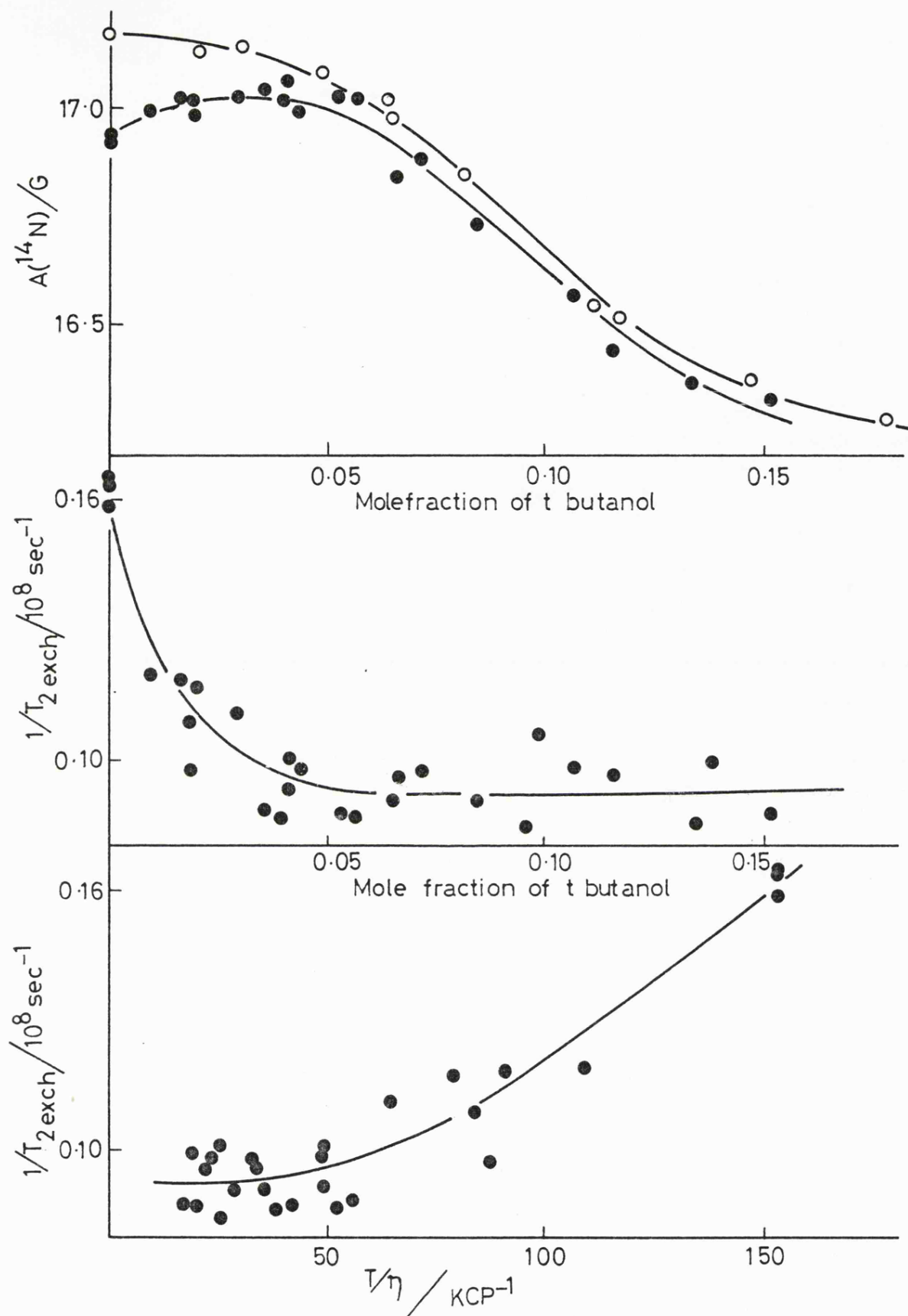
Probably, the most interesting feature of figures 5.6 and 5.7 is the deviation of the aqueous DTBN samples from the non-aqueous curve. We have already pointed out that the near linearity of figure 5.6 precludes the possibility of hydrogen bonding playing a significant rôle

in controlling the rate of exchange. From $A(^{14}\text{N})$ measurements in dilute solutions, we expect that DTBN is completely hydrogen bonded in water, at least 50 per cent hydrogen bonded in alcohols and non-bonded in aprotic solvents. Since the alcohols show no deviations from the non-aqueous line in figure 5.6, it would be reasonable to conclude that radical-solvent hydrogen bonding interactions do not cause the reduced exchange rate observed for DTBN in water. The low value of the exchange rate for DTBN in water could be due to two causes using a diffusional type model. This effect would be seen, if the translational motion of the nitroxide were restricted, or overlap between unpaired electrons of colliding radicals were reduced. The idea of a nitroxide radical held within a clathrate cage would certainly promote the second effect. The rôle of clathrate type solvation is known to be temperature sensitive, and a return to a more normal type behaviour is expected as the temperature increases. Figure 5.6 shows clearly that the aqueous data shows a stronger T/η dependence than the non-aqueous data, the two sets of data have almost converged at 900 KcP^{-1} ($\sim 350 \text{ K}$). This is consistent with the clathrate model. At 274 K , the experimentally determined rate constant for the exchange of a 10^{-2} M solution of DTBN in water, suggests that the interval between successive nitroxide-nitroxide collisions is of the order of $4 \times 10^{-8} \text{ sec}$. It is interesting to note that ultrasonic relaxation measurements on aqueous t-butanol solutions³⁰ show relaxation times of the order 10^{-7} to 10^{-8} secs . It has been suggested that these relaxation times are associated with the lifetime of a proposed clathrate structure. If we accept that ethanol is representative of the behaviour of a "free diffusion" controlled spin exchange process, then we would expect from the experimentally observed rate constant an interval of $\sim 1.8 \times 10^{-8} \text{ secs}$. The aqueous and ethanolic

systems are almost isoviscous at 274 K, thus we can see that the "clathrate effect" reduces the apparent radical-radical collision time by a factor of two.

The rôle of clathrate type solvation can be further probed by examining the nature of spin exchange in various aqueous t-butanol solutions. It has often been suggested that t-butanol has an ordering effect on the structure of water, when present in low concentrations in aqueous solution. Figure 5.6 shows the spin exchange rate constant observed for a $1.72 \times 10^{-2} \text{ M dm}^{-3}$ solution of DTBN in various t butanol-water mixtures, as a function of T/η . These results would appear to present an extension of the behaviour observed in the variable temperature study of exchange in water. Thus, the addition of t-butanol would appear to produce an extension of pure aqueous behaviour, rather than an enhancement of this behaviour.

The t-butanol behaviour is shown more clearly in figure 5.8. When the concentration dependent linewidths are plotted as a function of molefraction of t-butanol, we see a rapid fall in concentration dependent width in the 0 to 0.05 molefraction region. At concentrations of t-butanol greater than 0.05 mf the concentration dependent linewidth appears to be independent of further increase in t-butanol concentration. The plot of concentration dependent linewidth as a function of T/η shows that in the 0-0.05 mf region, the concentration dependent linewidth is a linear function of T/η , once the concentration has exceeded 0.05 mf ($T/\eta \sim 50 \text{ K cP}^{-1}$) the linewidth appears to be independent of further increase in T/η . The plots of $A(^{14}\text{N})$ against molefraction of t-butanol, for solutions containing $1.72 \times 10^{-2} \text{ M dm}^{-3}$ DTBN and $5 \times 10^{-5} \text{ M}$ DTBN are quite instructive. Initially the $1.72 \times 10^{-2} \text{ M dm}^{-3}$ shows an increase in $A(^{14}\text{N})$ in the 0 to 0.05 mf region. Since the $5 \times 10^{-5} \text{ M dm}^{-3}$ result



CAPTION TO FIGURE 5.8

Figure 5.8(i)

Plot of $A(^{14}\text{N})$ against molefraction of t-butanol for DTBN in various water-t-butanol solutions.

● = $1.72 \times 10^{-2} \text{ M dm}^{-3}$ DTBN

○ = $5 \times 10^{-5} \text{ M dm}^{-3}$ DTBN

Figure 5.8(ii)

Plot of the concentration dependent linewidth $1/T_2$ exch as a function of t-butanol concentration for a $1.72 \times 10^{-2} \text{ M}$ solution of DTBN in various t-butanol-water mixtures.

Figure 5.8(iii)

Plot of the concentration dependent linewidth $1/T_2$ exch as a function of T/η for a $1.72 \times 10^{-2} \text{ M}$ solution of DTBN in various t-butanol-water mixtures.

shows a plateau in this region, it would seem reasonable to attribute this increase in $A(^{14}\text{N})$ for the $1.72 \times 10^{-2} \text{ M dm}^{-3}$ sample, to a fall in spin exchange rate. Once the concentration of t-butanol exceeds 0.05 mf, $A(^{14}\text{N})$ for both samples begins to fall rapidly. Since both samples follow approximately parallel slopes, it is evident that the spin exchange rate is little effected by further increase in t-butanol concentration. The null effect of radical-solvent hydrogen bonding is demonstrated by the insensitivity of concentration dependent linewidth, in the 0.05 to 0.15 mf region, whilst the $A(^{14}\text{N})$ value of the $5 \times 10^{-5} \text{ M dm}^{-3}$ DTBN solution falls rapidly in this region.

Clearly, the t-butanol results can only be seen as an extrapolation of the pure water behaviour, as far as the concentration dependent linewidths are concerned. It is not possible to determine whether the levelling off of the decrease in concentration dependent width beyond 0.05 mf t-butanol is due to a return towards non-aqueous type behaviour or due to a balance between increase in dipolar contributions to the linewidth and ^{declining} exchange contributions as T/η increases. A continuation of aqueous type behaviour can be accommodated in terms of the clathrate model. In the low t-butanol concentration region, t-butanol and DTBN can be considered as being solvated in separate clathrate cages. This enclathration reduces nitroxide mobility and hinders efficient orbital overlap for the exchange process, thus decreasing the observed exchange rate to that expected for an aqueous sample. This behaviour is maintained at t-butanol concentrations greater than 0.05 mf, where cage sharing processes are thought to be of importance.³⁰ Here DTBN molecules will be forced to co-exist with t-butanol molecules in enlarged clathrate cages, since there are insufficient water molecules to form a clathrate network capable of accommodating each organic molecule in

separate cages. Cage sharing by t-butanol molecules in aqueous solutions has been postulated as the main reason for the intense ultrasonic absorption in the 0.05 to 0.2 molefraction regions.^{30,31} The similarity in magnitude for the time between radical-radical collisions calculated from the measured exchange rate, and the predicted lifetimes of t-butanol induced water structures as measured by ultrasonic relaxation measurements, lends some support to the "clathrate" idea.

Recently, Jolicoeur³² has examined the effects of hydrophobic interactions on relaxation processes, using the n.m.r. technique. The dipolar interactions between the t-butyl protons of t-butanol (or t-butylamine) and 2,2,6,6 tetramethyl piperidine-1-oxyl (TEMPO) in dilute solution, were measured in several solvents. Dipolar broadening of the alcohol's t-butyl protons was shown to be a linear function of the ratio of solvent viscosity to temperature. In aqueous solution the magnitude of dipolar broadening was significantly larger than experiment would predict for an isoviscous non-aqueous solvent. Jolicoeur et alia³² explained these results in terms of strong hydrophobic interactions between the alkyl residues of t-butanol and TEMPO in aqueous solution. An alternative explanation, in terms of the alcohol and nitroxide being held in separate clathrate cages, thus having restricted motion relative to each other, would clearly be consistent with the results of this spin exchange study. This would also imply that we have underestimated the importance of dipolar broadening in controlling the concentration dependent linewidth of DTBN in aqueous solutions. It is not possible to determine this effect accurately, but this should not effect the conclusions reached concerning the rôle of water structure in controlling the concentration dependent relaxation mechanisms examined.

5.4 Conclusions

The concentration dependent linewidths of DTBN in various non-aqueous and aqueous solvents have been carefully examined. In non-aqueous solvents the rate of increase in linewidth with increase of radical concentration are a linear function of the ratio of temperature to solvent viscosity. Careful examination of concentration dependent widths based on the Stokes-Einstein type prediction of the effects of Heisenberg spin exchange and dipolar broadening, have proved not to be valid. The possible importance of dipolar broadening effects and the discrepancy between solvent bulk viscosity and solvent microviscosity, have been acknowledged. It is proposed that the non-aqueous behaviour shows the effect of temperature and viscosity on the concentration dependent linewidth of DTBN in non-interacting solvent media. Possible effects due to radical-solvent hydrogen bonding have been discounted since the alkanes and alcohols show identical effects on the linewidths of the nitroxide probes studied.

Water behaves anomalously as a solvent and reduces the concentration dependent linewidth substantially. It is proposed that in aqueous solution the nitroxide is solvated in a clathrate cage. This "enclathration" of the nitroxide restricts the possibility of close approach of colliding radicals and reduces the translational freedom of probe molecules. The addition of t-butanol to the aqueous solutions appears to produce a continuation of the pure water behaviour. Initially, addition of small amounts of t butanol causes a decrease in concentration dependent linewidth along the T/η slope predicted from the pure water data. The decline in concentration dependent linewidth is arrested as the t-butanol concentration approaches 0.05 mf, and concentration dependent linewidth remains constant with further increase in t-butanol

behaviour. The retention of aqueous behaviour in the low molefraction region is attributed to the stabilisation of clathrate structures by the t-butanol molecules. The situation is less clear when the t-butanol concentration exceeds 0.05 mf. The levelling off of the curve could be interpreted as the beginnings of a return to "non-aqueous" type behaviour, or as a continuation of the aqueous behaviour masked by dipolar broadening effects. The latter suggestion implies the possibility of DTBN undergoing some cage sharing with t-butanol molecules, as the t-butanol concentrations increases the solution viscosity will increase causing a decline in exchange width cancelled by an increase in dipolar broadening. Clearly, this behaviour must be examined in more detail over a wider temperature range before more precise conclusions can be drawn.

REFERENCES TO CHAPTER FIVE

1. G. E. Pake and T. R. Tuttle, Phys. Rev. Letters, 1959, 3, 423.
2. D. Kivelson, J. Chem. Phys., 1960, 33, 1094.
3. M. T. Jones, J. Chem. Phys., 1963, 38, 2892.
4. T. A. Miller, R. N. Adams and P. M. Richards, J. Chem. Phys., 1966, 44, 4022.
5. C. S. Johnson, Mol. Phys., 1967, 12, 25.
6. M. P. Eastman, R. G. Kooser, M. R. Das and J. H. Freed, J. Chem. Phys., 1969, 51, 2690.
7. M. P. Eastman, G. V. Bruno and J. H. Freed, J. Chem. Phys., 1970, 52, 2511.
8. J. C. Lang and J. H. Freed, J. Chem. Phys., 1972, 56, 4103.
9. W. Plachy and D. Kivelson, J. Chem. Phys., 1967, 47, 3312.
10. P. Devaux, C. J. Scandella and H. M. McConnel, J. Mag. Res., 1973, 9, 474-485.
11. A. Abragam "The Principles of Nuclear Magnetism", Oxford University Press, London, 1961, p.289.
12. H. Lemaire, P. Rey, A. Rassat, A. de Combarieu and J. C. Michel, Mol. Phys., 1968, 14, 201.
13. K. Adamic, D. F. Bowman, T. Gillan and K. U. Ingold, J. Am. Chem. Soc., 1971, 93, 902.
14. C. Morat and A. Rassat, Tetrahedron, 1972, 28, 735.
15. L. J. Bernier, Acta Crystallog., 1970, B26, 1198.
16. See for example,
C. A. Coulson "Valence (2nd. Ed)", Oxford University Press, 1961, p.159.
17. D. J. Jones, Ph.D. Thesis, University of Leicester 1972.
18. C. E. Mount, H. C. Starkie, E. A. Smith and M. C. R. Symons. Unpublished results.
19. S. Ablett, M. D. Barratt and F. Franks, J. Solution Chem., 1975, 4, 497.
20. Y. Y. Lim, E. A. Smith and M. C. R. Symons, J.C.S. Faraday I, 1976, 72, 2876.

21. J. A. Riddick and W. B. Bunger "Organic Solvents. Physical Properties and Methods of Purification (3rd. Ed)", Wiley Interscience, 1970.
22. "Selected Values of Physical and Thermodynamic Properties of Hydrocarbons and Related Compounds". American Petroleum Institute of Research, Project 44, Carnegie Press, 1953.
23. S. Westmeier, Chem. Techn., 1977, 29, 218.
24. A. E. Stillman and R. N. Schwartz, J. Mag. Res., 1976, 22, 269.
25. A. K. Hoffman and A. T. Henderson, J. Am. Chem. Soc., 1961, 83, 4671.
26. See Appendix.
27. S. B. W. Roeder, W. Wun and O. H. Griffith, J. Phys. Chem., 1969, 73, 3510.
28. H. S. Gutowsky and J. C. Tai, J. Chem. Phys., 1963, 39, 208.
29. A. L. Kovarskii, A. M. Wasserman and A. L. Buchachenko, J. Mag. Res., 1972, 7, 225.
30. M. J. Blandamer, D. E. Clarke, N. J. Hidden and M. C. R. Symons, Trans. Faraday Soc., 1968, 64, 2691.
31. M. J. Blandamer and M. C. R. Symons "Hydrogen-Bonded Solvent Systems", Ed. A. K. Covington and P. Jones, Taylor & Francis, London, 1968.
32. C. Jolicoeur, P. Bernier, E. Firkins and J. K. Saunders, J. Phys. Chem., 1976, 80, 1908.

CHAPTER SIX

Frozen Solutions of Nitroxide Radicals

CHAPTER SIX

6.1 Introduction

The rôle of nitroxides, in probing solvation effects in fluid solution has been discussed in the earlier parts of this thesis. Studies of nitroxides in frozen solutions may be useful in further examining solvation effects. Until recently,^{1,2} studies of frozen solutions of nitroxides have been few. Determinations of the principal g and A tensors of nitroxides have been available from single crystal studies,^{3,4} for quite some time. Freed *et alia*^{2,5-7} have shown the importance of using accurate measurements of these magnetic parameters, when evaluating relaxation times of nitroxides in dilute solution. To obtain the relevant anisotropic g and A values, these authors have made accurate e.s.r. measurements on several nitroxides in a variety of frozen matrices. Unfortunately, the X-band e.s.r. spectrum of ditertiary butyl nitroxide in frozen solution is very broad. Figure 6.1 shows that only the principal g and A values along the nitrogen p_z orbital can be determined from this spectrum. To make accurate measurements of the complete g and A tensors of a dialkyl nitroxide, it is necessary to either use a perdeuterated nitroxide or to make e.s.r. measurements at Q-band (33 GHz) frequencies.

Recent measurements of the anisotropic nitrogen hyperfine splitting constants, $2B(^{14}\text{N})$ of various nitroxides^{8,9} have provided good estimates of the unpaired electron spin density in the p_z orbital on nitrogen in these radicals. These studies have demonstrated that both the isotropic g value and $2B(^{14}\text{N})$ are linear functions of $A(^{14}\text{N})$. An indication of the relationship of the principal g and A tensors to $A(^{14}\text{N})$ would be of interest.

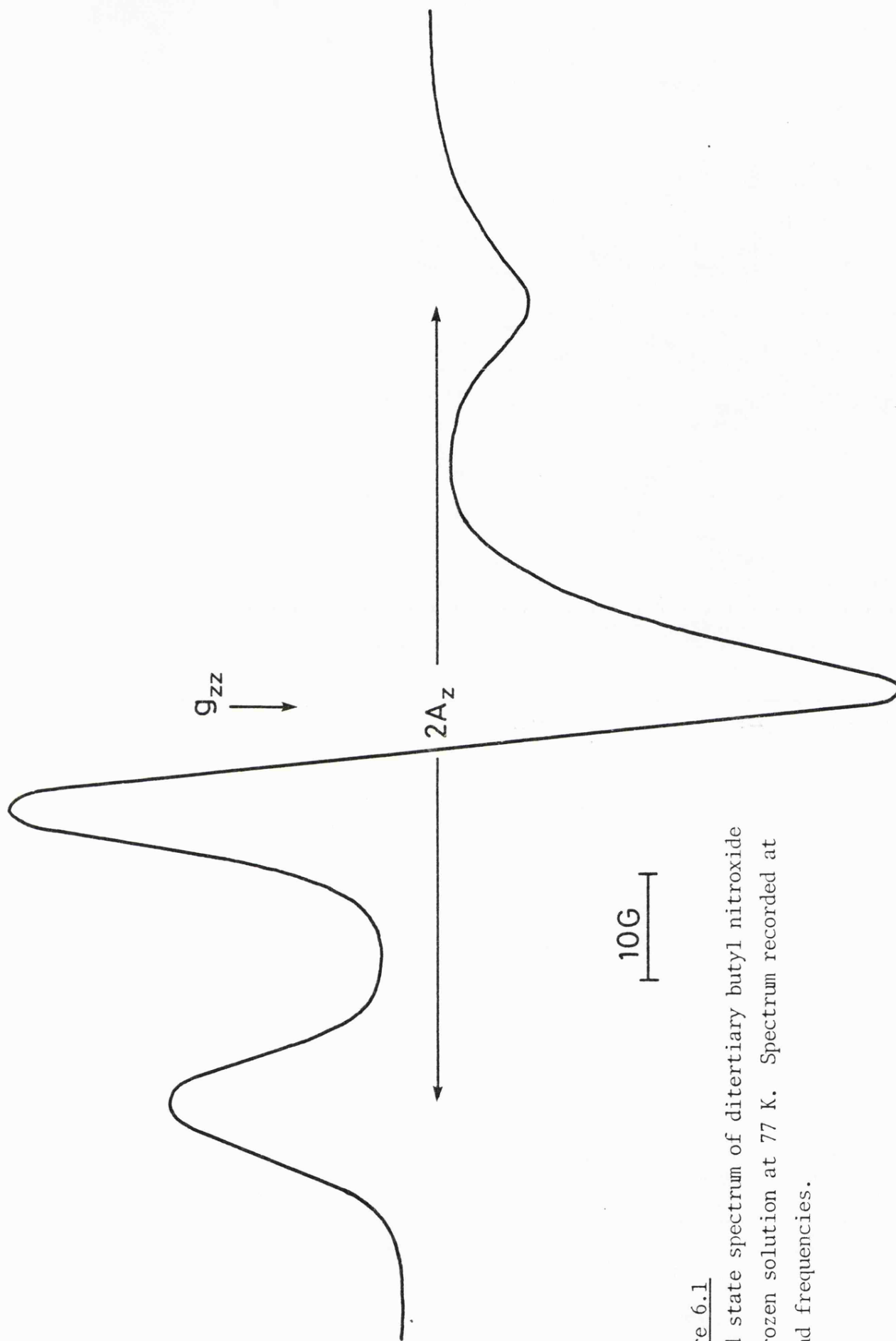


Figure 6.1
Solid state spectrum of ditertiary butyl nitroxide
in frozen solution at 77 K. Spectrum recorded at
X-band frequencies.

Jones¹⁰ has investigated the solid state spectrum of DTBN in various frozen aqueous matrices. This nitroxide shows a strong tendency to phase separate from water rich aqueous solutions at liquid nitrogen temperatures. This behaviour prevents accurate data being extracted from the spectra obtained, and thus no firm conclusions could be drawn from this work.

The purpose of the present work is to obtain good solid state data, for DTBN in a range of solvents and to examine the effects of solvation on the anisotropic spectrum. To obtain reliable data, the e.s.r. spectrum of DTBN in a variety of frozen matrices has been measured at Q-band frequencies and liquid nitrogen temperatures. The magnetic parameters are extracted from the Q-band spectrum using the computer simulation technique. The methods used are similar to those of Freed,^{2,5,6} of whose work we were unaware when this investigation was begun. The e.s.r. spectrum of the radical t-butyl-N-benzoyl nitroxide was examined at both X- and Q-band frequencies. It is hoped, from the parameters obtained, to infer something of the spin distribution within this radical.

6.2 Experimental Details

Ditertiary butyl nitroxide and d¹⁸ ditertiary butyl nitroxide were prepared as described in Chapter 3 of this thesis. Fremy's salt (peroxylamine disulphonate) was obtained from Alpha Inorganics, and was used as supplied. The radical t-butyl-N-benzoyl nitroxide was prepared by oxidation of an alkaline aqueous solution of the corresponding hydroxamic acid, using potassium ferricyanide as oxidizing agent. The reaction was allowed to proceed until the strong green colour of the radical appeared. Methylene chloride was then added to the reacting

mixture and the organic layer containing the bulk of the radical was separated off. The organic solution was dried over anhydrous sodium carbonate for several hours and the liquid was decanted off. The solvent was then removed using a rotary evaporator and the remaining green oil was t-butyl-N-benzoyl nitroxide. All solvents were purified using standard methods described previously.

The e.s.r. measurements were obtained using solutions with radical concentrations of 10^{-4} M or less. X-band spectra were recorded on a Varian E-3 spectrometer and the Q-band spectra were obtained using an instrument described in the literature.¹¹ X-band spectra were calibrated using either Fremy's salt in alkaline aqueous solution ($A(^{14}\text{N}) = 13.091$ G) or a 10^{-4} M aqueous solution of DTBN ($A(^{14}\text{N}) = 17.14$ G), to check the magnetic field. All g-values for X-band spectra were measured using diphenyl picryl hydrazyl, DPPH ($g_{\text{iso}} = 2.0036$) as a standard. The Q-band spectra were calibrated using a gaussmeter and the A_{\parallel} and g_{\parallel} values obtained from X-band measurements on the same sample. This method of calibration was not possible for the Q-band spectrum of t-butyl-N-benzoyl nitroxide, since even the parallel features of its spectrum are poorly resolved at X-band. These spectra were calibrated using a gaussmeter and a Q-band spectrum of Fremy's salt in a frozen 0.05 M aqueous solution of potassium carbonate ($A_{\parallel} = 29.8$ G, $g_{\parallel} = 2.0025$).² The frozen samples were maintained at 77 K by using liquid nitrogen in a standard finger dewar, for the X-band measurements. The small 8 mm cavity of the Q-band machine prevents the use of finger dewars and the whole cavity is immersed in liquid nitrogen instead.

The spectral simulations were produced using a FORTRAN computer program, written by Dr. T. Lund and based on the work of Pilbrow et

alia.¹² The simulation technique predicts the spectrum obtained using estimated values for A_x , A_y , g_x and g_y and the experimental values of A_z and g_z . The line shapes of the simulated spectrum are predicted using a Gaussian function and guessed values for the linewidths. Each variable is adjusted until the best fit of computer simulation and experiment is obtained. All simulations were produced using a CDC Cyber 72 computer and graphical output was obtained using the CULHAM GHOST plotting routines. The program is documented more fully in the appendix.

6.3 Ditertiary Butyl Nitroxide - results and discussion

The spectra obtained from the Q-band results together with their computer simulations are shown in figures 6.2 to 6.7. The experimental linewidths could be determined from the low and high field features of the X-band solid state spectrum or from the two high field features of the Q-band spectrum. These widths were measured as the half-width at half height, and were in the region of 4.5 to 5.5 G. The simulations gave the best fits to the Q-band spectrum using linewidths of the order 3 to 4 G. The "extra" broadness of the experimental spectrum probably is a function of the high degree of overlap of the spectral features. A small angular dependence of linewidth is seen for the Q-band spectra. On the whole the z features of the Q-band spectrum tend to be narrower than the x and y features. The magnetic x, y and z axes are those suggested by McConnell,³ with the x axis pointing along the N-O bond and the z axis defined by the nitrogen p_z orbital. The X-band results on d^{18} DTBN and Fremy's salt give much narrower lines, with the z features narrower than the x or y features. This angular dependence is similar to that observed by Freed. The widths used in simulating

Figure 6.2

X-band spectrum of Fremy's salt in a frozen solution of potassium carbonate in D_2O at 77 K.

— Experimental spectrum
 --- Computer simulation

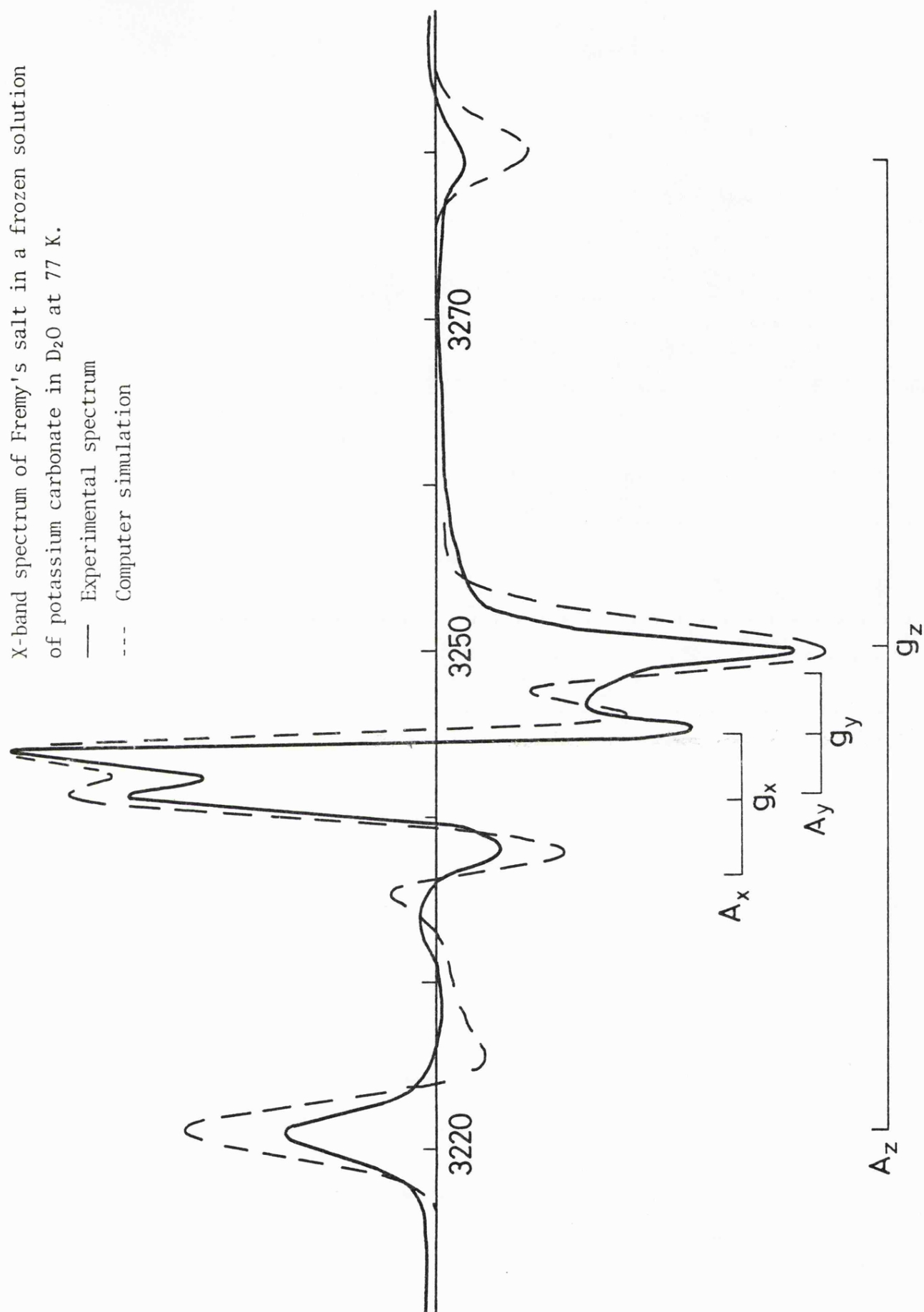


Figure 6.3

X-band spectrum of d^{18} ditertiary butyl nitroxide in a frozen solution of d^4 methanol at 77 K.

— Experimental spectrum
 --- Computer simulation

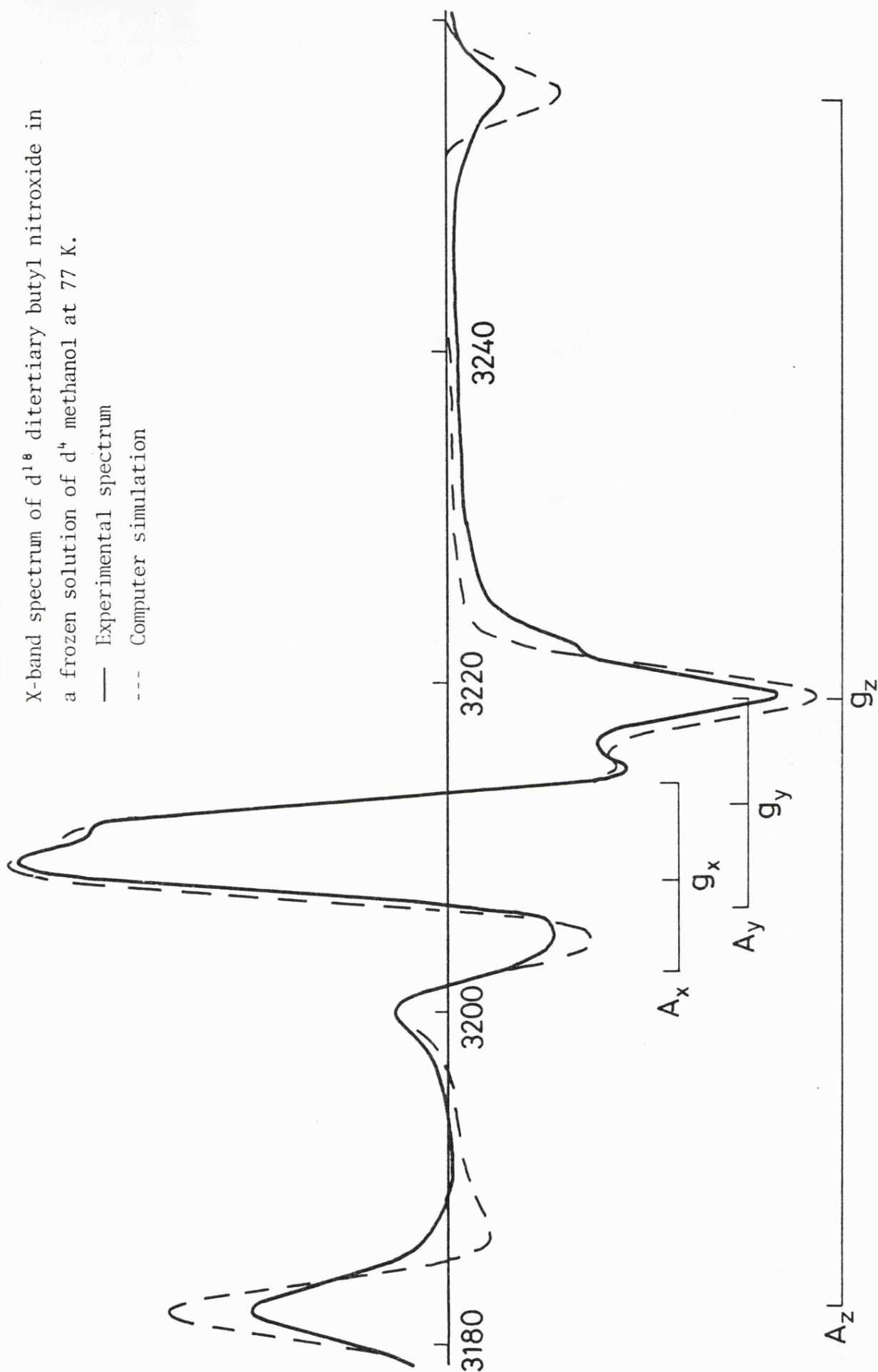
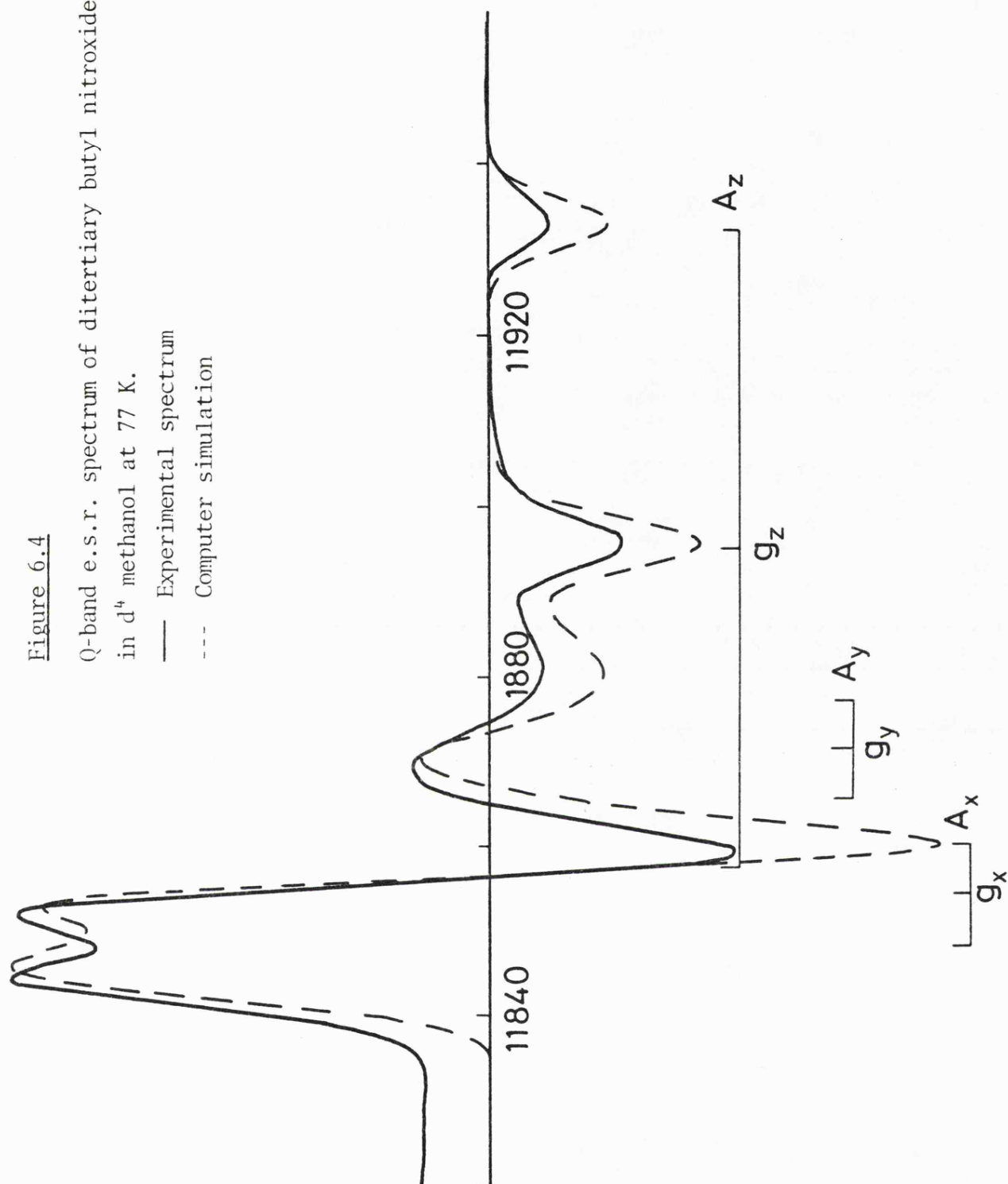


Figure 6.4

Q-band e.s.r. spectrum of ditertiary butyl nitroxide
in d^4 methanol at 77 K.

— Experimental spectrum

--- Computer simulation



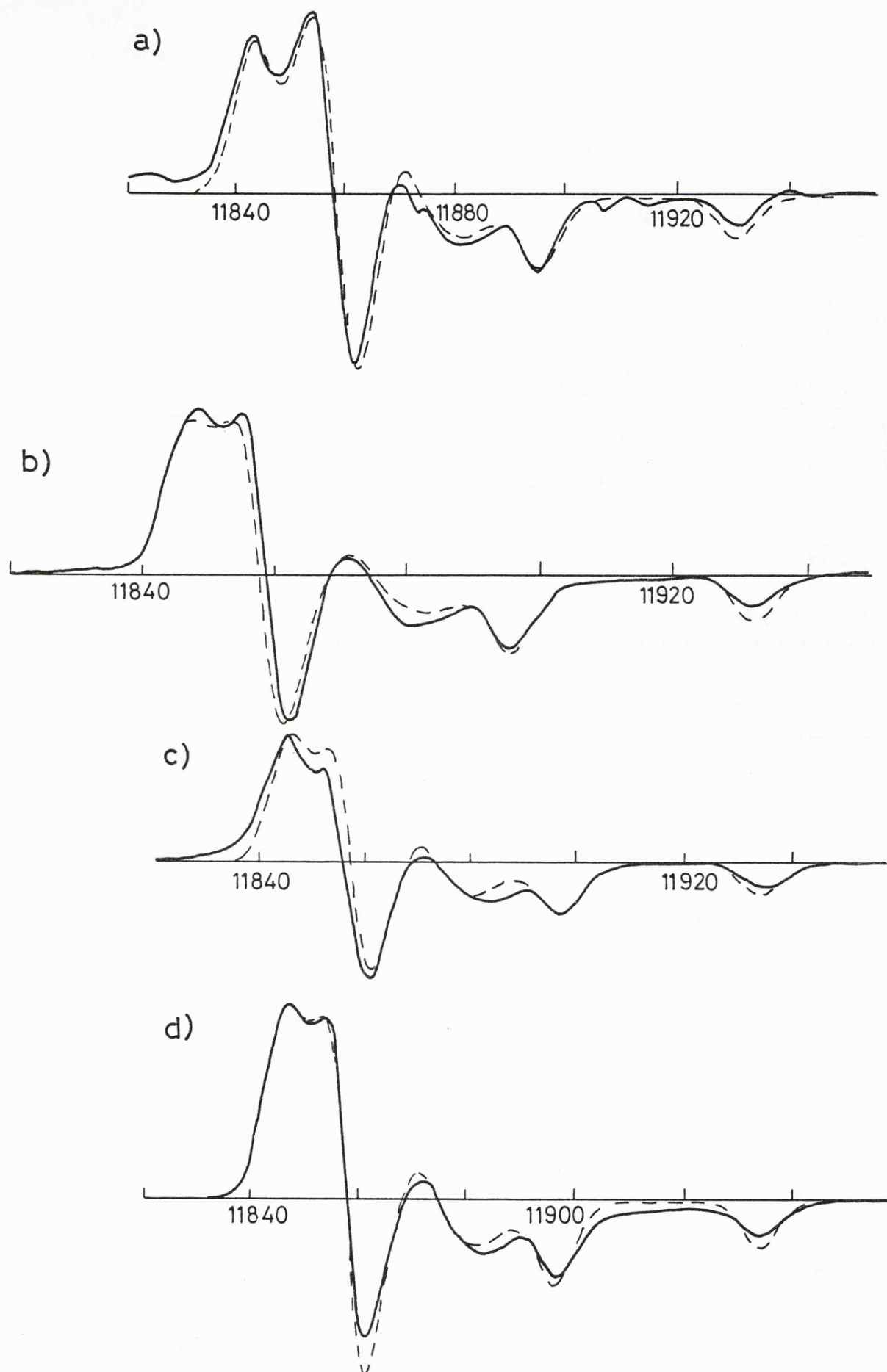


Figure 6.5

Q-band e.s.r. spectra of DTBN in
 a) toluene, b) 0.44 mf methanol-toluene, c) 0.735 mf methanol-toluene
 and d) 0.894 mf methanol-toluene, all at 77 K.

— Experimental spectrum

--- Computer simulation

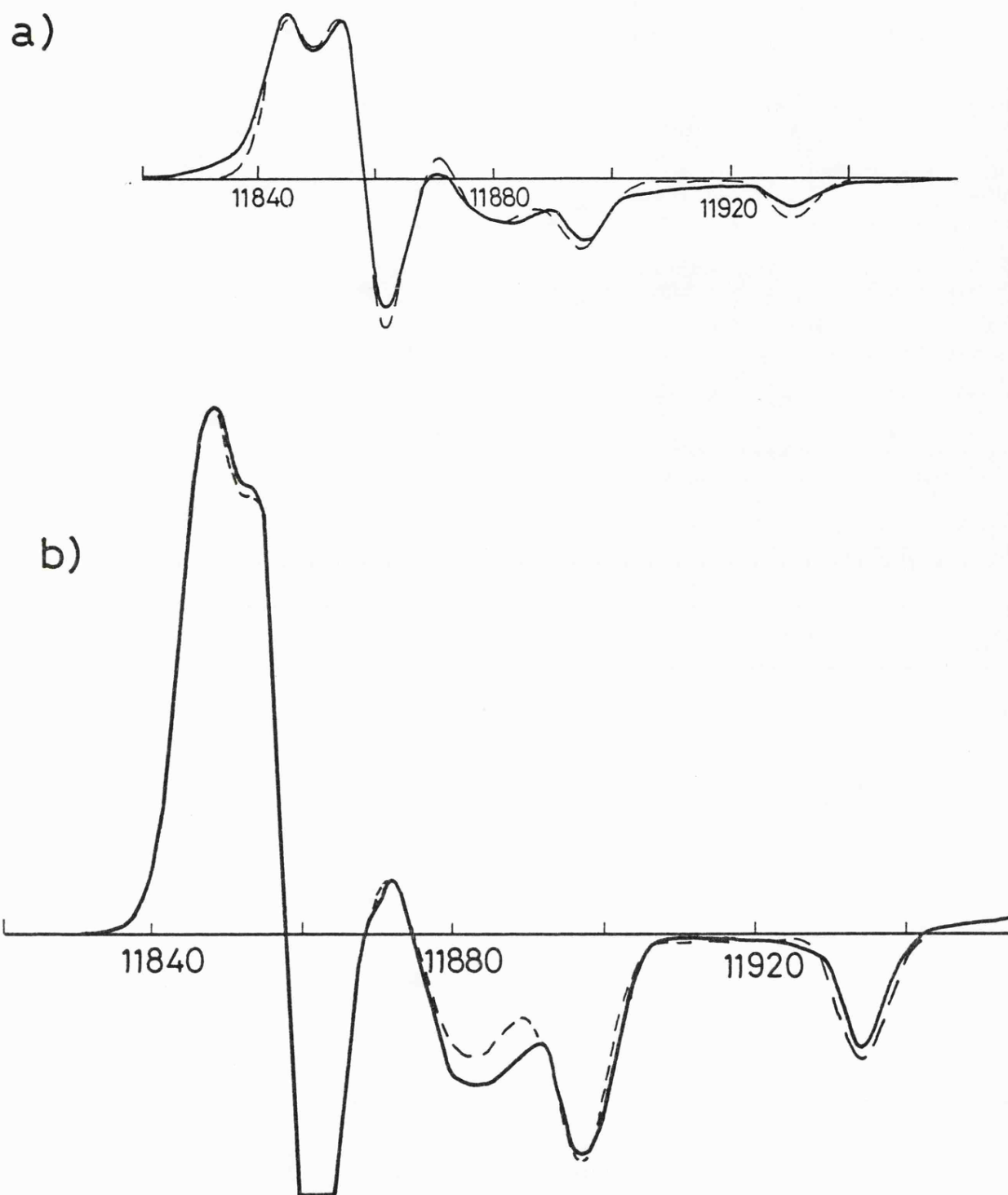


Figure 6.6

Q-band e.s.r. spectra of DTBN in a) d^3 methyl cyanide and b) methanol at 77 K.

— Experimental spectrum
 --- Computer simulation

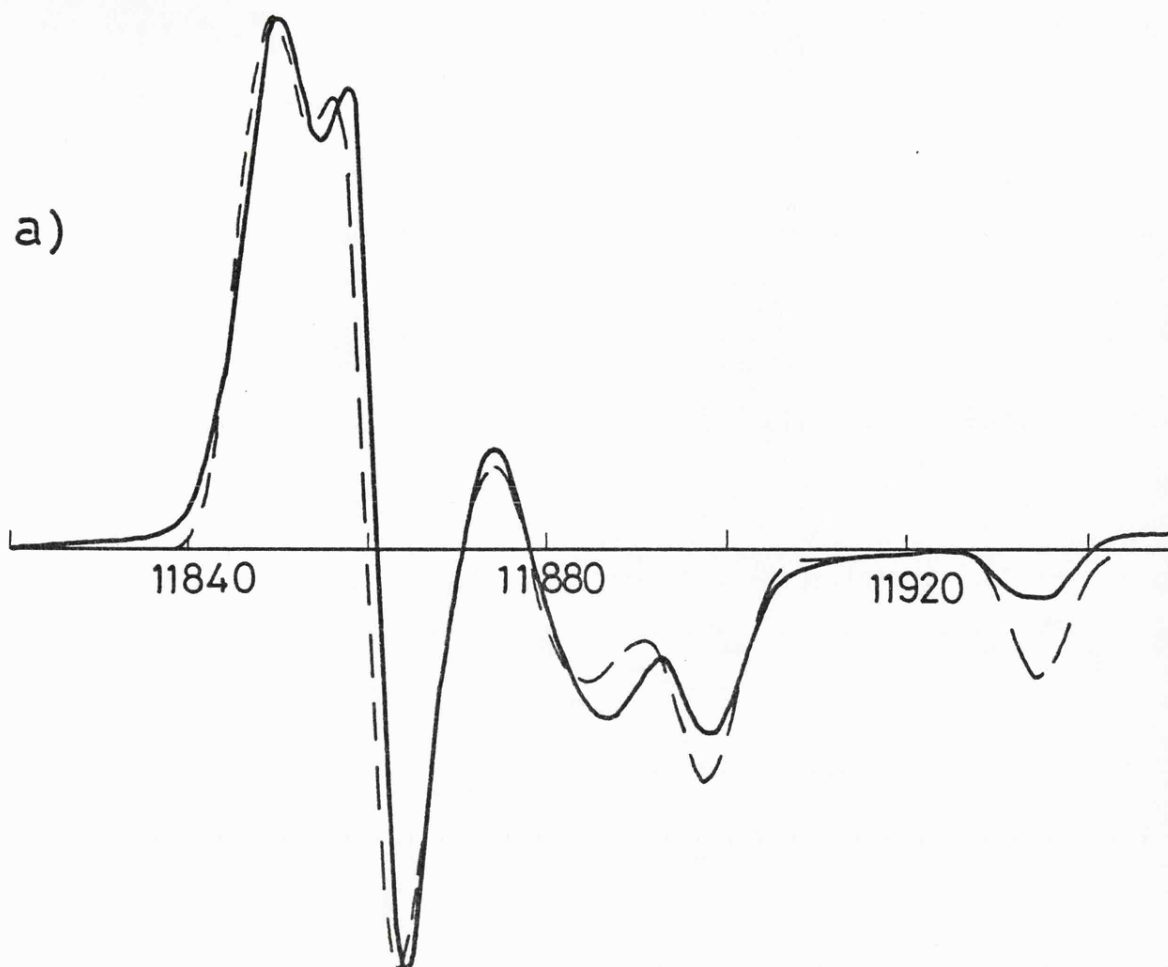
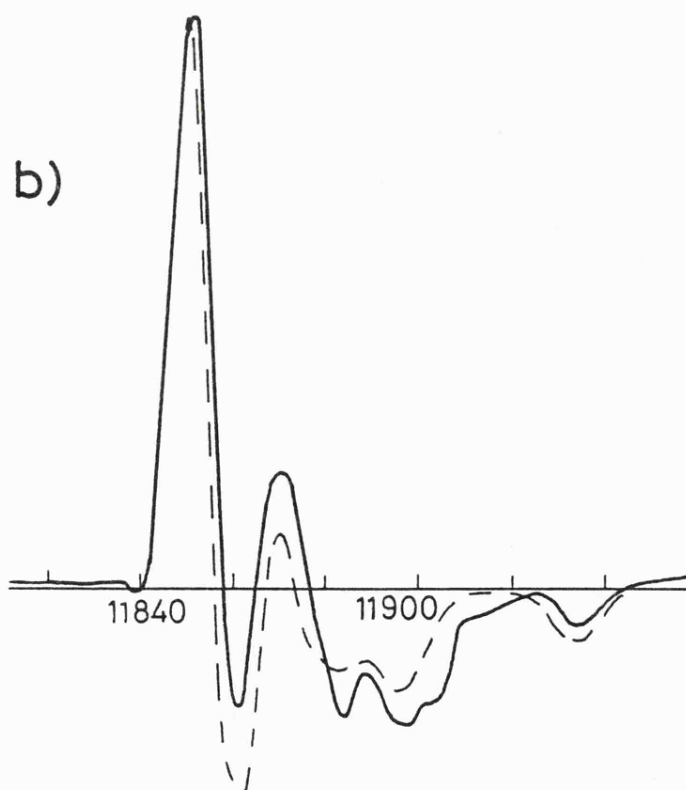


Figure 6.7

Q-band e.s.r. spectra of DTBN in frozen solutions of a) 0.180 mf t-butanol-water solution at 77 K; b) 0.0972 mf t-butanol-water solution at 77 K.

— Experimental spectrum
 --- Computer simulation



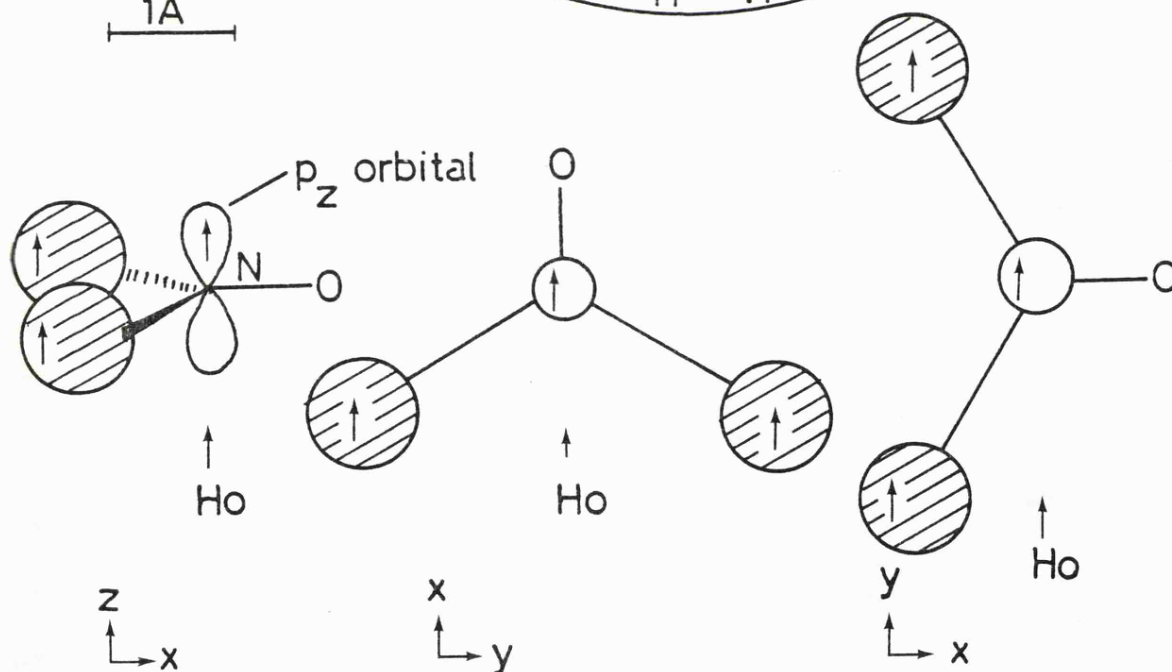
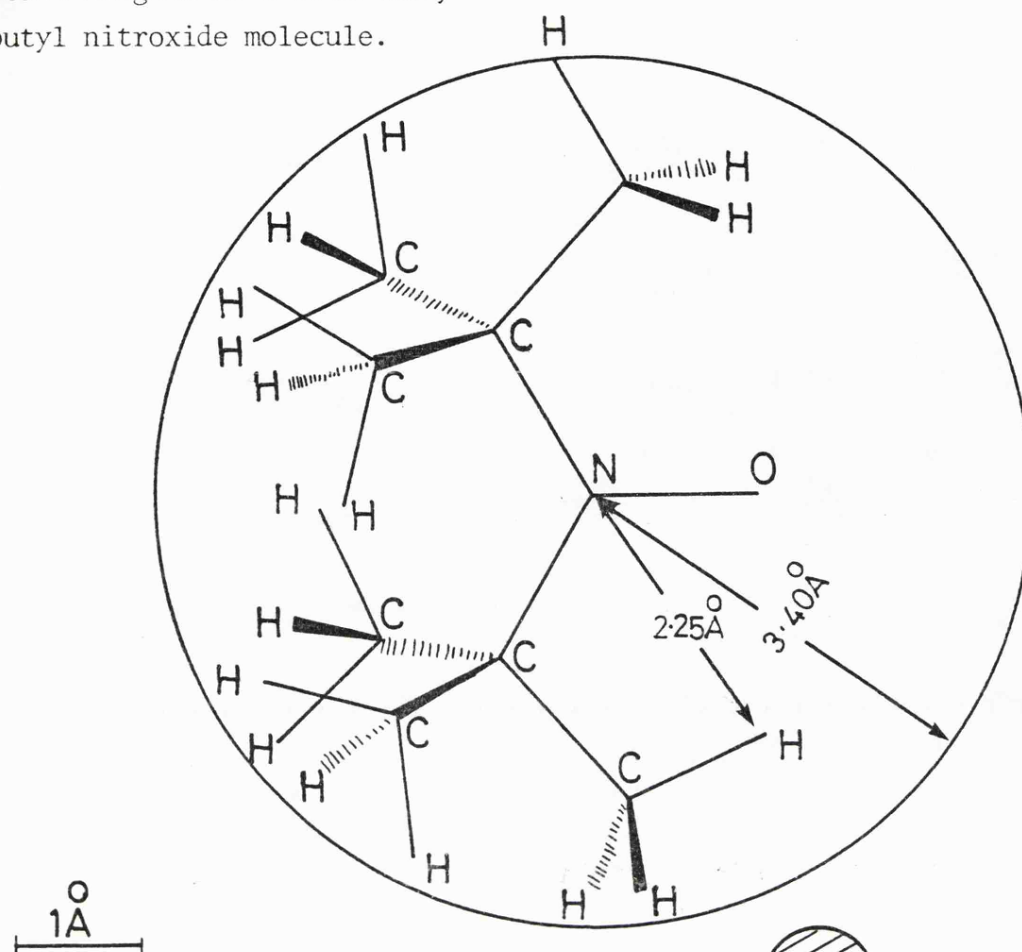
the d^{18} DTBN and Fremy's salt spectra (~ 1.6 G) were very close to the experimentally observed widths (2.0 and 1.6 G respectively).

The solid state spectra of dialkyl nitroxides are probably broadened by intramolecular coupling of the alkyl protons to the unpaired electron spin. This seems likely, because perdeuteration of the radical improves resolution of the spectra so dramatically. The effect of intermolecular coupling to solvent protons is small compared with this, since only a small narrowing of the DTBN solid state spectrum is seen, on switching to a perdeuterated matrix. Freed⁷ has proposed an anisotropic coupling of the methyl protons of 2,2,6,6-tetramethyl-4-piperidone-1-oxyl, TEMPOO, to the unpaired electron. This gives rise to a parallel coupling of -0.74 G and a perpendicular coupling of $+0.182$ G in the solid state.⁷ This coupling is larger than the isotropic proton coupling and can account for the broad solid state spectrum of TEMPOO as compared to the well resolved spectrum of the d^{16} radical. This anisotropic proton hyperfine coupling is probably due to an across space dipolar interaction with the unpaired electron. Rassatt has shown that the piperidone nitroxides undergo inversion between various conformers on a time scale of between 10^{-5} to 10^{-8} secs, at ambient temperatures. At 77 K TEMPOO may be thought of as residing in the more stable of its conformational states. The orientation of the methyl groups to the unpaired electron will be fixed by the rigid nature of the piperidone ring, although the methyl groups themselves may be free to rotate about the C-C bond. Thus, molecular motions would be incapable of averaging to zero the dipolar coupling between the protons and the unpaired electron, at 77 K.

The situation for DTBN is less clear; there is no ring structure to prevent free rotation of the t-butyl groups about the N-C bonds.

Figure 6.8

- a) Scale diagram of a ditertiary butyl nitroxide molecule.



- b) Point dipole representations of the anisotropic interaction between the t-butyl protons of DTBN and the unpaired electrons under the influence of an external magnetic field.

The spectrum of the t-butyl radical in some solvents at 77 K¹⁴ is typical of a freely rotating radical. This suggests that the t-butyl groups of DTBN may be free to rotate about the N-C axes even at 77 K. The protons of a freely rotating t-butyl group would still give an anisotropic coupling to the unpaired electron of DTBN. It is possible to demonstrate the presence of this coupling using the point dipole representation of DTBN shown in figure 6.8(b). Using molecular models, the average distance between the t-butyl protons and the nitrogen and oxygen atoms of DTBN, can be evaluated as 2.9 Å and 3.2 Å respectively. It is possible to approximate the t-butyl groups to single point nuclei 3 Å away from the unpaired electron. The method of Carrington and McLachlan¹⁵ used in conjunction with this model predicts a proton splitting of -1.15 G and -0.36 G, when the applied field lies along the z and x (or y) axes respectively. A large proton coupling of +2 G together with a smaller coupling of -0.36 G, will be observed if the applied field is orientated along one of the N-C bonds. It is encouraging that these very crude calculations give results of similar magnitude to Freed's⁷ estimates of the anisotropic proton coupling in TEMPOO. Perdeuterated nitroxides will give narrower features in their solid state spectra, since the ratio of the deuteron and proton magnetic moments predict a reduction in this anisotropic superhyperfine coupling to about one-sixth of the proton value.

Table 6.1 shows the experimentally observed principal g and A values obtained from Q- and X-band spectra of DTBN in frozen solutions of various solvents. Plots of the principal g and A values as functions of A(¹⁴N) are shown in figures 6.9 and 6.10 respectively. Both sets of parameters are linearly dependent on A(¹⁴N) and when subjected to a linear least squares type analysis show the following relationships.

TABLE 6.1

The principal g and A values of DTBN from computer simulation of Q-band spectra.

Results marked with an asterisk are from spectral simulation of X-band spectra of d¹⁸, DTBN or Fremy's salt. A_{av} is defined as $\frac{A_x + A_y + A_z}{3}$ and g_{av} is defined as $\frac{g_x + g_y + g_z}{3}$.

| Solvent | A _z (Gauss) | A _x (Gauss) | A _y (Gauss) | g _z | g _x | g _y | g _{av} | A _{av} (Gauss) | g _{iso} | A(¹⁴ N)(Gauss) |
|--|------------------------|------------------------|------------------------|----------------|----------------|----------------|-----------------|-------------------------|------------------|----------------------------|
| Toluene | 34.98 | 6.40 | 6.41 | 2.0024 | 2.0098 | 2.0063 | 2.0062 | 15.93 | 2.0061 | 15.50 |
| 0.440 mf MeOH in toluene | 36.16 | 6.72 | 6.73 | 2.0024 | 2.0091 | 2.0061 | 2.0059 | 16.54 | 2.0059 | 15.76 |
| 0.735 mf MeOH in toluene | 37.22 | 5.86 | 5.87 | 2.0024 | 2.0093 | 2.0063 | 2.0060 | 16.32 | 2.0058 | 16.30 |
| 0.894 mf MeOH in toluene | 37.12 | 6.40 | 6.41 | 2.0022 | 2.0091 | 2.0061 | 2.0058 | 16.64 | 2.0057 | 16.16 |
| Methanol | 37.23 | 6.61 | 5.98 | 2.0022 | 2.0090 | 2.0060 | 2.0057 | 16.61 | 2.0057 | 16.16 |
| d ⁴ Methanol | 37.22 | 5.86 | 5.87 | 2.0024 | 2.0093 | 2.0063 | 2.0060 | 16.32 | 2.0056 | 16.03 |
| d ³ Acetonitrile | 35.51 | 6.08 | 6.09 | 2.0025 | 2.0095 | 2.0063 | 2.0061 | 15.89 | 2.0060 | 15.69 |
| d ¹⁸ DTBN in * d ⁴ Methanol | 36.69 | 5.86 | 6.41 | 2.0023 | 2.0090 | 2.0060 | 2.0058 | 16.32 | 2.0057 | 16.08 |
| 0.0972 mf t-BuOH in water | 37.44 | 5.33 | 7.47 | 2.0022 | 2.0083 | 2.0063 | 2.0056 | 16.75 | 2.0058 | 16.67 |
| 0.180 mf t-BuOH in water | 36.48 | 6.40 | 5.87 | 2.0020 | 2.0087 | 2.0056 | 2.0054 | 16.25 | 2.0059 | 16.41 |
| Fremy's salt * in water | 29.41 | 4.48 | 3.63 | 2.0025 | 2.0083 | 2.0059 | 2.0056 | 12.51 | 2.0055 | 13.10 |

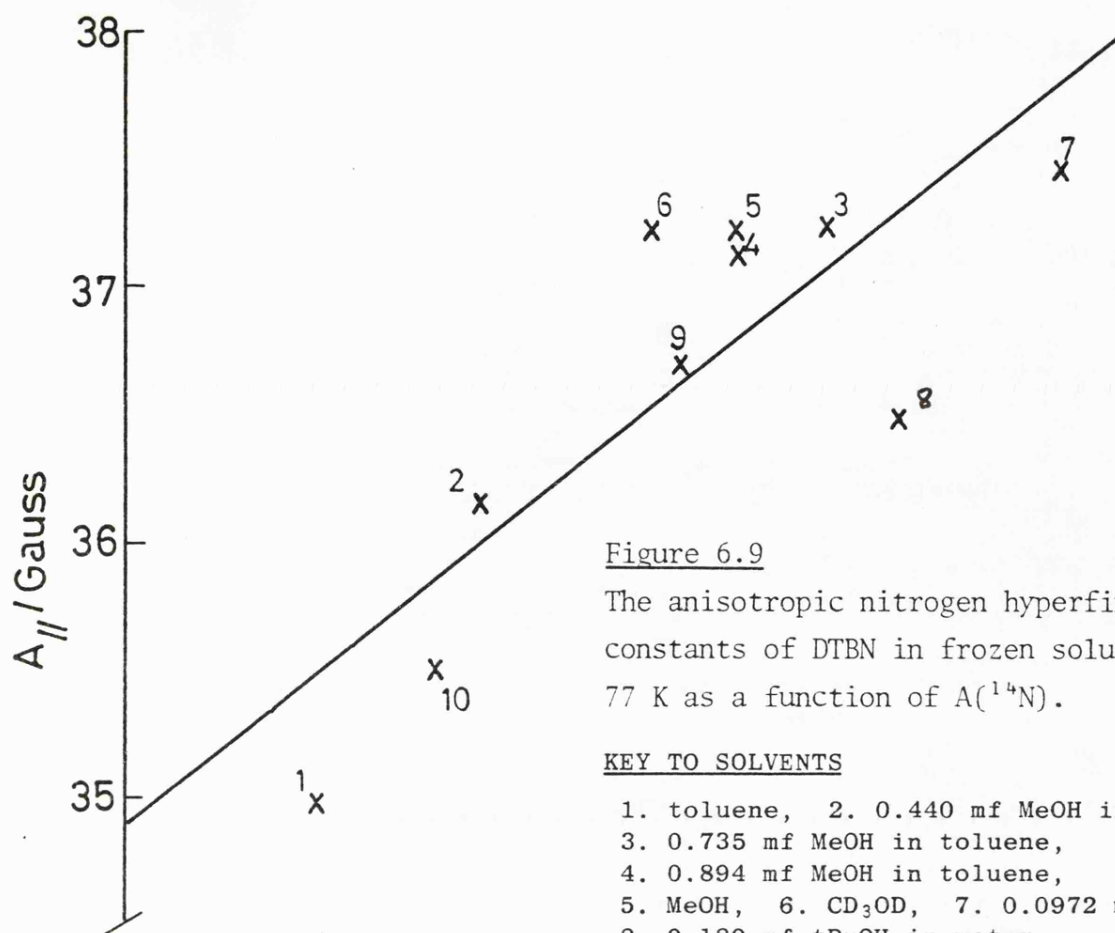


Figure 6.9

The anisotropic nitrogen hyperfine coupling constants of DTBN in frozen solutions at 77 K as a function of $A(^{14}\text{N})$.

KEY TO SOLVENTS

1. toluene, 2. 0.440 mf MeOH in toluene,
3. 0.735 mf MeOH in toluene,
4. 0.894 mf MeOH in toluene,
5. MeOH, 6. CD_3OD , 7. 0.0972 mf tBuOH in water,
8. 0.180 mf tBuOH in water,
9. d^{18} DTBN in CD_3OD ,
10. CD_3CN .

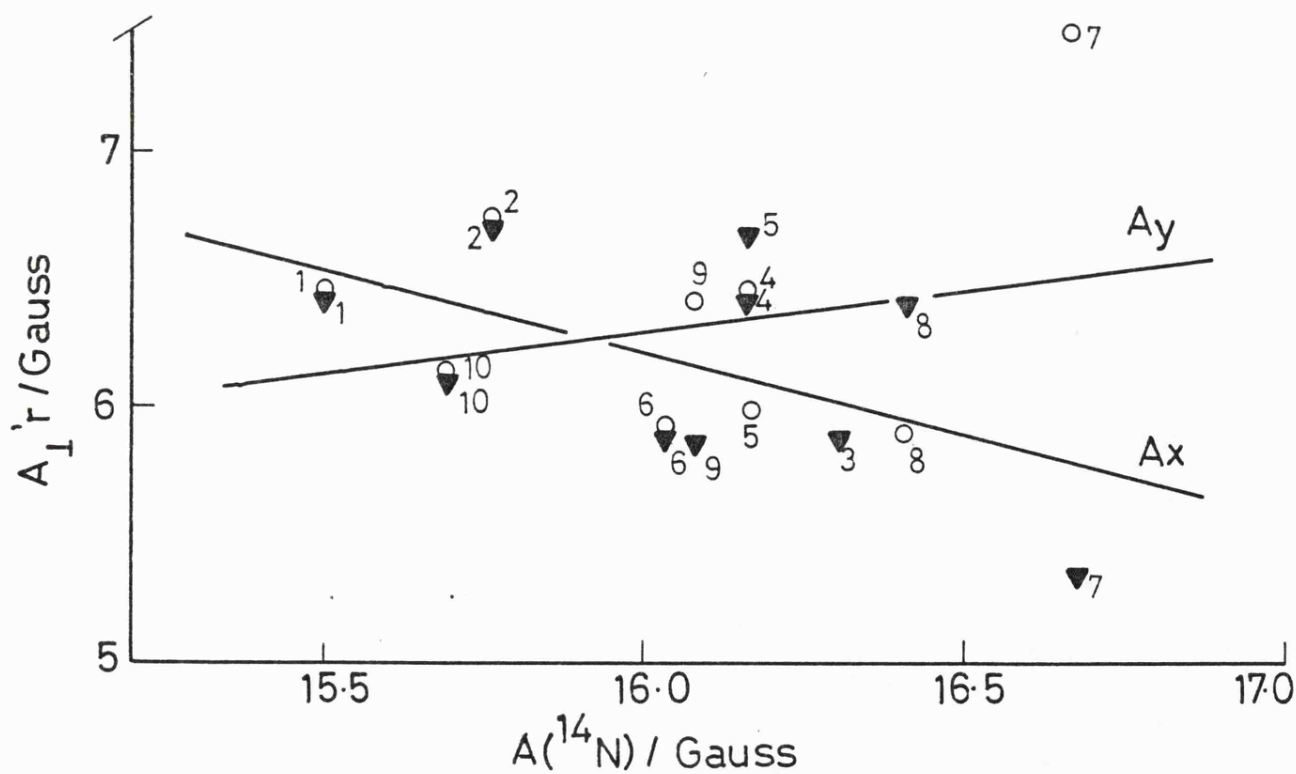
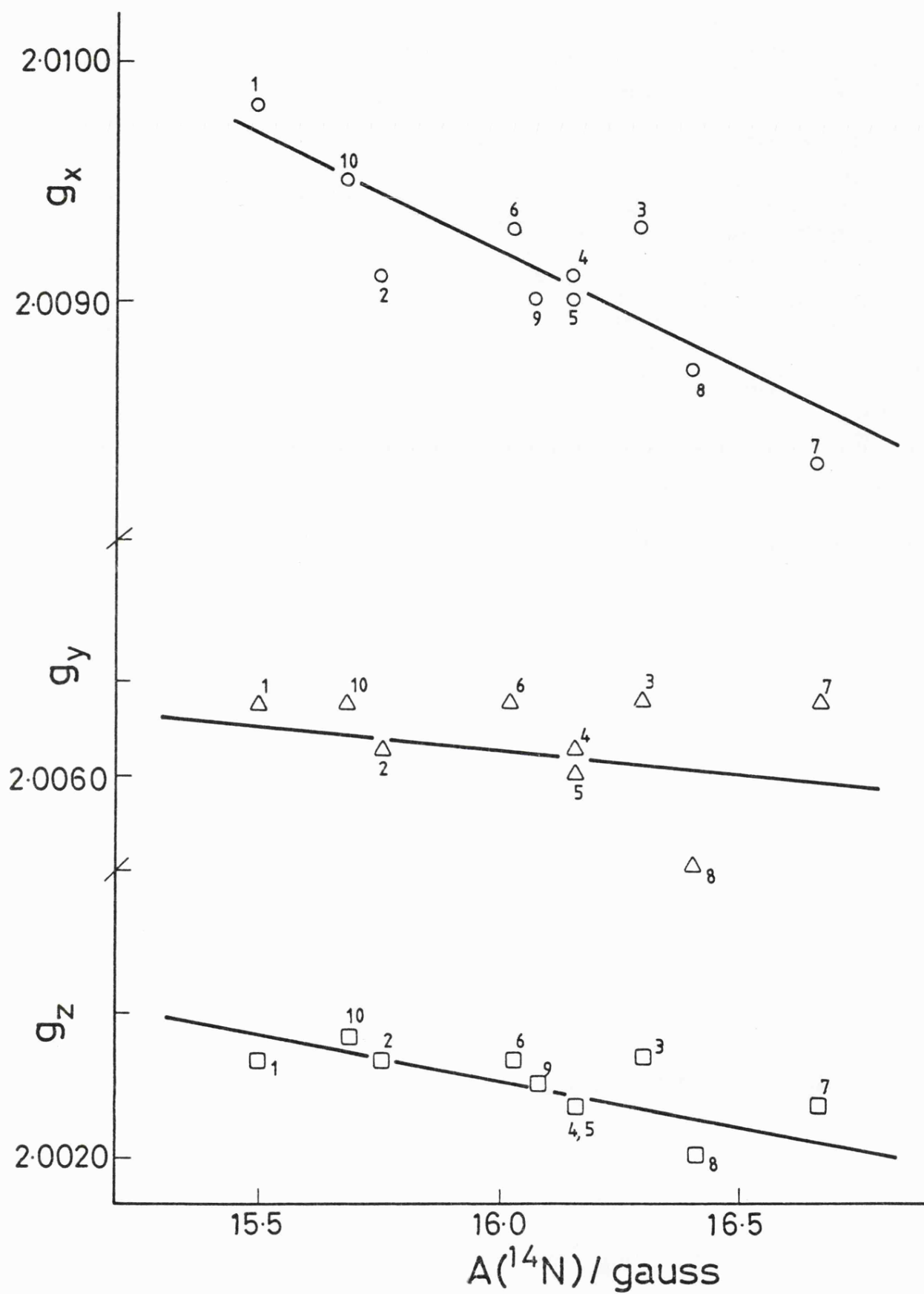


Figure 6.10

Plots of the principal g-values of DTBN as a function of $A(^{14}\text{N})$ in various frozen solutions at 77 K. [Key same as shown in Figure 6.9.]



$$g_x = 2.0257 - 0.00103 A(^{14}\text{N}) \quad (6.1)$$

$$g_y = 2.0092 - 0.00019 A(^{14}\text{N}) \quad (6.2)$$

$$g_z = 2.0070 - 0.00030 A(^{14}\text{N}) \quad (6.3)$$

$$A_x = -0.624 A(^{14}\text{N}) + 16.19 \text{ G} \quad (6.4)$$

$$A_y = 0.305 A(^{14}\text{N}) + 1.40 \text{ G} \quad (6.5)$$

$$A_z = 1.943 A(^{14}\text{N}) + 5.38 \text{ G} \quad (6.6)$$

These results are in line with the behaviour predicted in chapter two. Following Cohen and Hoffman,^{8,9} the anisotropic nitrogen hyperfine coupling constant, $2B(^{14}\text{N})$, can be evaluated as the difference between A_z and $A(^{14}\text{N})$. This gives a direct determination of the unpaired spin density in the nitrogen $2p_z$ orbital.^{8,9} A nitrogen spin density of ca. 0.58 is observed for DTBN in toluene, this rises to ca. 0.62 for DTBN in methanol. This substantiates the suggestion that hydrogen bonding to the oxygen atom of a dialkyl nitroxide pushes more unpaired electron density onto nitrogen. Phase separation of DTBN in pure aqueous solution at 77 K prevented any solid-state measurements being made on this radical in water. Extrapolation, using equation 6.6, predicts that a spin density of 0.64 on nitrogen will be observed for DTBN in pure water.

Variation in the principal g values follows the behaviour expected from the discussion in chapter two of this thesis. It can be shown that g_x can be derived from an equation of the form

$$g_x = 2.00232 + \frac{2p_o^\pi \lambda_o}{\Delta E_{nb-\pi^*}} \quad (6.7)$$

where p_o^π and λ_o are the unpaired spin density in the oxygen p_z orbital and the spin orbit coupling constant of oxygen respectively. $\Delta E_{nb-\pi^*}$ is the energy of the electronic transition from the oxygen p_y non-

bonding orbital and the lowest energy π antibonding orbital of the N-O group. This forms the barrier to orbital motion about the N-O bond. Since it has been shown that there is a decrease in the spin density on oxygen and a blue shift of the $n \rightarrow \pi^*$ transition of the N-O chromophore,¹⁶ as hydrogen bonding to a nitroxide increases, the trends in g_x are readily understood. The trends in g_y are a little more difficult to understand, since orbital motion about nitrogen is also possible. Using the model described in chapter two, orbital motion of the oxygen and nitrogen sp bonding orbitals and the oxygen sp non-bonding orbital will enhance spin orbit coupling about the y axis. This will give rise to the deviation of g_y from the free spin value. Recent work by Kikuchi¹⁷ suggests that variations in g_y are due to orbital motion about the y axis, facilitated by the excitation of the N-O σ electrons to the first π^* level. This L.C.A.O. type model postulates that the N-O σ -bond is formed from a linear combination of the oxygen and nitrogen p_x orbitals, thus denying the existence of an sp non-bonding orbital on oxygen. Fortunately, both models predict similar behaviour for g_y . To evaluate g_y , an equation similar in form to equation 6.7 can be derived, however the final term of 6.7 is replaced by a series of terms involving spin on both nitrogen and oxygen. Thus, as spin moves onto nitrogen, the reduction in g_y is partially offset by an increase in the contribution from orbital motion on nitrogen. This effect is likely to be small but appreciable, since the spin orbit coupling constant of oxygen is about twice that of nitrogen.¹⁸ A more important factor is the inverse dependence of the deviation of g from free spin on the energy barrier to rotation about the axis of interest. The barrier to orbital motion about the y axis is formed by the energy of the σ to π^* and possibly the sp non-bonding to π^* electronic transi-

tions. Both of these energies^{17,19} are thought to be greater than the energy of the p_y non-bonding to π^* electronic transition. Hence, as expected from equation 6.7, g_y should be smaller than g_x . It is expected that hydrogen bonding to a nitroxide will reduce the energy of the oxygen non-bonding orbitals, and produce smaller changes in the energies of the remaining N-O molecular orbitals. This implies that a larger proportional change in energy will be observed for the non-bonding to π^* electronic transition occurring at the longer wavelength. In terms of a relationship of the form of equation 6.7, it would be therefore expected that g_x would exhibit a stronger solvent dependence than g_y . The unpaired electron cannot participate in orbital motion about the molecular z axis and g_z remains close to the free spin value.

The solvent dependence of the anisotropic g and A values of DTBN, indicates the importance of measuring these parameters in the solvent of interest, when they are to be used to evaluate correlation times. Freed *et al.*⁵⁻⁷ have pointed out that accurate knowledge of the magnetic parameters of a radical is necessary if accurate correlation times are to be evaluated. Johnson²⁰ has shown that errors of up to 25% can occur in estimating the rotational correlation time of DTBN in various alcohols, if single crystal data rather than estimates of the anisotropic parameters obtained from measurements on frozen solutions, are used. Jolicoeur and Friedman^{21,22} have acknowledged the importance of the solvent dependence of spin parameters in the evaluation of correlation times. In the range of solvent systems studied by these authors,^{21,22} the spin parameters of the nitroxide probes used were thought to vary little and therefore have a minimal effect on correlation time estimates.

In view of the results obtained from the solid-state studies

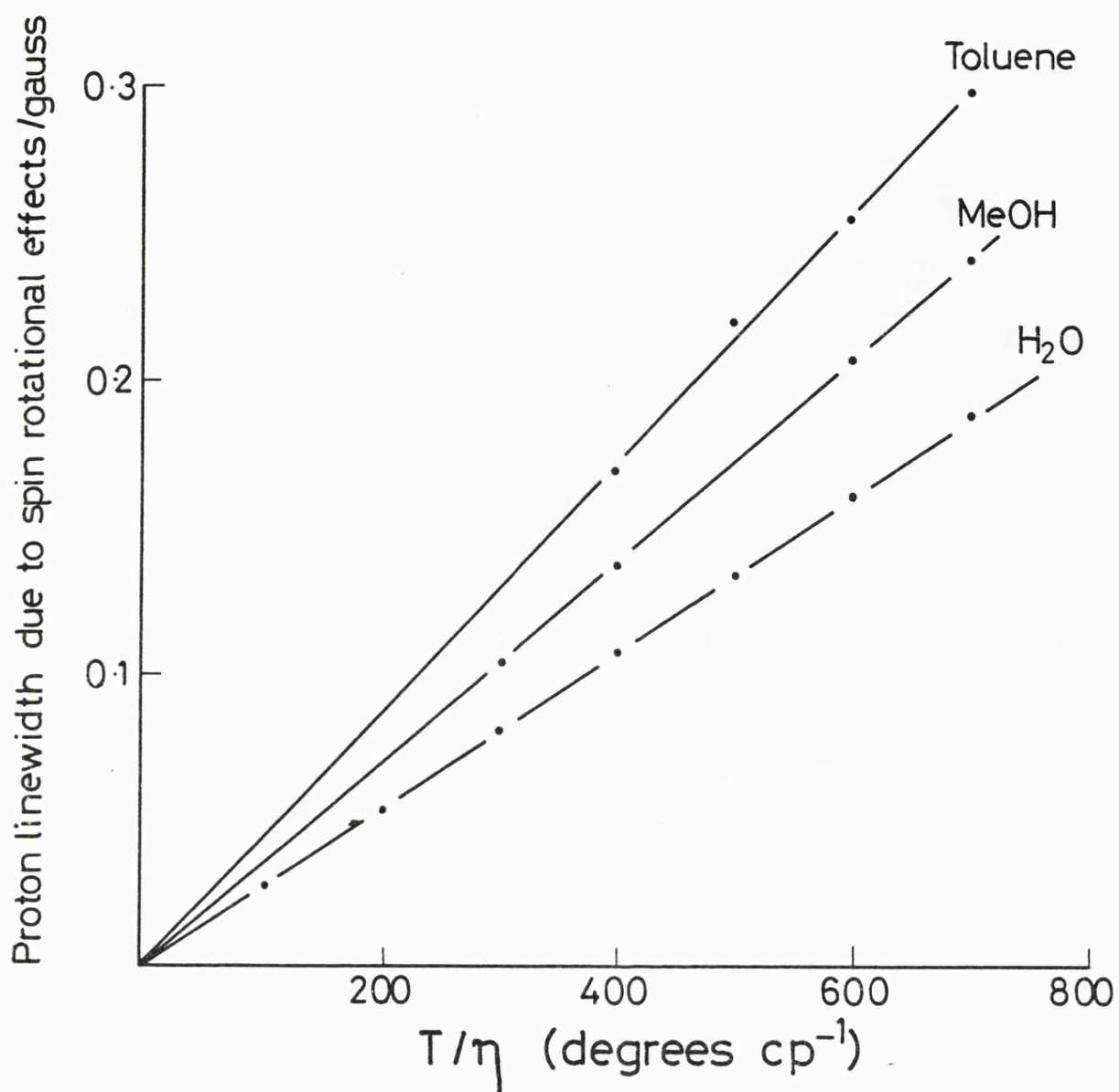


Figure 6.11

The linewidths, due to spin rotational effects, of each proton hyperfine component of the spectrum of DTBN as a function of temperature over viscosity. All linewidths were calculated using spectral parameters obtained from measurements on solid state spectra of DTBN in the solvent of interest.

described above, it would seem pertinent to examine the effect of changing spin parameters on relaxation parameters. Since the study of aqueous systems is of interest, a comparison of water with other solvents would be of use. Estimates of the principal g and A tensors of DTBN in water are shown in table 6.2, these values are obtained by extrapolation of equations 6.1 to 6.6. It is possible using the three principal g -values and equation 2.40 to predict the spin rotational linewidths of DTBN in various solutions. The results show that under identical conditions of the ratio temperature:viscosity, the spin rotational linewidth of DTBN in toluene is 1.6 times greater than that of DTBN in water. Figure 6.11 shows a comparison of the spin rotational behaviour of DTBN in water, toluene and methanol as a function of temperature and viscosity. The spin rotational linewidths of the proton components of the three nitrogen envelopes were calculated using equation 2.40, the experimental g -values, and a value of the hydrodynamic radius of the nitroxide known to give linewidths of a realistic order.^{21,22} The choice of hydrodynamic radius is quite arbitrary, but does not affect the conclusions reached. Using values of g perpendicular estimated, from the frozen X-band spectra and the value of g_{iso} measured in fluid solution, the same relative sizes of the spin rotational widths of DTBN are observed for these three solvents. Calculation of spin rotational widths using this method, gave results ca. 10% lower than those obtained using the Q-band parameters. Thus, the importance of solvent dependence of the anisotropic g -values has been established. It can be readily seen from the results given in chapter three, that this variation in g -values is insufficient to account for the dramatic reduction of spin rotational broadening observed for DTBN in aqueous solution.

Evaluation of the rotational correlation time τ_c using equation 2.28 was carried out. Correlation times calculated from the g and A cross term β , vary little from solvent to solvent, when solid state parameters from the glassy solvent measurements are used to evaluate them. However, these correlation times are ca. 20% less than would have been obtained if single crystal data³ were used in their calculation. Calculation of the rotational correlation time from the γ term of equation 2.28 shows a much greater sensitivity to the nature of the solvent. For example, if τ_c of DTBN in water is calculated using this γ term and the Q-band extrapolated g and A tensors, then a correlation time which is ca. 62% of that calculated using single crystal data is obtained. Similarly, for DTBN in toluene, the use of glassy solvent g and A values to calculate τ_c from the γ term, gives a value of about 80% of τ_c evaluated from single crystal data. Clearly, an accurate knowledge of the magnetic parameters of a nitroxide in the solvent of interest is required if accurate correlation times are to be calculated.

6.4 t-Butyl N benzoyl nitroxide - results and discussion

Recently, there have been several studies²⁰⁻²⁶ of a class of nitroxides known as the acyl nitroxides. In this class of nitroxides the nitroxyl group is adjacent to a carbonyl group. There have been a variety of attempts to determine the spin distribution in these compounds,²¹⁻²⁴ each study yielding differing spin density estimates. It is hoped using the techniques outlined in the earlier part of this chapter to give a reasonable picture of the spin distribution in acyl nitroxides.

Solid state spectra of t-butyl N benzoyl nitroxide in frozen ethanol at 77 K are shown in figures 6.12 and 6.13. The X-band spectrum

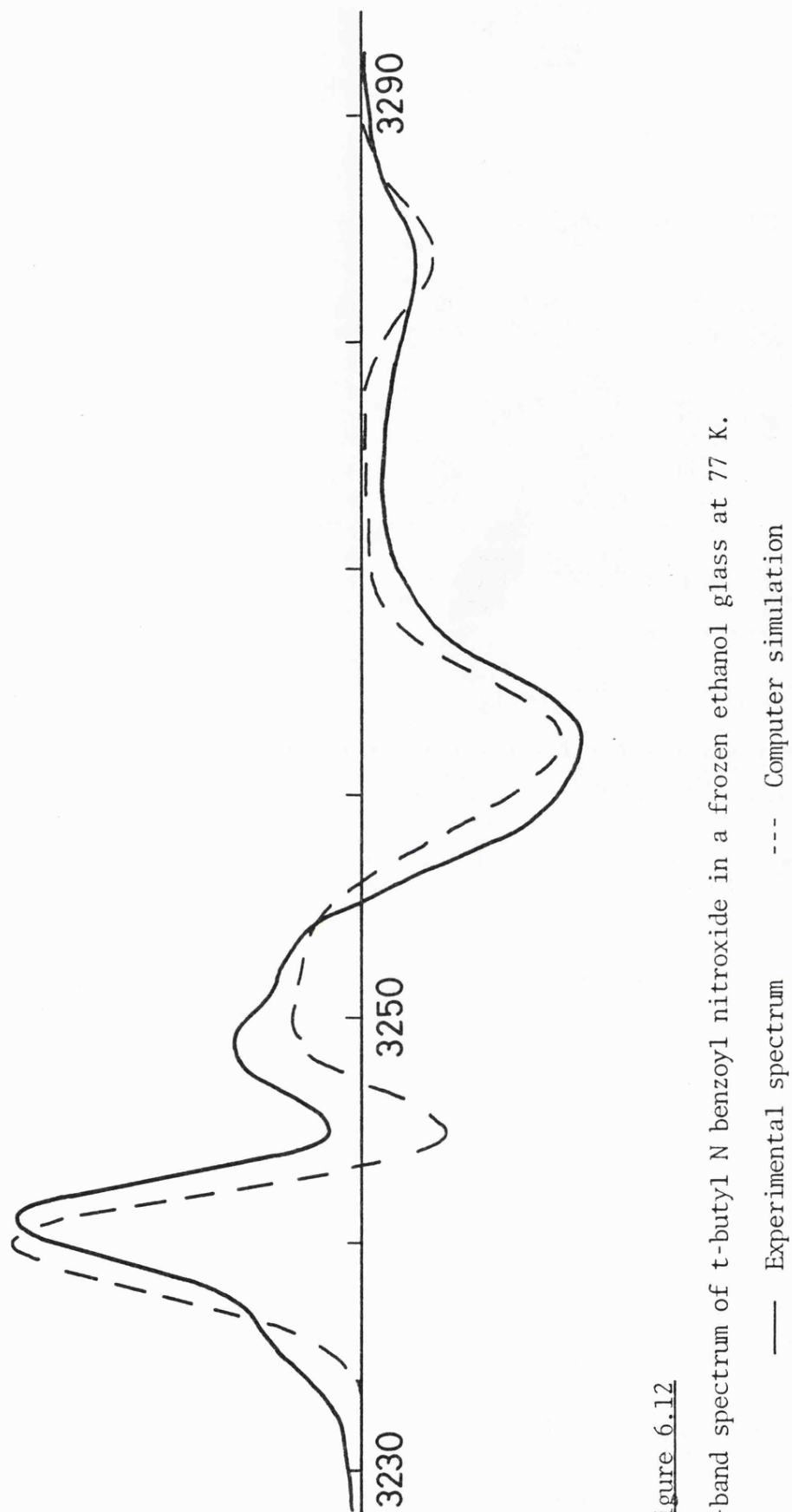


Figure 6.12

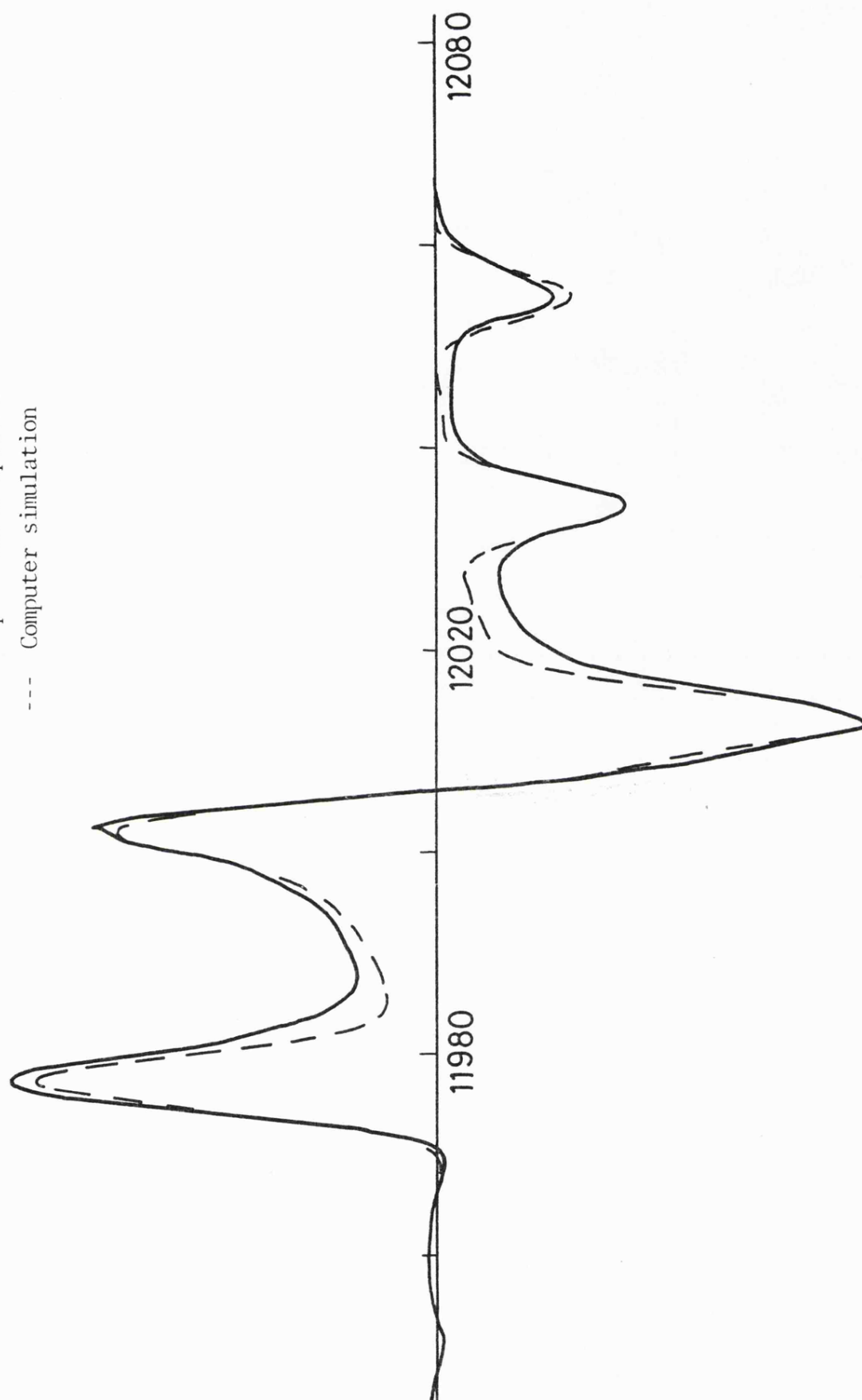
X-band spectrum of t-butyl N benzoyl nitroxide in a frozen ethanol glass at 77 K.

Figure 6.13

Q-band spectrum of t-butyl N benzoyl nitroxide in a frozen ethanol glass at 77 K.

— Experimental spectrum

--- Computer simulation



| | | | | | |
|----------|---|--------|----------|---|---------|
| g_x | = | 2.0080 | A_x | = | 5.49 G |
| g_y | = | 2.0059 | A_y | = | 6.64 G |
| g_z | = | 2.0020 | A_z | = | 38.67 G |
| g_{av} | = | 2.0053 | A_{av} | = | 16.93 G |

Table 6.2

The principal g and A parameters of aqueous ditertiary butyl nitroxide estimated by extrapolation of equations 6.1 to 6.6

is poorly resolved, making even g_z and A_z troublesome to evaluate. However, the Q-band spectrum is much more clearly resolved and the spectral parameters shown in Table 6.3 may be extracted after careful computer simulation. Using the experimental data, it is possible to estimate an anisotropic nitrogen coupling constant of 12.80 G. This value can be used to calculate^{8,9} a value of 0.382 for the unpaired spin density on nitrogen. Previous estimates for a variety of acyl nitroxides are 0.154,^{21,22} 0.25-0.30²³ and 0.234.²⁴ The method used in the present work is thought to be more direct than the INDO evaluations^{21,22} or Karplus-Fraenkel based evaluations from $A(^{14}\text{N})$ and $A(^{17}\text{O})$, previously used.

Previous estimates²¹⁻²⁴ have proposed that the bulk of the unpaired electron density resides on the nitroxyl oxygen. These studies were made using either INDO calculations or $\sigma \rightarrow \pi$ interaction parameters derived from measurements on nitroxides labelled with oxygen 17 in the N-O group. Values in the range 0.575 to 0.749 were proposed²¹⁻²⁴ for the unpaired electron density on oxygen. No oxygen 17 labelled nitroxide was available for the present study and hence no direct determination of spin density on oxygen could be made from solid state measurements. It is possible that the g-values of t-butyl-N-benzoyl nitroxide, in partic-

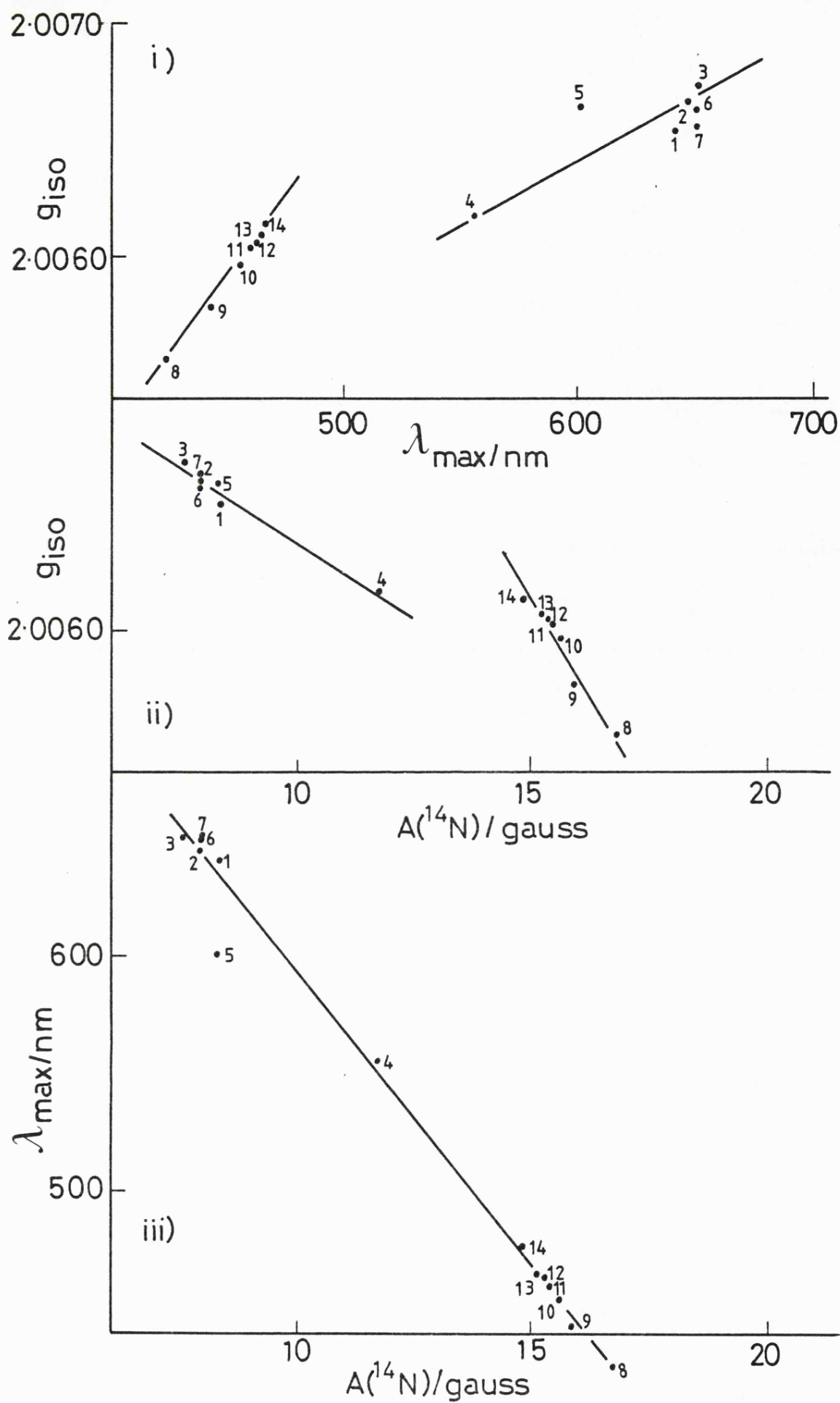
ular g_x , may give a reasonable guide to the spin density on oxygen. Using equation 6.7, g_x from Table 6.3 and the recorded wavelength of the $n \rightarrow \pi^*$ electronic transition²¹ of 646 nm; a spin density of 0.4 ± 0.05 can be estimated.

| | | | |
|-------------------|--------------------|---------------------------|-------------------------------------|
| $g_x = 2.0115$ | | $A_x = 0.11 \text{ G}$ | |
| $g_y = 2.0063$ | | $A_y = 1.60 \text{ G}$ | |
| $g_z = 2.0022$ | | $A_z = 20.75 \text{ G}$ | |
| $g_{av} = 2.0067$ | $g_{iso} = 2.0068$ | $A_{av} = 7.49 \text{ G}$ | $A(^{14}\text{N}) = 7.95 \text{ G}$ |

Table 6.3

The principal g and A parameters of *t*-butyl N benzoyl nitroxide in ethanol determined by computer simulation of the Q-band spectrum recorded at 77 K.

In view of this low value for spin density on oxygen, it may be reassuring to examine more closely the nature of the relationship between g -values and electronic transitions. Figure 6.14 shows linear relationships between the nitrogen hyperfine coupling constant and the isotropic g -value, and between the energy of the $n \rightarrow \pi^*$ electronic transition and the isotropic g -value. Here, and throughout the discussion of acyl nitroxides, the $n \rightarrow \pi^*$ transition is taken as the electronic transition between the oxygen p_y non-bonding orbital and the lowest energy π^* electronic level. It can be seen from figure 6.14, that the acyl nitroxides and dialkyl nitroxides behave differently. The energy of the $n \rightarrow \pi^*$ transition for an acyl nitroxide is expected to be lower than that for a dialkyl nitroxide for two reasons. Some degree of conjugation is to be expected in the acyl nitroxide π system, thus the energy of the lowest π^* electronic level will be lowered relative to that in a dialkyl nitroxide. Secondly, acyl nitroxides are



Caption to Figure 6.14

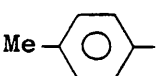
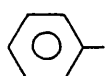
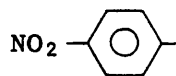
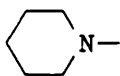
Comparison of the properties of dialkyl and acyl nitroxides expressed as plots of:

- a) Isotropic g-values as a function of λ_{\max} , the wavelength of maximum absorption of the $n \rightarrow \pi^*$ electronic transition.
- b) Isotropic g-values as a function of $A(^{14}\text{N})$.
- c) λ_{\max} as a function of $A(^{14}\text{N})$.

KEY

Results for the acyl nitroxides $\text{RCON} \begin{smallmatrix} \text{O} \\ \diagup \\ \text{X} \end{smallmatrix}$, 1-7 are taken from ref.

21, and R is:

1. 
2. 
3. 
4. 
5. $\text{MeO}-$
6. $\text{C}_{10}\text{H}_{21}-$
7. $\text{PhCH=CH}-$

Results for DTBN in solvents 8-14 are taken from ref. 16. Where the solvents are:

8. Water
9. MeOH
10. MeCN
11. Me_2CO
12. Toluene
13. CCl_4
14. Hexane

destabilised^{21,22} with respect to dialkyl nitroxides because of the strong electron withdrawing effect of the carbonyl group. This effect would also tend to reduce the energy of the lowest π^* orbital, shifting the $n \rightarrow \pi^*$ transition to longer wavelength. Figure 6.14 implies that it is the increased wavelength of the $n \rightarrow \pi^*$ transition rather than a large increase in spin on oxygen, which makes g_{iso} of an acyl nitroxide larger than that of a dialkyl nitroxide. The single linear dependence of λ_{max} , the wavelength of the $n \rightarrow \pi^*$ transition, on $A(^{14}N)$ is interesting. The effect of hydrogen bonding on $A(^{14}N)$ and λ_{max} is well known. It would appear that, the delocalising and inductive effects of the acyl grouping both lower the spin density on nitrogen and increase λ_{max} , in a manner mimicking the effects of hydrogen bonding on these parameters in dialkyl nitroxides. The behaviour exhibited in the plot of $A(^{14}N)$ against g_{iso} is to be expected from the form of the other two plots.

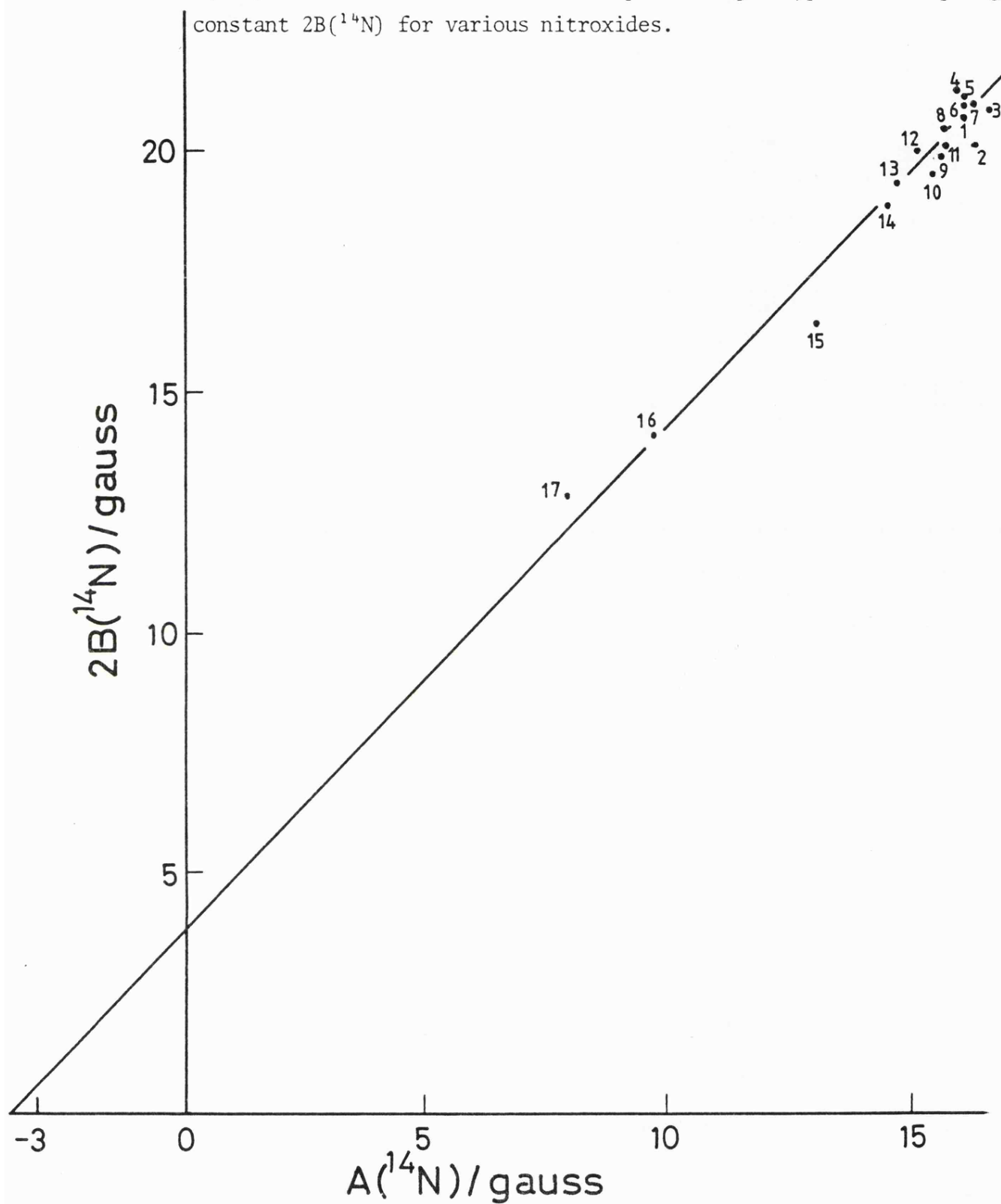
The Karplus-Fraenkel type relationships have been used on several occasions^{8,9,24} in discussing the spin distribution in nitroxide systems. Using a model, which assumes that the isotropic nitrogen coupling constant arises from a spin polarisation interaction with the unpaired electron in the molecular π system, it is possible to predict $A(^{14}N)$ from the following equation,

$$A(^{14}N) = p_N Q_{NN} + \sum_i p_i Q_{Ni} \quad (6.8)$$

Here p_N is the π electron density on nitrogen and p_i is the π electron density on an atom i adjacent to nitrogen. Q_{NN} and Q_{Ni} are the so-called "Karplus-Fraenkel" parameters. It would be expected that $A(^{14}N)$ would arise from a single positive contribution from spin on nitrogen and a smaller negative contribution from spin on other nuclei. In practice the term from spin on adjacent atoms has been proposed to be negligible²⁴ or positive.^{8,9} Following the method of Cohen and Hoffman,^{8,9} it should

Figure 6.15

The variation of the isotropic nitrogen hyperfine coupling constant $A(^{14}\text{N})$ as a function of the anisotropic nitrogen hyperfine coupling constant $2B(^{14}\text{N})$ for various nitroxides.



KEY TO FIGURE 6.15

1. d^{18} DTBN in CD_3OD (this work)
2. DTBN in 0.180 mf t-BuOH-water (this work)
3. DTBN in 0.097 mf t-BuOH-water (this work)
4. DTBN in CD_3OD (this work)
5. DTBN in MeOH (this work)
6. DTBN in 0.894 mf MeOH-toluene (this work)
7. DTBN in 0.735 mf MeOH-toluene (this work)
8. DTBN in 0.444 mf MeOH-toluene (this work)
9. DTBN in CD_3CN (this work)
10. DTBN in toluene (this work)
11. d^{16} TEMPOO in 85% d^4 glycerol- D_2O (ref. 6)
12. d^{16} TEMPOO in CD_3CD_2OD (ref. 6)
13. d^{16} TEMPOO in $(CD_3)_2CO$ (ref. 6)
14. d^{16} TEMPOO in d^8 toluene (ref. 6)
15. Fremy's salt in a solution of potassium carbonate in D_2O (this work)
16. Diphenyl nitroxide in benzophenone (ref. 26)
17. t-Butyl N benzoyl nitroxide in ethanol (this work)

be possible to predict the Karplus-Fraenkel parameters from a plot of $A(^{14}\text{N})$ as a function of $2B(^{14}\text{N})$. Such a plot is shown for several nitroxides in figure 6.15.

When treated by the method of least squares the data in figure 6.15 yields a relationship of the form:

$$A(^{14}\text{N}) = 0.958 \ 2B(^{14}\text{N}) - 3.59 \quad (6.9)$$

If spin is confined to the oxygen and nitrogen atoms, then the Karplus-Fraenkel parameters Q_{NN} and Q_{NO} can be evaluated from this data as 28.50 G and -3.59 G respectively. These Q-values and the proposed nitrogen spin density of 0.382 predict an $A(^{14}\text{N})$ of 8.67 G for t-butyl N benzoyl nitroxide in ethanol. This is in reasonable agreement with the experimental value. The negative "back term" is in line with the predictions of a spin polarisation model. It should be stressed however, that separate least squares plots on the data for DTBN and d^{16} TEMPOO yield Q_{NO} values of +8.81 G and -1.16 G respectively. Changes in the geometry at nitrogen,⁹ as we go from one type of nitroxide to another may account for some variation in fit for different nitroxides.

Work by Symons and Hunter²⁷ on spin polarisation effects may give a useful guide to the behaviour of $A(^{14}\text{N})$ as a function of $2B(^{14}\text{N})$ over the range of nitroxides shown in figure 6.15. These authors have shown that the adjacent atom term in equation 6.8 is a function of both, the hybridisation at and the magnetic moment of, the atom whose hyperfine coupling constant is being determined. The atom concerned will see little change in this adjacent atom effect as its hybridisation changes from sp^3 to sp^2 ; however as the s-character of this atom's orbitals further increases, a more significant increase in the size of this "back term" will be observed. Thus in the case of the nitroxides, the Q_{N1} terms in the Karplus-Fraenkel relationship should be identical for

all nuclei adjacent to nitrogen. The magnitude in the "back term" contribution to $A(^{14}\text{N})$ should therefore be only a function of the total spin delocalised onto the adjacent atoms and a single Q_{N1} value. The data and methods of Symons and Hunter²⁷ can be used to predict approximate values of Q_{NN} and the adjacent atom Q-value of +24 G and -5.5 G, respectively. This would yield a slope of +0.87 and an intercept of -5.5 G for a plot of $A(^{14}\text{N})$ as a function of $2B(^{14}\text{N})$. This is in good agreement with the slope and intercept calculated for figure 6.15. Thus, the single line drawn for all nitroxides shown in figure 6.15, seems to gain support from this type of analysis. Any loss of planarity at nitrogen should not effect the adjacent atom terms, but the increase in s-character of the unpaired electron will increase the size of $A(^{14}\text{N})$.

Discussion of the spin distribution in the carbonyl group in acyl nitroxides poses some difficulty. The proposed spin densities of ca. 0.38 and 0.40 on nitrogen and oxygen respectively, imply that about 22% of the unpaired electron density is out on the carbonyl group. This result does not differ greatly from the value of 15% proposed by Perkins²³ and the estimate of 19% proposed by Aurich.²⁴ Isotopic substitution experiments have shown O^{17} couplings of 4.4 G from the carbonyl oxygen²³ and 20.3 G at the nitroxide oxygen.²⁴ Following the simple proportionality method used by Perkins,²³ these results suggest that, if the spin density on the nitroxyl oxygen is 0.4, then that on the carbonyl oxygen will be ca. 0.09. This implies that the spin density on the carbonyl carbon is ca. 0.13. The spin density on the carbonyl carbon is small compared to the sum of the spin densities on the adjacent nitrogen and oxygen atoms. The coupling between the unpaired electron and carbon-13 in natural abundance at the carbonyl

site may well be negative due to a dominating adjacent atom effect. The carbon-13 splitting at the carbonyl group has been measured as ± 5.13 G, but its sign could not be determined. Thus, none of the experimental data currently available can give a really accurate measure of the spin distribution in the carbonyl group of an acyl nitroxide.

Spin delocalisation onto the phenyl ring of t-butyl-N-benzoyl nitroxide is very small. This is shown by the very low coupling of the phenyl protons to the unpaired electron, as determined from n.m.r. measurements.²¹ If the phenyl ring is replaced by a methyl group no significant change in $A(^{14}\text{N})$ is seen.^{20,24} This supports the suggestion that there is little delocalisation of the unpaired electron onto the phenyl ring of t-butyl-N-benzoyl nitroxide. X-ray structure determinations,²⁵ show that the phenyl ring is twisted by an angle of 40° out of the plane of the molecule. Overlap between the phenyl and carbonyl π systems should be a function of the square of the cosine of the angle that the two π systems are inclined to each other. This should only reduce the spin on the phenyl group to about 60% of the value expected, if the phenyl and carbonyl groups were coplanar. This does not satisfactorily account for the low coupling to the ring protons of this radical.

Having discussed the unpaired electron distribution of t-butyl-N-benzoyl nitroxide, it would be desirable to comment on a bonding scheme for this molecule. Normally²⁰⁻²⁵ a valence bond approach is used in describing the structure of this radical. Resonance structures of types I to V shown in figure 6.16 are used in this type of discussion. Spin on oxygen is derived from structures I and III; spin on nitrogen from structure II and spin on carbonyl from structures IV and V. The importance of structure III has been stressed, since it can be used to

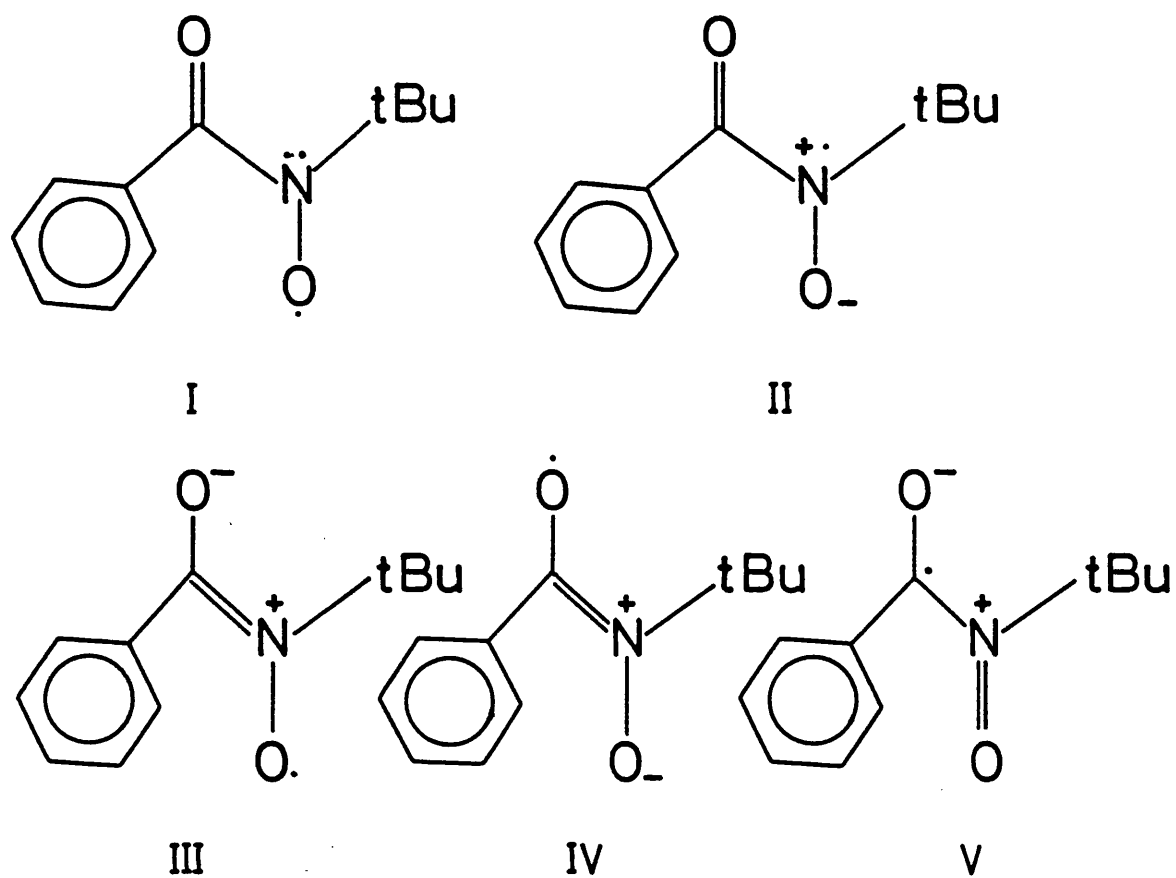
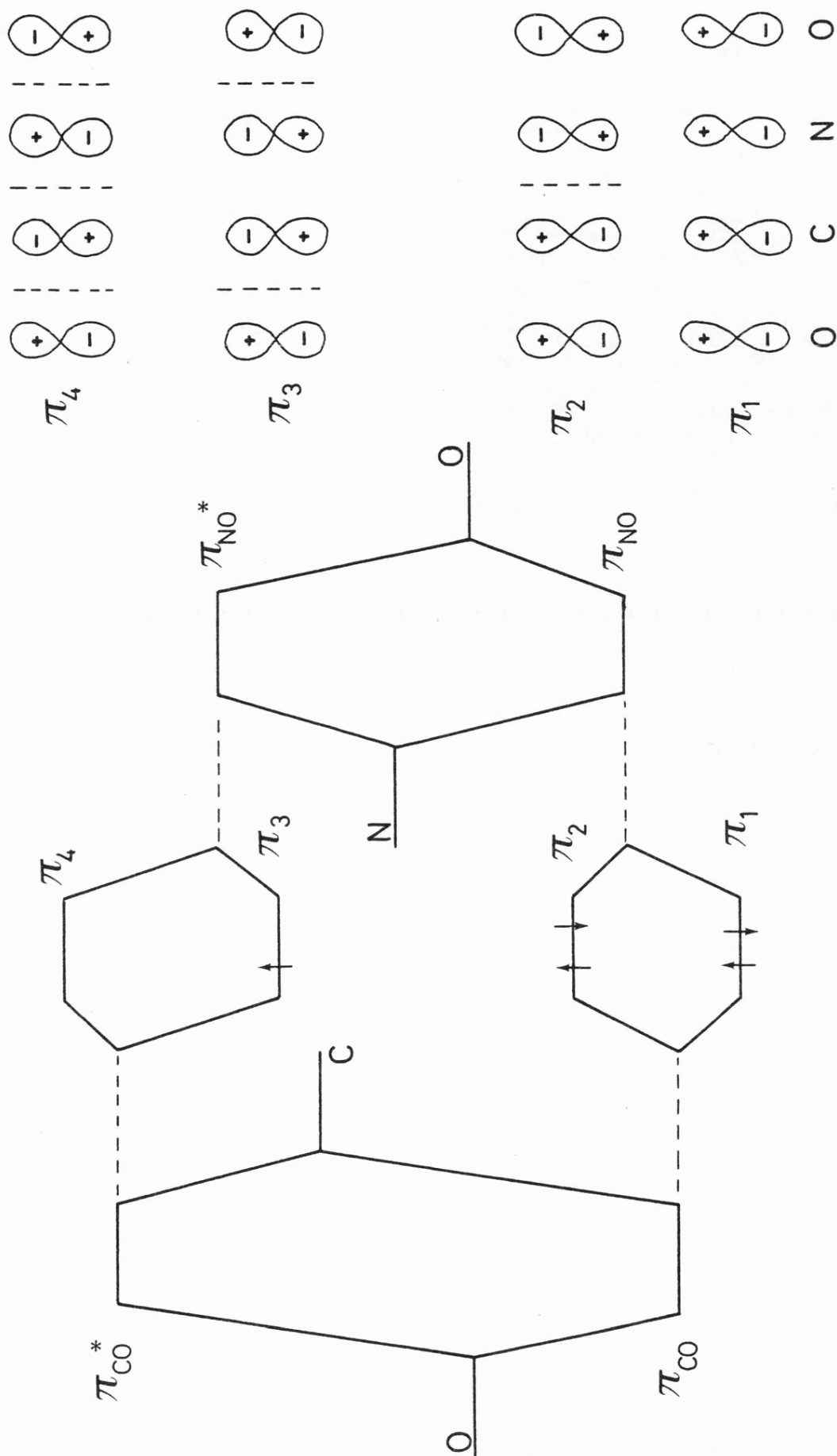


Figure 6.16

Valence bond structures proposed for the radical t-butyl
N benzoyl nitroxide.

Orbital correlation diagram showing the π orbitals of an acyl nitroxide. The π orbitals of the isolated nitroxide and carbonyl groups are designated π_{NO} and π_{CO} respectively. The orbitals of the conjugated π system are marked π_1 to π_4 . The phases of the four p-orbitals making up the four conjugated π orbitals are shown on the right.



account for the high spin density on the nitroxyl oxygen proposed for acyl nitroxides.²⁰⁻²⁴ The amide resonance III, could also be used to account for the effect on $A(^{14}\text{N})$ of adding substituents to the phenyl ring. The model proposed in this thesis reduces the spin on oxygen and hence diminishes the contribution from III to the overall bonding scheme. The present model will stress the importance of structures I and II, with lesser contributions from structures III, IV and V. X-ray results²⁵ suggest that structure III is still significant, since the measured carbon-nitrogen bond length of 1.384 Å is somewhat shorter than the accepted carbon-nitrogen single bond length of 1.47 Å.²⁸ The same results²⁵ show that the carbonyl C=O bond length is 1.207 Å, very close to the accepted value of 1.20 Å.²⁸ Clearly, this lack of deviation from normal carbonyl behaviour must limit the contribution from structures IV and V.

The above valence bond type treatment is simple and effective in describing the structure of an acyl nitroxide. In keeping with the practice already followed in this thesis, a molecular orbital description of the structure of an acyl nitroxide is shown in figure 6.17. The unpaired electron should be in the lowest π antibonding orbital π_3 , as shown in the diagram. This orbital is expected to be closer to a nitroxyl π^* orbital in both energy and character, than it is to a carbonyl π^* orbital. This would place the bulk of the unpaired electron spin in the nitroxyl group. Since a conjugated π system is proposed, it might be expected that the carbon-nitrogen separation might be shorter than the normally observed C-N single bond length. This molecular orbital description, although perhaps less simple than the valence bond description and less useful in accounting for ring substituent effects, can give an adequate description of the unpaired spin density distribu-

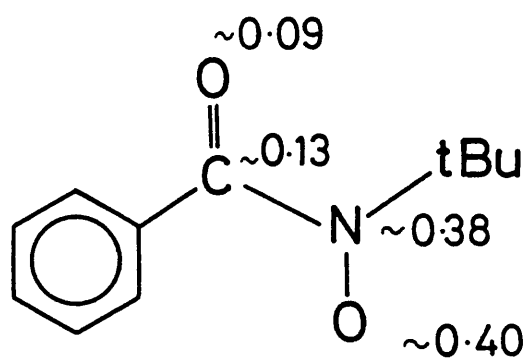


Figure 6.18

The unpaired electron distribution proposed for t-butyl N benzoyl nitroxide.

6.5 Conclusions

The technique of determining accurate principal g and A tensors of nitroxides, by making e.s.r. measurements on these radicals in frozen solutions, has been described. It is necessary to make these measurements on nitroxides using Q-band frequencies, or by examining perdeuterated nitroxides at X-band frequencies. The rôle of anisotropic coupling, between the unpaired electron and the alkyl protons of a nitroxide, in broadening the solid state spectra has been discussed. The solvent dependence of the anisotropic e.s.r. parameters of nitroxides fits in well with existing ideas concerning the solvation of these compounds. The need for accurate solid state parameters, taken in a frozen matrix of the solvent of interest, for use in measuring relaxation rates has been demonstrated.

Using Q-band e.s.r. measurements and other data from the literature, the structure of *t*-butyl-*N*-benzoyl nitroxide has been discussed at length. The spin distribution shown in figure 6.18 is proposed for this radical.

REFERENCES TO CHAPTER SIX

1. B. L. Bates, Chem. Phys. Letters, 1971, 10, 361.
2. S. A. Goldman, G. V. Bruno, C. F. Polnazek and J. H. Freed, J. Chem. Phys., 1972, 56, 716.
3. O. H. Griffith, D. W. Cornell and H. M. McConnell, J. Chem. Phys., 1965, 43, 2909.
4. S. Ohnishi, J. C. A. Boeyens and H. M. McConnell, Proc. Nat. Acad. Sci. U.S., 1966, 56, 809.
5. S. A. Goldman, G. V. Bruno and J. H. Freed, J. Chem. Phys., 1973, 59, 3071.
6. J. S. Hwang, R. P. Mason, L. P. Hwang and J. H. Freed, J. Phys. Chem., 1975, 79, 489.
7. C. F. Polnazek and J. H. Freed, J. Phys. Chem., 1975, 79, 2283.
8. A. H. Cohen and B. M. Hoffman, J. Amer. Chem. Soc., 1973, 95, 2061.
9. A. H. Cohen and B. M. Hoffman, J. Phys. Chem., 1974, 78, 1313.
10. D. Jones, Ph.D. Thesis, University of Leicester, 1972.
11. J. A. Brivati, J. M. Gross, M. C. R. Symons and D. J. A. Tinling, J. Chem. Soc., 1965, 6504.
12. J. R. Pilbrow and M. E. Winfield, Mol. Phys., 1973, 25, 1073.
13. R. Brière, H. Lemaire, A. Rassat, P. Rey and A. Rousseau, Bull. Soc. Chem. (Fr)., 1967, 12, 4479.
14. See, for example,
P. B. Ayscough "Electron Spin Resonance in Chemistry", Methuen & Co. Ltd., London, 1967, p.67.
15. A. Carrington and A. D. McLachlan "Introduction to Magnetic Resonance", Harper & Row, New York, 1967, p.105.
16. T. Kawamura, S. Matsumani and T. Yonezawa, Bull. Chem. Soc. Japan, 1967, 40, 1116.
17. O. Kikuchi, Bull. Chem. Soc. Japan, 1969, 42, 1187.
18. A. Carrington and A. D. McLachlan "Introduction to Magnetic Resonance", Harper & Row, New York, 1967, p.138.
19. See, for example,
M. Orchin and H. H. Jaffé "The Importance of Antibonding Orbitals", Houghton Mifflin Company, Boston, 1967, p.55.

20. H. G. Aurich and J. Trösken, *Leibrgs. Ann. Chem.*, 1971, 745, 159.
21. T. C. Jenkins, Ph.D. Thesis, Chelsea College, University of London, 1976.
22. T. C. Jenkins, M. J. Perkins and N. P. Y. Siew, *J.C.S. Chem. Comm.*, 1975, 880.
23. T. C. Jenkins, M. J. Perkins and B. Terem. To be published.
24. H. G. Aurich, K. Hahn, K. Stork and W. Weiss, *Tetrahedron*, 1977, 33, 969.
25. S. A. Hussain, Ph.D. Thesis, Chelsea College, University of London, 1978.
26. T. S. Lin, *J. Chem. Phys.*, 1972, 57, 2260.
27. T. F. Hunter and M. C. R. Symons, *J. Chem. Soc. (A)*., 1967, 1312.
28. I. L. Finar "Organic Chemistry - The Fundamental Principles, Vol. I", Longmans, London, 1967, p.25.

CHAPTER SEVEN

Study of t-Butyl-N-benzoyl nitroxide as a Spin Probe

CHAPTER SEVEN

7.1 Introduction

The use of e.s.r. spectroscopy as a tool for examining solvation phenomena has developed a good deal over recent years. Nitroxides, in particular the dialkyl nitroxides, have proved useful probes of the solvent environment. Studies of the effect of solvent on the e.s.r. parameters of the piperidine nitroxides¹⁻³ and ditertiary butyl nitroxide⁴⁻⁵ have provided insight into the nature of aqueous solutions. The solvent dependence of the e.s.r. spectra of other classes of nitroxide, such as the aryl⁶⁻⁷ and acyl⁷⁻⁹ nitroxides, have also been examined.

The behaviour of acyl nitroxides is rather different from that of the dialkyl nitroxides as far as solvation effects are concerned. Early studies of $A(^{14}\text{N})$ ^{8,9} of acyl nitroxides as a function of standard solvent parameters, such as the Dimroth-Reichardt E_T values or Kosower Z values, have shown anomalous results. Normally,¹⁰ a single relationship between $A(^{14}\text{N})$ and such parameters is seen, indicating that $A(^{14}\text{N})$ changes approximately in step with solvent polarity. The acyl nitroxides show a single dependence^{8,9} of $A(^{14}\text{N})$ on E_T in aprotic solvents. A weaker relationship between $A(^{14}\text{N})$ of these radicals and E_T is seen in alcoholic solutions. Jenkins⁹ showed that t-butyl-N-benzoyl nitroxide has similar values of $A(^{14}\text{N})$ in both aprotic and alcoholic solvents. A larger value of $A(^{14}\text{N})$ is observed for this radical in water. This behaviour contrasts with that of ditertiary butyl nitroxide, which shows a clear increase in $A(^{14}\text{N})$ as the solvent is changed from an aprotic solvent to an alcohol. It has been suggested,^{8,9} that this "odd" behaviour of acyl nitroxides is a function

of having two potential hydrogen bonding donor sites attached to the conjugated π system, which holds the unpaired electron.

Jenkins' work⁹ included a brief examination of the properties of acyl nitroxides in aqueous solutions. He was able to demonstrate the power of some bases in desolvating acyl nitroxides in aqueous solution. It is hoped to expand on this aspect of Jenkins' work in the following discussion. A wider range of solvent mixtures has been examined and the results used to infer something of the nature of the aqueous environment. It is expected that a comparison of the properties of the acyl nitroxide with DTBN in mixed solvent systems, will provide a good indication of its usefulness as a spin probe.

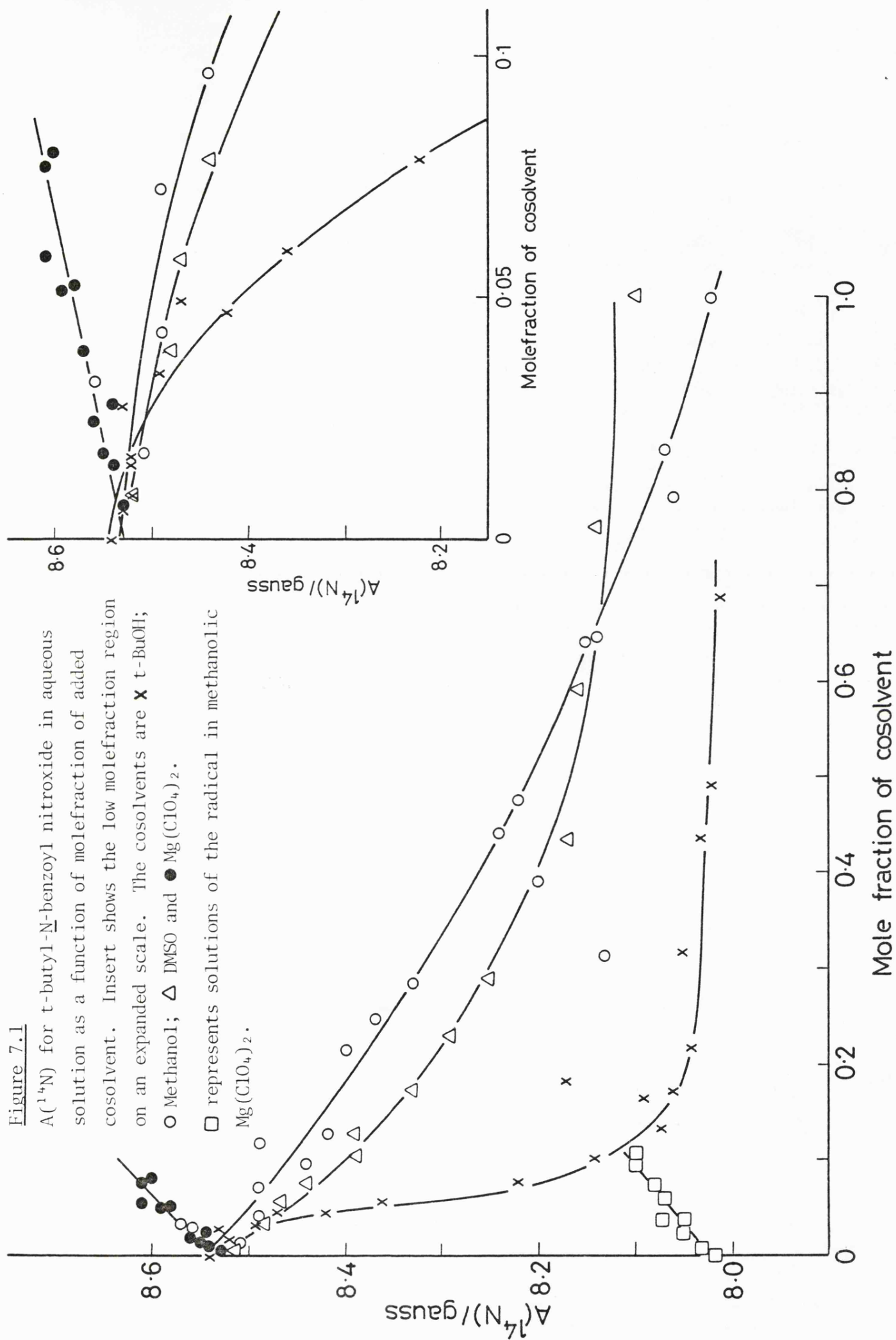
7.2 Experimental Details

All materials were prepared as described in earlier parts of this thesis. E.s.r. spectra were obtained using a Varian E109 spectrometer, fitted with a V6040 variable temperature accessory. All samples contained between 5×10^{-5} and 1×10^{-4} M dm⁻³ of t-butyl-N-benzoyl nitroxide and each sample was thoroughly degassed prior to use. The solvent and solution viscosities were obtained from standard sources.¹¹⁻¹³

7.3 Results and Discussion

The variation of $A(^{14}\text{N})$ of acyl nitroxides with solvent polarity has been the subject of two recent investigations.^{8,9} As was the case with the DTBN results, it is expected that this property will give a better insight into the nature of solvation effects than relaxation measurements. Solvation at either of the polar groups of an acyl nitroxide will effect the overall spin distribution. This makes the

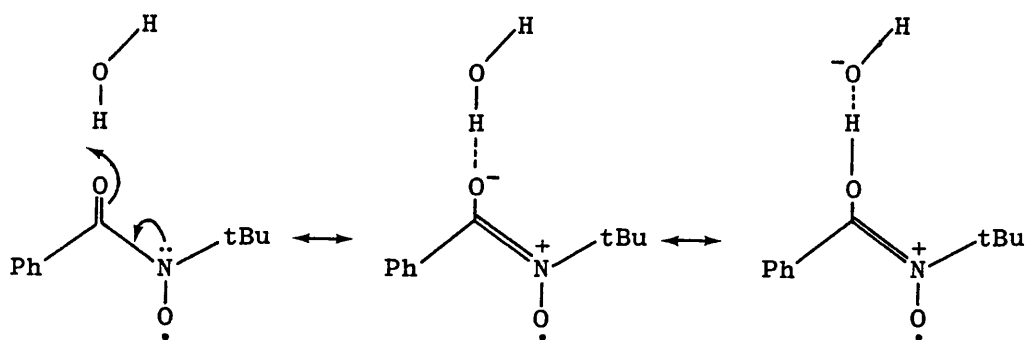
Figure 7.1



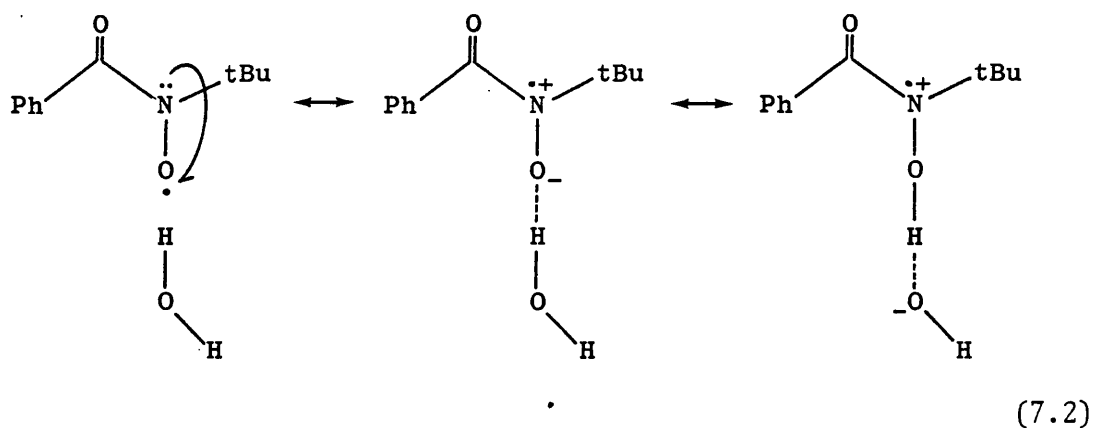
rôle of the solvent in controlling the size of the nitrogen hyperfine splitting of acyl nitroxides more difficult to understand.

Figure 7.1 shows a plot of $A(^{14}\text{N})$ of t-butyl-N-benzoyl nitroxide as a function of solvent composition. It can be readily seen that adding a basic solvent such as dimethyl sulphoxide or methanol to an aqueous solution of t-butyl-N-benzoyl nitroxide reduces $A(^{14}\text{N})$. The addition of magnesium perchlorate, on the other hand, causes an increase in $A(^{14}\text{N})$. These results are similar to those obtained for DTBN in mixed solvent systems. Figure 7.1 shows a plateau effect, similar to that seen in the DTBN study, in the 0 to 0.03 mole fraction region of the t-butanol-water curve.

In order to discuss these results, it is essential to examine the nature of hydrogen bonding to acyl nitroxides. Equilibria 7.1 and 7.2 show a valence bond description of this process. Hydrogen bonding to the carbonyl group will cause a migration of spin away from nitrogen onto oxygen, thus causing a fall in $A(^{14}\text{N})$. Solvation at the nitroxyl group should involve a movement of spin off oxygen onto nitrogen, increasing $A(^{14}\text{N})$.

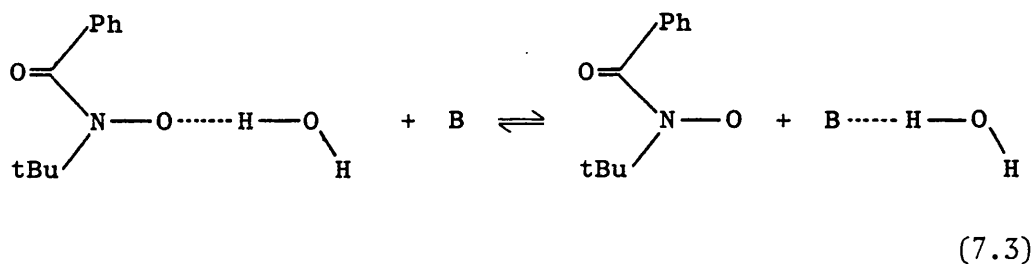


(7.1)



The molecular orbital treatment of the processes described above is not so clear. Essentially, hydrogen bonding at either site perturbs the electron distribution in the π system. Hydrogen bonding to the carbonyl oxygen is expected to attract π electron density towards the carbonyl group and push π^* electron density towards the nitroxyl oxygen. Hydrogen bonding to the nitroxyl oxygen on the other hand, will pull π electron density towards nitroxyl oxygen, increasing the unpaired spin density on nitrogen, thus causing an increase in $A(^{14}\text{N})$.

The fall in $A(^{14}\text{N})$ seen when a base is added to an aqueous solution of t-butyl-N-benzoyl nitroxide is indicative of a reduction of hydrogen bonding at the nitroxyl site. In the water rich region of these binary mixtures, a strong base such as DMSO is seen to be more effective in reducing $A(^{14}\text{N})$ than methanol. Jenkins⁹ measurements of $A(^{14}\text{N})$ of t-butyl-N-benzoyl nitroxide in a range of water-acetone and water-methanol binary mixtures are in good agreement with this observation. These trends resemble the changes in $A(^{14}\text{N})$ seen for DTBN in water-base mixtures, at low to medium base concentrations. An equilibrium of the type (7.3) is envisaged. Since hydrogen bonding to the carbonyl group of the acyl nitroxide is thought to cause a decrease in $A(^{14}\text{N})$, the curves drawn in figure 7.1 may hide a small increase in $A(^{14}\text{N})$, due to

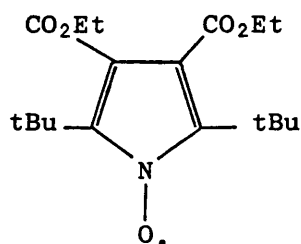


loss of hydrogen bonding to carbonyl. In the aprotic rich region of the curve, specific interactions between the probe and base may well control $A(^{14}\text{N})$. This seems likely, since in the base rich region, $A(^{14}\text{N})$ of *t*-butyl-*N*-benzoyl nitroxide is greater in a water-DMSO mixture than it is in a water-methanol mixture of the same strength.

The low value of $A(^{14}\text{N})$ of acyl nitroxides in alcohols has proved to be difficult to explain. Aurich⁸ has suggested that the low value of $A(^{14}\text{N})$ found for these radicals in alcohols is due to solvation at the carbonyl group. This would reduce the increase in $A(^{14}\text{N})$ expected from hydrogen bonding to nitroxyl alone. Water¹⁴ is expected to have a higher concentration of free hydroxyl groups, available for hydrogen bonding to the probe, than an alcohol. Hence, hydrogen bonding to both polar groups of the probe should be more extensive in aqueous solution than in alcoholic solution. A comparison of $A(^{14}\text{N})$ values suggests there are significant differences in the method of solvation of *t*-butyl-*N*-benzoyl nitroxide in water and alcohols. The low concentrations of free hydroxyl groups in alcoholic solutions of an acyl nitroxide may encourage preferential solvation at carbonyl giving a low value of $A(^{14}\text{N})$.

The spectroscopic and thermodynamic results of Drago et alia¹⁵ suggest that dialkyl nitroxides are more powerful bases than ketones. It therefore seems unlikely that the relative basicities of the polar

groups of an acyl nitroxide would favour solvation at carbonyl. Steric factors may induce preferential solvation at the carbonyl group. Crystallographic data¹⁶ suggests that t-butyl-N-benzoyl nitroxide is planar, with the carbonyl and nitroxyl groups anti to each other. Molecular models show that the nitroxide group lies "hidden" by the phenyl and t-butyl groups, whereas the carbonyl function is more exposed. An alcohol molecule would be inhibited from hydrogen bonding at the nitroxyl site because of the bulk steric interaction between the alkyl residue of the alcohol and the phenyl and t-butyl groups of the nitroxide. Hydrogen bonding to the carbonyl function is free of these steric effects. This effect would be less important in aqueous solution, since water is a smaller molecule than the alcohols and hydrogen bonding to both sites is possible. Rassat¹⁷ has noted that 2,5 di-t-butyl 3,4 diethoxycarbonyl pyrrol-1-oxyl



produces an e.s.r. spectrum with a value of $A(^{14}\text{N})$, which is independent of solvent. Hydrogen bonding to the nitroxyl group of this radical may also be inhibited by steric opposition from the t-butyl groups. Aurich⁸ has made measurements on t-butyl-N-acetyl nitroxide, which should show steric effects to a lesser extent than the bulkier t-butyl-N-benzoyl nitroxide. Comparison of the results of Aurich⁸ and Jenkins⁹ indicate that in alcoholic solution there is little difference in the extent of hydrogen bonding to the nitroxyl sites of these two radicals. This

clearly makes the suggestion, that selective solvation at carbonyl is caused by steric factors, less acceptable.

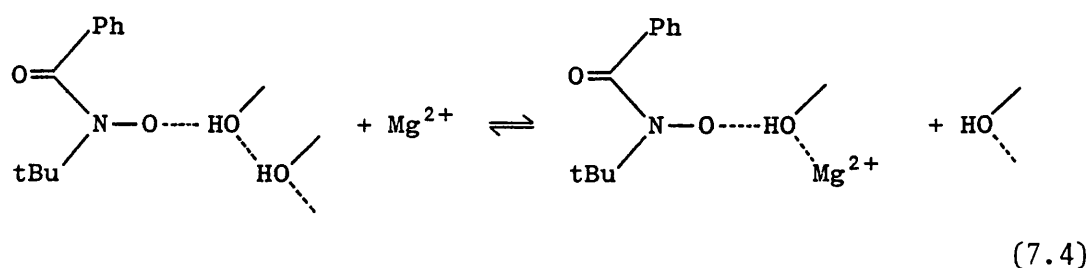
It is possible to account for the trends in $A(^{14}\text{N})$ of acyl nitroxides, without invoking the possibility of selective solvation. The close proximity of the carbonyl and nitroxyl groups in these molecules is expected to reduce the basic strength of both functions. Thus, *t*-butyl-*N*-benzoyl nitroxide is expected to be less basic than a dialkyl nitroxide. In alcoholic solution, an acyl nitroxide may be too weak a base to compete favourably with the excess free lone pairs of the solvent for free hydroxyl groups. The acyl nitroxide is pictured as being hydrogen bonded to a very small extent at either site in these solutions. In aqueous solution there is a sufficiently high concentration of free hydroxyl groups to allow hydrogen bonding to the radical. Basic solvents can be expected to form loose dipolar complexes with acyl nitroxides, thus increasing $A(^{14}\text{N})$. These complexes would be similar to the DTBN-methyl cyanide complex proposed in chapter 3. Small, highly basic solvent molecules would be expected to interact with the acyl nitroxide most readily. The high $A(^{14}\text{N})$ observed by Aurich⁸ for *t*-butyl-*N*-acetyl nitroxide in methyl cyanide supports this view of dipolar solvation.

The curve of $A(^{14}\text{N})$ of *t*-butyl-*N*-benzoyl nitroxide in *t*-butanol - water mixtures shown in figure 7.1 is very similar to that seen for DTBN in the same solvent system. In solutions containing less than 0.03 mf *t*-butanol, the fall in $A(^{14}\text{N})$ is very gradual. This can be ascribed to solvation of the acyl nitroxide molecule and the cosolvent molecules in separate clathrate type cages. The nitroxide, as indicated by its high $A(^{14}\text{N})$ value, is expected to be hydrogen bonded to the walls of its host clathrate cage. Once the *t*-butanol concentration exceeds

ca. 0.04 mf, there is insufficient water present to maintain this clathrate structure and a cage sharing process is thought to come into play. The t-butanol molecules can now more readily desolvate the nitroxide. The limiting low value of $A(^{14}\text{N})$ is approached at lower concentrations of added t-butanol for aqueous t-butyl-N-benzoyl nitroxide (ca. 0.2 mf) than it is for aqueous DTBN (ca. 0.3 mf). This may well reflect the proposed weaker basicity of t-butyl-N-benzoyl nitroxide.

The rôle of an electrolyte in controlling $A(^{14}\text{N})$ in aqueous and methanolic solutions of t-butyl-N-benzoyl nitroxide was examined. Figure 7.1 shows that the rates of increase of $A(^{14}\text{N})$ of the probe with increase of magnesium perchlorate concentration are similar in both water and methanol solvents. This result differs from the measurements made on DTBN in methanolic and aqueous solutions of the same electrolyte; where the increase in $A(^{14}\text{N})$ is more rapid in methanolic solution. The processes controlling $A(^{14}\text{N})$ of the acyl nitroxide in salt solutions are expected to be similar to those described by equilibria 4.1 to 4.6 of chapter 4.

The formation of hydrogen bonds between the acyl nitroxide and the solvation co-sphere of the cation as shown in equilibrium 7.4:



is thought to influence $A(^{14}\text{N})$ significantly. The increased acidity of the protons of the cation solvation shell is expected to increase

the strength of the hydrogen bond to the nitroxide. This would increase $A(^{14}\text{N})$. The electrolyte is expected to modify the number of free hydroxyl groups present in these solutions. A small highly charged cation, like magnesium, should increase the concentration of free hydroxyl groups. In chapter 4, it was suggested that this increase in concentration of (OH) free would have a significant effect on $A(^{14}\text{N})$ of DTBN in methanolic solution, since only ca. 50 per cent of DTBN is expected to be hydrogen bonded in this solvent. In aqueous solution DTBN is thought to be almost completely hydrogen bonded and no increase in $A(^{14}\text{N})$ due to an increase in concentration of (OH) free is expected.

It has been suggested that t-butyl-N-benzoyl nitroxide is a weaker base than DTBN. If this is the case, desolvation of the acyl nitroxide by the anion in electrolyte solutions may become important. Hence, the increase in $A(^{14}\text{N})$ produced by the extra (OH) free generated by the magnesium cations in aqueous solution would be offset by desolvation of the acyl nitroxide by the perchlorate anion. In methanolic solution both effects are expected to be minimal, since the acyl nitroxide is expected to be largely non-hydrogen bonded in this case. The law of mass action would limit the importance of the cation effect and the low concentration of hydrogen bonded radical would minimise the anion effect. It is tentatively suggested that the increase of $A(^{14}\text{N})$ of t-butyl-N-benzoyl nitroxide in both aqueous and methanolic solutions of salts is predominantly caused by the process shown in equilibrium 7.4. This would account for the similar rates of increase of $A(^{14}\text{N})$ with concentration of added salt, for this radical in methanolic and aqueous solution. It is stressed that these conclusions must be treated with caution, since they are based on a small number of results.

Figure 7.2 provides a comparison of the properties of t-butyl-N-

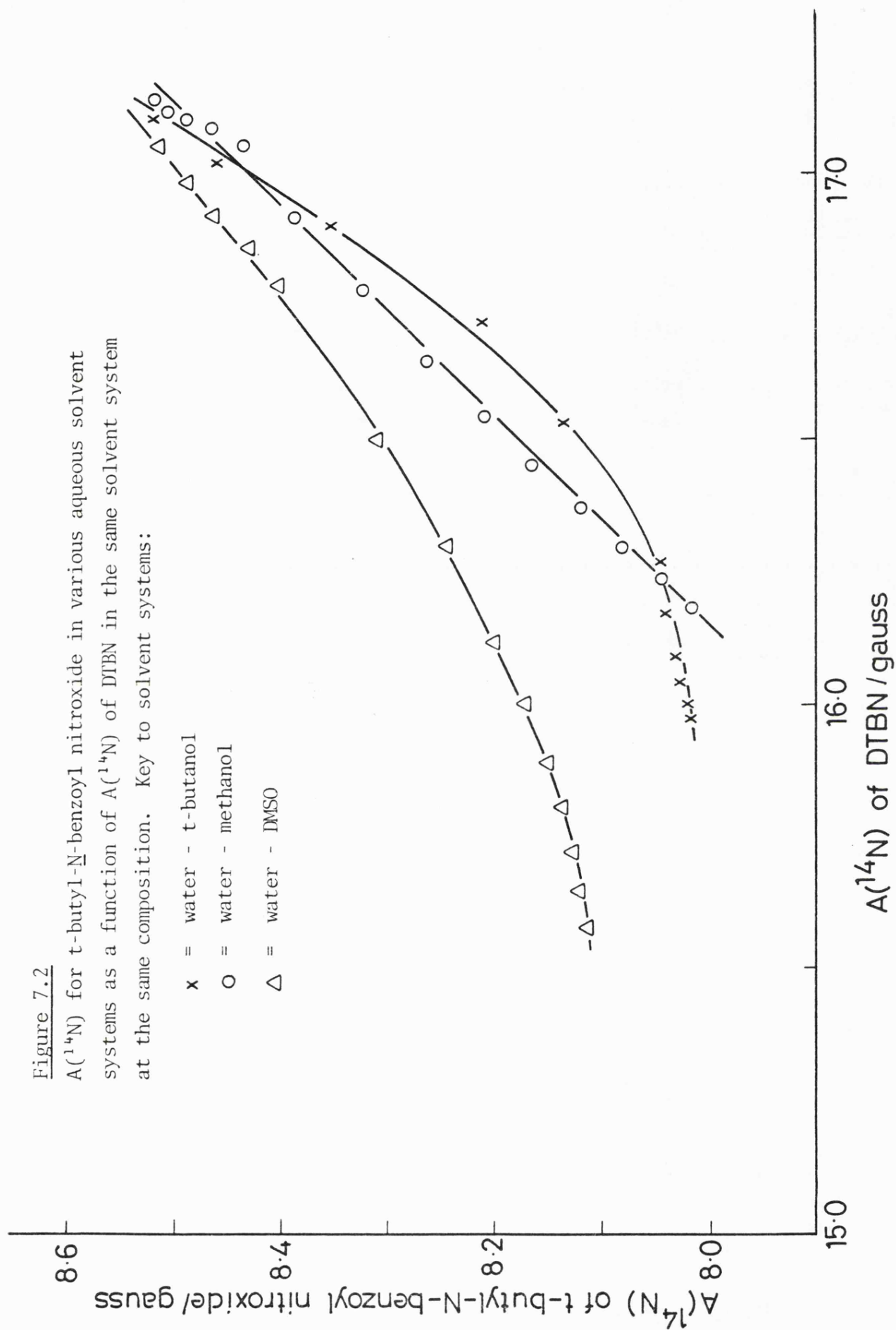
Figure 7.2

$A(^{14}\text{N})$ for t-butyl-N-benzoyl nitroxide in various aqueous solvent systems as a function of $A(^{14}\text{N})$ of DTBN in the same solvent system at the same composition. Key to solvent systems:

x = water - t-butanol

O = water - methanol

Δ = water - DMSO



benzoyl nitroxide and DTBN in a range of mixed solvents. The linear slope of the water-methanol plot suggests that the changes in concentration of (OH) free, as the methanol concentration increases, control $A(^{14}\text{N})$ of both radicals. A curved plot is obtained from the water-DMSO data. This implies that the fall in $A(^{14}\text{N})$, seen as the supply of (OH) free groups diminishes, is arrested by a second process in the case of the acyl nitroxide. This second process may well be the formation of dipolar complexes between the acyl nitroxide and the base. This effect should be less important for DTBN, since by virtue of its stronger basicity, this radical is expected to cling more tenaciously to any solvating water molecules. This would hinder the formation of a dipolar pair between the probe and base. Consequently, base-nitroxide complex formation is expected to become important for *t*-butyl-N-benzoyl nitroxide at lower base concentrations than it does for DTBN. Clathrate effects are expected to be important in determining the form of the water-*t*-butanol curve. The almost linear portion of this curve corresponds to *t*-butanol concentrations of between 0 and 0.08 mf. This corresponds to the initial plateau region and the region of rapid descent of $A(^{14}\text{N})$ with added *t*-butanol. Here the solvation of both radicals is thought to be controlled by similar processes. The curvature beyond this region is probably a function of the weaker basicity of the acyl nitroxide. It has already been pointed out that, in mixtures of *t*-butanol and water, *t*-butyl-N-benzoyl nitroxide reaches the limiting value of $A(^{14}\text{N})$ at lower molefractions of the alcohol than DTBN. The curvature of the *t*-butanol-water curve of figure 7.2 merely echoes this type of behaviour.

Jenkins⁹ has shown that $A(^{14}\text{N})$ of *t*-butyl-N-benzoyl nitroxide in aprotic solvents increases as the temperature is raised. It was

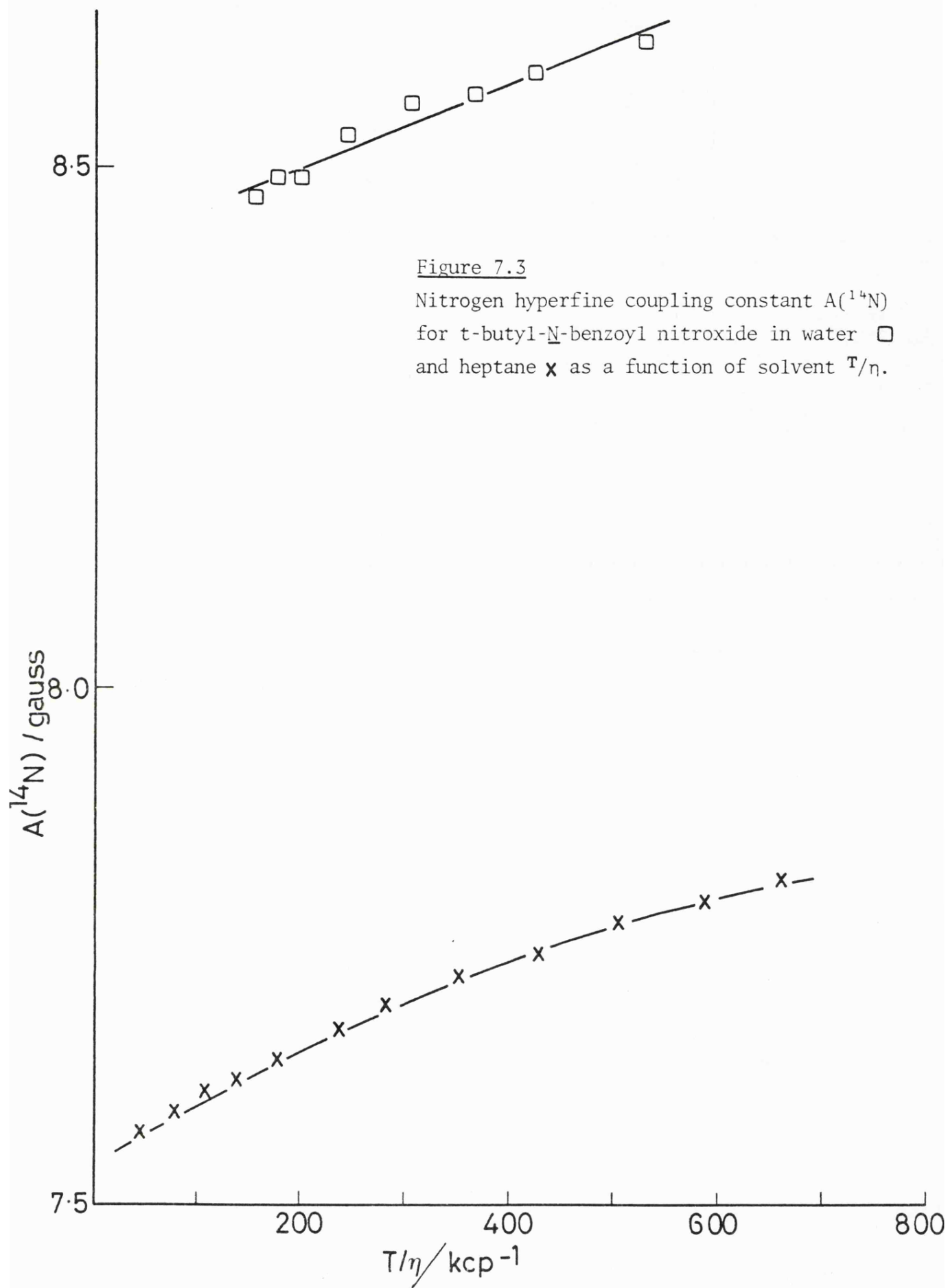


Figure 7.3

Nitrogen hyperfine coupling constant $A(^{14}\text{N})$
for *t*-butyl-*N*-benzoyl nitroxide in water □
and heptane x as a function of solvent T/η .

suggested that this temperature dependence of $A(^{14}\text{N})$ may be due either to an increase in out-of-plane vibrational activity about nitrogen or to changes in solvation. In order to probe this effect further, the variation of $A(^{14}\text{N})$ of t-butyl-N-benzoyl nitroxide in water and heptane solvents was examined as a function of temperature. Figure 7.3 shows that $A(^{14}\text{N})$ appears to be dependent on both temperature and solvent viscosity. Jenkins⁹ suggests that the temperature dependence of $A(^{14}\text{N})$ of t-butyl-N-benzoyl nitroxide is given by:

$$A(^{14}\text{N}) = b \exp (-c/T) \quad (7.5)$$

where b and c are constants. A plot of the reciprocal of temperature as a function of the natural logarithm of $A(^{14}\text{N})$ was made to check this behaviour. As expected from figure 7.3, the aqueous results exhibit a linear dependence in agreement with equation 7.5, whilst the heptane results show a small curvature.

On the basis of the measurements made on DTBN, it seems that $A(^{14}\text{N})$ of a nitroxide in aqueous solution should fall as the temperature rises. This is thought to be due to changes in solvation as the temperature increases. The planarity of DTBN has been established by electron diffraction measurements.¹⁸ Steric interactions between the two t-butyl groups¹⁸ are thought to be responsible for the near planarity at nitrogen in the DTBN molecule. This same steric interaction should inhibit any out-of-plane vibration about nitrogen. In contrast to the DTBN results, $A(^{14}\text{N})$ of t-butyl-N-benzoyl nitroxide increases as the temperature is raised. This increase in $A(^{14}\text{N})$ can be more readily accounted for in terms of an increase in vibrational freedom than by solvation effects.

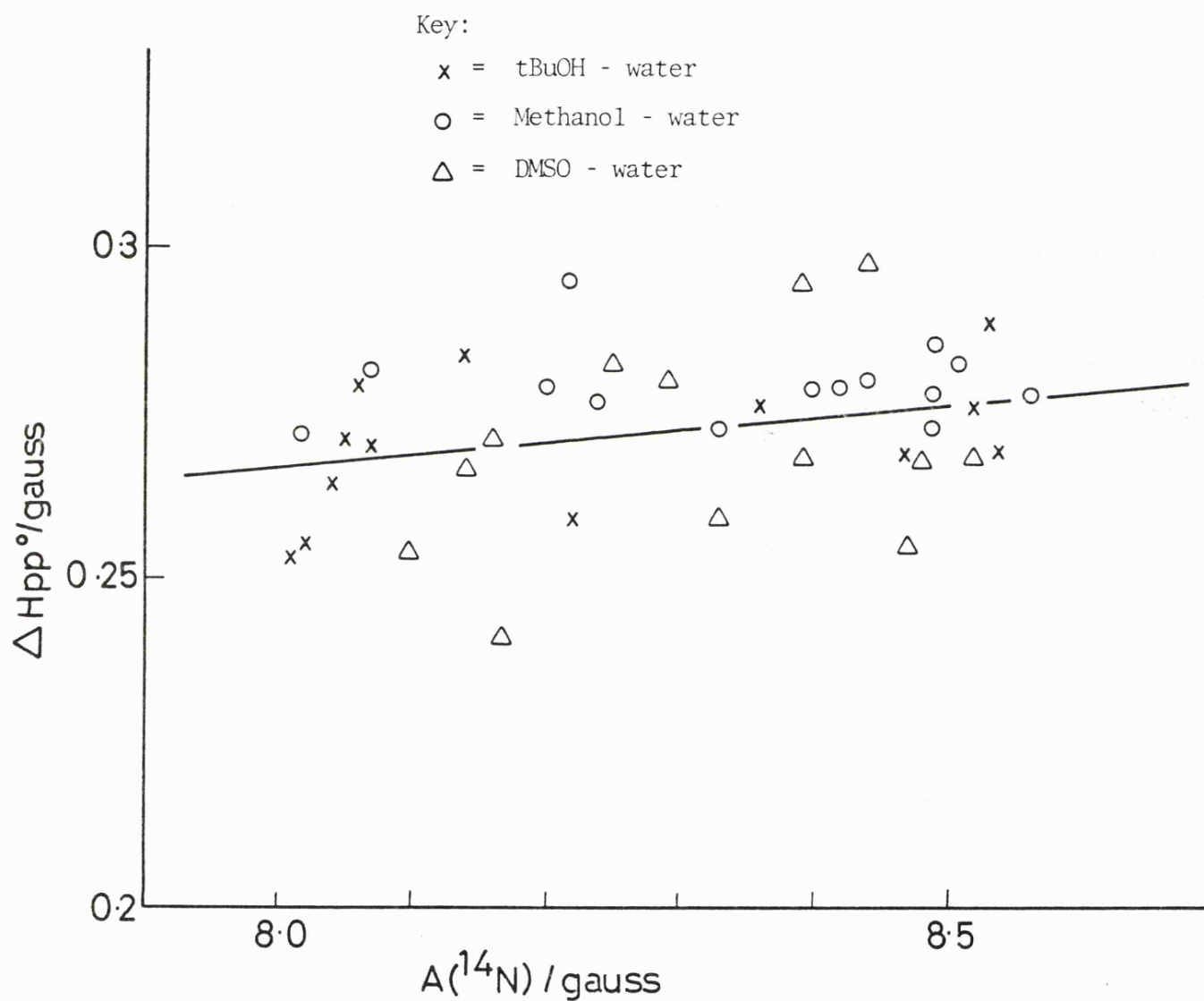
The dependence of $A(^{14}\text{N})$ of t-butyl-N-benzoyl nitroxide on the

ratio of temperature and viscosity implies that diffusion control of $A(^{14}\text{N})$ is appreciable. This seems likely since the energy required to facilitate out-of-plane bending is transferred through intermolecular collisions. The aqueous results shown in figure 7.3 show a linear form, whilst the heptane results show a slight curve. This difference is not thought to be significant, since the water results were obtained over a narrower temperature range.

The results shown in figure 7.3 should be borne in mind when considering solvation effects. Jenkins⁹ pointed out that t-butyl-N-benzoyl nitroxide in a 10 M solution of lithium chloride in water has a lower value of $A(^{14}\text{N})$ than the same radical in pure water. This was attributed to the lithium cation disordering the bulk water structure to a large enough extent to disturb the solvation of the probe. At 15°C T/η , the temperature over viscosity ratio, of a 10 M aqueous lithium chloride solution is of the order 60 KcP⁻¹. Extrapolation of the water slope of figure 7.3, suggests that at a T/η value of 60 KcP⁻¹, the $A(^{14}\text{N})$ value of this probe in water should be ca. 8.44 G. In pure water at 15°C, $A(^{14}\text{N})$ of t-butyl-N-benzoyl nitroxide was found to be 8.53 G. Due to calibration differences, the values of $A(^{14}\text{N})$ presented here are slightly lower than those reported by Jenkins. At 15°C Jenkins⁹ quotes a value of 8.586 G for $A(^{14}\text{N})$ of this radical in pure water and a value of 8.510 G for the probe in a 10 M aqueous solution of lithium chloride. This fall in $A(^{14}\text{N})$ appears to be within the range predicted from the data in figure 7.3 on viscosity grounds. This fall in $A(^{14}\text{N})$ may well be due to a decrease in out-of-plane bending about nitrogen, caused by an increase in solvent viscosity on addition of lithium chloride. If this is true, then the picture of lithium chloride as a water structure breaker may be false. Indeed comparison of the magnesium perchlorate

Figure 7.4

Plot of $A(^{14}\text{N})$ of *t*-butyl-*N*-benzoyl nitroxide as a function of ΔH_{pp}^0 , the linewidth of the central nitrogen component, in various aqueous solvent mixtures.



data from figure 7.1 with the results of chapter 4 implies that the lithium cation should increase $A(^{14}\text{N})$ of t-butyl-N-benzoyl nitroxide in water.

The rôle of relaxation processes in reflecting solvation phenomena has been outlined for several nitroxides.¹⁻⁵ The possibility of obtaining useful solvation information from linewidth measurements on t-butyl-N-benzoyl nitroxide in solution, was examined. Figure 7.4 shows the variation of ΔH_{pp}^0 , the peak to peak linewidth of the central feature of the e.s.r. spectrum of this radical, as a function of $A(^{14}\text{N})$. Within the scatter of points obtained no clear dependence of ΔH_{pp}^0 on $A(^{14}\text{N})$ can be discerned, in contrast with DTBN. Changes in ΔH_{pp}^0 with $A(^{14}\text{N})$ for DTBN were explained partially in terms of a variation of proton super-hyperfine coupling constant, $A(^1\text{H})$ with $A(^{14}\text{N})$. In the case of t-butyl-N-benzoyl nitroxide there are four possible types of proton with which the unpaired electron should couple. Table 7.1 lists the values of $A(^1\text{H})$ due to coupling to each of these four proton types. It is not clear how $A(^1\text{H})$ of each proton type and hence ΔH_{pp}^0 vary with $A(^{14}\text{N})$ of this radical. Perhaps $A(^1\text{H})$ for all protons is virtually

| | |
|--------------------|------------------------------------|
| Ortho ring protons | $A(^1\text{H}) = +0.036 \text{ G}$ |
| Meta ring protons | $A(^1\text{H}) = +0.001 \text{ G}$ |
| Para ring proton | $A(^1\text{H}) = -0.036 \text{ G}$ |
| t-butyl protons | $A(^1\text{H}) = +0.054 \text{ G}$ |

Table 7.1

The proton hyperfine coupling constants of t-butyl-N-benzoyl nitroxide as determined from n.m.r. measurements. The results were obtained from reference 9.

independent of $A(^{14}\text{N})$. Alternatively self compensating changes in $A(^1\text{H})$ of the aryl and alkyl protons may produce a null change. In any case interpretation of the linewidths is very difficult and computer simulation of the individual proton hyperfine lines was not attempted. This seems justified in light of the lack of knowledge of how $A(^1\text{H})$ of this radical varies and the small changes in linewidth involved.

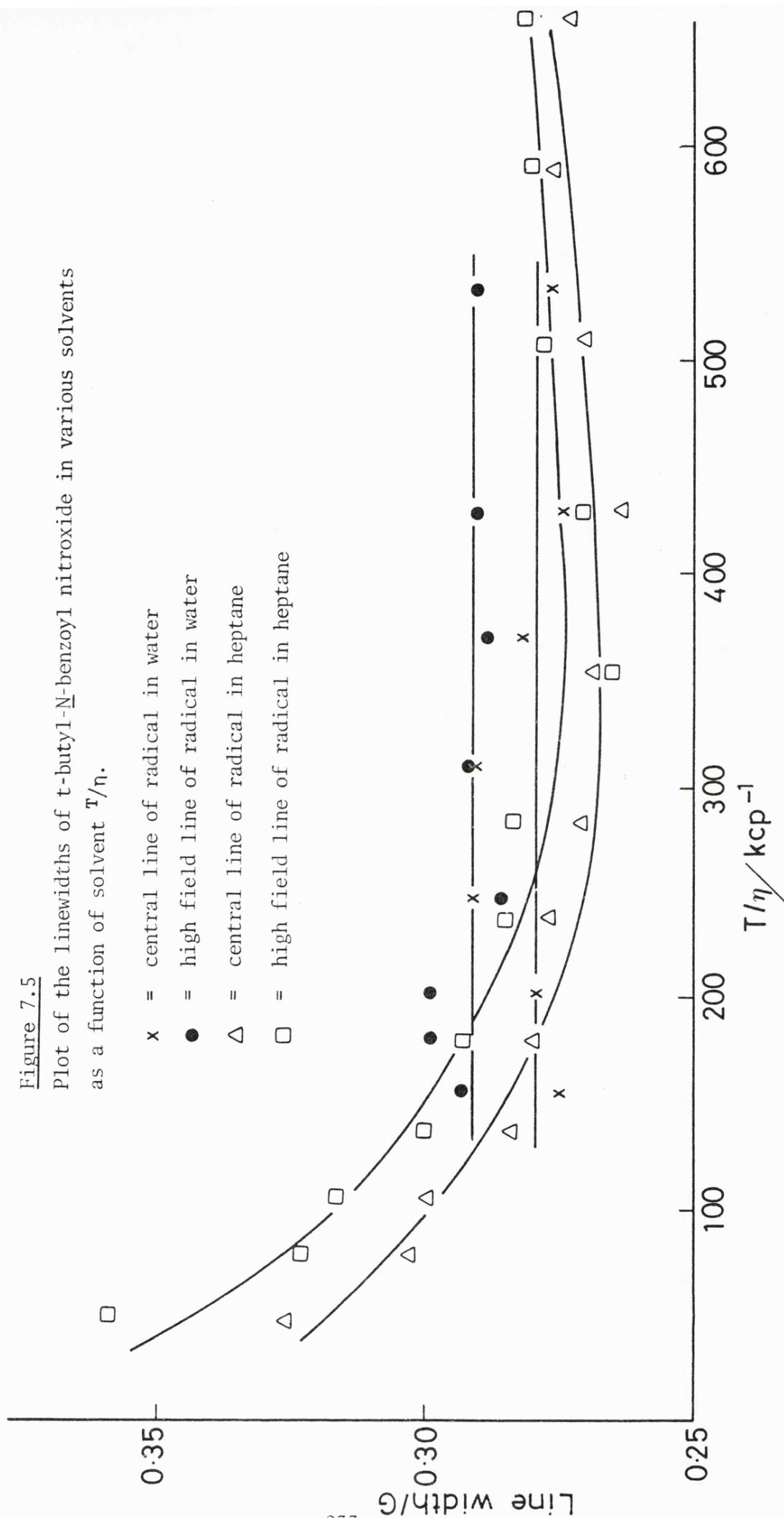
The variation of linewidths of t-butyl-N-benzoyl nitroxide with T/η was examined for the radical in solution in heptane and water. The results are presented in figure 7.5. The insensitivity of linewidth to changes in T/η in the region 150 to 600 KcP^{-1} is interesting. This implies that spin rotation is of minor importance as a relaxation mechanism. The large anisotropy of the g tensor of t-butyl-N-benzoyl nitroxide, discussed in the previous chapter, would predict a large contribution to the linewidth from spin rotation. However, scale drawings based on X-ray diffraction measurements,¹⁶ suggest that the t-butyl-N-benzoyl nitroxide molecule is almost cylindrical in shape, having a long axis of ca. 9.5 Å and a radius of ca. 3.25 Å. The size of the probe reduces its mobility in solution and hence decreases the contribution of spin rotational broadening to the linewidth.

It should be possible to calculate reasonably accurate correlation times from the heptane results. Using the β and γ terms of equation 2.28, as discussed in chapter 3, a series of correlation times was calculated from the widths of the three nitrogen hyperfine components. The results of these calculations are shown in table 7.2. To produce linewidth differences of the kind observed, equation 2.30 demands that the probe has a hydrodynamic radius of 1.5 Å. Equation 2.40, when used to evaluate the spin rotational results, requires a hydrodynamic radius of ca. 4.3 Å. This latter result is closer to the molecular radius

| Temperature K | ΔH_{pp}^{+1} (Gauss) | ΔH_{pp}^0 (Gauss) | ΔH_{pp}^{-1} (Gauss) | τ_c calculated from γ term of eqn. 2.28 (secs) | τ_c calculated from β term of eqn. 2.28 (secs) |
|------------------|---------------------------------|------------------------------|---------------------------------|--|---|
| 183.3 | 0.325 | 0.326 | 0.359 | 3.704×10^{-11} | 1.459×10^{-11} |
| 194.3 | 0.304 | 0.303 | 0.323 | 2.503×10^{-11} | 7.105×10^{-12} |
| 202.9 | 0.291 | 0.300 | 0.317 | 1.045×10^{-11} | 1.030×10^{-11} |
| 211.5 | 0.286 | 0.284 | 0.300 | 2.174×10^{-11} | 5.075×10^{-12} |
| 221.2 | 0.271 | 0.280 | 0.293 | 5.460×10^{-12} | 8.418×10^{-12} |
| 232.4 | 0.278 | 0.277 | 0.285 | 1.163×10^{-11} | 2.468×10^{-12} |
| 240.5 | 0.271 | 0.271 | 0.284 | 1.621×10^{-11} | 4.889×10^{-12} |
| 251.8 | 0.265 | 0.269 | 0.266 | -9.243×10^{-12} | 3.494×10^{-13} |
| 262.4 | 0.268 | 0.264 | 0.271 | 1.394×10^{-11} | 1.050×10^{-12} |
| 273.6 | 0.272 | 0.271 | 0.279 | 1.163×10^{-11} | 2.468×10^{-12} |
| 282.8 | 0.280 | 0.277 | 0.281 | 9.243×10^{-12} | 3.494×10^{-13} |
| 291.2 | 0.282 | 0.275 | 0.283 | 1.844×10^{-11} | 3.494×10^{-13} |

TABLE 7.2

Correlation times and linewidths for t-butyl-N-benzoyl nitroxide in heptane at various temperatures



predicted above, from the X-ray data. This is unlikely to be significant, since the hydrodynamic radius of a radical determined by e.s.r. relaxation measurements and the Debye theory, is usually smaller than than predicted from molecular models. Thus, the relaxation data shown in figure 7.5 gives no real indication of the mobility of t-butyl-N-benzoyl nitroxide in solution.

Since the above mentioned relaxation mechanisms cannot account for the linewidth trends of t-butyl-N-benzoyl nitroxide in solution, alternative relaxation processes must be considered. The out-of-plane bending about nitrogen, already discussed, may have a line broadening effect. This could be seen as a chemical exchange between a planar form of the probe with a low value of $A(^{14}\text{N})$ and a bent form of the radical, with a higher value of $A(^{14}\text{N})$. Such a process would be expected to broaden the outer hyperfine lines of the e.s.r. spectrum more than the central feature. Thus, this exchange broadening is expected to take a similar form to the differential broadening produced by rotational averaging of the anisotropic g and A tensors of the probe. The measured linewidth differences are smaller than expected on the basis of the long τ_c values predicted by the slope of figure 7.5. Thus, it seems that invoking out-of-plane bending as a source of line broadening does nothing to improve the understanding of the linewidth variations observed for this probe in solution.

The lack of success in understanding the variation of linewidth of t-butyl-N-benzoyl nitroxide as a function of solvent T/η may be due to anisotropic re-orientation of the probe. The equations quoted in chapter two are based on isotropic diffusion of the probe through the solvent and may be inapplicable in cases where the molecular motion is anisotropic. A nearly spherical molecule such as Fremy's salt¹⁹ has

been shown to undergo anisotropic motion in solution. It has already been pointed out that t-butyl-N-benzoyl nitroxide is a cylindrical molecule, which suggests that it may tumble anisotropically in solution. A full discussion of anisotropic re-orientation is beyond the scope of this thesis. The insensitivity of linewidth to changes in solvent suggests that such a discussion would yield little insight into the solvation of this radical.

7.4 Conclusions

A study of the rôle of t-butyl-N-benzoyl nitroxide as a spin probe has been attempted. The results are by no means exhaustive, but reveal that this radical is less suitable for probing solvation effects than the dialkyl nitroxides. Further investigations of the behaviour of acyl nitroxides in solution would be useful, in examining the nitroxides in general as solvation probes.

The variation of $A(^{14}\text{N})$ with solvent composition shows broad similarities between the solvation behaviour of t-butyl-N-benzoyl nitroxide and DTBN. The main differences between the two radicals are thought to arise from the weaker basicity of the acyl nitroxide and the possibility of hydrogen bonding to the two polar sites of this radical. From the trends followed by $A(^{14}\text{N})$, it would appear that hydrogen bonding to the nitroxyl group has the greater effect on $A(^{14}\text{N})$. Hydrogen bonding to carbonyl is thought to have the opposite effect on $A(^{14}\text{N})$, but produces smaller changes. Where changes are small, the effects of solvation on $A(^{14}\text{N})$ may be masked or enhanced, by increases in $A(^{14}\text{N})$ caused by increased out-of-plane vibrational activity of the radical. It is proposed that the acyl nitroxide is hydrogen bonded in water to an appreciable extent. The radical is thought to be hydrogen bonded to

a very small degree in alcoholic solution, whilst in aprotic solvents dipolar interactions may be appreciable.

Linewidth studies on *t*-butyl-*N*-benzoyl nitroxide in solution yield less information than corresponding studies on dialkyl nitroxides. The linewidths of the acyl nitroxide are insensitive to solvent, viscosity and temperature changes; except at lower temperatures, when modulation of the anisotropic *g* and *A* tensors seems to be of some importance. The linewidth theories presented in chapter two fail to describe adequately this behaviour. Alternative line broadening mechanisms have been tentatively considered, but yield no firm explanation of the linewidth variations observed. A more detailed linewidth study is required to provide an insight into the relaxation processes, which make the linewidths of *t*-butyl-*N*-benzoyl nitroxide so insensitive to the solvent environment.

REFERENCES TO CHAPTER SEVEN

1. C. Jolicoeur and H. L. Friedman, Ber. Bunsenges. Physik. Chem., 1971, 75, 248.
2. C. Jolicoeur and H. L. Friedman, J. Solution Chem., 1974, 3, 15.
3. S. Ablett, M. D. Barratt and F. Franks, J. Solution Chem., 1975, 4, 497.
4. Y. Y. Lim, E. A. Smith and M. C. R. Symons, J.C.S. Faraday I, 1976, 72, 2876.
5. S. E. Jackson, E. A. Smith and M. C. R. Symons, Disc. Faraday Soc., 1977, 64, 173.
6. Y. Deguchi, Bull. Chem. Soc. Japan, 1962, 35, 260.
7. H. G. Aurich, K. Hahn, K. Stork and W. Weiss, Tetrahedron, 1977, 33, 969.
8. H. G. Aurich and J. Trösken, Leibigs. Ann. Chem., 1971, 745, 159.
9. T. J. Jenkins, Ph.D. Thesis, Chelsea College, University of London, 1976.
10. B. Knauer and J. J. Napier, J. Amer. Chem. Soc., 1976, 98, 4395.
11. "Selected Values of Physical and Thermodynamic Properties of Hydrocarbons and Related Compounds", American Petroleum Institute of Research Project 44, Carnegie Press, 1953.
12. J. A. Riddick and W. B. Bunger, "Organic Solvents. Physical Properties and Methods of Purification (3rd. Ed)", Wiley Interscience, 1970.
13. S. J. Baxter and W. P. Baxter, "International Critical Tables Vol. V", p.12, Kynoch Press, Birmingham, 1930.
14. M. C. R. Symons, Phil. Trans. Roy. Soc. (Lond)., 1975, B272, 13.
15. R. S. Drago, G. C. Vogel and T. E. Needham, J. Amer. Chem. Soc., 1971, 93, 6014.
16. S. A. Hussain, Ph.D. Thesis, Chelsea College, University of London, 1978.
17. R. Ramasseul and A. Rassat, Bull. Chem. Soc. (Fr)., 1970, 12, 4330.
18. B. Anderson and P. Anderson, Acta Chem. Scand., 1966, 20, 2728.
19. S. A. Goldman, G. V. Bruno, C. F. Polnaszek and J. H. Freed, J. Chem. Phys., 1975, 79, 489.

APPENDIX

Computer Programs

APPENDIX

A.1 Introduction

Over recent years computers have been increasingly used by scientists to analyse large amounts of data. The computer by use of a set of instructions, usually programmed in a high level language, can rapidly translate raw data into processed results. In this way lengthy, repetitive calculations can be executed, saving time and eliminating the possibility of arithmetic errors (provided that the program itself is correct). In addition to its power as a "number cruncher" the modern computer may be used to store large amounts of data on magnetic media such as tape or disc. Results obtained from computer calculations can be presented neatly, especially when graphical output facilities are available.

Typically, scientific applications are programmed in one of two high level languages - ALGOL or FORTRAN, although other languages may be used. The programs presented in this thesis were all written in FORTRAN, and were run on the University of Leicester's CDC Cyber 72 computer. FORTRAN was chosen for several reasons. The most complicated and frequently used program PLOWSY, which simulates e.s.r. powder spectra, was already written in FORTRAN by Dr. T. Lund. In order to keep consistency the remainder of the programs were also written in this language. The implementation of ALGOL on the Cyber 72 is inferior to the FORTRAN implementation; it runs much more slowly and offers poor string handling capabilities. Programs written in FORTRAN are portable, i.e. they can be transferred from one machine to another with the minimum number of changes.

Four programs are described in the ensuing sections of this

Appendix. They are:

 PLOWSY: a program to simulate the e.s.r. powder spectrum of a paramagnetic species, with electronic spin $S = \frac{1}{2}$ and any nuclear spin.

 SWACK: a program to simulate the envelope produced by overlap of a number of Lorentzian first derivative curves, having relative intensities given by a binomial distribution.

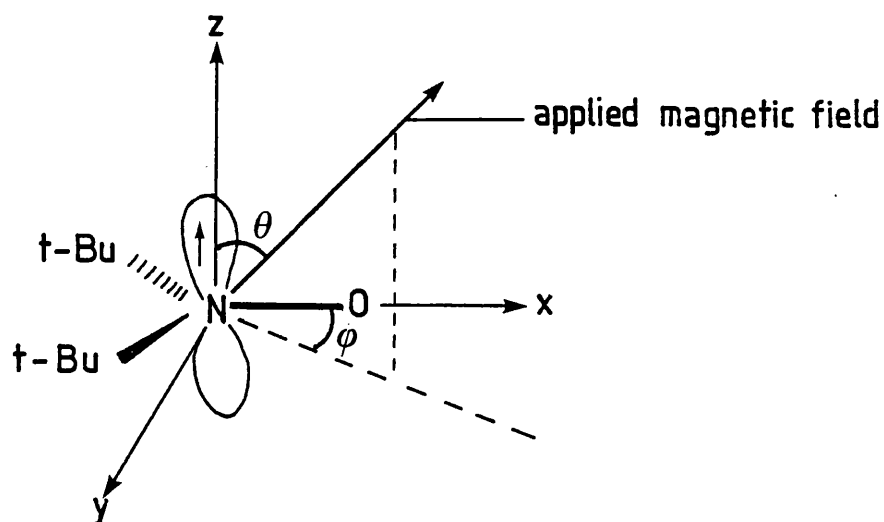
 REXTAU: a program to calculate rotational correlation times from linewidth data and the equations of Johnson.¹

 TUGGER: this program analyses linewidth data as a function of probe concentration, using a linear least squares fit.

Each program is described in more detail below. Where the logic of a program is difficult to follow a flow diagram is presented to clarify matters. Although it was not written by the current author, PLOWSY is described in this Appendix since it does not appear to be adequately documented elsewhere. The listings of each program are given at the end of this Appendix.

A.2 The Solid State Simulation Program - PLOWSY

PLOWSY is a FORTRAN program, which calculates the first derivative e.s.r. spectrum of an immobilised radical (with $S = \frac{1}{2}$) trapped in a rigid matrix. The program was written by Dr. T. Lund and is based on the work of Pilbrow et alia,² which calculates the e.s.r. spectrum to second order. The program calculates the e.s.r. spectrum of a rigidly held radical, with the direction of the magnetic field given by the polar angles θ and ϕ , shown below:



The stick spectrum produced is then adjusted to the correct intensity by calculating the transition probability at the given θ and ϕ . The stick spectrum is then fitted to a first derivative Gaussian lineshape of given width. The values of θ and ϕ are then changed and the spectrum for this new orientation is similarly calculated and added to the first spectrum. Both θ and ϕ are varied from 0 to 90°, in pre-defined steps; and the spectrum for each orientation is added into the summed spectrum. The final accumulated spectrum is the spectrum of the radical summed over all orientations within the solid matrix.

The following data is required by the program and is input in the order given below:

"Initial value g_z , final value g_z , increment for g_z "

"Initial value g_x , final value g_x , increment for g_x "

"Initial value g_y , final value g_y , increment for g_y "

"Initial value A_z , final value A_z , increment for A_z "

"Initial value A_x , final value A_x , increment for A_x "

"Initial value A_y , final value A_y , increment for A_y "

"Initial value quadrupole coupling, final value quadrupole coupling, increment for quadrupole coupling"

"Asymmetry parameter for quadrupole coupling"

"Angle between x axes of g and A tensors"
"Linewidth z features, linewidth x features, linewidth y features"
"Nuclear spin quantum number"
"Microwave frequency"
"Number of steps required to scan θ from 0 to 90°"
"Number of steps required to scan ϕ from 0 to 90°"
"Initial magnetic field, Final magnetic field, Magnetic field increment"
"Scaling factor for graphical output"

The formats for each parameter can be easily obtained from the listing given later. All angles are given in degrees, the microwave frequency is given in MHz, and the linewidths are given in gauss. The hyperfine splitting constants are given in units of $\text{cm}^{-1} \times 10^{-5}$, since the program was originally developed to examine transition metal complexes. Graphical output is achieved by using the CULHAM GHOST curve plotting package. For the DTBN work, the literature values of 6° for the angle between the x axes of the g and A tensors³ and 0.000 133 42 cm^{-1} (4MHz) for the quadrupole coupling⁴ were tried. Since these values did not appear to significantly change the observed spectrum, both of these quantities were taken as zero in all remaining simulations.

A flow diagram for PLOWSY is given on page

The CULHAM GHOST routines allow the graphical spectrum to be drawn to exactly the same scale as the experimental spectrum, which is being fitted. This provides a useful method for visually comparing the computed and experimental spectra and helps in deciding which parameters to alter in the next computation to improve the fit. Typically θ and ϕ are stepped through in 30 increments each, from 0° to 90°. A further increase in the number of steps is found to extend the execution time,

Exit.

without greatly improving the accuracy of the computed spectrum.

A.3 The Proton Envelope Simulation Program - SWACK

This program was written to simulate the nitrogen hyperfine envelopes formed by overlap of the proton superhyperfine lines of DTBN. The program requires that the predicted value of the proton superhyperfine coupling constant, $A(^1\text{H})$, and the number of protons coupling to the unpaired electron, are provided as input. The first step in the program is to calculate the binomial distribution of the proton line intensities and then $A(^1\text{H})$ is converted from units of gauss to radians sec^{-1} . The linewidth of the proton superhyperfine lines is varied from 0.1 to 1.0 G in steps of 0.1 G. For each proton linewidth an envelope spectrum is computed. This is done by scanning through a given frequency range of 59.925×10^9 radians sec^{-1} to 60.025×10^9 radians sec^{-1} in steps of 5×10^5 radians sec^{-1} . The resonance of the central proton superhyperfine line is fixed at the middle of this frequency sweep. At each frequency point the intensity of absorption of each proton line is calculated using a first derivative Lorentzian lineshape function. The absorption due to each value of the proton nuclear spin is scaled by a factor equal to its binomial coefficient. The intensities due to each proton superhyperfine feature at that frequency point are totalled and the result stored. When all frequency points have been analysed in this way the spectrum is printed to the lineprinter. This is repeated for each value of the proton linewidth.

A.4 Program to Calculate Rotational Correlation Times - REXTAU

This program evaluates rotational correlation times from equations

3.2 and 3.3 of chapter 3. Both equations contain expressions for the non-secular contributions to the linewidth, such expressions are often solved by the iterative method used by Jones.⁵ The program described in this section uses the Newton-Ralphson method⁶ for evaluating these non-secular terms. The Newton-Ralphson method appears to home in on an accurate solution to these equations more quickly than the iterative process.

The program requires the parameters given below in the following order as input:

"Number of principle g and A values to use, microwave frequency, magnetic field, the probe's moment of inertia"

For each set of principle g and A values, the following input is required:

"g_z, g_x, g_y, A_z, A_x, A_y"

"Number of points for this set of g and A values"

And for each point

"Width of low-field line, Width of centre line, Width of high-field line, temperature".

The data for the next set of g and A values should then be input, the process being repeated until all the required data is known to the program. The frequency is given in units of MHz, magnetic field is given in gauss, g values should be multiplied by 10⁴ and A values are in units of 1/100th gauss. The probe's moment of inertia and the temperature are required to evaluate τ_J from equation 3.4. The central linewidth, after broadening caused by τ_c effects have been subtracted out, is used in the calculation of τ_J . This program is limited to use for calculations involving radicals of nuclear spin, I = 1. Meaningful

values of τ_J can only be obtained if proton linewidths are used.

A.5 Program to Analyse the Concentration Dependence of Linewidths - TUGGER

This program takes probe concentration data and linewidth data and from them calculates the pseudosecond order rate constant for Heisenberg Spin Exchange and the linewidth of the probe at infinite dilution. This information is evaluated using a linear least squares analysis on the available data. Standard errors for the rate constant and limiting linewidth were also calculated to give an idea of the goodness of fit. Several sets of data can be analysed in one execution of this program. The probe concentration data can be corrected for variations between the temperature at which the samples are made up and the temperature at which the sample is run. Graphical output is provided using the CULHAM GHOST software package.

This program requires the following data:

"Number of sets of data to be analysed, High limit of probe concentration, maximum linewidth".

For each set of data to be analysed, the following input is required:

"Number of points in this set, temperature samples made up, density of solvent at that temperature, temperature coefficient of density of the solvent".

And then:

"Probe Concentration, Linewidth"

for each data point, followed by:

"Solvent viscosity, sample temperature, probe molecular radius, exchange integral".

The next set of data points should be input in the same way, this pro-

cess is repeated until all the required data has been entered. The linewidths should be in units of gauss. The probe concentration is given in M dm^{-3} , this is corrected for temperature, by multiplying by the ratio of the solvent density at the run temperature: the solvent density at the temperature at which the sample was made up. The solvent density at run temperature is calculated from the temperature coefficient of density of the solvent. Temperatures are given in degrees Kelvin. The probe's molecular radius, exchange integral, sample temperature and the solvent viscosity are used in making theoretical estimates of the exchange rate. This is done either by using the theories of Freed⁷ or the Smoluchowsky rate equation given by equation 5.1.

A.6 Listings

The listings of the programs described above are given in this section.

A.6.1 PLOWSY

```
      PROGRAM PLOWSY(INPUT,OUTPUT,TAPE7=INPUT,TAPE2=OUTPUT)
C     SIMULATES EPR SPECTRA FROM IONS WITH S=1/2
C     USES THREE PRINCIPAL G VALUES , AND THREE PRINCIPAL HYPERFINE
C     CONSTANTS
C     THE G AND A TENSORS HAVE THE SAME Z AXIS
C     BUT THERE MAY BE AN ANGLE ALPHA BETWEEN THEIR X AXES
C     REFERENCE: PILBROW, MOL. PHYS. (1973)25,1073
C     QUADRUPOLE COUPLING IS INCLUDED VIA THE PARAMETERS Q,ETA
C     OUTPUT IS BY GRAPH PLOTTER
      REAL JEX,MWF
      DIMENSION CX(91),THETA(91),CPHI(91),SX(91),SPHI(91)
      COMMON L,LTOT,LINT,GZ,GX,GY,AZ,AX,AY,SIGZ,SIGX,SIGY,ALPHA,
1 RNS,MWF,STORE(1001),FIELD(1001),Q,ETA,LI
      READ(7,100) NGZ1,NGZ2,NGZ3
      READ(7,100) NGX1,NGX2,NGX3
      READ(7,100) NGY1,NGY2,NGY3
      READ(7,100) NAZ1,NAZ2,NAZ3
      READ(7,100) NAX1,NAX2,NAX3
      READ(7,100) NAY1,NAY2,NAY3
      READ(7,100) NQ1,NQ2,NQ3
      READ(7,100) NETA
      READ(7,101) ALPHA
      READ(7,100) NSIGZ,NSIGX,NSIGY
      READ(7,102) RNS
      READ(7,102) MWF
      READ(7,100) NANG
      READ(7,100) MANG
      READ(7,100) L,LTOT,LINT
      READ(7,102) HEIGHT
100  FORMAT(3I5)
101  FORMAT(2F5.0,I5)
102  FORMAT(F6.1)
      CALL PAPER(1)
      CALL GARGS(1)
      ETA=FLOAT(NEGA)/100.
      SIGZ=FLOAT(NSIGZ)/10.
      SIGX=FLOAT(NSIGX)/10.
      SIGY=FLOAT(NSIGY)/10.
      SIGZS=SIGZ*SIGZ
      SIGXS=SIGX*SIGX
      SIGYS=SIGY*SIGY
      RNSQ=RNS*RNS+RNS
      BETA=0.46688E-4
      W=0.3336E-4*MWF
      WSQ=W*W
      LI=(LTOT-L)*10/LINT+1
      RL=FLOAT(L)
      RLINT=FLOAT(LINT)/10.
      HMIN=FLOAT(L)
      HMAX=FLOAT(LTOT)
      RNSS=RNS*2.
```



```

N2=INT(RNSS+0.5)
N1=-INT(RNSS+0.5)
CA=COS(0.01745*ALPHA)
SA=SIN(0.01745*ALPHA)
C2A=COS(0.0349*ALPHA)

```

C
C
C

```

SET ANGLE INTERVALS

```

```

INN=INT(0.4222*FLOAT(NANG))
THC=0.733
CSTH=COS(THC)
INNT=INN+1
INNTT=INN+2
NANGI=NANG+1
DO 1 I=1,INNT
  THETA(I)=THC*(I-1)/INN
  CX(I)=COS(THETA(I))
1 SX(I)=SIN(THETA(I))
DO 2 I=INNTT,NANGI
  CX(I)=CSTH*(NANG+1-I)/(NANG-INN)
2 SX(I)=SQRT(1.-CX(I)*CX(I))
MANGI=MANG+1
DO 3 I=1,MANGI
  PHI=1.5708*FLOAT(I-1)/FLOAT(MANG)
  CPHI(I)=COS(PHI)
3 SPHI(I)=SIN(PHI)

```

C
C
C

```

INSERT DO LOOPS TO VARY PARAMETERS AT THIS POINT

```

```

DO 19 NGZ=NGZ1,NGZ2,NGZ3
DO 19 NGX=NGX1,NGX2,NGX3
DO 19 NGY=NGY1,NGY2,NGY3
DO 19 NAZ=NAZ1,NAZ2,NAZ3
DO 19 NAX=NAX1,NAX2,NAX3
DO 19 NAY=NAY1,NAY2,NAY3
DO 19 NQ=NQ1,NQ2,NQ3
GZ=FLOAT(NGZ)/10000.
GX=FLOAT(NGX)/10000.
GY=FLOAT(NGY)/10000.
AZ=FLOAT(NAZ)/100000.
AX=FLOAT(NAX)/100000.
AY=FLOAT(NAY)/100000.
Q=FLOAT(NQ)/100000.
GZS=GZ*GZ
GXS=GX*GX
GYS=GY*GY
AZS=AZ*AZ
AXS=AX*AX
AYS=AY*AY
TXX=AXS*CA*CA+AYS*SA*SA
TYY=AXS*SA*SA+AYS*CA*CA
TXY=(AXS-AYS)*SA*CA
QESQ=Q*Q*ETA*ETA/9.
DO 4 I=1,LI

```

```

STORE(I)=0.
FIELD(I)=HMIN+FLOAT((I-1)*LINT)/10.
4 CONTINUE

```

```

C
C WORK OUT TRANSITION FIELDS AND PROBABILITIES FOR EACH ANGLE
C

```

```

DO 18 I=1,NANGI
  IF(I-INNT) 5,5,6
5 DCOS=CX(I)-CX(I+1)
  GO TO 7
6 DCOS=CSTH/(NANG-INN)
7 IF(I.EQ.1.OR.I.EQ.NANGI) DCOS=0.5*DCOS
  CS=CX(I)
  SN=SX(I)
  CSS=CS*CS
  SNS=SN*SN
  DO 17 J=1,MANGI
    CP=CPHI(J)
    SP=SPHI(J)
    CPS=CP*CP
    SPS=SP*SP
    GSQ=GXS*SNS*CPS+GYS*SNS*SPS+GZS*CSS
    G=SQRT(GSQ)
    GPERPS=GXS*CPS+GYS*SPS
    ASQ=(TXX*GXS*SNS*CPS+TTY*GYS*SNS*SPS+2.*GX*GY*SNS*CP*SP*TXY
1 +AZS*GZS*CSS)/GSQ
    A=SQRT(ASQ)
    BSQ=(GXS*TXX*CPS+GYS*TTY*SPS+2.*GX*GY*SP*CP*TXY)/GPERPS
    TAU1SQ=BSQ*A*ZS/ASQ
    TAU2SQ=AXS*AYS/BSQ
    TAUBIT=SP*CP*(AXS-AYS)*((GXS-GYS)*SA*CA-GX*GY*C2A)
    TAUBSQ=AZS*GZS/(BSQ*GPERPS)*TAUBIT*TAUBIT/(ASQ*GSQ*GPERPS)
    TAU3SQ=TAUBSQ*CSS
    TAU4SQ=GZS*GPERPS*(BSQ-A*ZS)*(BSQ-A*ZS)*SNS*CSS/(ASQ*GSQ*GSQ)
    TAU5SQ=TAUBSQ*SNS*BSQ*GPERPS/(AZS*GZS)
    QUADSQ=Q*Q*BSQ*GPERPS*SNS/(ASQ*ASQ*GSQ*GSQ)
    QUAD1=2.*QUADSQ*A*ZS*GZS*CSS/(A*W)
    QUAD2=.5*QUADSQ*BSQ*GPERPS*SNS/(A*W)
    BDIFS=AXS*GXS*CPS-AYS*GYS*SPS
    QUAD3=2.*QESQ*(AZS*GZS*CSS*SNS*BDIFS*BDIFS/(ASQ*GSQ)
1 -4.*AXS*AYS*GXS*GYS*SNS*CPS*SPS)/(A*ASQ*BSQ*GSQ*GPERPS*W)
    QUAD4=.5*QESQ*((AZS*A*ZS*GZS*GZS*CSS*CSS+ASQ*ASQ*GSQ*GSQ)
1 *BDIFS*BDIFS/(ASQ*GSQ)+16.*AXS*AYS*A*ZS*GXS*GYS*GZS*CSS*CPS*SPS)/
2 (A*ASQ*BSQ*BSQ*GSQ*GPERPS*GPERPS*W)
    QUAD1=QUAD1+QUAD3
    QUAD2=QUAD2+QUAD4
    GT=(GXS*GYS*SNS+GYS*GZS*(SPS+CSS*CPS)+GZS*GXS*(CPS+CSS*SPS))/GSQ
    WEIGHT=GT*DCOS
    IF(J.EQ.1.OR.J.EQ.MANGI) WEIGHT=WEIGHT*0.5
    PP=WEIGHT
    SIGMAS=(GXS*SNS*CPS*SIGXS+GYS*SNS*SPS*SIGYS+GZS*CSS*SIGZS)/GSQ
    S=SQRT(SIGMAS)
    SS=3.*S
    ISS=INT(SS/RLINT+0.5)
    HO=W/(G*BETA)

```

```

C
C AND FOR EACH M ( NUCLEAR SPIN QUANTUM NUMBER ) AT THAT ANGLE
C
      DO 17 M=N1,N2,2
      RM=FLOAT(M)/2.
      H=HO*(1.-A*RM/W-(TAU1SQ+TAU2SQ+TAU3SQ)*(RNSQ-RM*RM)/(4.*WSQ)
1    - (TAU4SQ+TAU5SQ)*RM*RM/(2.*WSQ)
2    +QUAD1*RM*(4.*RNSQ-8.*RM*RM-1.)-QUAD2*RM*(2.*RNSQ-2.*RM*RM-1.))

C
C SPECTRUM IS FITTED IN THIS SECTION OF PROGRAM
C
      IF(ABS(H).GT.20000.) GO TO 25
      KH=INT((H-RL)/RLINT+0.5)+1
      LS=KH-ISS
      LF=KH+ISS
      IF(LS.LT.1) LS=1
      IF(LF.GT.LI) LF=LI
      DO 24 K=LS,LF
      DELTA=H-((K-1)*RLINT+HMIN)
      FACT=-0.5*DELTA*DELTA/(S*S)
      STORE(K)=STORE(K)+DELTA*PP*EXP(FACT)/(S*S*S)
24  CONTINUE
25  CONTINUE
17  CONTINUE
18  CONTINUE
      CALL TITLE
      CALL NORM(HEIGHT)
      CALL PSPACE(0.1,0.9205,0.1,0.529)
      CALL MAP(HMIN,HMAX,-6.,+6.)
      CALL BORDER
      CALL AXES
      CALL PTPLOT(FIELD,STORE,1,LI,-1)
      CALL FRAME
      CALL GREND
19  CONTINUE
      STOP
      END

      SUBROUTINE TITLE
      REAL JEX,MWF
      COMMON L,LTOT,LINT,GZ,GX,GY,AZ,AX,AY,SIGZ,SIGX,SIGY,ALPHA,
1    RNS,MWF,STORE(1001),FIELD(1001),Q,ETA,LI
      WRITE(2,99) Q,ETA
      WRITE(2,100) GZ,GX,GY,AZ,AX,AY,ALPHA,SIGZ,SIGX,SIGY,MWF,RNS
99  FORMAT(1H1,6HPLOWSY,6X,2HQ=,F7.5,3X,4HETA=,F4.2)
100 FORMAT(1H ,3HGZ=,F6.4,1X,3HGX=,F6.4,1X,3HGY=,F6.4,1X,3HAZ=,F7.5,
1    2X,3HAX=,F7.5,2X,3HAY=,F7.5,2X,6HALPHA=,F3.0,2X,5HSIGZ=,F3.1,2X,
2    5HSIGX=,F3.1,3X,5HSIGY=,F3.1,2X,4HMWF=,F6.0,2X,2HI=,F3.1)
      RETURN
      END

```

```

SUBROUTINE NORM(FACTOR)
REAL JEX,MWF
COMMON L,LTOT,LINT,GZ,GX,GY,AZ,AX,AY,SIGZ,SIGX,SIGY,ALPHA,
1 RNS,MWF,STORE(1001),FIELD(1001),Q,ETA,LI

```

```

C
C NORMALISE SPECTRUM TO FIT LINEPRINTER
C

```

```

    DMODM=ABS(STORE(1))
    DO 1 N=1,LI
    DMODN=ABS(STORE(N))
    IF(DMODM.GT.DMODN) GO TO 1
    DMODM=DMODN
1 CONTINUE
    PEAK=DMODM
    DO 2 K=1,LI
    STORE(K)=STORE(K)*FACTOR/PEAK
2 CONTINUE
    RETURN
    END

```

A.6.2 SWACK

```
PROGRAM SWACK(INPUT,OUTPUT,TAPE7=INPUT,TAPE2=OUTPUT)
COMMON BINOM(100),WHH,ALPHA(201)
```

```
C
C PROGRAM TO CALCULATE ENVELOPE WIDTHS FROM A GIVEN VALUE OF THE PROTN
C HYPERFINE WIDTH AND THE PROTON SUPER HYPERFINE COUPLING CONSTANT
C
```

```
      READ(7,10) NAH,NOEL
10  FORMAT(215)
```

```
C
C GET BINOMIAL COEFFICIENT AND PUT CONSTANTS INTO CORRECT FORMAT
C
```

```
      FAKE=1
      BINOM(1)=1
      DO 20 I=1,NOEL
        JIM=I+1
        FAKE=FAKE*(NOEL+1-I)/I
        BINOM(JIM)=FAKE
20  CONTINUE
      WRITE(2,30)
      WRITE(2,35) (BINOM(K),K=1,JIM)
30  FORMAT(1H1,2X,21HBINOMIAL COEFFICIENTS)
35  FORMAT(1H ,F10.0)
      AH=FLOAT(NAH)/100.
      WRITE(2,40) AH
40  FORMAT(1H ,F5.3,30HPROTON SUPERHYPERFINE COUPLING)
      AH=AH*1.76083*10000000.
```

```
C
C LOOP THROUGH DESIRED LINEWIDTHS
C
```

```
      DO 80 NWH=1,10
        WHH=FLOAT(NWH)/10.
        WH=WHH*15249095.
        WH=1/WH
        DO 65 K=1,201
65  ALPHA(K)=0
        H=59975.*1000000.
        DO 75 NOG=1,201
          W=((59925.*10)+5*(NOG-1))*100000.
          BETA=0
          DO 70 M=1,JIM,1
            R=M-((0.5*NOEL)+1)
            Y=H+R*AH
            X=W-Y
            RE=(-(4*BINOM(M)*WH*WH*WH*X)/(3.1416*((1+(WH*WH*X*X))**2)))
70  BETA=BETA+(RE*(10.**14))
          ALPHA(NOG)=BETA
75  CONTINUE
          CALL GRAPH
80  CONTINUE
      STOP
      END
```

```

SUBROUTINE GRAPH
DIMENSION LINE(120)
COMMON BINOM(100),WHH,ALPHA(201)

```

```

C
C SUBROUTINE TO DRAW OUT PROTON ENVELOPES
C

```

```

DATA STAR,BLANK,HYPHEN,AXIS/1H*,1H ,1H-,1HI/
WRITE(2,5)WHH
5 FORMAT(1H0,F6.4,17HPROTON LINE WIDTH)
N=0
DMODM=ABS(ALPHA(1))
DO 10 NL=1,201
N=N+1
DMODN=ABS(ALPHA(N))
IF(DMODM.GT.DMODN) GO TO 10
DMODM=DMODN
10 CONTINUE
PEAK=DMODM
FACTOR=50.
DO 80 K=1,N
FIELD=(K-1)*0.0283956
ALPHA(K)=ALPHA(K)*FACTOR/PEAK
LOC=INT(ALPHA(K)+0.5)
LOC=60-LOC
IF(K.GT.1)GO TO 40
DO 30 M=1,120
30 LINE(M)=HYPHEN
LINE(LOC)=STAR
GOTO 60
40 DO 50 M=1,120
50 LINE(M)=BLANK
LINE(60)=AXIS
LINE(LOC)=STAR
60 WRITE(2,70) FIELD,(LINE(JJ),JJ=1,120)
70 FORMAT(1H ,F6.4,2X,120A1)
80 CONTINUE
RETURN
END

```

A.6.3 REXTAU

PROGRAM REXTAU(INPUT,OUTPUT,TAPE7=INPUT,TAPE2=OUTPUT)

```
C
C  FORTRAN VERSION OF EASTAUC.  CALCULATES ROTATIONAL CORRELATION
C  TIMES FOR NITROXIDE FREE RADICALS.  USES THE NEWTON-RALPHSON
C  METHOD IN EVALUATING THE CORRELATION TIME
C  REFERENCE:POGGI AND JOHNSON J.MAG.RES.1970.
C
C  INPUT THE NUMBER OF POINTS WITH DIFFERENT G&A VALUES
C  THE FREQUENCY IN M.HZ., THE FIELD IN GAUSS; ALL IN I5 FORMAT
C  AND THE MOMENT OF INERTIA*10**38 IN F10.6 FORMAT
C  NEXT LINE:INPUT GZ,GX&GY(ALL*10000); AND AZ,AX,AY(ALL*100)
C  ALL IN I5 FORMAT
C
      READ(7,10) NIP,NEU,IFIELD,TIA
10  FORMAT(3I5,F10.6)
      FREQ=FLOAT(NEU)/1000.
      FIELD=FLOAT(IFIELD)
      DO 4 KIP=1,NIP
      READ(7,77) IGZ,IGX,IGY,IAZ,IAX,IAY
77  FORMAT(6I5)
      GX=FLOAT(IGX)/10000.
      GY=FLOAT(IGY)/10000.
      GZ=FLOAT(IGZ)/10000.
      AX=FLOAT(IAX)/100.
      AY=FLOAT(IAY)/100.
      AZ=FLOAT(IAZ)/100.
      DELG=(GZ-(GX+GY)/2)*8.793955868*10**6
      G=(GX+GY+GZ)/3
      DELA=(2*G*(AZ-(AX+AY)/2)*8.793955868*10**6)/3
      W=6.28318530*FREQ*10**9
      DELAM=20/(DELA**2)
      DELAN=15/(DELA*DELG*FIELD)
C
C  INPUT NO OF POINTS FOR THAT G&A VALUE IN I3 FORMAT
C
      READ(7,20) NUMED
20  FORMAT(I3)
C
C  READ IN THE WIDTHS OF EACH HYPERFINE LINE IN GAUSS, ALL IN F10.6
C  FORMAT, AND THE TEMPERATURE IN KELVIN IN F10.6 FORMAT
C  CALCULATION OF CORRELATION TIMES BEGINS HERE
C
      DO 30 I=1,NUMED
      READ(7,25) FIRST,ZERO,HIGH,TEMP
25  FORMAT(3F6.4,F10.6)
      AM=FIRST+HIGH-2*ZERO
      AN=FIRST-HIGH
      AM=AM*G*DELAM*7.615789*10**6
      AN=AN*DELAN*G*7.615789*10**6
```

```

TAUR=1.0/(10**10)
TAUC=TAUR
DO 40 INK=1,10
FTAUR=5*W*W*TAUR*TAUR*TAUR-AM*W*W*TAUR*TAUR+4*TAUR-AM
FDAUR=15*W*W*TAUR*TAUR-2*AM*W*W*TAUR+4
DTAUR=FTAUR/FDAUR
TAUR=TAUR-DTAUR
FTAUC=8*W*W*TAUC*TAUC*TAUC-AN*W*W*TAUC*TAUC+14*TAUC-AN
FDAUC=24*W*W*TAUC*TAUC-2*AN*W*W*TAUC+14
DTAUC=FTAUC/FDAUC
TAUC=TAUC-DTAUC
WRITE(2,45) TAUR,TAUC
45 FORMAT(2E16.7)
40 CONTINUE
WRITE(2,50) TAUR,TAUC
50 FORMAT(1H ,18HCORRELATION TIMES=,E16.7,2X,3HAND,E16.7)
WRITE(2,98) DELA,DELG,AM,AN
WRITE(2,99) GX,GY,GZ,AX,AY,AZ
98 FORMAT(1H ,8HA ANISO=,E16.7,2X,12HDELTA GAMMA=,E16.7,2X,
1 7H2*BETA=,E16.7,2X,8H2*GAMMA=,E16.7)
99 FORMAT(1H ,3HGX=,F10.6,2X,3HGY=,F10.6,2X,3HGZ=,F10.6,2X,3HAX=,
1 F10.6,2X,3HAY=,F10.6,2X,3HAZ=,F10.6)

```

C
C
C

SECTION TO ADD IN SPIN ROTATIONAL CORRELATION TIME

```

TAU=(TAUC+TAUR)/2
BAIT=TIA*(1.5/(1.38044*TEMP))
ZERO=ZERO*G*7.615789*10**6
WING=1/(1+W*W*TAU*TAU)
ZULU=(DELA*DELA*(3+7*WING)/20)+((DELG*DELG*FIELD*FIELD)*
1 (4+3*WING)/45)
ZULU=ZULU*TAU
DULL=((GX-2.00232)**2+(GY-2.00232)**2+(GZ-2.00232)**2)
ZING=ZERO-ZULU
TAUJ=(ZING*BAIT)/DULL
TAUJ=TAUJ*1.E-22
ZING=ZING/(G*7.61578*10**6)
WRITE(2,88) TAUJ,ZING
88 FORMAT(1H ,5HTAUJ=,E16.7,2X,15HSPIN ROT WIDTH=,F10.6)
30 CONTINUE
4 CONTINUE
STOP
END

```


A.6.4 TUGGER

```
      PROGRAM TUGGER(INPUT,OUTPUT,TAPE7=INPUT,TAPE2=OUTPUT)
C  PROGRAM TO PRODUCE RATE CONSTANTS FOR SPIN EXCHANGE
      DIMENSION X(1000),Y(1000),Z(1000)
      CALL PAPER(1)
      CALL GARGS(1)
      READ(7,4) NOK,XLIM,YLIM
4  FORMAT(I5,2F10.7)
      YLIM=YLIM*15.24909468*10**6
      CALL BLKPEN
      CALL PSPACE(0.1,0.75,0.1,0.90)
      CALL MAP(0.0,XLIM,0.0,YLIM)
      CALL BORDER
      CALL AXES
      CALL CTRSET(4)
      DO 5 K=1,NOK
C
C  THIS SECTION FITS THE DATA TO A STRAIGHT LINE USING A LEAST
C  SQUARES ROUTINE, AND CORRECTS RADICAL CONC FOR TEMPERATURE
C  D2 IS THE DENSITY OF THE SOLVENT AT TEMPERATURE T2
C  DDT IS THE TEMPERATURE COEFFICIENT OF DENSITY
C
      S1=0
      S2=0
      S3=0
      S4=0
      READ(7,10)N,T2,D2,DDT
      READ(7,11) (X(I),Y(I),I=1,N)
      READ(7,19)VISC,T,RAD,EXCH
      WRITE(2,18)
      WRITE(2,11) (X(I),Y(I),I=1,N)
      DO 12 I=1,N
      X(I)=X(I)*(D2+(T2-T)*DDT)/D2
      Y(I)=Y(I)*15.24909468*10**6
      S1=S1+X(I)
      S2=S2+Y(I)
      S3=S3+X(I)*Y(I)
12  S4=S4+X(I)*X(I)
      C=N*S4-S1*S1
      A=(N*S3-S1*S2)/C
      B=(S2*S4-S1*S3)/C
      R7=0
      DO 8 I=1,N
      Z(I)=X(I)*A+B
      QT=Z(I)-Y(I)
      QTS=QT*QT
8  R7=R7+QTS
      B=B/(15.24909468*10**6)
      WRITE(2,20) A,B
      RMSA=SQRT((N*R7)/((N-2)*C))
```

```

RMSB=SQRT(S4*R7/((N-2)*C))
RMSB=RMSB/(15.24909468*10**6)
WRITE(2,28) RMSA,RMSB
10 FORMAT(I5,3F10.6)
11 FORMAT(2F10.7)
18 FORMAT(1H1,6HTUGGER)
19 FORMAT(4F10.6)
20 FORMAT(1H ,33HPSEUDOSECOND ORDER RATE CONSTANT=,E16.7,3X,
1 15HRESIDUAL WIDTH=,F10.7)
28 FORMAT(1H ,18HMEAN SQUARE ERRORS,E16.7,3X,14H=RATE CONSTANT,
1 3X,E16.7,10H=RES WIDTH)
WRITE(2,31) (Y(I),X(I),I=1,N)
31 FORMAT(1H ,E16.7,12X,F8.5)

```

C
C THIS SECTION HAS BEEN ADDED TO GIVE A THEORETICAL RATE CONSTANT
C VISCOSITY IS IN CENTIPOISE, TEMP IN DEGREES K, RADIUS IN ANGSTROMS
C AND EXCH IN RAD*SEC-1
C

```

WRITE(2,24)
24 FORMAT(1H ,24HFREED DIFFUSION ANALYSIS)
TAU1=9.103163209*RAD*RAD*RAD*VISC/T
TAU1=TAU1/(10**10)
TAU2=VISC/(11.08335061*T*10**6)
EXCH=EXCH*10**10
EXCH2=(EXCH*EXCH*TAU1*TAU1)/(1+EXCH*EXCH*TAU1*TAU1)
COLK=EXCH2/TAU2
HEIK=2*COLK/3
WRITE(2,35) TAU1,TAU2,COLK,HEIK
35 FORMAT(1H ,5HTAU1=,E16.7,3X,5HTAU2=,E16.7,3X,8HCOLRATE=,E16.7,
1 3X,9HEXCHRATE=,E16.7)
SMOL=22.17066667*T*10**6/VISC
EXSM=SMOL/3
WRITE(2,36) SMOL,EXSM
36 FORMAT(1H ,18HSMOLUCHOWSKY RATE=,E16.7,2X,14HEXCHANGE RATE=,
1 E16.7)
IF(K.EQ.1.OR.K.EQ.5.OR.K.EQ.7.OR.K.EQ.9)CALL BLKPEN
IF(K.EQ.2.OR.K.EQ.6.OR.K.EQ.8.OR.K.EQ.11)CALL GRNPEN
IF(K.EQ.3.OR.K.EQ.4.OR.K.EQ.10)CALL REDPEN
DO 15 I=1,N
CALL PLOTNC(X(I),Y(I),62)
15 CONTINUE
CALL PTPLLOT(X,Z,1,N,-1)
5 CONTINUE
CALL BLKPEN
CALL FRAME
CALL GREND
STOP
END

```

REFERENCES FOR THE APPENDIX

1. G. Poggi and C. S. Johnson, J. Mag. Res., 1970, 3, 436.
2. J. R. Pilbrow and M. E. Winfield, Mol. Phys., 1973, 25, 1073.
3. L. J. Libertini and O. H. Griffith, J. Chem. Phys., 1970, 53, 1359.
4. J. S. Hyde, C. W. Chien and J. H. Freed, J. Chem. Phys., 1968, 48, 4421.
5. D. Jones, Ph.D. Thesis, University of Leicester, 1972.
6. See, for example,
P. Macdonald "Mathematics and Statistics for Scientists and Engineers", Van Nostrand, London, 1966, p.75.
7. M. P. Eastman, R. G. Kooser, M. R. Das and J. H. Freed, J. Chem. Phys., 1969, 51, 2690.



ELECTRON SPIN RESONANCE STUDIES OF SOLVATION USING NITROXIDE RADICALS
AS PROBES

By Edward Andrew Smith

The electron spin resonance spectrum of a paramagnetic substance, present in low concentration in solution, can give much information concerning the solvent environment. In the work described, nitroxide radicals are used as spin probes. Changes in the nitrogen hyperfine coupling constant and the measured linewidths of the Q radical are indicative of changes in solvation. Two nitroxide radicals are used in this context:- ditertiary butyl nitroxide and t-butyl-N-benzoyl nitroxide.

This thesis is mainly concerned with aqueous and methanolic solutions. The structure and properties of water, together with certain aspects of e.s.r. are reviewed in the earlier parts of the thesis. Studies of ditertiary butyl nitroxide in binary aqueous mixtures imply that this probe is very sensitive to changes in the solvent environment. The probe is thought to be completely hydrogen-bonded in aqueous solution, about fifty per cent hydrogen-bonded in methanol and non-hydrogen bonded in aprotic solvents. The changes in hydrogen-bonding to the nitroxide in aqueous solution on addition of a cosolvent are examined.

The study is extended to incorporate an investigation into the solvation of ions in aqueous and methanolic solution. Heisenberg Spin Exchange Studies, of ditertiary butyl nitroxide in various solvents, reveal that water behaves anomalously as a solvent. The e.s.r. spectrum of ditertiary butyl nitroxide in frozen solutions is examined. This study is extended to include the radical t-butyl-N-benzoyl nitroxide and hence to infer something of the spin distribution within this molecule. Finally, the usefulness of t-butyl-N-benzoyl nitroxide as a spin probe is examined and a comparison with ditertiary butyl nitroxide is made.